

Technical University of Munich



TUM School of Life Sciences

Leaf and whole-tree physiology and morphology of mature Norway spruce and European beech under repeated summer drought and subsequent recovery

Kyohsuke Hikino

Vollständiger Abdruck der von der

TUM School of Life Sciences

der Technischen Universität München zur Erlangung

eines Doktors der Naturwissenschaften (Dr. rer. nat.)

genehmigten Dissertation.

Vorsitz:

Prof. Dr. Thomas Knoke

Prüfer*innen der Dissertation:

1. apl. Prof. Dr. Thorsten E. E. Grams

2. Prof. Dr. Dr. h.c. Hans Pretzsch

3. Dr. Tamir Klein

Die Dissertation wurde am 26.10.2022 bei der Technischen Universität München eingereicht und durch die TUM School of Life Sciences am 14.03.2023 angenommen.

Summary

Forest ecosystems serve important functions for human society especially as a huge storage of terrestrial carbon (C). As a consequence of the ongoing climate change, trees in global forests have been suffering from severe drought and mortality, and are further expected to increasingly experience frequent and long-term drought events in their lifetime. However, responses of mature trees to a multiyear drought and subsequent recovery are poorly understood. To fill this knowledge gap, this doctoral thesis aims to reveal physiological and morphological drought responses and their recovery processes of the two dominant tree species in the Central Europe, Norway spruce (*P. abies* [L.] KARST.) and European beech (*F. sylvatica* L.), during five years of repeated drought and three years of subsequent recovery.

This study was conducted as part of Kranzberg forst roof (KROOF) project, which was initiated to expose more anisohydric mature European beech trees and more isohydric mature Norway spruce trees to five years of drought from 2014 to 2018. Roofs built beneath the forest canopy completely excluded precipitation throughfall during the five entire growing seasons. In the early summer of the sixth drought year in 2019, the previously drought-stressed trees were watered over 2 days with c. 90 mm to investigate their recovery processes. During the five years of drought and the three years of subsequent recovery, predawn leaf water potential, leaf gas exchange, sap flow density, sap flow profile, leaf and shoot morphology, and total leaf area were investigated to reveal the short- and long-term physiological and morphological responses of both trees species. Furthermore, the whole-tree C transport and allocation in spruce trees during the first weeks after drought release were investigated using a continuous ^{13}C labeling experiment performed in parallel with the watering. Fate of newly assimilated C to growth and CO_2 efflux was thereby tracked along branches, stems, coarse- and fine roots, ectomycorrhizae and root exudates to soil CO_2 efflux during the first weeks of drought release.

According to the iso- and anisohydric framework, more isohydric spruce showed larger drought effects both at the leaf and whole-tree level compared to more anisohydric beech. Both species regulated water loss through stomatal closure as a first drought response, with stronger reduction in stomatal conductance and sap flow density in spruce (by up to 85% reduction) compared to beech (by up to 40% reduction). As a long-term response, only spruce reduced their total leaf area by 50-60% compared to the controls through production of shorter needles and shoots, which was accompanied by a reduction along sap flow profile, reinforcing the whole-tree level regulation of water loss at the expense of C uptake. The combination of these responses led to stronger reduction of water use in spruce compared to beech throughout the

drought period. In addition, both species increased predawn leaf water potential under similar soil water conditions in the last drought years, likely through belowground acclimations under repeated drought such as in root morphology, physiology, and micorrhizal/bacterial community. Therefore, stomatal control, reduction in the total leaf area (only spruce), and increased leaf water potential likely facilitated the survival of both species under the long-term drought.

Following the stronger drought effect on the leaf and whole-tree physiology and morphology, spruce trees opened their stomata slower than beech after drought release, likely due to ABA accumulation in spruce needles. Furthermore, among drought stressed spruce trees, severity of the soil water deficit during the drought phase was positively correlated with the ABA concentration before drought release. Thus, more severe drought led to a slower recovery of the stomatal conductance and CO₂ assimilation rates. This correlation between drought severity and recovery processes was not observed for beech. At the whole-tree level, due to the lack of significant change in the total leaf area during the drought, beech trees likely recovered their whole-tree C uptake and water use within one growing season, along with a full recovery in the leaf gas exchange. In contrast, the whole-tree C uptake and water use of spruce trees did not fully recover due to the slow recovery of their total leaf area within the study period of 3 years, even after the full recovery of the stomatal conductance and CO₂ assimilation rates at the leaf level. Nevertheless, spruce trees showed a full recovery of the whole-tree C transport speed within two weeks after drought release, ensuring C supply to sinks. Furthermore, recovering spruce trees produced seven times as much fine roots as controls during the four weeks after the drought release to regenerate their water absorbing system. These enhanced C sinks were supplied by a preferential allocation of newly assimilated C, without any indication of C starvation, supporting the recovery of water uptake and tree physiology. However, only half of the C used for the fine root growth was met by newly assimilated C, and the other half was supplied with stored C, indicating an importance of stored C during drought recovery in addition to newly assimilated C.

Interestingly, even 2 years after the drought release, previously drought-stressed spruce trees showed still lower stomatal conductances than controls accompanied by a higher ABA concentration in leaves. Under non-limited water conditions, this water-conserving leaf-physiological responses together with the slow recovery of the total leaf area can delay the recovery of the stem growth and tree productivity. However, under repeated and frequent drought predicted in the future, the pronounced negative “drought legacy” of spruce can be of

advantage for its survival during future drought events by reduced water consumption. Since frequency and duration of drought are increasing, trees recovering from a long-term drought most likely experience another drought event in the near future. Further researches should focus on “drought legacy” effect on tree performance and mortality during the next drought event to better understand forest developments under future climate change.

Kurzfassung

Waldökosysteme erfüllen wichtige Funktionen für die Menschheit, insbesondere als großer Speicher von terrestrischem Kohlenstoff (C). Als Folge des fortschreitenden Klimawandels erfahren Wälder weltweit schweren Trockenstress und Mortalität. Außerdem wird erwartet, dass sie im Laufe ihres Lebens immer häufiger und länger anhaltende Dürreereignisse erleben werden. Die Reaktionen erwachsener Bäume auf mehrjährige Dürreperioden und während der anschließenden Erholungsphase sind jedoch nur unzureichend bekannt. Die Ziele dieser Doktorarbeit sind, die physiologischen und morphologischen Reaktionen der beiden wichtigsten Baumarten in Mitteleuropa, der Rotbuche (*F. sylvatica* L.) und der Gemeinen Fichte (*P. abies* [L.] KARST.), unter fünfjährigen Trockenstressbedingungen und während der anschließenden dreijährigen Erholungsphase, zu untersuchen.

Diese Studie wurde im Rahmen des Kranzberg Roof Projekt (KROOF) durchgeführt. Dabei wurden eher anisohydrisch reagierende, erwachsene Rotbuchen und isohydrischere erwachsene Fichten einem fünfjährigen Trockenstress, von 2014 bis 2018, ausgesetzt. Dächer, die unter dem Kronendach errichtet wurden, schlossen den Niederschlag während der fünf Vegetationsperioden vollständig aus. Im Frühsommer des sechsten Dürrejahres (2019) wurden die zuvor trockenheitsgestressten Bäume über zwei Tage mit ca. 90 mm bewässert, um ihre Erholungsprozesse zu untersuchen. In den fünf Dürrejahren und den drei Jahren der anschließenden Erholungsphase wurden Blattwasserpotenzial, Blattgasaustausch, Dichte und radiales Profil des Xylemflusses, Blatt- und Sprossmorphologie, und Gesamtblattfläche untersucht, um die kurz- und langfristigen physiologischen und morphologischen Reaktionen beider Baumarten zu ermitteln. Außerdem wurden der C-Transport und die C-Allokation in Fichten in den ersten Wochen nach der Bewässerung mit Hilfe eines kontinuierlichen ¹³C Labeling untersucht, das parallel zur Bewässerung durchgeführt wurde. Die Allokation des neu assimilierten C wurde entlang der Äste, Stämme, Grob- und Feinwurzeln, Ektomykorrhizen und Wurzelexsudate bis hin zur Bodenatmung verfolgt.

Gemäß dem Konzept von Iso- und Anisohydrie zeigte die isohydrischere Fichte sowohl auf der Blatt- als auch auf der Baumebene größere Trockenstresseffekte als die anisohydrischere Buche. Beide Baumarten regulierten den Wasserverbrauch durch Schließung der Stomata als eine der ersten Reaktionen auf den Trockenstress, wobei die stomatäre Leitfähigkeit und die Xylemflussdichte bei der Fichte (um bis zu 85 %) stärker abnahmen als bei der Buche (um bis zu 40 %). Als eine langfristige Reaktion verringerte nur die Fichte die Gesamtblattfläche um 50-60 % im Vergleich zu den Kontrollbäumen durch die Produktion kürzerer Nadeln und Triebe, was die Regulierung des Wasserverbrauchs auf Blattebene auf Kosten der C-Aufnahme verstärkt. Die Kombination dieser Reaktionen führte zu einer stärkeren Verringerung des Wasserverbrauchs bei der Fichte im Vergleich zur Buche während der gesamten Dürreperiode. Darüber hinaus erhöhten beide Arten in den letzten Dürrejahren unter ähnlichen Bodenwasserbedingungen das Blattwasserpotenzial, wahrscheinlich durch unterirdische Anpassungen, z. B. Änderung der Wurzelmorphologie und -physiologie, und der mikorrhizischen/bakteriellen Gemeinschaft. Deshalb haben die Kontrolle der Stomata, die Verringerung der Blattfläche (nur bei der Fichte) und das erhöhte Blattwasserpotenzial das Überleben der beiden Baumarten in der Langzeitdürre ermöglicht.

Infolge der stärkeren Auswirkungen des Trockenstresses auf die Physiologie und Morphologie auf Blatt- und Baumebene, öffneten die Fichten ihre Stomata nach der Bewässerung langsamer als die Buchen, was wahrscheinlich auf die ABA-Akkumulation zurückzuführen ist. Darüber hinaus korrelierte bei Fichten, das Bodenwasserdefizit während des Trockenstresses positiv mit der ABA-Konzentration vor der Bewässerung. Ein stärkerer Trockenstress führte also zu einer langsameren Erholung der stomatären Leitfähigkeit und der CO₂-Assimilationsrate. Diese Korrelation zwischen der Trockenstressdosis und den Erholungsprozessen wurde bei der Buche nicht beobachtet. Da sich die Gesamtblattfläche während des Trockenstresses nicht signifikant veränderte, erholte sich bei der Buche innerhalb einer Vegetationsperiode die C-Aufnahme und der Wasserverbrauch auf Baumebene, zusammen mit einer Erholung des Blattgasaustausches und der Xylemflussdichte. Im Gegensatz dazu, pendelten sich die C-Aufnahme und der Wasserverbrauch von Fichten auf der Baumebene innerhalb von drei Jahren nicht vollständig ein, selbst nach der vollständigen Erholung der stomatären Leitfähigkeit sowie der CO₂-Assimilationsrate auf Blattebene. Dies ist auf die langsame Erholung ihrer gesamten Blattfläche zurückzuführen. Dennoch erholten sich die C-Transportgeschwindigkeit der Fichten innerhalb von zwei Wochen nach der Bewässerung vollständig, wodurch die C Versorgung der Senken sichergestellt werden kann. Darüber hinaus produzierten die Fichten in den ersten vier Wochen nach der Bewässerung siebenmal so viele Feinwurzeln wie die Kontrollbäume. Diese

stimulierten C-Senken wurden durch eine bevorzugte Allokation von neu assimiliertem C versorgt, ohne Anzeichen von C-Mangel, was die Erholung der Wasseraufnahme und der Baumphysiologie unterstützt. Allerdings wurde nur die Hälfte des für das Feinwurzelwachstum verbrauchten C durch neu assimiliertes C gedeckt, während die andere Hälfte aus gespeichertem C stammte. Das deutet darauf hin, dass neben dem neu assimilierten C auch der gespeicherte C bei der Erholung vom Trockenstress eine große Rolle spielt.

Interessanterweise wiesen zuvor trockenheitsgestresste Fichten selbst zwei Jahre nach der Bewässerung bei hohem Wasserpotenzial niedrigere stomatäre Leitfähigkeit als die Kontrollbäume auf, begleitet von einer höheren ABA-Konzentration in den Blättern. Unter normalen Wasserbedingungen können diese wassersparenden blattphysiologischen Reaktionen zusammen mit der langsamen Erholung der gesamten Blattfläche dazu führen, dass die Erholung des Stammzuwachses sich verzögert. Aber bei wiederholten Dürreperioden, welche für die Zukunft vorhergesagt werden, kann diese verzögerte Erholung der Fichte ein großer Vorteil sein, um den Wasserverlust zu begrenzen, und ihr Überleben zu erleichtern. Da Häufigkeit und Dauer von Dürren zunehmen, werden Bäume, die sich vom wiederholtem Trockenstress erholen, in naher Zukunft höchstwahrscheinlich ein weiteres Dürreereignis erleben. Weitere Forschungen sollten die Auswirkungen der verzögerten Erholung auf die Leistung und die Mortalität der Bäume während der nächsten Dürreereignisse aufzeigen, um die Entwicklung der Wälder unter dem künftigen Klimawandel besser zu verstehen.

Table of Contents

Summary	2
Kurzfassung.....	4
Table of Contents	7
List of Abbreviations.....	9
List of Figures	11
List of Tables.....	11
List of Publications.....	12
1. Introduction	13
1.1 Forest ecosystems under global climate change	13
1.2 Isohydic and anisohydic strategies	14
1.3 Tree responses to a long-term drought.....	14
1.4 Recovery from drought	16
1.5 Critical time for C supply: C transport and allocation during drought recovery	17
1.6 Norway spruce and European beech in the Central European forestry and their opposing drought strategies	18
1.7 The aims of the study	19
2. Overview of materials and methods.....	20
2.1 KROOF experimental site.....	20
2.2 Weather data.....	22
2.3 Measurement of soil water conditions	23
2.3.1 Soil moisture	23
2.3.2 Soil water deficit	23
2.4 Measurement of physiology	24
2.4.1 Leaf gas exchange	24
2.4.2 Leaf water potential.....	24
2.4.3 Abscisic acid (ABA) concentrations in leaves	24
2.4.4 Sap flow density, radial profile, and tree water consumption.....	25
2.5 Measurement of morphology	26
2.5.1 Leaf characteristics and shoot length growth.....	26
2.5.2 Total leaf area of beech	26
2.5.3 Total leaf area of spruce	27
2.6 Calculation of Resilience	29
2.7 ¹³ C Labeling	29

2.7.1	CO ₂ exposure and assessment of canopy air	30
2.7.2	Sample collection and measurement of stable C isotopic composition ($\delta^{13}\text{C}$), rates of CO ₂ efflux, and root exudates	30
2.7.3	Calculation of label arrival time and C transport rates (CTR)	34
2.7.4	Calculation of C sink activity	36
2.7.5	Calculation of fraction of labeled C (f_{Label}) and contribution of C _{new} to each C sink (contC _{new})	39
2.7.6	Calculation of allocation of newly assimilated C (C _{new}) to each C sink	40
2.7.7	Calculation of the amount of osmolytes remobilized from leaves and fine-roots upon drought release	41
3.	Abstracts and contributions to the single chapters	43
3.1	Chapter I: Physiological and morphological acclimation of mature trees to five years of experimental summer drought at the leaf and crown level	43
3.2	Chapter II: Repeated summer drought changes the radial xylem sapflow profile in mature <i>Picea abies</i> (L.) Karst.	44
3.3	Chapter III: High resilience of carbon transport in long-term drought-stressed mature Norway spruce trees within 2 weeks after drought release	45
3.4	Chapter IV: Dynamics of initial carbon allocation after drought release in mature Norway spruce - Increased belowground allocation of current photoassimilates covers only half of the carbon used for fine-root growth	46
4.	General discussion.....	48
4.1.	More isohydric spruce was more affected by repeated drought than more anisohydric beech.....	48
4.2.	Acclimation belowground during the repeated drought.....	49
4.3.	Correlation between drought severity and physiological recovery	52
4.4.	Positive “Drought legacy”? - Correlation between morphological and physiological responses in spruce.....	55
4.5.	C sink activity and C supply in spruce during the critical time of drought recovery: Did C starvation occur under enhanced C sink activity?	56
4.6	What can be expected in the forests and their C cycle dynamics in the future?	58
5.	Conclusion and outlook.....	61
6.	References	62
7.	Acknowledgements	85
8.	Appendix	86

List of Abbreviations

ABA	Abscisic acid
A_n	Total leaf area of each needle age
A_{sat}	Light-saturated CO_2 assimilation rates at CO_2 concentration of 400 ppm
C	Carbon
CA	Projected canopy area of beech
C_i/C_a	Ratio of intercellular to ambient CO_2 concentration
CO	Control
CO_2	Carbon dioxide
C_{new}	Newly assimilated C
$contC_{new}$	Contribution of C_{new} to each C sink
CTR	Carbon transport rates
CTR_{above}	Aboveground carbon transport rates from crown to trunk base
CTR_{below}	Belowground carbon transport rates from trunk base to soil CO_2 efflux
CRDS	Cavity ring-down spectroscopy
CR_{mean}	Mean canopy radius of beech
c_w	Concentration of the water solution
D	Needle density in each shoot
DBH	Diameter at breast height
DOY	Day of year
DRM	Total initial dry fine-root biomass
ECM	Ectomycorrhizae
f_{Label}	Fraction of labeled C
g_s	Leaf stomatal conductance to water vapor
HFD	Heat field deformation system
IRIS	Isotope ratio infrared spectrometer
IRMS	Isotope ratio mass spectrometer
iSWD	Time-integrated soil water deficit
KROOF	Kranzberg roof experiment
LA	Total leaf area
LA/SA	Ratio of leaf to sapwood area
L_b	Total length of the needled branches

L_n	Needle length
L_s	Length of each shoot
LWC	Leaf water content
LWM	Leaf water mass per tree
MRT	Mean residence time of leaf sugars
N_n	Total number of needles of each needle age
N_s	Number of shoots of each needle age
OE	Molar osmolytes equivalent
PAW	Plant available water
PLA	Projected leaf area
PPFD	Photosynthetically Active Photon Flux Density
$RO_{\text{sucrose/pinitol/prolin}}$	Total amount of remobilized osmolytes
RWC	Root water content
RWM	Total water mass in fine-roots
π_o	Osmotic potential of the leaf at full turgor
Ψ_{PD}	Predawn leaf water potential
$\Psi_{50/88}$	Water potential inducing 50/88% of loss of xylem conductivity
SA	Sapwood area
SLA	Specific leaf area
TD	Thermal dissipation system
TDR	Time Domain Reflectometry
TE	Throughfall exclusion
u_{daily}	Mean sap flow density per day
VPD	Vapor pressure deficit
$\delta^{13}C$	stable C isotopic composition
$\delta^{13}C_a$	$\delta^{13}C$ in tree crowns
$\delta^{13}C_{\text{old}}$	Mean $\delta^{13}C$ before the start of labeling
$\delta^{13}C_{\text{phloem}}$	$\delta^{13}C$ of phloem sugars
$\delta^{13}C_{\text{new}}$	$\delta^{13}C$ at the new isotopic equilibrium
$\delta^{13}C_{\text{sample}}$	$\delta^{13}C$ of each measurement
$\delta^{13}C_{\text{stem}}$	$\delta^{13}C$ of stem CO_2 efflux
$\delta^{13}C_{\text{soil}}$	$\delta^{13}C$ of soil CO_2 efflux

List of Figures

Fig. 1: Map of the Kranzberg forest experimental site.....	21
Fig. 2: a) Monthly mean temperature, b) monthly mean vapour pressure deficit (VPD), and c) monthly precipitation of Kranzberg forest from 2014 to 2021 measured above forest canopy	22
Fig. 3: Calculation of time-integrated soil water deficit (iSWD) using soil water content measured by TDR (Time Domain Reflectometry).....	23
Fig. 4: Additional information for the calculation of the total leaf area of spruce.....	28
Fig. 5: (a) Overview of the two ¹³ C-labeled plots and (b) Picture of the structure for the ¹³ C labeling	29
Fig. 6: Overview of C sinks and sampling/calculation methods used for this study	31
Fig. 7: Overview of the carbon transport paths assessed in this study.....	35
Fig. 8: Relationship between Ψ_{PD} (predawn leaf water potential) of both species (CO: control and TE: throughfall exclusion) and PAW (plant available water, a,b) or iSWD (time-integrated soil water deficit, c,d) at 0-70 cm soil depth.	51
Fig. 9: Relationships in spruce trees between Resilience of leaf physiological parameters and iSWD (time-integrated soil water deficit during the five years of drought phase) at 0-70 cm soil depth before (day -7) and after drought release (day 0-56).....	53
Fig. 10: Relationships in beech trees between Resilience of leaf physiological parameters and iSWD (time-integrated soil water deficit during the five years of drought phase) at 0-70 cm soil depth before (day -7) and after drought release (day 0-56).....	54
Fig. 11: Relationships between Resilience of leaf physiological parameters and Resilience of LA/SA (ratio of leaf area to sapwood area) in the second and third recovery year (2020-2021).....	56

List of Tables

Table 1: Parameters used to calculate the amount of osmolytes remobilized from leaves and fine-roots of the recovering trees upon drought release.	42
---	----

List of Publications

Included in this thesis

Chapter III and IV have been published in peer reviewed international journals:

-**Hikino, K.**, Danzberger, J., Riedel, V. P., Rehschuh, R., Ruehr, N. K., Hesse, B. D., Lehmann, M. M., Buegger, F., Weigl, F., Pritsch, K., & Grams, T. E. E. (2022). High resilience of carbon transport in long-term drought-stressed mature Norway spruce trees within 2 weeks after drought release. *Global Change Biology*, 28, 2095– 2110. <https://doi.org/10.1111/gcb.16051>

-**Hikino, K.***, Danzberger, J.*, Riedel, V. P., Hesse, B. D., Hafner, B. D., Gebhardt, T., Rehschuh, R., Ruehr, N. K., Brunn, M., Bauerle, T. L., Landhäusser, S. M., Lehmann, M. M., Rötzer, T., Pretzsch, H., Buegger, F., Weigl, F., Pritsch, K., & Grams, T. E. E. (2022). Dynamics of initial carbon allocation after drought release in mature Norway spruce— Increased belowground allocation of current photoassimilates covers only half of the carbon used for fine-root growth. *Global Change Biology*, 00, 1– 17. <https://doi.org/10.1111/gcb.16388>

Additional publications published during the PhD period of the candidate that are not part of this thesis:

- Brunn, M., Hafner, B.D., Zwetsloot, M.J., Weigl, F., Pritsch, K., **Hikino, K.**, Ruehr, N.K., Sayer, E.J. and Bauerle, T.L. (2022). Carbon allocation to root exudates is maintained in mature temperate tree species under drought. *New Phytol*, 235: 965-977. <https://doi.org/10.1111/nph.18157>

- Grams, T. E. E., Hesse, B. D., Gebhardt, T., Weigl, F., Rötzer, T., Kovacs, B., **Hikino, K.**, Hafner, B. D., Brunn, M., Bauerle, T. L., Häberle, K.-H., Pretzsch, H., & Pritsch, K. (2021). The Kroof experiment: realization and efficacy of a recurrent drought experiment plus recovery in a beech/spruce forest. *Ecosphere*, 12(3). <https://doi.org/10.1002/ecs2.3399>

- Agathokleous, E., Kitao, M., Shi, C., Masui, N., Abu-ElEla, S., **Hikino, K.**, Satoh, F., Koike, T. (2021). Ethylenediurea (EDU) spray effects on willows (*Salix sachalinensis* F. Schmid) grown in ambient or ozone-enriched air: implications for renewable biomass production. *J. For. Res.* 33, 397–422 (2022). <https://doi.org/10.1007/s11676-021-01400-1>

1. Introduction

1.1 Forest ecosystems under global climate change

Forest ecosystems cover one-third of the Earth's terrestrial area (FAO and UNEP, 2020) and have been serving important functions for human society, e.g. primarily with wood and non-wood products to generate income (FAO and UNEP, 2020). Even more important is the role of forests as a huge storage of terrestrial carbon (C), which, especially in a form of carbon dioxide (CO₂), is the most influential greenhouse gas for global climate (Collins et al., 2013; IPCC, 2021). Forests store ~45% of terrestrial C (Bonan, 2008) and exchange a large amount of C and water with the surrounding atmosphere through photosynthesis and respiration (Brüggemann et al., 2011; Gower, 2003). Tree canopy absorbs CO₂ via stomata on leaves at the expense of water loss. A part of the absorbed C is used for growth and storage, and thus remains in forests for long periods i.e. years (Chapin et al., 1990; Hartmann & Trumbore, 2016; Pretzsch et al., 2018). Other parts are released from C sinks as respiration for maintenance and repair (Penning de Vries, 1975). C uptake and accompanied water loss, C transport and allocation, sink activity (e.g. respiration and growth), and the balance among them determine productivity and C storage of forests, unless C removal occurs through disturbances (Alkama & Cescatti, 2016; Noormets et al., 2015).

Atmospheric CO₂ concentration has been rising by more than 100 ppm since the 19th century mainly through anthropogenic CO₂ emission and land use changes especially from forests into agricultural lands (IPCC, 2014, 2021). As a consequence, the mean global temperature has been increasing and is predicted to further increase by c. 1 - 4 °C by the end of the 21st century (IPCC, 2021), causing various climate changes. Drought, including soil and atmospheric drought (Basarin et al., 2020), is one of the most influential events on forest ecosystems under climate changes (McDowell et al., 2022). Drought has been causing tree mortality across large areas in global forests (Allen et al., 2010; Hammond et al., 2022; Hartmann et al., 2018; Schuldt et al., 2020). Moreover, the frequency and duration of natural droughts have been increasing (e.g. 2015, 2018, 2019, and 2022, Hartmann et al., 2018; Schuldt et al., 2020; Toreti et al., 2022), and are predicted to further increase in the future (IPCC, 2021). Therefore, trees in global forests are expected to increasingly experience frequent and long-term drought events in their lifetime. Conditions of forests feedback affect the future of human society, not only directly through reduced income derived from wood and non-wood products, but indirectly through altered C storage and C exchange between forests and the atmosphere (Collins et al., 2013). For

this reason, it is essential to understand to what extent changing water availability affects the abovementioned C source (i.e. photosynthesis including accompanied water loss) and sink (i.e. growth, storage, and respiration) activities, and the processes connecting them i.e. C transport and allocation. However, comprehensive analyses including all the C- and water-related processes are still rare and thus poorly understood especially for mature forest stands under long-term drought und subsequent recovery (Hartmann et al., 2018).

1.2 Isohydic and anisohydric strategies

Stomatal regulation is one of the first mechanisms of plants to tackle a drought (Choat et al., 2018; Cochard et al., 1996; Limousin et al., 2009), which inevitably limits C uptake. The stomatal behavior under changing water availability can be described as a continuum between the isohydric and the anisohydric strategy (Hartmann et al., 2021; Tardieu & Simonneau, 1998), which plays an important role for C and water relations under drought and subsequent recovery (Kannenbergh et al., 2019). Isohydric species close their stomata early after onset of the drought to keep a constant midday plant water potential at the expense of C uptake. In contrast, anisohydric species keep their stomata longer open under water limitation. While stomatal opening of anisohydric species seems to be controlled mainly through hydraulic regulation, that of isohydric species is regulated additionally by an accumulation of abscisic acid (ABA, Gallé et al., 2013) synthesized during drought (Christmann et al., 2013; Pierce & Raschke, 1980), inducing stomatal closure (Blackman et al., 2009; Li et al., 2021; Lovisolo et al., 2008; Thalmann & Santelia, 2017). The anisohydric responses enable plants to continue C uptake, but allow midday water potentials to decline, thus may be prone to a hydraulic failure (McDowell et al., 2008; 2022). In contrast, early stomatal closure of isohydric species prevents from hydraulic failure, but may cause C starvation if the drought persists long (McDowell et al., 2008). Thus, the different strategies largely affect C and water relations under changing water availability (Kannenbergh et al., 2019). However, most of the observations to date are based on potted plants and thus iso- and anisohydric responses of mature trees are still poorly understood (Kannenbergh et al., 2019; Yin & Bauerle, 2017).

1.3 Tree responses to a long-term drought

Under drought, tree survival primarily depends on the extent to which tree function is affected (Lloret et al., 2011). C sink and source activity and water use are often down-regulated under water limitation (e.g. Bréda et al., 2006; Meir et al., 2008; van der Molen Calcerrada et al., 2011

and literatures therein). To date, a large body of literature reported negative drought effects on growth (Peñuelas et al., 2011; Pretzsch et al., 2013), respiration (e.g. Leaf: Flexas et al., 2006, Stem: Rodríguez-Calcerrada et al., 2021, soil: Huang et al., 2018; Schindlbacher et al., 2012), C uptake (e.g. Ciais et al., 2005), and water consumption (e.g. Gartner et al., 2009; Peiffer et al., 2014) mostly under a seasonal drought, whose extent is species-specific, depending on tree age (Niinemets, 2010) and drought level (Nolan et al., 2021).

Under a long-term drought, in comparison, it is of further importance for tree's survival to adjust to the water-limiting conditions (Flexas et al., 2006; Limousin et al., 2013) and to prepare for further repeated drought events (Gessler et al., 2020; Niinemets, 2010). Previous studies revealed non-linear responses of trees to a long-term drought due to their ability to adjust to new environmental conditions especially in their leaf morphology and physiology (Barbeta et al., 2013; Beier et al., 2012; Feichtinger et al., 2014; Leuzinger et al., 2011; Liu et al., 2015). Leaf morphological adjustments include a modification in leaf thickness (i.e. SLA, specific leaf area, Anderegg & Hillerislambers, 2016; Poorter & Nagel, 2000) and total leaf area mostly through leaf shedding (Ambrose et al., 2018; Arend et al., 2022; Limousin et al., 2009; Poyatos et al., 2013). These responses may change the root to shoot ratio (Bloom, 1985; Hertel et al., 2013; Poorter & Nagel, 2000) or the leaf to sapwood area ratio (LA/SA, Hudson et al., 2018; Limousin et al., 2012; Martínez-Vilalta et al., 2009; Martin-StPaul et al., 2013; Mencuccini et al., 2019; Poyatos et al., 2007; Rosas et al., 2019) to balance water uptake and transpiration loss at the expense of C uptake (Bréda et al., 2006; Pritzkow et al., 2021; Trugman et al., 2018). Leaf physiological adjustments comprise stomatal regulation, increased photosynthetic capacity (Benomar et al., 2016; Schönbeck et al., 2022; Sperlich et al., 2016), and osmotic adjustments (Mitchell et al., 2008; Morgan, 1984; Tomasella et al., 2018). Compared to morphology, physiological adjustments have been less investigated and its capacity seems to be more limited (Brodribb et al., 2020; Poorter et al., 2012). Furthermore, there have been studies indicating morphological adjustments to induce physiological improvements (Bert et al., 2021; Flexas et al., 2006; Gao et al., 2017; Grassi & Bagnaresi, 2001; Reich et al., 1997).

To predict the development of forest ecosystems in the future, responses of mature trees to long-term and repeated drought are invaluable information, but still poorly understood (Anderegg et al., 2020; Beier et al., 2012; Feichtinger et al., 2017; Harfouche et al., 2014; Leuzinger et al., 2011). To date, there are only a few experiments investigating effect of a long-term drought (> 1 year) on mature trees, either with a throughfall exclusion (Barbeta & Peñuelas, 2016; da Costa et al., 2010; Grossiord et al., 2017) or an irrigation of naturally dry forests (Bose et al., 2022).

This lack of knowledge causes large uncertainties in the predictions of future forests (McDowell et al., 2020; Venturas et al., 2021), since current models predicting C fluxes and forest productivity do not consider potential non-linear responses under repeated drought (Choat et al., 2018; McDowell et al., 2022; Smith & Dukes, 2013; Zhou et al., 2019). Thus, analyses of mature trees exposed to repeated drought are essential to better understand the development of forests under future climate change (Bose et al., 2022; Kramer et al., 2020).

1.4 Recovery from drought

Frequent drought events predicted in the future (IPCC, 2021) are associated with frequent drought release. For surviving trees, it is crucial to respond quickly to available water and recover their restricted function back to the pre-drought (or unstressed control) level after drought release (Lloret et al., 2011). In addition to the drought effect per se, therefore, recovery is another important process for long-term tree survival (Choat et al., 2018; Schwalm et al., 2017). In contrast to drought effects, however, responses to drought release have been less investigated especially for mature trees (Ruehr et al., 2019; Vilonen et al., 2022).

Leaf physiology might recover within hours and days (Ruehr et al., 2019) depending on the degree of isohydry as observed in young trees. In isohydric species, the accumulation of ABA in leaves may delay stomatal responses even after the recovery of leaf water potential (Brodribb & McAdam, 2013; Lovisolo et al., 2008). Whereas the delayed stomatal opening (Belfiore et al., 2021; Duan et al., 2020) hinders fast reaction to available water at the leaf level, it can facilitate embolism repair (Lovisolo et al., 2008; Tombesi et al., 2015) and refilling of water storage (Schulze et al., 1985). Indeed, after moderate drought, anisohydric species tend to recover faster than isohydric species due to rapid stomatal opening upon watering and a resistant xylem structure to cavitation (Pou et al., 2012; Sade et al., 2012; Urli et al., 2013). However, the recovery time can increase with the degree of loss of hydraulic conductivity during drought (Kannenberg et al., 2019) and therefore with the severity of drought (Brodribb & Cochard, 2009). Previous studies observed that loss of hydraulic conductivity in stems delayed recovery of photosynthesis after a severe drought (Garcia-Fornier et al., 2017; Rehschuh et al., 2020), and anisohydric species even showed a slower recovery compared to isohydric species due to a greater loss of hydraulic conductivity during drought (Brodribb & Cochard, 2009; Kannenberg et al., 2019; Yin & Bauerle, 2017).

In contrast to leaf physiology, recovery speed of leaf morphology might be much slower and might differ between deciduous and evergreen species (Zweifel et al., 2020). Since shoot and

leaf growth is mainly pre-determined by the number of shoot and leaf units built during bud-formation (Bollmark et al., 1995; Chen et al., 1996; Cochard et al., 2005), but depends also on current conditions during the shoot and leaf development (Lanner, 2017; Sutinen et al., 2015; Zhu et al., 2022), full recovery of leaf morphology can take at least for one growing season. While deciduous trees can produce new leaves in the next growing season after drought release, evergreen trees keeping older leaves might need years for leaf morphological recovery, further restricting whole-tree level C uptake and water use even after a full recovery of leaf physiology. Therefore, recovery at the whole-tree level can be completely uncoupled with that at the leaf level, and thus recovery of leaf and crown morphology must be taken into account.

1.5 Critical time for C supply: C transport and allocation during drought recovery

In addition to the C source activity, C sink activity and sufficient C supply from both newly assimilated C (C_{new}) and stored C are important prerequisites for tree survival under changing water availability (Hartmann et al., 2020; McDowell & Sevanto, 2010; Ruehr et al., 2019). Especially drought recovery is a critical time for C supply, since both aboveground and belowground C sinks can be stimulated after drought release for embolism repair (Brodersen & McElrone, 2013; Ruehr et al., 2019; Zang et al., 2014), C storage (Galiano et al., 2017; Rehschuh et al., 2022), and root production or microbial activity (Gao et al., 2021; Hagedorn et al., 2016; Joseph et al., 2020). Whether the enhanced C sink activity can be met by available C depends on both C transport rates (CTR) and allocation (Ruehr et al., 2019). Previous studies revealed that C transport and allocation were both altered under changing water availability. CTR to belowground sinks typically decreases under drought due to slower sugar export from leaves (Dannoura et al., 2019; Epron et al., 2012; Hesse et al., 2019; Ruehr et al., 2009), and slower phloem transport in woody tissues (Epron et al., 2016; Hesse et al., 2019; Woodruff, 2014), restricting C supply to sinks. This slower C transport can limit C supply to sinks after drought release, if it does not recover fast enough (Hartmann, Ziegler, & Trumbore, 2013; Sevanto, 2014; Winkler & Oberhuber, 2017). For C allocation, different patterns have been observed in previous studies. Drought can reduce (Joseph et al., 2020; Ruehr et al., 2009; Zang et al., 2014) or increase (Blessing et al., 2015; Chuste et al., 2020; Gaul et al., 2008; Hart et al., 2021) C allocation to belowground sinks for growth and maintenance. During drought recovery, recent studies revealed that C_{new} plays an important role especially in belowground sinks (Gao et al., 2021; Hagedorn et al., 2016; Joseph et al., 2020). However, C allocation dynamics after

drought release are still understudied especially in mature trees (Gao et al., 2021; Joseph et al., 2020) and the role of stored C during drought recovery has not been assessed yet. Furthermore, not only leaf-level photosynthesis, but also recovery of the amount of photosynthesis apparatus i.e. total leaf area, is crucial to ensure the supply with C_{new} in a long run. Thus, combined analyses of C transport, sink activity, and allocation including belowground sinks, which have been often restricted to young trees (Brüggemann et al., 2011; Hartmann et al., 2018), together with the recovery of leaf physiology and morphology are a necessary approach to understand the recovery of mature trees after drought release.

1.6 Norway spruce and European beech in the Central European forestry and their opposing drought strategies

One-third of the Europe's total land area is covered with forests and the majority of it is under management for timber production (Forest Europe 2015). In forest ecosystems in the Central Europe, Norway spruce (*Picea abies* (L.) Karst.) and European beech (*Fagus sylvatica* L) are dominant tree species, accounting for 30% of the forest areas (Pretzsch, Biber, et al., 2014). Norway spruce is the most frequent tree species in the forestry of the Central Europe although its natural distribution is restricted to mountainous regions (LWF, 2020). European beech is one of the most important deciduous trees for the forestry in the Central Europe (Leuschner, 2020; LWF, 2020), the most competitive tree species in non-limited climate and soil conditions, and thus has the largest natural distribution area in the Central Europe.

These two species show different strategies under changing water availability. While European beech deploys a more anisohydric strategy, keeping stomata longer open (Leuschner, 2020; Magh et al., 2019), Norway spruce exhibits a more isohydric strategy, closing stomata earlier under water limitation (Hartmann, Ziegler, Kolle, et al., 2013; Oberhuber et al., 2015). Under recent severe drought events, both Norway spruce and European beech trees have been showing crown diebacks (Arend et al., 2022; Frei et al., 2022), growth declines (Bottero et al., 2021; Knutzen et al., 2017; Martinez del Castillo et al., 2022; Walthert et al., 2021), and tree mortality (Arend et al., 2021; Braun et al., 2020; Schuldt et al., 2020). To better understand tree responses and their effects on forest ecosystem C cycles under changing water availability, we need comprehensive research during drought and subsequent recovery. However, there are huge knowledge gaps regarding responses of mature trees to a long-term drought and subsequent recovery processes. To this end, the Kranzberg forest roof (KROOF) project was initiated in 2010 in Freising, Southern Germany (Grams et al., 2021; Pretzsch, Rötzer, et al., 2014). In the

first phase of the KROOF project (KROOF I), mature European beech and Norway spruce were exposed to five years of repeated summer drought between 2014 and 2018 by precipitation throughfall exclusion from spring to late fall. To assess the recovery processes after the repeated drought, the KROOF project was shifted to the second phase (KROOF II) in the sixth drought year 2019, applying a controlled watering of drought-stressed trees.

1.7 The aims of the study

To fill the knowledge gaps mentioned above, this doctoral thesis aims to investigate C source and sink activity, C transport, C allocation dynamics, and related water use during a long-term drought and subsequent recovery, taking advantage of the unique long-term KROOF project in a mature forest stand. Main objectives of this study were:

- 1: To determine isohydric and anisohydric responses of mature spruce and beech trees to a repeated drought in carbon and water relations both at the leaf- and whole-tree level
- 2: To address the effect of the drought responses on their recovery processes

Chapters I and II mainly focus on the drought phase and reveal physiological and morphological responses of Norway spruce and European beech to repeated drought. Chapter I shows detailed physiological and morphological responses to the repeated drought and its effect on the whole-tree water use. We hypothesized that more isohydric spruce would reduce water consumption more than beech due to stronger stomatal control as a first drought response, and that the water consumption would be regulated not only by stomatal control but also by morphological acclimation under repeated drought. Chapter II then focuses on the xylem sap flow profile to reveal if sap flow profile changes during drought and recovery after drought release.

Chapters III and IV then focus on C relations of Norway spruce trees during the recovery phase, the critical time for C supply. Chapter III assesses the recovery of the whole-tree C transport and hypothesized that both above- and belowground C transport rates would recover within two weeks after drought release. Chapter IV then discusses the whole-tree C sink activity and allocation during recovery. We hypothesized that spruce trees recovering from a long-term drought would increase belowground C sink activity and preferentially allocate newly assimilated C (C_{new}) belowground. Additionally we also tested if the contribution of C_{new} would decrease under enhanced sink activity.

The results of this doctoral thesis improve the mechanistic understanding of tree responses to repeated drought and subsequent recovery. Short-term and long-term responses of two

dominant tree species in the Central Europe both at the leaf and the whole-tree level provide essential information to predict the development of forests under climate change with increasing drought frequency and severity.

2. Overview of materials and methods

This capital summarizes the general information and the main works for this thesis done by the author. The other detailed methods and statistical analyses are described in each chapter (I, II, III, IV).

2.1 KROOF experimental site

Kranzberg forest roof project (KROOF) was initiated in 2010 in a mixed forest in southern Germany/Bavaria (11°39'42"E, 48°25'12"N; 490 m a.s.l.) with c. 90 year-old European beech (*F. sylvatica* L.) and 70-year-old Norway spruce (*P. abies* [L.] KARST.) (Fig. 1). The long-term mean temperature (1998-2010) during growing season is 15.5 °C and the annual mean precipitation is 844 mm (Waldklimastation Freising, Bayerische Landesanstalt für Wald und Forstwirtschaft). At this site, a long-term throughfall exclusion (KROOF I) and subsequent watering experiment (KROOF II) were conducted as described in detail in Grams et al. (2021). There are 12 plots (110 - 220 m²) at this site, consisting of 3-7 beech and spruce trees, respectively. The half of the (even numbered six) plots are equipped with the roofs at c. 2-5 m height above the forest floor to exclude the throughfall of precipitation (TE). The other half (uneven numbered six plots) is without roofs defined as control plots (CO). All plots were trenched to 1 m soil depth four years before the onset of the drought treatment and are separated by plastic tarps from the surrounding soil to prevent trees from growing roots outside the plots (Pretzsch, Rötzer, et al., 2014). Water exclusion started in spring 2014. The roofs were closed during the entire growing season (from March to November). After the growing season, the roofs were opened and TE trees received the natural precipitation until next spring. Accordingly, 459 ± 21 mm (69 ± 7% of the annual precipitation) was excluded each year. In total, TE trees had been exposed to recurrent summer droughts for five consecutive growing seasons from 2014 to 2018. To investigate the recovery processes after a long-term drought, all TE plots were watered in early summer 2019 and thereby supplied with c. 90 mm over 36 h to increase the soil water content to the level of CO plots (Grams et al., 2021). The canopy crane located next

to the plots enabled to assess leaf-level photosynthesis and collect samples in the sun-exposed crowns in the plots 1-8.

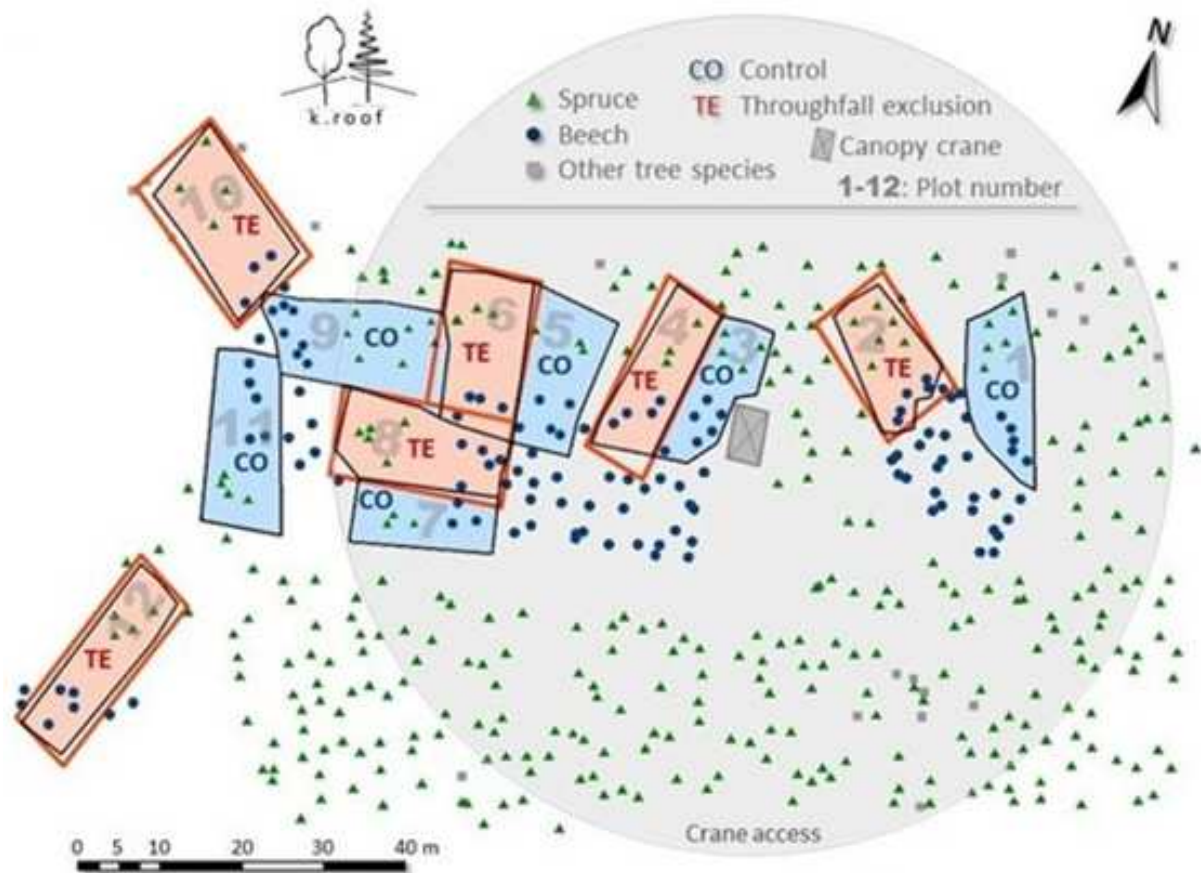


Fig. 1: Map of the Kranzberg forest experimental site, taken from Grams et al., (2021). Blue plots are control plots (CO, uneven number) without roofs and red plots are throughfall exclusion plots (TE, even number) equipped with roofs beneath the canopy to exclude precipitation throughfall. Canopy crane enabled measurements and sampling in the tree crowns in the plot 1-8.

2.2 Weather data

Fig. 2 displays mean monthly temperature, vapor pressure deficit (VPD), and monthly precipitation. Mean temperature above the forest canopy was 11.2 ± 7.8 (SD) °C during the experiment (2014-2021) and mean VPD was 0.37 ± 0.42 (SD) kPa. Mean annual precipitation was 679 ± 118 (SD) mm, and varied between 491 mm in 2015 and 854 mm in 2021.

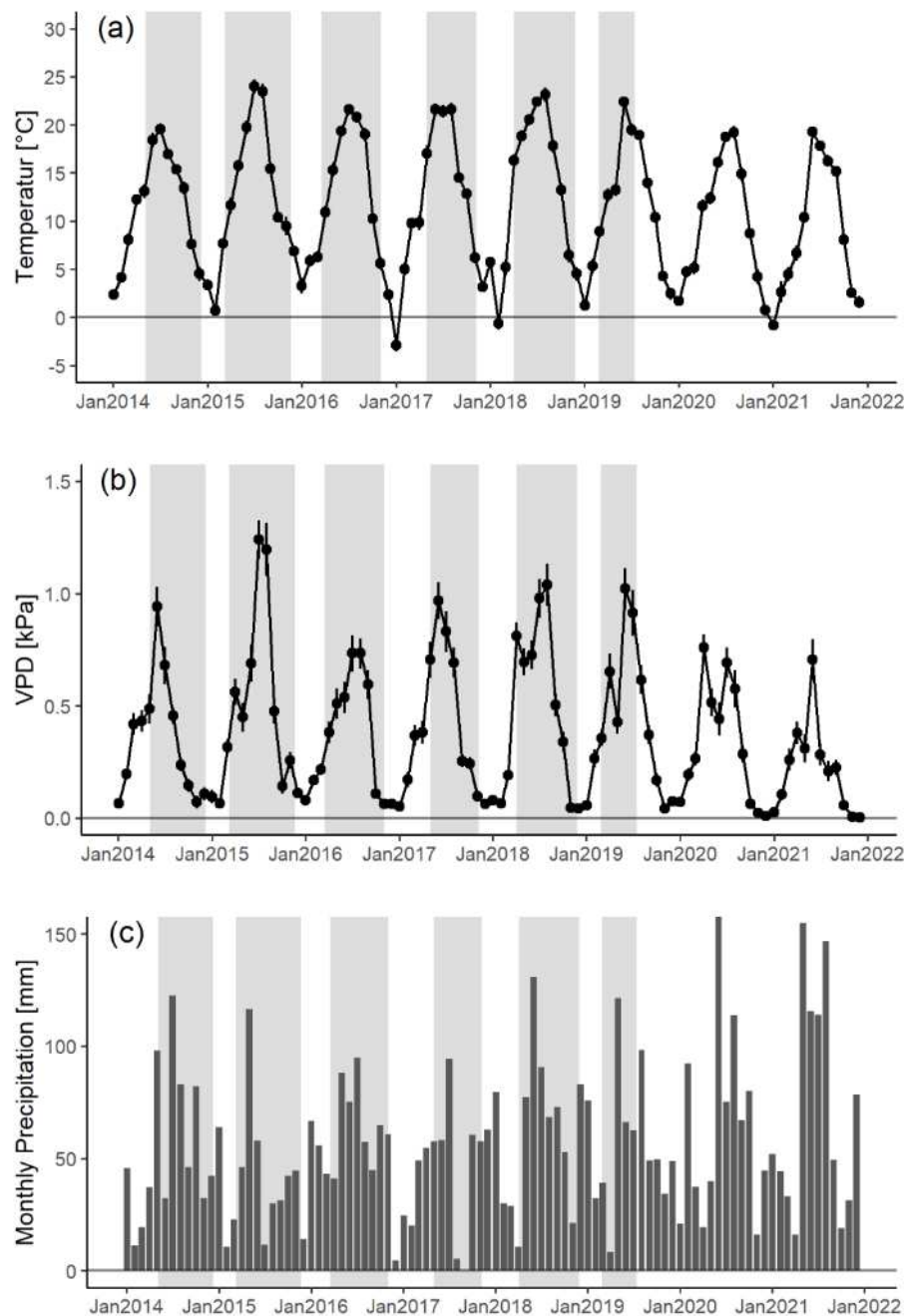


Fig. 2: a) Monthly mean temperature, b) monthly mean vapour pressure deficit (VPD), and c) monthly precipitation of Kranzberg forest from 2014 to 2021 measured above the forest canopy. Shaded areas indicate the periods when the roofs were closed.

2.3 Measurement of soil water conditions

2.3.1 Soil moisture

Soil moisture was measured every week at four depth (0–7 cm, 10–30 cm, 30–50 cm, and 50–70 cm) using Time Domain Reflectometry (TDR100, Campbell Scientific, Logan, CT, USA). The sensors were buried at three positions per plot (within beech trees, between beech and spruce groups, and within spruce trees). Plant available water (PAW) was calculated considering permanent wilting point (threshold soil water content below which no water is available to plants), which was determined by Grams et al., (2021).

2.3.2 Soil water deficit

Using the weekly data of the TDR measurements, time-integrated soil water deficit (iSWD in $\text{day cm}_{(\text{H}_2\text{O})}^3 \text{cm}_{(\text{soil})}^{-3}$) was calculated following Hesse et al., (2019) (Fig. 3). For each soil layer, the maximum soil water content measured in the years (2011–2013) before the start of the throughfall exclusion was defined as the water saturation (unpublished data). The difference between this saturation and the measured soil water content was calculated for each measurement day and TDR probe. Then, the cumulative sum of the difference from April.01 was calculated for each year and TDR probe. Finally, the cumulative sum of the four soil layers (0–7 cm, 10–30 cm, 30–50 cm, 50–70 cm) were summed up, and defined as iSWD. For trees standing in a mixture, the mean iSWD of TDR probe within the species group and TDR in the mixture was used.

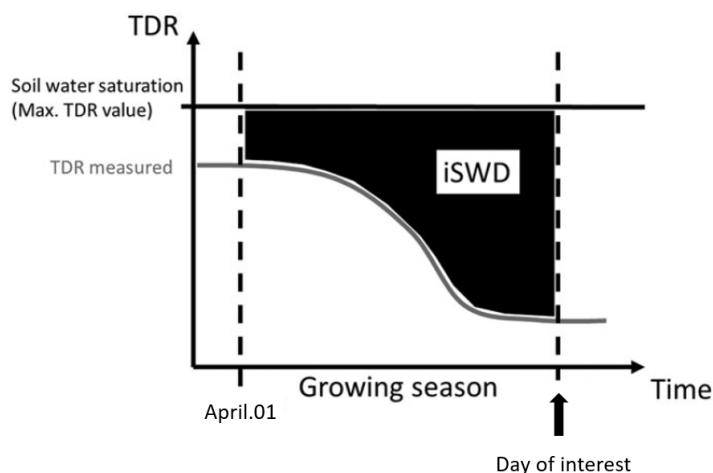


Fig. 3: Calculation of time-integrated soil water deficit (iSWD) using soil water content measured by TDR (Time Domain Reflectometry). Modified from Hesse et al. (2019).

2.4 Measurement of physiology

2.4.1 Leaf gas exchange

Light-saturated CO₂ assimilation rates at CO₂ concentration of 400 ppm (A_{sat}) and leaf stomatal conductance to water vapor (g_s) were measured between 8 am and 3 pm (CET) using open gas exchange systems LI-6400 and LI-6800 (Li-Cor Inc., Lincoln, NE, USA). Two trees per plot and species were assessed ($n = 8$, but $n = 6$ for TE spruce due to mortality in 2015 through bark beetle attack). For beech, 3-5 sun-exposed leaves per tree were randomly chosen in each measurement campaign. For spruce, we chose 1-3 sun-exposed twig with one-year-old needles per tree. In TE trees, when annual branch growth was not sufficiently long to cover the measurement chamber, needles from the previous year(s) were also included. During the measurement, the light intensity (PPFD, Photosynthetically Active Photon Flux Density) was set on $1500 \mu\text{mol m}^{-2} \text{s}^{-1}$ and the leaf temperature at 25 °C. Relative humidity was kept between 60-65%, resulting in VPD of c. 1.3 kPa. After each growing season, the spruce needles were harvested and scanned (Epson Perfection 4990 Photo, Epson Deutschland GmbH, Meerbusch, Germany). The projected leaf area was determined with ImageJ (version 1.53a, National Institute of health, USA) and multiplied by the factor 3.2 to determine the total leaf area (Goisser et al., 2016; Homolová et al., 2013).

In the drought phase (KROOF I) from 2014-2018, 1-2 measurement campaigns per year were conducted: mid- (July) and/or late-summer (August). In the recovery phase (KROOF II), the following measurement campaigns were conducted: D-14 (14 days before watering), D1, D3, D7, D14, D21, D56 (2019, watering year), D365, D425 (2020, second recovery year), D730, and D790 (2021, third recovery year).

2.4.2 Leaf water potential

Predawn water potential (Ψ_{PD} in MPa) of sun-exposed twigs was assessed on the same days as leaf gas exchange measurements with a Scholander pressure bomb (mod. 1505D, PMS Instrument Co., Albany, OR, USA) before sunrise (3 am – 5 am CET).

2.4.3 Abscisic acid (ABA) concentrations in leaves

Leaf samples for the measurements of abscisic acid (ABA) concentration were collected around noon (CET) on the measurement days of the leaf gas exchange during the recovery phase. Three

beech leaves and ten spruce one-year-old needles were randomly sampled from sun crowns and immediately put on dry ice. Within one hour, 3-5 needles (spruce) or 3-5 leaf discs with a diameter of 4 mm (beech) were taken, weighed, put in 80% MeOH solution, and subsequently stored at -21°C at least for 72 h until further procedures.

After MeOH was evaporated using low heat (35 °C), the plant material (5-50 mg) was placed in a 2 mL bead beater tube (CKMix-2 mL, Bertin Technologies, Montigny le Bretonneux, France), filled with ceramic balls (zirconium oxide; mix beads of 1.4 mm and 2.8 mm), an aliquot (10 µL) of a solution of the internal standard ((+)*cis,trans* abscisic acid d6 (2.5 µg/mL)) in acetonitrile was added and incubated for 30 min at room temperature. Then, the tube was made up with ethyl acetate (1mL). After extractive grinding (3 × 20 s with 40 s breaks; 6000 rpm) using a bead beater homogenizer (Precellys Homogenizer, Bertin Technologies, Montigny le Bretonneux, France) the supernatant was membrane filtered, evaporated to dryness, resumed in acetonitrile (70 µL) and injected into the LC–MS/MS-system (2 µL). ABA quantification was carried out by means of the stable isotope dilution assay methodology after establishing calibration curves with the help of commercially available references. The final concentrations were expressed in pmol g⁻¹ fresh weight.

2.4.4 Sap flow density, radial profile, and tree water consumption

Sap flow density was measured every 10 min with Granier-type thermal dissipation sensors (TD, Granier, 1985; 1987) during the entire growing seasons from 1st April to 31st October. Two trees per plot and species were equipped with two sensors (north and south side) in the outer xylem sapwood (0-2 cm depth) at breast height. Average of the two sensors were used and the mean sap flow density per day (u_{daily} in L dm⁻² d⁻¹) was calculated for each tree.

In addition to the outer 2 cm of sapwood, radial sap flow profile at breast height was assessed with TD and heat field deformation system (HFD, Nadezhdina et al., 2012) in summer 2016, 2019, 2020, and 2021. TD sensors were installed at 0-2 cm, 2-4 cm, and 4-6 cm from the cambium, whereas HFD sensors monitor sap flow density at more detailed sapwood depths (0.5, 1.5, 2.5, 3.5, 4.5, 5.5, 6.5, and 7.5 cm from the cambium). Radial sap flow profile was calculated by relating values of each xylem depth to the values at the outermost measurement point (in %) for each tree.

Using u_{daily} , radial profile, and sapwood area (0-8 cm xylem depth as determined by the measurements of radial profile), annual tree water use was calculated as an integrated sum of the water flow.

2.5 Measurement of morphology

2.5.1 Leaf characteristics and shoot length growth

Specific leaf area (SLA in $\text{cm}^2 \text{g}^{-1}$) and shoot length growth (cm) of both species were recorded annually. Five to ten beech leaves or c. 150 needles were randomly collected and scanned (Epson Perfection 4990 Photo, Epson Deutschland GmbH). Then the software Image J (version 1.53a, National Institute of health, USA) was used to calculate the leaf area. After the samples were oven-dried at 64°C for three days, dry weight was recorded and SLA was determined. For the shoot growth, 2 to 5 branches per tree were chosen every year after the growing season and their length were recorded.

For spruce, additional leaf characteristics were determined such as needle length (mm) and needle density (n cm^{-1} shoot). For needle length, five needles per tree from different branches were randomly selected. The needle density was determined by collecting a representative shoot per tree and counting the needles per length unit.

2.5.2 Total leaf area of beech

To estimate the total leaf biomass of the beech trees, litter bags were equipped below the canopy base in two positions per plot, in the middle of spruce and beech tree groups. Five litter bags (0.25 m^2 each) were arranged in each position and they were collected every 1 - 4 month. The collected beech leaves were sorted, dried and weighed. Beech leaves found in the bags below the spruce tree groups were considered to derive from neighboring beech trees in the same plot. We calculated the mean dry leaf biomass per bag/plot, reflecting the leaf biomass per 0.25 m^2 projected canopy area. Projected canopy area (CA) of each tree was estimated using mean canopy radius (CR_{mean}), calculated from eight canopy radii as followed (Pretzsch, 2019).

$$CR_{\text{mean}} = \sqrt{\frac{CR_i^2 + CR_{ii}^2 + CR_{iii}^2 + CR_{iv}^2 + CR_v^2 + CR_{vi}^2 + CR_{vii}^2 + CR_{viii}^2}{8}} \quad (\text{Epn. 1}),$$

where CR_N is the eight canopy radii measured on cite.

Then, projected canopy area (CA) was calculated:

$$CA = \pi * CR_{\text{mean}}^2 \quad (\text{Eqn. 2})$$

Mean dry leaf biomass per litterbag was then extrapolated to the mean CA of all trees in each plot, and converted to total leaf area ($\text{LA m}^2 \text{ tree}^{-1}$) using SLA determined above.

2.5.3 Total leaf area of spruce

Total leaf area (LA m² tree⁻¹) was estimated from three CO and six TE spruce trees. First, in late summer 2020, we counted the number of branches in the sun and the shade crown for each tree. Then, the number of shoots of each needle age (N_s , in n cm⁻¹ needled branch length) was counted on one representative branch in the middle of the sun crown (at c. 5 m from the top) and one representative branch in the middle of the shade crown (red lines in Fig. 4). For the chosen two branches and one additional branch at the bottom of the sun crown (orange lines in Fig. 4) we measured the length of the needled branch part (green area in Fig. 4) and the needleless part (white area in Fig. 4). Then, the total length of the needled branches (L_b in cm) was estimated for sun and shade crowns using the total number of branches. For sun crowns, we assumed a linear increase of both needled and needleless parts towards the bottom of the sun crowns as observed on-site (Fig. 4a). For shade crowns, we observed a constant length of needled and needleless parts of all branches (Fig. 4a). Subsequently, the total number of needles of each needle age (N_n , separated into sun/shade crown) was calculated with N_s , L_b , length of each shoot (L_s in cm, measured for sun and shade crowns), and needle density in each shoot (D in n cm⁻¹, measured for each tree for sun and shade crowns):

$$N_n = N_s \times L_b \times L_s \times D \text{ (Eqn. 3)}$$

Then, the total leaf area of each needle age (A_n in m²) was calculated using needle length (L_n in mm, measured for sun and shade crowns) following (Riederer et al., 1988):

$$A_n = \frac{N_n \times (3.279 \times L_n - 16.31)}{1000000} \text{ (for current year needles, Eqn. 4)}$$

$$A_n = \frac{N_n \times (4.440 \times L_n - 24.78)}{1000000} \text{ (for older needles, Eqn. 5),}$$

For the surface area of shade needles, A_n was multiplied with a factor (0.71) to account for the different leaf thickness between sun and shade needles, determined earlier for the spruce trees on the experimental site (Patzner, 2004). Finally, the surface area of each needle age was summed up to determine the total leaf area (LA) of each tree in 2020.

Based on the data of 2020, we retrospectively calculated annual LA between 2014 and 2019 and for 2021, making the following four assumptions: 1) N_s in sun crowns remained constant if a branch at the same distance from the top would be assessed every year (red line in Fig. 4b). In this case, the lowest whorl at the bottom of the sun crown (three to four branches) is removed

from the calculation of L_b every year. 2) The needle age distribution remains constant throughout the calculation period. 3) For shade crowns, N_s and the number of branches remain constant throughout the calculation period. 4) Since L_s , D , and L_n of shoots older than 2013 could not be recorded, we averaged the values of 2013-2020 for CO spruce and used the values of 2013 for TE spruce, since drought effects were observed after 2014 in TE trees.

The calculated LA of CO trees in each year (2014-2021) corresponded to values (insignificant difference, $p > 0.9$) estimated with a site-specific allometric relationship between DBH and LA determined by Patzner (2004) after a whole-tree harvest. Leaf to sapwood area ratio (LA/SA) was further calculated with DBH and sapwood area of outer 8 cm, based on the sap flow profil measurement.

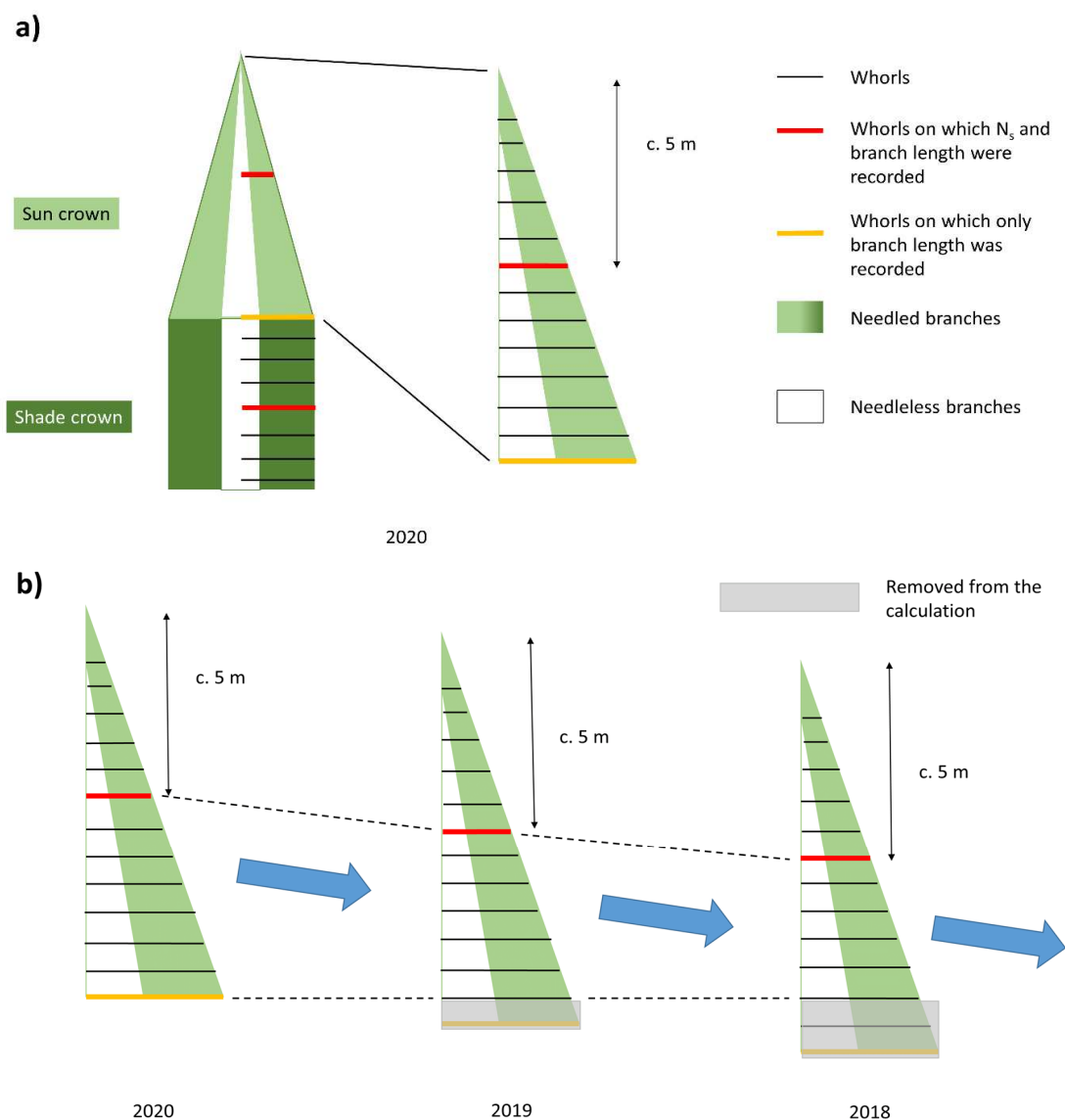


Fig. 4: Additional information for the calculation of the total leaf area of spruce (taken from Chapter II). For details see the text above.

2.6 Calculation of Resilience

In this study, the resilience was defined as the ability of trees to recover to the level of control trees after drought release (Ruehr et al., 2019). According to Hesse (2021), Resilience of leaf physiological parameters (Ψ_{PD} , A_{sat} , g_s , and ABA) and LA/SA of spruce were calculated as TE values divided by mean CO values:

$$Resilience_{i,x} = \frac{TE_{i,x}}{Mean(CO_i)} \quad (\text{Eqn. 6})$$

where i is each individual measurement point and x is each individual tree.

2.7 ^{13}C Labeling

To assess the C transport and allocation of spruce trees during the critical time of recovery from the repeated drought, a whole-tree and continuous ^{13}C labeling was conducted in parallel with the watering in the early summer 2019. The objectives of this experiment were spruce trees on the Plot 3 (four CO) and the Plot 4 (three TE trees).

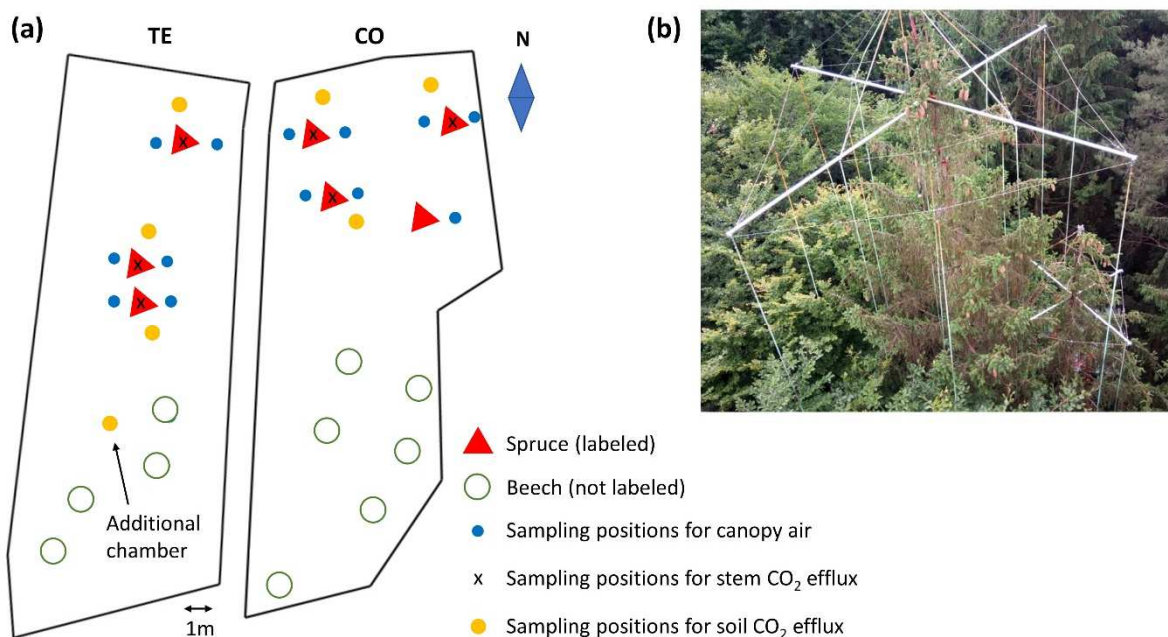


Fig. 5: (a) Overview of the two ^{13}C -labeled plots (CO = control, TE = throughfall exclusion), giving positions of trees (red triangles = labeled spruce trees, green open circles = beech), sampling positions of canopy air (blue circles), stem CO₂ efflux (x), and soil CO₂ efflux (yellow circles). (b) Picture of the structure for the ^{13}C labeling with PVC tubes hanging vertically through the spruce crowns. Taken from Chapter III.

2.7.1 CO₂ exposure and assessment of canopy air

The whole crowns of all, i.e. four spruce trees in plot 3 (CO) and three spruce trees in plot 4 (TE) (Fig. 5a) were exposed to ¹³C-depleted air using the isoFACE-System (Grams et al., 2011) with ¹³C-depleted tank CO₂ ($\delta^{13}\text{C}$ of $-44.3 \pm 0.2\text{‰}$). Each tree crown was equipped with a spider-web shaped construction with 9-17 vertically hanging PVC fumigation tubes (Fig. 5b) connected to the CO₂ tank.

The atmospheric CO₂ concentration and $\delta^{13}\text{C}$ in tree crowns ($\delta^{13}\text{C}_a$) were continuously monitored during the labeling in the sun-lite crowns at 1 m distance from the stem (in west and east orientation) using a cavity ring-down spectroscopy (CRDS, ESP-1000, PICARRO, Santa Clara, CA, USA). A sample point above the canopy was used as a reference. The sample air was continuously transported to the CRDS by membrane pumps via PVC tubes. A computer-automated multiplexer system switched every five minutes among measurement positions and the values of the last three minutes were used for further analyses. According to the mean CO₂ concentration of all 13 measurement points in canopy, which was measured continuously by an infra-red gas analyzer (BINOS 100 4P, Rosemount-Emerson Electric Co., St. Louis, MO, USA), a mass flow controller regulated the amount of the labeled CO₂ added to the crowns.

The ¹³C-labeling started on July.04.2019 (day 0) in parallel with the watering and continued for 14 days until July.17.2019 (day 13), from 5 am until 7 pm (CET). The mean CO₂ concentration in canopy air was targeted at + 130 ppm relative to the ambient air, creating a shift of -8.3 ‰ in $\delta^{13}\text{C}_a$. Mean CO₂ concentration and $\delta^{13}\text{C}$ of the ambient air above the canopy were 413 ppm and -9.2 ‰ during labeling hours.

2.7.2 Sample collection and measurement of stable C isotopic composition ($\delta^{13}\text{C}$), rates of CO₂ efflux, and root exudates

To determine C sink activity and to track the transport speed and the fate of the newly assimilated C (C_{new}) after drought release, samples were continuously or repeatedly collected from stem phloem, stem CO₂ efflux, fine roots, ectomycorrhizae (ECM), root exudates, and soil CO₂ efflux, and once after the growing season 2019 from tree rings in three different heights and coarse roots (Fig. 6).

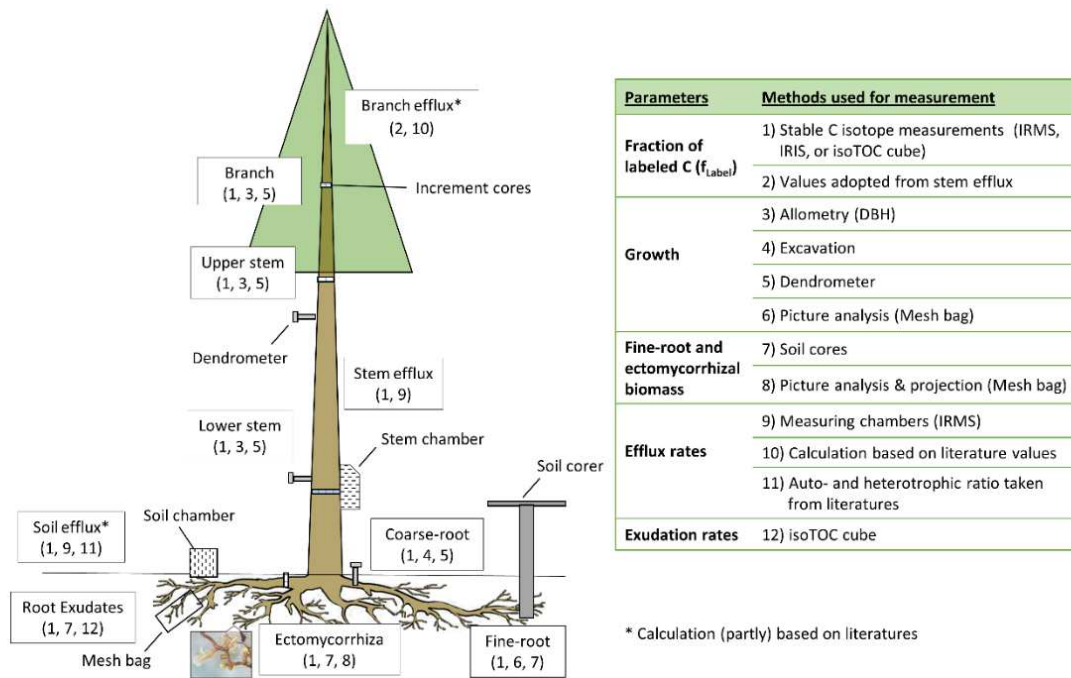


Fig. 6: Overview of C sinks and sampling/calculation methods used for this study. In few cases, data from literature were adopted for calculations (i.e. branch CO₂ efflux and autotrophic soil CO₂ efflux). Taken from Chapter IV.

2.7.2.1 Stem phloem sugar

Samples of phloem tissues were collected on day -1, 7, 13, and 21 around midday at the breast height of labeled trees (four CO and three TE trees) using a cork borer (two discs with diameter of 5 mm for each tree). The samples were immediately frozen on dry ice. Subsequently, they were freeze-dried, ground using a steel ball-mill (Retsch, Haan, Germany), and sent to Swiss Federal Institute for Forest, Snow and Landscape Research (WSL). Then, about 70 mg per sample were mixed with 1.5 ml deionized water (for details see Lehmann et al., 2020). Next, in water bath at 85 °C, water-soluble compounds were extracted for 30 min and purified to neutral sugars with ion-exchange cartridges (OnGuard II H, A, & P, Dionex, Sunnyvale, CA, USA). Afterwards, 1 mg of the neutral sugar was put in silver capsules (Saentis Analytical AG, Teufen, Switzerland), frozen at -20 °C, and freeze-dried. Finally, the carbon isotopic composition of phloem sugars ($\delta^{13}\text{C}_{\text{phloem}}$) was measured using thermal conversion elemental analyser (PYRO cube, Elementar, Hanau, Germany) coupled via a ConFlo III reference system to an isotope ratio mass-spectrometer (Finnigan Delta Plus XP, all supplied by Thermo Fisher Scientific, Bremen, Germany).

2.7.2.2 Stem CO₂ efflux

Rates of stem CO₂ efflux and its stable C isotope composition ($\delta^{13}\text{C}_{\text{stem}}$) were recorded at breast height (Fig. 6) using an isotope ratio infrared spectrometer (IRIS, DeltaRay, Thermo Fisher

Scientific). A total of 12 spruce trees were measured, three ^{13}C -labeled and three non-labeled trees in each treatment, i.e. CO and TE ($n = 3$). The non-labeled trees were used to correct for changes in ^{13}C discrimination caused by the watering and weather fluctuations. Plexiglas (Röhme GmbH, Darmstadt, Germany) chambers (61 to 204 cm^2) were attached at ca. 1 m height on each stem after removing mosses, lichens, and algae. After a leak test using a slight overpressure (c. 2000 Pa), each chamber was supplied with reference air of a constant CO_2 concentration of c. 413 ppm. Excess air was exhausted before entering the chamber to avoid an overpressure. The sample air (mixture of the reference air and the stem-derived CO_2) was transported via PVC tubes to a computer-automated manifold with 16 channels, which switched the chambers connected to the IRIS every five minutes. The CO_2 concentration and the stable C isotope composition of the reference air were determined between measurement cycles (c. every 80 min).

The rates of stem-derived CO_2 efflux were calculated according to mass balance equation (Gammitzer et al., 2009), using the mean values of the closest 2 measurements of the reference air.

$$\text{Stem } \text{CO}_2 \text{ efflux } (\mu\text{mol m}^{-2} \text{ s}^{-1}) = \frac{F_{\text{air}}}{V_{\text{mol}} A_{\text{chamber}}} ([\text{CO}_2]_{\text{sample}} - [\text{CO}_2]_{\text{reference}}) \quad (\text{Eqn.7}),$$

where F_{air} gives the air flow through the chamber (L s^{-1}); V_{mol} , the molar volume of gases (22.4 L mol^{-1}); A_{chamber} , the chamber base area (m^2); $[\text{CO}_2]_{\text{sample}}$ and $[\text{CO}_2]_{\text{reference}}$, the CO_2 concentration (ppm) of sample air from stem chambers and reference air, respectively.

$\delta^{13}\text{C}_{\text{stem}}$ was calculated using a two end-member mixing model (Dawson et al., 2002),

$$\delta^{13}\text{C}_{\text{stem}}(\text{‰}) = \frac{([\text{CO}_2]_{\text{sample}} \times \delta^{13}\text{C}_{\text{sample}}) - ([\text{CO}_2]_{\text{reference}} \times \delta^{13}\text{C}_{\text{reference}})}{[\text{CO}_2]_{\text{sample}} - [\text{CO}_2]_{\text{reference}}} \quad (\text{Eqn. 8}),$$

where $\delta^{13}\text{C}_{\text{sample}}$ and $\delta^{13}\text{C}_{\text{reference}}$ give the $\delta^{13}\text{C}$ signature of sample air from stem chambers and that of reference air, respectively.

In addition to the purpose of ^{13}C labeling experiment, stem CO_2 efflux rates of additional trees were measured during drought recovery. In this way, a total of 28 trees (5 beech and 9 spruce per treatment) were assessed. The measurement started one week before the watering and continued until December 2019. In parallel, the stem temperature of two beech and two spruce trees were recorded next to the stem chambers.

2.7.2.3 Branch, Stem, and Coarse roots

Increment cores (diameter 0.5 cm) were collected from three different stem heights (at breast height, crown base, and middle of crown) and from coarse-roots after the growing season 2019 (Fig. 6). The samples were immediately dried at 64 °C for 72 hours, tree rings from 2019 were separated with a razor blade, and subsequently thin-sliced (c. 5 µm) in radial direction using a microtome (Sledge Microtome G.S.L.1, Schenkung Dapples, Zürich, Switzerland). $\delta^{13}\text{C}$ of tree ring slices were determined with an isotope ratio mass spectrometer (IRMS, delta V Advantage, Thermo Fisher Scientific, Bremen, Germany) coupled to an Elemental Analyzer (Euro EA, Eurovector, Milano, Italy).

2.7.2.4 Fine roots and ectomycorrhizae

In April 2019, vital fine-roots (diameter ≤ 2 mm) found within the upper 10 cm of the soil were photographed, put into 1/3 soil filled ingrowth nylon mesh bags (12.5 x 6.5 cm, mesh width 80 µm, open area of 29%), moisturized and covered with soil (Fig. 6). The mesh bag roots were then harvested and photographed 7 days before and weekly after the watering, while additional fine-roots from 0 – 10 cm depth were daily and randomly taken to gain a more detailed time resolution of the C isotope signatures. After sampling, vital ectomycorrhizae (ECM) and non-mycorrhizal root tips were distinguished by the presence and absence of a hyphal mantle using a stereomicroscope (M125, Leica, Wetzlar, Germany), and dried for 1 h at 60 °C. $\delta^{13}\text{C}$ of vital root tips (ECM and non-mycorrhizal) were determined with the same IRMS used for tree ring slices coupled to an Euro EA.

2.7.2.5 Root exudates

Root exudates were collected according to the method described by Phillips et al., (2008). Excavated root branches were rinsed with a nutrient solution (0.5 mM NH_4NO_3 , 0.1 mM KH_2PO_4 , 0.2 mM K_2SO_4 , 0.15 mM MgSO_4 , 0.3 mM CaCl_2) after attached soil was removed. Roots were then left to recover in a 1:1 mixture of native soil from the site and sand for 48 hours, cleaned, and placed into 30 ml glass syringes with sterile glass beads. Syringes were flushed three times with the nutrient solution, equilibrated for 48 hours, flushed again and left shielded with aluminum foil and leaf litter. Between days -5 and 7, and 20 and 24, exudates trapped in the syringes were collected from the same root branches every 48 hours by adding 30 ml of nutrient solution and extracted using a membrane pump, and stored at -20 °C. Root branches were harvested after exudate collection, dried, and total dry biomass recorded to normalize exudation rates to root mass. $\delta^{13}\text{C}$ and total organic C concentration of root exudate samples were analyzed with an isoTOC cube (Elementar, Hanau, Germany).

2.7.2.6 Soil CO₂ efflux

Soil CO₂ efflux rates and its isotopic C composition ($\delta^{13}\text{C}_{\text{soil}}$) were measured using a Li-8100 automated soil CO₂ flux system with a Li-8150 multiplexer (Li-Cor Inc., Lincoln, NE, USA), connected to an IRIS. Three automatically operating soil chambers (8100-104) per treatment i.e. CO and TE, were installed with 1 m distance from the labeled spruce trees (Fig. 5a). $\delta^{13}\text{C}_{\text{soil}}$ was calculated using the Keeling plot approach (Keeling, 1958; 1961). One additional chamber was placed in the labeled TE plot under unlabeled trees, which was used to correct for the effect of watering and weather fluctuation on $\delta^{13}\text{C}_{\text{soil}}$.

2.7.3 Calculation of label arrival time and C transport rates (CTR)

For the calculation of arrival time and the corresponding C transport rates (CTR), we used the following two changes in $\delta^{13}\text{C}_a$ created by the labeling. 1) ¹³C-depleted tracer assimilated after the turn-on of the CO₂ exposure on the day of the watering (day 0). 2) Ambient/unlabeled carbon (unlabeled tracer hereafter) assimilated after the turn-off of the CO₂ exposure on day 13. Using these two tracers, we determined the C transport rates in the first week after the watering and two weeks after the watering. The entire carbon transport from canopy (needles) to soil CO₂ efflux was divided into two parts (Fig. 7). 1) Aboveground carbon transport from canopy to trunk base (aboveground transport hereafter). 2) Belowground carbon transport from trunk base to soil CO₂ efflux (belowground transport hereafter). As a third process, 3) Carbon transport from trunk base to fine root tips was assessed.

The arrival time of the two tracers (¹³C-depleted tracer after the start of labeling, and unlabeled tracer after the end of labeling) in stem/soil CO₂ efflux and living root tips was determined by fitting the courses of $\delta^{13}\text{C}$ with piecewise function (see Figure 4 in Chapter III). The arrival time of the ¹³C-depleted tracer was defined as the point when $\delta^{13}\text{C}$ started to decrease. First, $\delta^{13}\text{C}$ data of each C sink was cut to contain only two linear segments before and after the arrival of the tracers. Then, we performed a linear regression for the $\delta^{13}\text{C}$ data (“lm” function, R package “stats”, version: 3.6.1). Finally, the intersection of two linear fits were determined using “segmented” function (R package “segmented”, version: 1.3-0, red lines fitted to the $\delta^{13}\text{C}$ data). This intersection was then defined as the arrival time of the ¹³C-depleted tracer (red vertical lines in Figures 4a-f in Chapter III). After the end of labeling, $\delta^{13}\text{C}$ of each C sink started to increase again, as the unlabeled tracer arrived. This point of increasing $\delta^{13}\text{C}$ was calculated with the same method described above (blue lines fitted to the $\delta^{13}\text{C}$ data) and was then defined as the arrival time of the unlabeled C (blue vertical lines in Figures 4a-f in Chapter

III). In the case of root tips, it was not possible to assign each root to the belonging tree. Therefore, all values were pooled for each treatment (Figure 4e,f in Chapter III), providing only one arrival time for each treatment.

Using the arrival time in stem and soil CO₂ efflux, the CTR_{above} (aboveground carbon transport rates from crown to trunk base in m h⁻¹, Fig. 7) and CTR_{below} (belowground carbon transport rates from trunk base to soil CO₂ efflux in m h⁻¹, Fig. 7) were calculated by:

$$\text{CTR (m h}^{-1}\text{)} = \frac{d}{tl} \text{ (Eqn. 9)}$$

For CTR_{above}, *tl* (in h) gives the time-lag between the start respectively end of labeling and the arrival time of the tracers at trunk base (stem CO₂ efflux). *d* (in m) represents the distance between the mean crown height (the middle of the crown) of the tree and the height of the stem chamber. For CTR_{below}, *tl* (in h) gives the time-lag between the arrival time of the tracers at trunk base and the arrival time at soil CO₂ efflux, with *d* (in m) representing the height of the stem chamber plus 1 m, since each soil chamber was placed at 1 m distance from each trunk. We did not calculate CTR to living root tips, since the transport distance was unknown due to random sampling positions. Therefore, for the incorporation time of current photoassimilates in fine roots, the time-lags between the arrival time of the tracers at trunk base and the arrival time at root tips were compared between CO and TE trees instead.

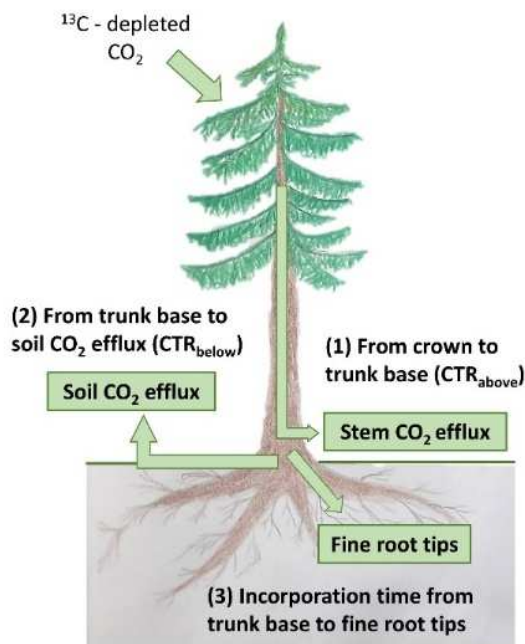


Fig. 7: Overview of the carbon transport paths assessed in this study. (1) Aboveground carbon transport rates (CTR_{above}, in m h⁻¹) from crown to trunk base (assessed as stem CO₂ efflux), (2) Belowground carbon transport rates (CTR_{below}, in m h⁻¹) from trunk base to soil CO₂ efflux, and (3) Incorporation time (in h) of current photoassimilates from trunk base to fine root tips. Taken from Chapter III.

2.7.4 Calculation of C sink activity

To assess the whole-tree C sink activity and the allocation of newly assimilated (C_{new}) and stored C, different above- and belowground sinks were considered (Fig. 6). Below, cumulative sum of C sink activity during 28 days after drought release (in $\text{g C tree}^{-1} 28\text{days}^{-1}$) was calculated for each C sink.

2.7.4.1 Calculation of stem and branch growth

The total growth during the 2019 growing season (Y in kg tree^{-1}) was determined with an allometric function provided for Norway spruce by Forrester et al., (2017), using the diameter at breast height (DBH, d in cm) as input parameter:

$$\text{For stem} \quad \ln(Y) = -2.5027 + 2.3404 \cdot \ln(d) \quad (\text{Eqn. 10}),$$

$$\text{For branch} \quad \ln(Y) = -3.3163 + 2.1983 \cdot \ln(d) \quad (\text{Eqn. 11}),$$

As crown length was c. 1/3 of the total tree height, 1/9 of the total stem growth was assigned to the upper stem (from top to crown base) and the remaining 8/9 to the lower stem (from crown base to trunk base).

The total annual growth in 2019 was then multiplied by the proportional growth (in %) during the 28 days after watering (ratio of the radial growth during 28 days to the total annual growth), determined by automatic point dendrometers (DR-type, Ecomatik, Dachau, Germany) installed at 50% tree height (used for branch and upper stem) and breast height (used for lower stem). The dendrometer data at 6 am (CET) was used and fitted with the following sigmoid curve:

$$X = d + \frac{a-d}{1 + e^{\frac{DOY-c}{b}}} \quad (\text{Eqn. 12}),$$

where X is the output voltage (in mV), DOY is the day of year, a is the starting value of X before the growing season, b the slope coefficient of the regression, c the inflection point of the curve, and d the end value of X after the growing season.

Using these fits, proportional growth was calculated by relating the growth during the 28 days to the total annual growth. The % C of samples was ascertained by IRMS measurement (same for coarse-root growth, fine-root growth, and ECM).

2.7.4.2 Calculation of branch CO_2 efflux

Total branch and twig surface area was estimated for each tree using field data including length, number, and mean diameter of branches and twigs, separated into each needle class and

sun/shade crowns. Based on earlier studies on spruce trees at the same site (Kuptz et al., 2011; Reiter, 2004), maintenance respiration rates (R_M), growth respiration rates (R_G), and total CO_2 efflux of branch CO_2 efflux were calculated as follows:

$$R_{branch} = R_M + R_G \quad (\text{Eqn. 13}),$$

$$R_M = R_{M10} \cdot Q_{10}^{\frac{T-10}{10}} \quad (\text{Eqn. 14}),$$

$$R_G = \frac{330-DOY}{330-130} \cdot R_{G10max} \cdot Q_{10}^{\frac{T-10}{10}} \quad (\text{Eqn. 15}),$$

where R_{M10} represents the maintenance respiration rates at 10 °C (0.13 $\mu\text{mol m}^{-2} \text{s}^{-1}$ for sun branch, and 0.048 $\mu\text{mol m}^{-2} \text{s}^{-1}$ for shade branch), R_{G10max} the maximum growth respiration at 10 °C (0.23 $\mu\text{mol m}^{-2} \text{s}^{-1}$ for sun branch, and 0.12 $\mu\text{mol m}^{-2} \text{s}^{-1}$ for shade branch), Q_{10} the temperature sensitivity (2.45 for both sun and shade branches), and T the temperature.

2.7.4.3 Calculation of stem CO_2 efflux

Stem CO_2 efflux rates of each tree were multiplied by the stem surface area, which were calculated with the DBH and tree height, assuming a conical shape of the stems. For stems above 6.5 m, efflux rates at breast height were multiplied with 1.4 as previously assessed with spruce trees at the same site (Kuptz et al., 2011). The mean rates of stem CO_2 efflux of three measured control trees were used for the fourth control tree, which was not assessed in this study.

2.7.4.4 Calculation of coarse-root growth

Coarse-roots were counted, and the length of one coarse root per tree was estimated on site after excavating. Using root wood density of 0.416 g cm^{-3} (Pretzsch et al., 2018), mean diameter, length, and ring width from 2019 based on coring, the total coarse-root growth in 2019 was determined, which was then, multiplied by the proportional growth during the 28 days after watering, according to automatic dendrometers installed at one coarse-root (diameter of 9.4 ± 1.1 cm) on each tree (Ecomatik) as described above for stem and branch growth.

2.7.4.5 Calculation of fine-root growth and ectomycorrhizae (ECM)

To avoid massive soil disturbance in the long-term plots, not more than one coarse-root per tree was excavated and thus it was not able to assign the samples of ECM, non-mycorrhizal root tips, and root exudates unequivocally to a specific tree. For this reason, the total C sink activity of fine-root growth, ECM, and root exudates was first extrapolated to the area occupied by spruce trees (Fig. 5a). The total C sink activity belowground underneath the spruce trees was

then assigned to individual trees according to the area occupied by each tree using a positive exponential relationship between DBH and root biomass (Häberle et al., 2012).

The initial fine-root biomass per soil volume (mg cm^{-3}) was determined with fine-roots taken from ten soil cores (diameter of 1.4 cm) within the first 10 cm of the uppermost soil layers on day -7. To calculate the fine-root biomass at 10 - 30 cm depth and thus the total initial fine-root biomass from 0 – 30 cm soil depth (M_{FR30}), a root biomass ratio between upper (0 – 10 cm) and lower (10 – 30 cm) soil layer was used, measured in summer 2018 on the same plots. The total fine-root gain per spruce area was calculated, assuming a constant fine-root diameter:

$$\text{Fine root biomass gain per initial biomass} = \frac{\text{root length growth}}{\text{initial root length in mesh bag}} \quad (\text{Eqn. 16}),$$

where the initial root length on day -7 and root length growth was determined by image analysis of respective pre- and post-harvest mesh bag root pictures via ImageJ (version 1.53a, National Institute of Health, USA). The biomass gain per soil volume (mg cm^{-3}) was then calculated (Eqn. 17) and extrapolated to the soil volume of the plot at 0 – 30 cm depth.

$$\text{fine root biomass gain} = \text{fine root biomass gain per initial biomass} \times \text{dry mass per soil volume} \quad (\text{Eqn. 17})$$

Within mesh bag roots, we found that 96% of the sampled fine-roots in control and 57% in recovering trees were colonized by ectomycorrhizal fungi. Assuming no significant change in ECM biomass on root tips during our study period of 28 days, since full formation of ECM takes longer (Ineichen & Wiemken, 1992), the biomass of mycorrhized fine-roots (M_{FR_ECM}) at 0-30 cm depth was calculated based on the initial fine-root biomass at 0-30 cm (M_{FR30} , Table 2):

$$M_{FR_ECM} = \frac{M_{FR30}}{100} \times 96 \text{ (or 57)} \quad (\text{Eqn. 18})$$

As ECM make up 28% of one spruce fine-root's biomass as determined under the same terms as in our study (root diameter < 2mm, most fine-roots found within 0-10 cm depth, Helmisaari et al., 2007, 2009), ECM biomass (M_{ECM}) was calculated:

$$M_{ECM} = \frac{M_{FR_ECM}}{100} \times 28 \quad (\text{Eqn. 19})$$

2.7.4.6 Calculation of root exudates

The total amount of root exudates was calculated for the soil at 0-30 cm depth using the organic C concentration in root exudates and the total fine-root biomass determined by soil cores.

2.7.4.7 Calculation of soil CO₂ efflux

Soil CO₂ efflux rates were multiplied by the area belowground occupied by each tree (as determined for C sink activity of fine root). The mean rates of soil CO₂ efflux close to the three measured control trees were used for the fourth control tree, which was not assessed. For the contribution of autotrophic respiration (root-derived including rhizosphere) to total soil respiration (autotrophic + heterotrophic), we used 51% in control and 38% in recovery trees based on previous measurements under drought with the spruce trees at the same experimental site (Nikolova et al., 2009). We assumed that the contribution of autotrophic respiration did not significantly change after drought release, as soil CO₂ efflux rates remained unaffected by the drought release.

2.7.5 Calculation of fraction of labeled C (f_{Label}) and contribution of C_{new} to each C sink ($contC_{new}$)

f_{Label} was calculated at each measurement point using the following equation (Kuptz et al., 2011):

$$f_{Label} = \frac{\delta^{13}C_{old} - \delta^{13}C_{sample}}{\delta^{13}C_{old} - \delta^{13}C_{new}} \text{ (Eqn. 20),}$$

where $\delta^{13}C_{old}$ gives the mean $\delta^{13}C$ before the start of labeling, $\delta^{13}C_{sample}$ is the $\delta^{13}C$ of each measurement, and $\delta^{13}C_{new}$ represents $\delta^{13}C$ at the new isotopic equilibrium. Rarely occurring negative f_{Label} values were set to zero. f_{Label} of stem CO₂ efflux was used for branch CO₂ efflux, which was not assessed in this study.

$\delta^{13}C_{new}$ was calculated as described by Kuptz et al. (2011):

$$\delta^{13}C_{A-O} (\text{‰}) = \left(\frac{1000 + \delta^{13}C_{Air-Unlabeled}}{1000 + \delta^{13}C_{old}} - 1 \right) \times 1000 \text{ (Eqn. 21),}$$

which gives the mean apparent ¹³C discrimination ($\delta^{13}C_{A-O}$) between unlabeled crown air (reference air above canopy, $\delta^{13}C_{Air-Unlabeled}$) and $\delta^{13}C_{old}$.

$$\delta^{13}C_{new} (\text{‰}) = 1000 \times \frac{1000 + \delta^{13}C_{Air-Labeled}}{1000 + \delta^{13}C_{A-O}} - 1000 \text{ (Eqn. 22),}$$

where $\delta^{13}\text{C}_{\text{Air-Labeled}}$ is the mean $\delta^{13}\text{C}$ of crown air of each tree (aboveground sinks and coarse-roots) or each treatment (all other belowground sinks) during labeling.

$\text{contC}_{\text{new}}$, representing f_{Label} at the new isotopic equilibrium, was determined by fitting the course of f_{Label} with the following sigmoid curve.

$$f_{\text{Label}} = \frac{\text{contC}_{\text{new}}}{1 + e^{-\frac{t-t_0}{b}}} \quad (\text{Eqn. 23}),$$

where t is the time of measurement, t_0 the inflection point of the curve, and b the slope coefficient of the regression. $\text{contC}_{\text{new}}$ would be 1 if C sink was supplied solely with C_{new} and zero if supplied exclusively by stored C. Since f_{Label} decreased again after the end of labeling, only f_{Label} before reaching the maximum were used for the fitting. $\text{contC}_{\text{new}}$ to soil CO_2 efflux was divided by the contribution of autotrophic part to calculate the $\text{contC}_{\text{new}}$ to autotrophic soil CO_2 efflux.

2.7.5.1 Methods used for branch, stem, and coarse-root growth

For branch, stem, and coarse-root growth, $\delta^{13}\text{C}_{\text{old}}$ and $\delta^{13}\text{C}_{\text{sample}}$ (for Eqn. 20) were determined by fitting the $\delta^{13}\text{C}$ of tree ring slices with a piecewise function as used for the calculation of CTR (see Figure S5 and S6 in Chapter IV). The $\delta^{13}\text{C}$ value, when $\delta^{13}\text{C}$ started to decrease (marked by the green horizontal dashed lines in Figure S5a,b in Chapter IV) was defined as $\delta^{13}\text{C}_{\text{old}}$. The minimum $\delta^{13}\text{C}$ value (purple horizontal dashed lines) was then defined as $\delta^{13}\text{C}_{\text{sample}}$. In addition to the labeled trees, we also determined the natural shifts of $\delta^{13}\text{C}$ of non-labeled control trees for each treatment ($n = 3$) to correct $\delta^{13}\text{C}_{\text{sample}}$ for the effect of watering, weather fluctuation, and seasonal changes (Helle & Schleser, 2004). Finally, using $\delta^{13}\text{C}_{\text{old}}$, corrected $\delta^{13}\text{C}_{\text{sample}}$, and Eqn. 20, f_{Label} was calculated.

For the course of f_{Label} , C transport rates determined above were used to define the day on which the first ^{13}C -depleted tracer arrived at each tree height (i.e. when f_{Label} started to increase, Figure S6 in Chapter IV). A linear increase of f_{Label} was assumed until the new isotopic equilibrium was reached, that is $\text{contC}_{\text{new}}$. $\text{contC}_{\text{new}}$ calculated with the samples from the middle of the crown was used for branch and upper stem growth. For the lower stem growth, we used the mean $\text{contC}_{\text{new}}$ calculated for the crown base and breast height.

2.7.6 Calculation of allocation of newly assimilated C (C_{new}) to each C sink

Total amount of C_{new} allocated to each C sink during 28 days after drought release was calculated as a cumulative sum of C_{new} after multiplying C sink activity and their respective

f_{Label} . As soon as f_{Label} started to decrease due to the end of labeling, sigmoid curves (Eqn. 23) or in case of branch, stem, and coarse-root growth a constant f_{Label} were used. For soil CO₂ efflux, total C sink activity (autotrophic + heterotrophic efflux) was multiplied with respective f_{Label} , since C isotopic signatures and f_{Label} comprise the mixed signal of both autotrophic and heterotrophic efflux. Using the amount of C_{new} (in g C), proportional allocation of C_{new} (in %) to each sink was calculated for each tree.

2.7.7 Calculation of the amount of osmolytes remobilized from leaves and fine-roots upon drought release

For leaves, the leaf mass was first calculated using projected leaf area (PLA) and the specific leaf area (SLA in m² kg⁻¹) of the recovering spruce at the experimental site (see Table 1, Hesse, 2021). Then, leaf water mass per tree (LWM in L) was calculated by:

$$LWM = \frac{PLA}{SLA} * LWC \quad (\text{Eqn. 24}),$$

where LWC is the leaf water content in % (ratio of water to dry leaf mass).

For fine-roots, the total water mass in fine-roots (RWM) of the three recovering trees was calculated with total initial dry fine-root biomass (DRM) and root water content (RWC in %, ratio of water to dry fine-root mass, Table 1) determined with soil cores.

$$RWM = DRM * RWC \quad (\text{Eqn. 25}),$$

According to the van't Hoff formula, we calculated the concentration change of the water solution in leaves and fine-roots of recovering trees after watering by:

$$c_W = \frac{\Delta\pi_0}{R*T} * 1000 \quad (\text{Eqn. 26}),$$

where c_W is the concentration of the water solution (mol L⁻¹), $\Delta\pi_0$ is the difference in the leaf osmotic potential between day -6 and day 22 (MPa) (Hesse et al., submitted), R describes the ideal gas constant (8.134 J K⁻¹ mol⁻¹), and T temperature in K (here 293.15 K). Here, since osmotic potential of fine-roots was not assessed, the difference between day -6 and day 22 was assumed to be same as that of leaves (Dichio et al., 2006). The calculated c_W was then multiplied with the LWM or RWM to determine the molar osmolytes equivalent (OE in mol), which were remobilized after the watering until day 22. For this study, we chose the three most important osmolytes: sucrose, pinitol, and prolin (Peuke et al., 2002; Schiop et al., 2017). By multiplying

with each molar mass, we calculated the total amount of remobilized osmolytes ($RO_{\text{sucrose/pinitol/prolin}}$ in g C, separately for each osmolyte).

*Table 1: Parameters used to calculate the amount of osmolytes remobilized from leaves ($n = 6$) and fine-roots of the recovering trees in the labeling plot 4 upon drought release. PLA; total projected leaf area per tree, DRM; total initial dry root biomass of the three recovering trees, SLA; specific leaf area, leaf water content (LWC, ratio of water to dry leaf mass), root water content (RWC, ratio of water to dry fine-root mass), leaf water mass per tree (LWM), root water mass in the three recovering trees (RWM), π_0 ; osmotic potential, $\Delta\pi_0$; difference in the osmotic potential between day -6 and day 22, c_w : calculated water solution concentration, molar osmolytes equivalent (OE), RO; total amount of remobilized osmolytes calculated for the three osmolytes: sucrose, pinitol, and prolin. Leaf values are calculated by Hesse (2021). All errors represent SE. * taken from Hesse et al. (submitted).*

Parameter	Leaf (per recovering tree)	Fine-roots (total of three recovering trees in plot 4)
PLA (m ²) / DRM (g)	67 ± 13 (m ²)	14170 (g)
SLA (m ² kg ⁻¹)	4.3 ± 0.2	-
Leaf/root water content (%)	107.5 ± 8.3	431
Leaf/root water mass (L)	16.8 ± 3.4	61
π_0 on day -6 (MPa)*	-2.44 ± 0.05	-
π_0 on day 22 (MPa)*	-2.00 ± 0.04	-
$\Delta\pi_0$ (MPa)	0.44 ± 0.19	Assumed to be same
c_w (mol L ⁻¹)	0.185 ± 0.032	Assumed to be same
Molar osmolytes equivalent (mol)	3.47 ± 1.02	11.29
RO_{Sucrose} (g C)	499 ± 147	1625
RO_{Pinitol} (g C)	291 ± 86	948
RO_{Prolin} (g C)	208 ± 61	677

3. Abstracts and contributions to the single chapters

3.1 Chapter I: Physiological and morphological acclimation of mature trees to five years of experimental summer drought at the leaf and crown level

Hesse, B. D.*, Hikino, K.*, Gebhardt, T.*, Motte, F., Rötzer, T., Weigl, F., Pritsch K., Hafner, B. D., Pretzsch, H., Häberle, K-H. & Grams, T. E. E. Physiological and morphological acclimation of mature trees to five years of experimental summer drought at the leaf and crown level. (draft)

As a consequence of the ongoing climate change, global forests have been suffering from severe natural drought, causing immense growth decline and tree mortality. Since frequency and duration of drought events are predicted to increase, ability to acclimate to a long-term and repeated drought is crucial for tree survival. To elucidate long-term physiological and morphological responses of mature Norway spruce (*Picea abies* [L.] KARST.) and European beech (*Fagus sylvatica* L.) to repeated drought, we conducted detailed analyses of leaf and whole-tree level physiology and morphology during five years of experimental summer drought. We thereby measured predawn leaf water potential, leaf gas exchange, sap flow density, whole-tree water consumption, and morphological parameters such as shoot growth and total leaf area. In accordance with the iso- and anisohydric framework, more isohydric spruce reduced their water consumption more strongly than more anisohydric beech, through more drought-sensitive stomatal control as a first drought response. As a long-term response starting from the third drought year, only spruce trees reduced their total leaf area by more than 50% through production of shorter shoots and needles. This response led to a significant decrease in leaf to sapwood area ratio in spruce after the third drought year, which ensures higher water transport capacity per leaf area. Indeed, drought effect on leaf gas exchange and sap flow density became smaller after the reduction of the total leaf area. Thus, under repeated drought, reduction in the total leaf area regulated the leaf and whole-tree physiology in spruce, in addition to the strong stomatal control. However, the reduction of spruce leaf area cannot be quickly reversed, limiting water consumption and carbon uptake even after drought release. Therefore, further studies are needed to elucidate the long-term consequences of the morphological drought acclimation on tree performance under future climate change.

Contributions: I finalized the experimental design, collected and processed the samples, analyzed and interpreted the data, and wrote the manuscript. Benjamin D. Hesse and Timo Gebhardt finalized the design, collected and processed the samples, analyzed and interpreted the data, and wrote the manuscript together with me. Thorsten E. E. Grams and Karl-Heinz Häberle originally designed the study and helped interpreting the data. Florian Motte, Thomas Rötzer, Fabian Weikl, Karin Pritsch, Benjamin D. Hafner, and Hans Pretzsch collected and processed samples, supported me to analyze and interpret data. About 50% of the work was done by myself.

3.2 Chapter II: Repeated summer drought changes the radial xylem sapflow profile in mature *Picea abies* (L.) Karst.

Gebhardt, T.*, Hesse, B. D.*, **Hikino, K.**, Kolovrat, K., Hafner, B. D., Grams, T. E. E., & Häberle, K-H. Repeated summer drought changes the radial xylem sapflow profile in mature *Picea abies* (L.) Karst. (submitted to Agricultural and Forest Meteorology)

Water consumption of trees is one of the most important processes connected to their survival under ongoing climate change and extreme events such as drought. Radial profiles of xylem sap flow density are an integral component to quantify the water transport for the level of an individual tree and that of ecosystems. However, knowledge of such radial profiles, in particular under stress, is very scarce. Here we show the radial profile of the xylem sap flow density in mature European beech (*Fagus sylvatica* L) and Norway spruce (*Picea abies* (L) Karst.) under repeated summer drought induced by throughfall exclusion (TE) and subsequent recovery compared to untreated control trees (CO). We measured xylem sap flow density (u_{daily} in $\text{L dm}^{-2} \text{ d}^{-1}$) down to 8 cm sapwood depth at breast height using two different approaches, a thermal dissipation system and the heat field deformation method. In beech, repeated throughfall exclusion did not affect the radial xylem sap flow profile. However, in spruce, u_{daily} was strongly reduced across the profile under repeated drought, changing the profile from a linear to a logarithmic regression. Even two years after drought release, the xylem sap flow profile did not fully recover in TE spruce. The reduction of u_{daily} along the radial profile was accompanied by a reduction of the leaf area in TE spruce by c. 50%, while sapwood depth remained constant. The reduction of the xylem sap flow density along the profile reduced the calculated water consumption of TE spruce trees by more than 33% compared to CO trees, also after drought release. The impact of stressors such as repeated drought on the xylem sap flow density across

the radial profile and its consequences for trees' and stands' water consumption needs to be addressed in more detail to minimize uncertainties in quantifying ecosystem water cycles.

Contributions: I collected, analyzed, and interpreted the data of the total leaf area of spruce trees. Benjamin D. Hesse and Timo Gebhardt finalized the experimental design, collected and processed the samples, analyzed and interpreted the data, and wrote the manuscript. Thorsten E. E. Grams and Karl-Heinz Häberle originally designed the study and helped interpreting the data. Katarina Kolovrat and Benjamin D. Hafner collected and analyzed the data. All authors thoroughly read and revised the manuscript. About 30% of the work was done by myself.

3.3 Chapter III: High resilience of carbon transport in long-term drought-stressed mature Norway spruce trees within 2 weeks after drought release

Hikino, K., Danzberger, J., Riedel, V. P., Rehschuh, R., Ruehr, N. K., Hesse, B. D., Lehmann, M. M., Buegger, F., Weigl, F., Pritsch, K., & Grams, T. E. E. (2022). High resilience of carbon transport in long-term drought-stressed mature Norway spruce trees within 2 weeks after drought release. *Global Change Biology*, 28, 2095– 2110.

Under ongoing global climate change, drought periods are predicted to increase in frequency and intensity in the future. Under these circumstances, it is crucial for tree's survival to recover their restricted functionalities quickly after drought release. To elucidate the recovery of carbon (C) transport rates in c. 70-year-old Norway spruce (*Picea abies* [L.] KARST.) after five years of recurrent summer droughts, we conducted a continuous whole-tree ¹³C labeling experiment in parallel with watering. We determined the arrival time of current photoassimilates in major C sinks by tracing the ¹³C label in stem and soil CO₂ efflux, and tips of living fine roots. In the first week after watering, aboveground C transport rates (CTR) from crown to trunk base were still 50% lower in previously drought-stressed trees ($0.16 \pm 0.01 \text{ m h}^{-1}$) compared to controls ($0.30 \pm 0.06 \text{ m h}^{-1}$). Conversely, CTR below ground, that is, from the trunk base to soil CO₂ efflux were already similar between treatments (c. 0.03 m h^{-1}). Two weeks after watering, aboveground C transport of previously drought-stressed trees recovered to the level of the controls. Furthermore, regrowth of water-absorbing fine roots upon watering was supported by faster incorporation of ¹³C label in previously drought-stressed (within $12 \pm 10 \text{ h}$ upon arrival at trunk base) compared to control trees ($73 \pm 10 \text{ h}$). Thus, the whole-tree C transport system from the crown to soil CO₂ efflux fully recovered within 2 weeks after drought release, and hence showed high resilience to recurrent summer droughts in mature Norway spruce forests.

This high resilience of the C transport system is an important prerequisite for the recovery of other tree functionalities and productivity.

Contributions: I finalized the experimental design, collected and processed the samples, analyzed and interpreted the data, and wrote the manuscript. Thorsten E. E. Grams and Karin Pritsch originally designed the study and helped me interpret the data. Jasmin Danzberger, Vincent P. Riedel, Romy Rehschuh, Nadine K. Ruehr, Benjamin D. Hesse, Marco M. Lehmann, Franz Buegger, and Fabian Weikl collected and processed samples, supported me to analyze and interpret data. All authors thoroughly read and revised the manuscript. About 85% of the work was done by myself.

3.4 Chapter IV: Dynamics of initial carbon allocation after drought release in mature Norway spruce - Increased belowground allocation of current photoassimilates covers only half of the carbon used for fine-root growth

Hikino, K.*, Danzberger, J.*, Riedel, V. P., Hesse, B. D., Hafner, B. D., Gebhardt, T., Rehschuh, R., Ruehr, N. K., Brunn, M., Bauerle, T. L., Landhäusser, S. M., Lehmann, M. M., Rötzer, T., Pretzsch, H., Buegger, F., Weikl, F., Pritsch, K., & Grams, T. E. E. (2022). Dynamics of initial carbon allocation after drought release in mature Norway spruce—Increased belowground allocation of current photoassimilates covers only half of the carbon used for fine-root growth. *Global Change Biology*, 00, 1– 17.

After drought events, tree recovery depends on sufficient carbon (C) allocation to the sink organs. The present study aimed to elucidate dynamics of tree-level C sink activity and allocation of recent photoassimilates (C_{new}) and stored C in c. 70-year-old Norway spruce (*Picea abies*) trees during a four week period after drought release. We conducted a continuous, whole-tree ^{13}C labeling in parallel with controlled watering after five years of experimental summer drought. The fate of C_{new} to growth and CO_2 efflux was tracked along branches, stems, coarse- and fine-roots, ectomycorrhizae (ECM) and root exudates to soil CO_2 efflux after drought release. Compared to control trees, drought recovering trees showed an overall 6% lower C sink activity and 19% less allocation of C_{new} to aboveground sinks, indicating a low priority for aboveground sinks during recovery. In contrast, fine-root growth in recovering trees was 7 times greater than that of controls. However, only half of the C used for new fine-root growth was comprised of C_{new} while the other half was supplied by stored C. For drought recovery of mature spruce trees, in addition to C_{new} , stored C appears to be critical for the regeneration of the fine-root system and the associated water uptake capacity.

Contributions: I finalized the experimental design, collected and processed the samples, analyzed and interpreted the data, and wrote the manuscript. Jasmin Danzberger finalized the experimental design, collected and processed the samples, analyzed and interpreted the data, and wrote the manuscript together with me. Thorsten E. E. Grams and Karin Pritsch originally designed the study and helped interpreting the data. Vincent P. Riedel, Benjamin D. Hesse, Benjamin D. Hafner, Timo Gebhardt, Romy Rehschuh, Nadine K. Ruehr, Melanie Brunn, Taryn L. Bauerle, Simon M. Landhäuser, Marco M. Lehmann, Thomas Rötzer, Hans Pretzsch, Franz Buegger, and Fabian Weikl collected and processed the samples and helped analyzing the data. All authors thoroughly read and revised the manuscript. About 50% of the work was done by myself.

4. General discussion

This part aims to integrate the four chapters and discuss tree responses to the repeated drought together with responses during the subsequent recovery.

4.1. More isohydric spruce was more affected by repeated drought than more anisohydric beech

In accordance with the iso- and anisohydric framework, mostly determined by saplings (Hartmann et al., 2021; Kannenberg et al., 2019; Tardieu & Simonneau, 1998), mature beech and spruce responded differently at the leaf level to the repeated drought. During the drought phase, stomata of more isohydric spruce closed to a larger extent and earlier than those of more anisohydric beech (Chapter I). The stomatal opening of spruce was regulated at least partially through ABA accumulation, which was not observed in beech (Hesse et al., submitted). The strong stomatal closure prevents leaves, branches, and stems from water loss and hydraulic failure (Lovisolo et al., 2008; Mitchell et al., 2016; Wilkinson & Davies, 2002), which is crucial, especially for spruce trees maintaining their needles for several years.

As a consequence of the reduced A_{sat} , g_s , and sap flow density at the outer 2 cm (Chapter I), annual water use of spruce trees was more strongly reduced (by 65-75%) under repeated drought than that of beech trees (by 10-35%, Chapter I), indicating that the whole-tree water use was first regulated by leaf-level stomatal closure. Aside from the stomatal regulation, total leaf area determines whole-plant hydraulic conductance and water use (Mencuccini, 2003), and thus its modification can potentially alleviate drought impacts (Farquhar et al., 2002; Jump et al., 2017; Levanic et al., 2011). During the present long-term drought treatment, TE spruce trees significantly reduced their total leaf area (by >50%, Chapter I), accompanied by a reduction along the radial sap flow profile (Chapter II) and stronger depletion of stem water storage (Knüver et al., 2022), whereas TE beech did not significantly modify their total leaf area (Chapter I) nor their sap flow profile (Chapter II) along with less depleted stem water storage (Knüver et al., 2022). These different responses can also be related to their iso- and anisohydric strategies. The drought treatment caused fine root mortality and reduction of root growth, thus the water-absorbing root system was impaired in both species (Nickel et al., 2018; Nikolova et al., 2020; Zwetsloot & Bauerle, 2021). To compensate for the root loss, TE beech increased the production of thin fine roots with high specific fine-root area and high respiration rates in deeper, moister soil layers (i.e. a fast ecological strategy, Nikolova et al., 2020; Zwetsloot & Bauerle, 2021). Likely because this response contributes to maintaining the water uptake but

also causes belowground C cost, the total C uptake of TE beech were not strongly downregulated under drought (according to sink-control theory: Fatichi et al., 2014; Gavito et al., 2019; Hagedorn et al., 2016; Körner, 2015): i.e. through maintaining stomatal conductance and total leaf area, which is in accordance with more anisohydric strategy of beech. Maintained water uptake also likely explains only slight depletion of stem water storage in beech (Knüver et al., 2022), confirming a low reliance of more anisohydric beech on stem water storage (Hartmann et al., 2021; Jiang et al., 2021). In contrast, TE spruce trees increased suberization and longevity of fine roots, decreasing water uptake but also belowground C cost for growth and respiration (slower ecological strategy, Nikolova et al., 2020, Chapter III, IV). Furthermore, while the decline of stem and fine root growth in spruce trees already started in the first drought year (Pretzsch et al., 2020; Zwetsloot & Bauerle, 2021), the reduction of the total leaf area was observed only after the third drought year through production of shorter shoots and needles (Chapter I). Thus, reduced sink activity possibly downregulated C uptake through strong stomatal closure in the first two drought years, and additionally by reduced leaf area after the third drought years, reflecting more isohydric strategy of spruce. Earlier downregulation of C sink activity than the leaf area may also explain the lack of C starvation in TE spruce (Hesse et al., 2021). This response may have balanced reduced water uptake and transpiration loss (Bréda et al., 2006; Pritzkow et al., 2021; Schönbeck et al., 2018; Trugman et al., 2018), and maintained the leaf-specific hydraulic conductivity (Limousin et al., 2010, 2012; Munné-Bosch & Alegre, 2004). Whole-tree water balance was further supported by a stronger use of stem water storage compared to beech (Knüver et al., 2022), confirming a high reliance of more isohydric spruce on stem water storage (Hartmann et al., 2021; Jiang et al., 2021). Therefore, not only at the leaf level, but at the whole-tree level, more isohydric spruce seem to have downregulated C sink activity, C uptake, and related water use more strongly than more anisohydric beech, which is in line with the iso- and anisohydric framework. However, decrease in the leaf osmotic potential during the drought was similar in both species (Hesse et al., submitted; Tomasella et al., 2018). Thus, the C sinks for the osmotic regulation were similarly upregulated in both species and the relative C allocation to these sinks increased more strongly in spruce than in beech, at the expense of other C sinks such as stem and root growth.

4.2. Acclimation belowground during the repeated drought

Aside from the leaf and whole-tree level responses discussed above, both tree species showed an acclimation during long-term drought likely caused by belowground responses. Despite the similar soil water conditions at 0-70 cm depth throughout the drought period in terms of both

current plant available water (PAW, Fig. 8a,b) and time-integrated soil water deficit (iSWD, Fig. 8c,d), Ψ_{PD} increased in the last three drought years in both species as a long-term response. At given PAW and iSWD, Ψ_{PD} of both species was higher in the last three drought years (2016-2018) than in the first two drought years (2014-2015). This acclimation may be possible through a change in a) Root morphology, b) Root physiology, and/or c) Mycorrhizae/bacteria community. In the first case (a), root morphology includes e.g. increased fine root production in deeper, moister layers as observed only in beech (Brunn et al., 2022; Zwetsloot & Bauerle, 2021), or a change in root-soil contact (Duddek et al., 2022). In the first drought years, shrinkage or suberization of roots might have increased the hydraulic resistance of the root-soil interface in both species (Brunner et al., 2015). Furthermore, longer fine roots with a smaller diameter can uptake soil resources more efficiently with a low carbon cost compared to thick roots (Bergmann et al., 2020; Encinas-Valero et al., 2022; Hodge, 2004; Ma et al., 2018). Beech has shown a high plasticity in fine root morphology and anatomy of both saplings (Knutzen et al., 2015) and mature trees (Förster et al., 2021; Kirfel et al., 2017). Under seasonal drought, the present beech trees also increased specific root area and decreased the diameter of fine roots (Nikolova et al., 2020). As Kirfel et al., (2017) speculates, fine roots with a high conductivity were possibly increasingly produced in wetter soil layers, as found earlier in the depth of fine root growth (Brunn et al., 2022; Zwetsloot & Bauerle, 2021). In contrast, fine root distribution, water uptake depth, and root morphology of spruce fine roots seem to be less plastic under drought, thus less likely than those of beech (Brinkmann et al., 2019; Meusburger et al., 2022; Nikolova et al., 2020; Zwetsloot & Bauerle, 2021). b) Another possibility is root physiology. Rates of root exudation and proportional C allocation to root exudates both increased in the present TE trees of both species, with a larger increase in spruce compared to beech (Brunn et al., 2022). Exuded mucilage can improve the rhizosphere environment (e.g. root-soil contact: Ahmed et al., 2014; Jakoby et al., 2020) and facilitates root water uptake (Carminati et al., 2016). Other possible physiological mechanisms are osmotic adjustments (Hart et al., 2021; Hodge, 2004) and upregulating of aquaporin activity to increase leaf/root hydraulic conductivity (Domec et al., 2021; Johnson et al., 2014; J. Liu et al., 2014; McLean et al., 2011; Rodríguez-Gamir et al., 2019). Under a seasonal drought, both species at the experimental site showed an accumulation of non-structural carbohydrates specifically in the transport fine roots (Nikolova et al., 2020), indicating an osmotic acclimation belowground (Leuschner, 2020). Especially, more anisohydric beech might have a higher potential of osmotic adjustment than more isohydric spruce (Hartmann et al., 2021). Finally, c), Mycorrhizae/bacteria community might have played an important role. Mycorrhiza has been proven to mitigate drought impact

on host trees e.g. directly through the increased absorbing surface area, improvement of soil filtration and water storage, or synthesis of osmolytes (Brunner et al., 2015; Lehto & Zwiazek, 2011; Mohan et al., 2014; Usman et al., 2021). Nickel et al., (2018) found that in the first drought years, the ectomycorrhizae (ECM) supporting long-distance water transport increased in both species in TE plots, whereas ECM with short and medium rhizomorphs decreased. This qualitative change possibly mediated the drought effect in a long run. Alternatively, adaptation in the soil microbial community has also been reported under drought (Canarini et al., 2021; Fitzpatrick et al., 2018; Lau & Lennon, 2012). Soil microbiome and bacteria can potentially support host plants via plant hormones and biochemical processes against water stress (Yandigeri et al., 2012), or even support ECM establishment (Reis et al., 2021). Although further studies are necessary to reveal the mechanisms behind this acclimation, both tree species seem to have adjusted the belowground water-absorbing system during the long-term drought.

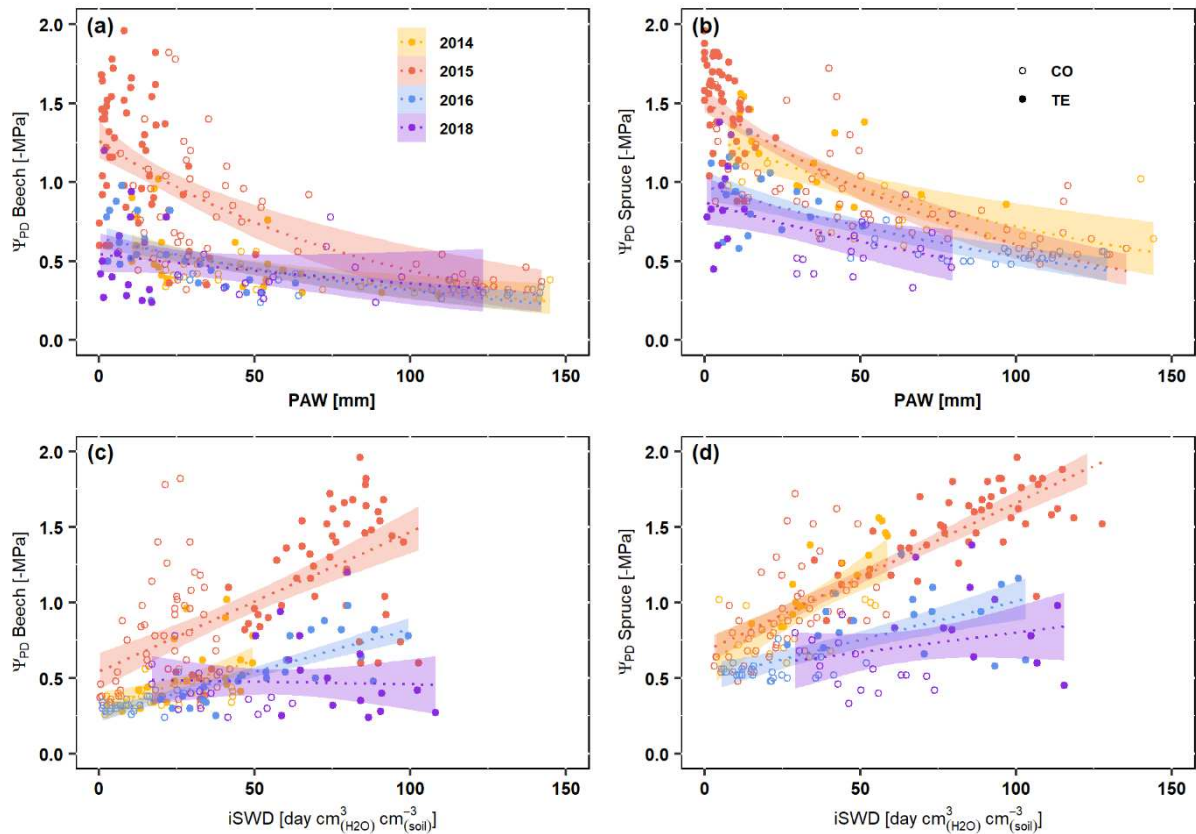


Fig. 8: Relationship between Ψ_{PD} (predawn leaf water potential) of both species (CO: control and TE: throughfall exclusion) and PAW (plant available water, a,b) or iSWD (time-integrated soil water deficit, c,d) at 0-70 cm soil depth. Both treatments (CO and TE) are fitted together for each year, with a linear regression (after log transformation of Ψ_{PD} in case of a and b). The dotted lines and the shaded area display the prediction of the regression and its 95% confidence interval.

4.3. Correlation between drought severity and physiological recovery

Following the less drought effect on the leaf and whole-tree physiology and morphology in more anisohydric beech compared to more isohydric spruce (Chapter I), beech trees opened their stomata faster than spruce after drought release, likely due to ABA accumulation during the drought observed only in spruce leaves (Hesse et al., submitted). As Ruehr et al. (2019) suggested, however, it deserves further attention if resilience, i.e. ability to recover to the level of control after stress release, is correlated with the drought severity among TE trees. According to their framework, trees that had experienced more severe drought would show lower resilience compared to trees with less severe drought. This trend was observed in spruce (Fig. 9) but not in beech trees (Fig. 10). TE spruce trees with higher iSWD (time-integrated soil water deficit) during the five drought growing seasons tended to show lower resilience in leaf physiology during the first week after the drought release (although often not significant, Fig. 9), whereas TE beech trees did not show any clear correlation pattern (Fig. 10). This species difference can also be explained by their iso- and anisohydric strategies. Spruce trees experiencing more severe drought showed higher leaf ABA concentration before watering (Fig. 9d), which then likely delayed the recovery of the leaf photosynthesis. In contrast, stomatal opening of beech was not mainly controlled by ABA, leading to no clear correlation pattern between the resilience of the leaf photosynthesis and the drought severity. It should be noted, however, that Ψ_{PD} of TE trees during the drought phase was as low as -1.8 MPa (Grams et al., 2021), which is far above the Ψ_{50} (water potential inducing 50% of loss of xylem conductivity) of spruce and Ψ_{88} of beech at the experimental site (both around -4MPa, Knüver et al., 2022; Tomasella et al., 2018). Therefore, no severe xylem cavitation occurred during the drought. Since embolism delays the recovery of g_s and A_{sat} , especially in anisohydric species (Kannenbergh et al., 2019; Peguero-Pina et al., 2018; Rehschuh et al., 2020; Skelton et al., 2017), drought severity may affect resilience also in beech trees during recovery from more severe drought, directly affecting the recovery of water use and C uptake at the whole-tree level.

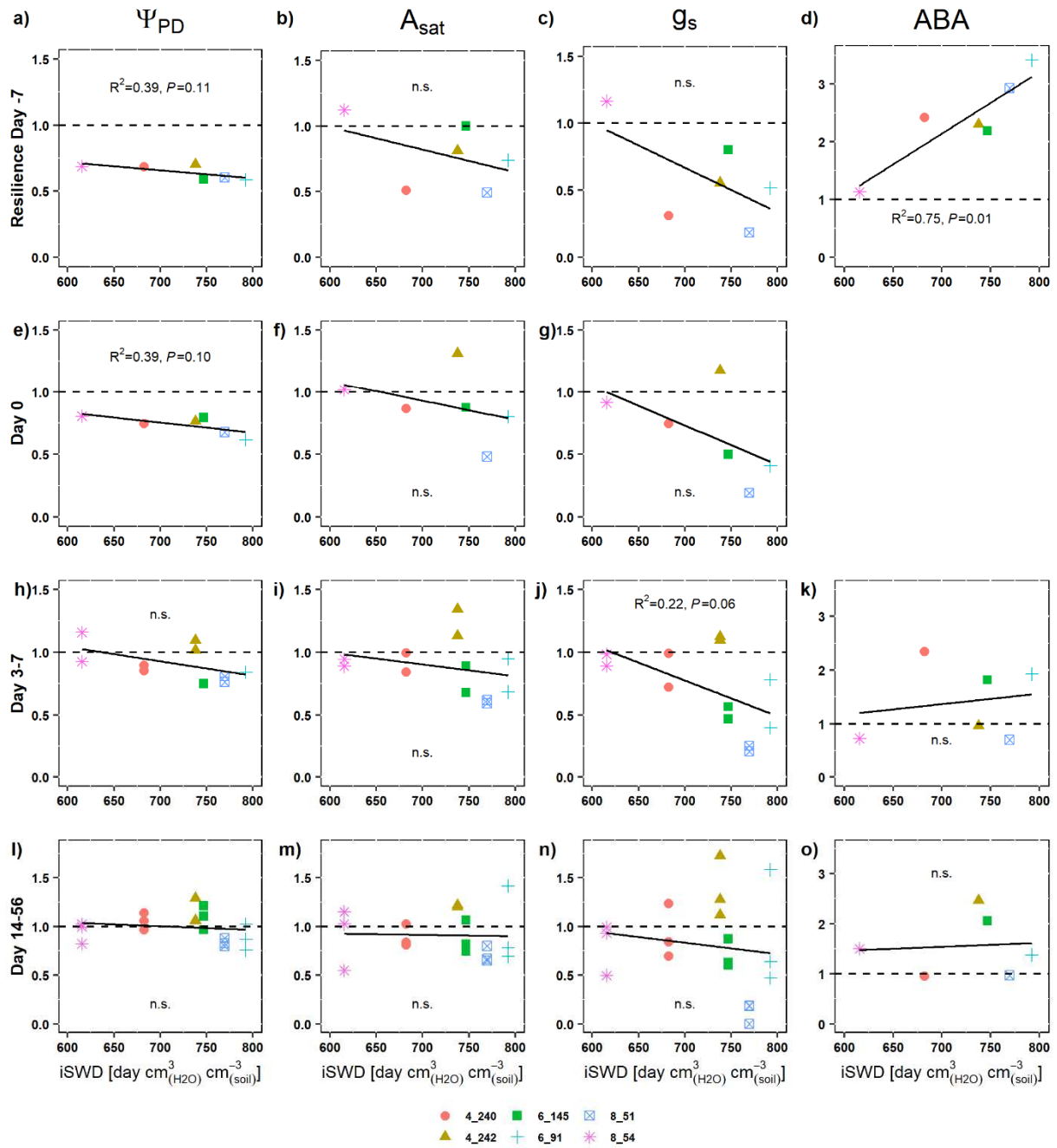


Fig. 9: Relationships in spruce trees between Resilience of leaf physiological parameters (Ψ_{PD} ; predawn leaf water potential, A_{sat} ; light-saturated CO_2 assimilation rates, g_s ; leaf stomatal conductance, ABA; concentration of abscisic acid in leaves) and iSWD (time-integrated soil water deficit during the five years of the drought phase) at 0-70 cm soil depth, before (day -7) and after drought release (day 0-56). Resilience is calculated as TE values divided by mean CO values: Resilience of 1 means the same value as the average of CO trees. Each color and symbol represents individual TE (throughfall-exclusion) trees. R^2 , p-values, n.s. (no significance), and solid lines indicate the results of linear regression applied for each data.

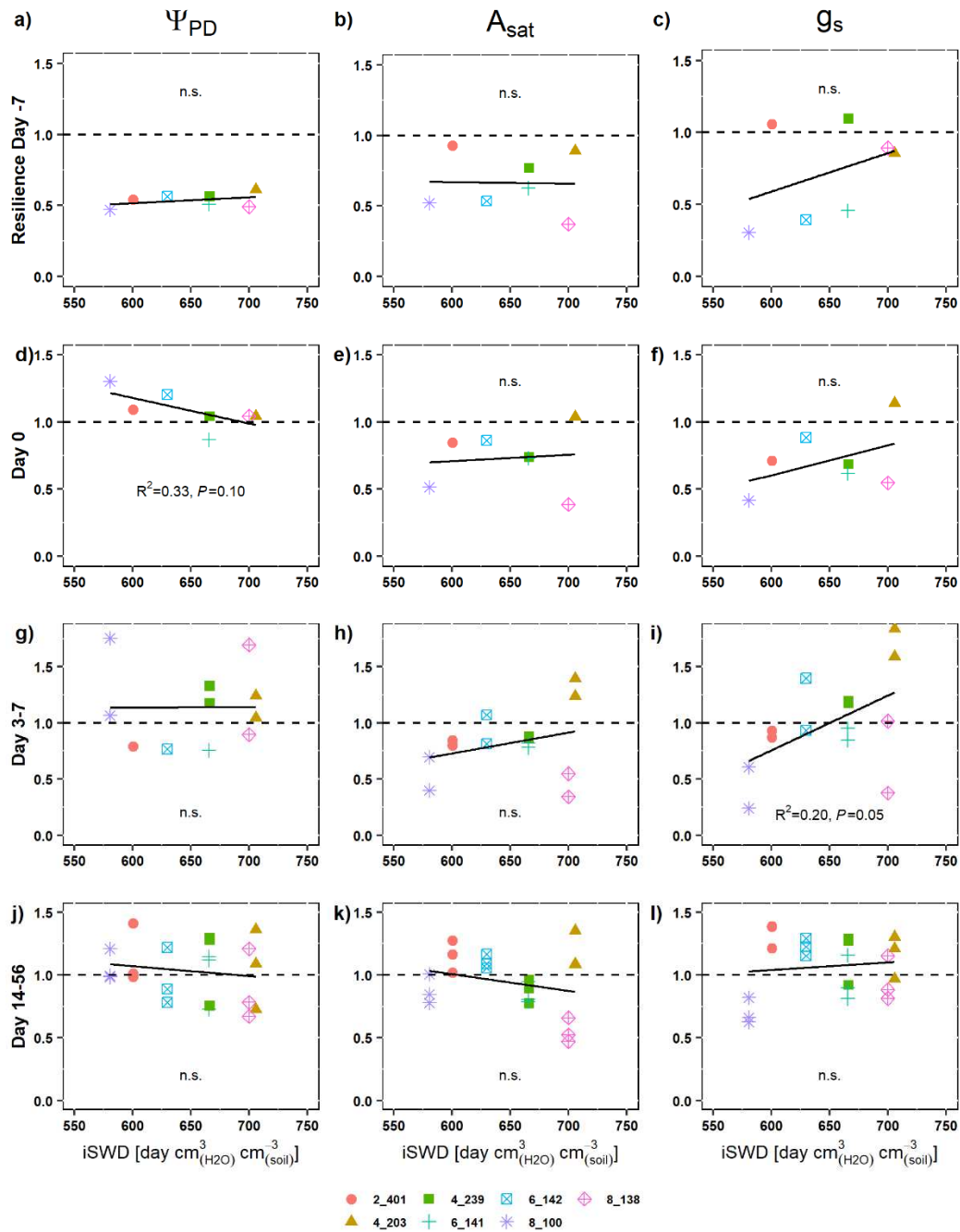


Fig. 10: Relationships in beech trees between Resilience of leaf physiological parameters (Ψ_{PD} ; predawn leaf water potential, A_{sat} ; light-saturated CO_2 assimilation rates, g_s ; leaf stomatal conductance, ABA; concentration of abscisic acid in leaves) and iSWD (time-integrated soil water deficit during the five years of the drought phase) at 0-70 cm soil depth, before (day -7) and after drought release (day 0-56). Resilience is calculated as TE values divided by mean CO values: Resilience of 1 means the same value as the average of CO trees. Each color and symbol represents individual TE (throughfall-exclusion) trees. R^2 , p-values, n.s. (no significance), and solid lines indicate the results of linear regression applied for each data.

4.4. Positive “Drought legacy”? - Correlation between morphological and physiological responses in spruce

In contrast to beech trees with no significant reduction in their total leaf area during drought (Chapter I), spruce trees did not recover their total leaf area within three years after drought release (Chapter II). Previous reports indicate that morphological responses can improve physiology (Bert et al., 2021; Flexas et al., 2006; Gao et al., 2017; Grassi & Bagnaresi, 2001; Reich et al., 1997), e.g. since smaller total leaf area can be advantageous for leaf-level physiology at given soil water availability. Indeed, during the drought phase, annual water use per leaf area likely increased in the TE spruce after the reduction in the total leaf area and the parallel change in the sap flow profile (Chapter II), considering the constant annual water use of TE spruce throughout the drought years (Chapter I). Interestingly, even one year after the drought release, the total leaf area was correlated with leaf physiology. In the second and third recovery year (2020-2021), even though Ψ_{PD} was similar between treatments and the soil water content under TE spruce was higher than those of CO spruce (Hesse, 2021), Resilience of Ψ_{PD} , A_{sat} , and g_s was rather positively correlated with Resilience of leaf to sapwood area ratio (LA/SA) (Fig. 11a-c). The positive correlation between leaf physiological parameters and LA/SA was accompanied by a negative correlation between ABA concentration and LA/SA (Fig. 11d). Therefore, spruce trees with a stronger reduction in total leaf area rather displayed a more conservative water strategy with lower g_s and associated A_{sat} at the leaf level even two years after drought release, reinforcing the reduction of water use and C uptake at the whole-tree level. This observation is in accordance with the framework of Ruehr et al. (2019) that speed and intensity of recovery become lower with increasing severity of drought. Under non-limited water conditions, the slow recovery of the total leaf area together with the water-conserving leaf-physiological responses can delay the recovery of the stem growth and tree productivity compared to species such as beech showing faster recovery. However, under repeated and frequent drought predicted in the future, the pronounced negative “drought legacy” of spruce might be advantageous for its survival during future drought by the reduced water consumption (and can be seen as “acclimation”, see Gessler et al., 2020). Further studies should consider the relationship between the degree of the morphological responses to the first drought and the physiological performances during the next drought events.

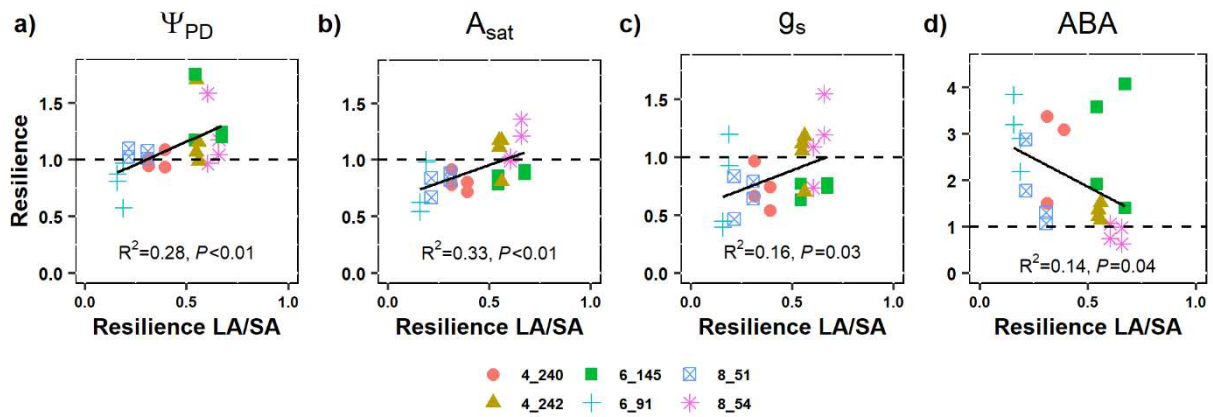


Fig. 11: Relationships between Resilience of leaf physiological parameters (Ψ_{PD} ; predawn leaf water potential, A_{sat} ; light-saturated CO_2 assimilation rates, g_s ; leaf stomatal conductance, ABA; concentration of abscisic acid in leaves) and Resilience of LA/SA (leaf to sapwood area ratio) in the second and third recovery year (2020–2021). Resilience is calculated as TE values divided by mean CO value: Resilience of 1 means the same value as the average of CO trees. LA/SA was used instead of LA to consider different tree sizes. Each color and symbol represents individual TE (throughfall-exclusion) spruce trees. R^2 , p -values, and solid lines indicate the results of linear regression applied for each data.

4.5. C sink activity and C supply in spruce during the critical time of drought recovery: Did C starvation occur under enhanced C sink activity?

The strong reduction in the water use especially in spruce, caused by stomatal control and reduced total leaf area (Chapter I), necessarily impacts whole-tree C balance (Chapter II). Indeed, during the drought phase, spruce trees significantly reduced stem growth (Pretzsch et al., 2020), fine-root growth (Nickel et al., 2018; Zwetsloot & Bauerle, 2021), total C uptake (Brunn et al., 2022), and C storage pools (Hesse et al., 2021). After drought release, fine root growth was a high priority for spruce trees (Chapter IV) to regrow their impaired water-absorbing system during drought (Nickel et al., 2018; Zwetsloot & Bauerle, 2021). However, total C uptake of previously drought-stressed spruce was still likely significantly lower than controls due to the slow recovery of the total leaf area (Chapter II), although full recovery of photosynthesis at the leaf level was observed within one growing season (Fig. 9). Thus, the high C sink activity belowground can cause local C starvation. Indeed, the whole-tree C transport rates (CTR) of spruce trees were reduced by more than 50% under drought and did not immediately recover after drought release (Chapter III), which can limit the supply of newly assimilated C (C_{new}) especially due to long transport distances from C source organs. However, similar to the observations during the first drought years (Hesse et al., 2021), recovering spruce trees showed similar or higher concentration of non-structural C in fine roots compared to the

control trees after drought release (Jasmin Danzberger personal communication), thus no sign of C starvation in the enhanced C sink. This is likely because the regrowth of the fine root system was supported by a preferential allocation of C_{new} and additionally by an increased use of stored C derived from starch conversion and release of osmolytes (Chapter IV). Especially, remobilization of osmolytes may be a huge C source during recovery (Hesse, 2021; Tsamir-Rimon et al., 2021), since released osmolytes calculated solely from leaves and fine-roots (c. 1200 - 3000 g C, Table 1) can potentially cover >70% of the total stored C used for the fine-root growth (c. 1700 g C, Chapter IV), depending on the share of each osmolyte. The full recovery of the whole-tree CTR within 2 weeks (Chapter III), which can double the amount of C transport, also contributed to the increased allocation of C_{new} towards belowground sinks. However, after the use of the released osmolytes and stored C, long-term C sink activity must be largely met by C_{new} (Lynch et al., 2013; Matamala et al., 2003). Especially, C storage might not be completely depleted due to its higher priority over growth as observed earlier (Galiano et al., 2017; Huang et al., 2021; Rehschuh et al., 2022). Fine root production of TE spruce remained higher or as high as that of CO trees at least until the end of the 2019 growing season (Jasmin Danzberger, personal communication), although the total leaf area of TE spruce was significantly smaller during the 3 years of recovery (Chapter II). Moreover, necessary fine root biomass to support the leaf area may be smaller in TE spruce than that of CO trees. Therefore, further analyses of the whole-tree C balance including development of above- and belowground biomass partitioning are needed to understand whether and how belowground C sinks are supplied in a long-term recovery period as well as to reveal the long-term consequences of the observed C allocation shift.

Since we only assessed C allocation of three recovery trees in one plot, it was not possible to relate the allocation pattern with the severity of the previous drought. So far there has been no experiment comparing C allocation of trees during recovery from different drought levels. Observations during drought indicate that C allocation towards roots increases with drought severity, at the expense of shoot growth and/or leaf maintenance (Encinas-Valero et al., 2022; Jacobs et al., 2009; Moser et al., 2015; Poorter et al., 2012). Further studies should consider potential changes in allocation patterns after different drought levels, which is still widely unknown, especially for mature trees (Ruehr et al., 2019).

The CTR and allocation of C_{new} of beech trees were not assessed in this study. On the one hand, fast recovery of the phloem transport speed can be expected for the beech trees within a few days after drought release in parallel with Ψ_{PD} , because a) phloem transport speed in beech

branches is correlated with Ψ_{PD} (Hesse et al., 2019), and b) the phloem diameter of beech branches were not significantly modified under drought (Petit et al., 2022). On the other hand, however, recovery of the mean residence time of leaf sugars (MRT) was possibly slower. This is because MRT was correlated with iSWD rather than with current Ψ_{PD} (Hesse et al., 2019) and the complete recovery of the leaf osmotic potential (π_o) took more than 2 weeks (Hesse et al., submitted), possibly delaying recovery of the whole-tree CTR, as observed in spruce trees (Chapter III). Furthermore, continuous C investment of beech trees into fine root growth observed during drought (Nikolova et al., 2020; Zwetsloot & Bauerle, 2021) was also detected after drought release (Jasmin Danzberger, personal communication), whereas stimulation of aboveground sinks is unlikely according to unchanged stem efflux rates after drought release (data not shown). Total C uptake of recovering beech trees likely became similar to that of the control trees within one growing season, considering the recovery of leaf photosynthesis within one week (Fig. 10), sap flow density within one growing season (Hesse et al., submitted), and unchanged total leaf area (Chapter I) and radial sap flow profile during drought (Chapter II). Further studies should address total belowground C sink activity (e.g. fine root growth and ECM) to discuss the whole-tree C balance of beech trees after drought release.

4.6 What can be expected in the forests and their C cycle dynamics in the future?

Recent studies reported mortality of both species through natural severe drought events (Arend et al., 2021; Braun et al., 2020; Schuldt et al., 2020). The present drought treatment also induced a mortality rate of 1.46% for beech and 7.45% for spruce (Pretzsch et al., 2020). In particular, TE spruce trees with the smallest radial stem growth ($\leq 1.5 \text{ mm year}^{-1}$) died from bark beetle attacks in the second drought year 2015 (Grams et al., 2021). However, only a few TE trees showed mortality solely through drought. The tree responses discussed in this study likely contributed to the survival of the TE trees through: a) stomatal control as a short-term drought response (Chapter I), b) reduced total leaf area as a long-term drought response (only for spruce, Chapter I, II), c) increased Ψ_{PD} under similar plant available water (PAW) after 3 years of drought (Fig. 8), d) along with a decrease in the leaf osmotic potential reported earlier (Tomasella et al., 2018). Therefore, once beech and spruce trees manage to survive the first drought phase, they seem to be able to adjust to the new water-limiting conditions. This acclimation is one possible explanation for the development of the stem radial growth, which increased after the third drought year in TE trees (Pretzsch et al., 2020).

After drought release, total C uptake and water use of beech trees likely recovered within one year to the control level. Faster recovery of the leaf and whole-tree level physiology and morphology may reflect a faster recovery of the stem growth compared to spruce. Furthermore, even spruce trees, showing larger drought effect both at the leaf and whole-tree level compared to beech, were able to respond quickly to the available water through recovery of C transport speed (Chapter III) and preferential C allocation towards fine roots (Chapter IV), enabling recovery in the water and C uptake, and the leaf level physiology. However, recovery of spruce at the whole-tree level requires non-water limiting conditions for much longer than three years, due to the slow recovery of the total leaf area (Chapter II). Considering frequency of recent drought events (e.g. 2015, 2018, 2019, and 2022, Hartmann et al., 2018; Schuldt et al., 2020; Toreti et al., 2022), spruce trees might maintain a new balance between water uptake and transpiration loss after release from repeated drought rather than completely recover their total leaf area and total C uptake. According to the sink control theory (Fatichi et al., 2014; Gavito et al., 2019; Hagedorn et al., 2016; Körner, 2015), necessary C uptake may be still low if the whole-tree C sink activity remains low. This is, however, still an open question and has to be investigated in further studies.

The slow recovery of the total leaf area and high ABA concentration even two years after the drought release (Fig. 11) in spruce can also be beneficial to cope with future drought events (Gessler et al., 2020; Pritzkow et al., 2021). An advantage of this “drought legacy” might be an increase in soil water content through smaller water use, which was observed under TE trees in the second recovery year (Hesse, 2021). Thus, soil water content before the onset of the next drought event is likely higher under previously drought-stressed spruce trees, compared to that under spruce experiencing the drought for the first time. Second, the smaller water use of spruce can further delay soil drying after the onset of drought. In mixed-species stands, this can even benefit other neighboring tree species at least in the initial drought phase (Costa et al., 2018; Pretzsch et al., 2013). During the drought periods, TE beech trees possibly benefitted from the reduced water use of neighboring TE spruce trees (Hesse, 2021), considering unchanged sap profile and associated leaf area of beech during drought (Chapter II). This is another possible explanation for the increased stem growth after the third drought year, especially in the TE beech trees (Pretzsch et al., 2020). Although the slow recovery of the total leaf area might reflect a slow recovery of stem growth and thus forest productivity (Zweifel et al., 2020), increase in soil water content and delayed soil drying together with the remaining strong stomatal control through ABA accumulation may facilitate survival of spruce and even neighboring tree species under frequent and prolonged drought predicted in the future.

The observed tree responses also affect the C storage capacity of forest ecosystems, feedback influencing the global climate (Collins et al., 2013; IPCC, 2021). Increased growth of thinner fine-roots (Nikolova et al., 2020; Zwetsloot & Bauerle, 2021) in parallel with decreased C uptake (Chapter I) and stem growth (Pretzsch et al., 2020) in beech might have accelerated C turnover of the forest ecosystem, because C turnover of fine roots (0 - 1 yr, Gill & Jackson, 2000; Kengdo et al., 2023; Lukac, 2012; McCormack et al., 2014) is much shorter than that of stems (Erb et al., 2016; Stephenson & Mantgem, 2005). In contrast, a decline in root growth and respiration as well as increase in root life span in spruce (Nikolova et al., 2020; Zwetsloot & Bauerle, 2021), in parallel with a strong reduction in C uptake (Chapter I) and stem growth (Pretzsch et al., 2020), might have rather decelerated C exchange and turnover of the forest ecosystem with the surrounding atmosphere. After drought release, the increased C allocation towards fine roots (Chapter IV) might enhance C sequestration in soil (Lützow et al., 2006; Obersteiner & Klein, 2022; Villarino et al., 2021). However, if the C allocation shift persists for years, C absorbed by trees may be released with relatively shorter turnover time, compared to C allocated to stem growth, even though the total C uptake increases through physiological and morphological recovery. Although changes of the C allocation contribute to tree recovery and survival, C storage time and capacity can remain low for years after drought release, which has been observed as “drought legacy” on stem growth (Anderegg et al., 2015; Kannenberg et al., 2020; Montwé et al., 2014; Peltier et al., 2016). Further studies on long-term dynamics of C storage including soil organic C are necessary to better predict ecosystem C cycles under future climate change, which still includes large uncertainties (Müller & Bahn, 2022; Obersteiner & Klein, 2022).

5. Conclusion and outlook

This comprehensive study presents leaf and whole-tree level physiology and morphology of mature Norway spruce and European beech to repeated drought and subsequent recovery. Spruce showed larger drought effect and slower recovery in both leaf and whole-tree level physiology and morphology compared to beech. Nevertheless, recovering spruce trees increased C transport speed and allocation of newly assimilated and stored C towards fine roots, indicating an ability to respond to the available water even after a long-term drought. These observed physiological and morphological responses are invaluable to understand the current and future development of the forest productivity. Under a short-term drought, whole-tree level C uptake and water use seem to be regulated solely through stomatal control without morphological changes unless leaf shedding occurs under more severe drought. In this case, fast recovery of the leaf and whole-tree level C uptake and water use can be expected after drought release, as observed in beech trees. In comparison, under a long-term and repeated drought, morphological responses can be induced as observed in spruce trees, which significantly delay the post-drought recovery of the whole-tree level C uptake and water use and thus tree productivity, especially in evergreen trees. However, one question still arises for further studies where the tipping point in the severity and the duration of a drought event is, leading to tree mortality (Arend et al., 2021; McDowell et al., 2022). Furthermore, the observed C allocation shift towards belowground sinks can also delay the recovery of the aboveground growth and forest productivity if it persists long. Since frequency and duration of drought are increasing, trees recovering from a long-term drought most likely experience another drought event before full recovery. It is therefore strikingly important to know whether physiological and morphological responses to a previous drought and subsequent recovery have a positive or negative effect on responses to the next drought events. Further researches should focus on this “drought legacy” effect on tree performance and mortality during repeated drought to better understand forest developments under future climate change.

6. References

- Ahmed, M. A., Kroener, E., Holz, M., Zarebanadkouki, M., & Carminati, A. (2014). Mucilage exudation facilitates root water uptake in dry soils. *Functional Plant Biology*, *41*(11), 1129. <https://doi.org/10.1071/FP13330>
- Alkama, R., & Cescatti, A. (2016). Biophysical climate impacts of recent changes in global forest cover. *Science*, *351*(6273), 600–604. <https://doi.org/10.1126/science.aac8083>
- Allen, C. D., Macalady, A. K., Chenchouni, H., Bachelet, D., McDowell, N., Vennetier, M., Kitzberger, T., Rigling, A., Breshears, D. D., Hogg, E. H. (Ted), Gonzalez, P., Fensham, R., Zhang, Z., Castro, J., Demidova, N., Lim, J.-H., Allard, G., Running, S. W., Semerci, A., & Cobb, N. (2010). A global overview of drought and heat-induced tree mortality reveals emerging climate change risks for forests. *Forest Ecology and Management*, *259*(4), 660–684. <https://doi.org/10.1016/j.foreco.2009.09.001>
- Ambrose, A. R., Baxter, W. L., Martin, R. E., Francis, E., Asner, G. P., Nydick, K. R., & Dawson, T. E. (2018). Leaf- and crown-level adjustments help giant sequoias maintain favorable water status during severe drought. *Forest Ecology and Management*, *419–420*, 257–267. <https://doi.org/10.1016/j.foreco.2018.01.012>
- Anderegg, L. D. L., & Hillerislambers, J. (2016). Drought stress limits the geographic ranges of two tree species via different physiological mechanisms. *Global Change Biology*, *22*(3), 1029–1045. <https://doi.org/10.1111/gcb.13148>
- Anderegg, W. R. L., Schwalm, C., Biondi, F., Camarero, J. J., Koch, G., Litvak, M., Ogle, K., Shaw, J. D., Shevliakova, E., Williams, A. P., Wolf, A., Ziaco, E., & Pacala, S. (2015). Pervasive drought legacies in forest ecosystems and their implications for carbon cycle models. *Science*, *349*(6247), 528–532. <https://doi.org/10.1126/science.aab1833>
- Anderegg, W. R. L., Trugman, A. T., Badgley, G., Konings, A. G., & Shaw, J. (2020). Divergent forest sensitivity to repeated extreme droughts. *Nature Climate Change*, *10*(12), 1091–1095. <https://doi.org/10.1038/s41558-020-00919-1>
- Arend, M., Link, R. M., Patthey, R., Hoch, G., Schuldt, B., & Kahmen, A. (2021). Rapid hydraulic collapse as cause of drought-induced mortality in conifers. *Proceedings of the National Academy of Sciences*, *118*(16). <https://doi.org/10.1073/pnas.2025251118>
- Arend, M., Link, R. M., Zahnd, C., Hoch, G., Schuldt, B., & Kahmen, A. (2022). Lack of hydraulic recovery as a cause of post-drought foliage reduction and canopy decline in European beech. *New Phytologist*, *234*(4), 1195–1205. <https://doi.org/10.1111/nph.18065>
- Barbeta, A., Ogaya, R., & Peñuelas, J. (2013). Dampening effects of long-term experimental drought on growth and mortality rates of a Holm oak forest. *Global Change Biology*, *19*(10), 3133–3144. <https://doi.org/10.1111/gcb.12269>
- Barbeta, A., & Peñuelas, J. (2016). Sequence of plant responses to droughts of different timescales: lessons from holm oak (*Quercus ilex*) forests. *Plant Ecology & Diversity*, *9*(4), 321–338. <https://doi.org/10.1080/17550874.2016.1212288>

- Basarin, B., Lukić, T., & Matzarakis, A. (2020). Review of Biometeorology of Heatwaves and Warm Extremes in Europe. *Atmosphere*, *11*(12), 1276. <https://doi.org/10.3390/atmos11121276>
- Beier, C., Beierkuhnlein, C., Wohlgemuth, T., Penuelas, J., Emmett, B., Körner, C., de Boeck, H., Christensen, J. H., Leuzinger, S., Janssens, I. A., & Hansen, K. (2012). Precipitation manipulation experiments - challenges and recommendations for the future. *Ecology Letters*, *15*(8), 899–911. <https://doi.org/10.1111/j.1461-0248.2012.01793.x>
- Belfiore, N., Nerva, L., Fasolini, R., Gaiotti, F., Lovat, L., & Chitarra, W. (2021). Leaf gas exchange and abscisic acid in leaves of Glera grape variety during drought and recovery. *Theoretical and Experimental Plant Physiology*, *33*(3), 261–270. <https://doi.org/10.1007/s40626-021-00211-3>
- Benomar, L., Lamhamedi, M. S., Rainville, A., Beaulieu, J., Bousquet, J., & Margolis, H. A. (2016). Genetic Adaptation vs. Ecophysiological Plasticity of Photosynthetic-Related Traits in Young *Picea glauca* Trees along a Regional Climatic Gradient. *Frontiers in Plant Science*, *7*. <https://doi.org/10.3389/fpls.2016.00048>
- Bergmann, J., Weigelt, A., van der Plas, F., Laughlin, D. C., Kuyper, T. W., Guerrero-Ramirez, N., Valverde-Barrantes, O. J., Bruelheide, H., Freschet, G. T., Iversen, C. M., Kattge, J., McCormack, M. L., Meier, I. C., Rillig, M. C., Roumet, C., Semchenko, M., Sweeney, C. J., van Ruijven, J., York, L. M., & Mommer, L. (2020). The fungal collaboration gradient dominates the root economics space in plants. *Science Advances*, *6*(27). <https://doi.org/10.1126/sciadv.aba3756>
- Bert, D., le Provost, G., Delzon, S., Plomion, C., & Gion, J.-M. (2021). Higher needle anatomic plasticity is related to better water-use efficiency and higher resistance to embolism in fast-growing *Pinus pinaster* families under water scarcity. *Trees*, *35*(1), 287–306. <https://doi.org/10.1007/s00468-020-02034-2>
- Blackman, C. J., Brodribb, T. J., & Jordan, G. J. (2009). Leaf hydraulics and drought stress: response, recovery and survivorship in four woody temperate plant species. *Plant, Cell & Environment*, *32*(11), 1584–1595. <https://doi.org/10.1111/j.1365-3040.2009.02023.x>
- Blessing, C. H., Werner, R. A., Siegwolf, R., & Buchmann, N. (2015). Allocation dynamics of recently fixed carbon in beech saplings in response to increased temperatures and drought. *Tree Physiology*, *35*(6), 585–598. <https://doi.org/10.1093/treephys/tpv024>
- Bloom, A. (1985). Resource Limitation in Plants--An Economic Analogy. *Annual Review of Ecology and Systematics*, *16*(1), 363–392. <https://doi.org/10.1146/annurev.ecolsys.16.1.363>
- Bollmark, M., Chen, H.-J., Moritz, T., & Eliasson, L. (1995). Relations between cytokinin level, bud development and apical control in Norway spruce, *Picea abies*. *Physiologia Plantarum*, *95*(4), 563–568. <https://doi.org/10.1111/j.1399-3054.1995.tb05523.x>
- Bonan, G. B. (2008). *Forests and Climate Change: Forcings, Feedbacks, and the Climate Benefits of Forests*. <https://www.science.org>
- Bose, A. K., Rigling, A., Gessler, A., Hagedorn, F., Brunner, I., Feichtinger, L., Bigler, C., Egli, S., Etzold, S., Gossner, M. M., Guidi, C., Lévesque, M., Meusburger, K., Peter, M.,

- Saurer, M., Scherrer, D., Schleppi, P., Schönbeck, L., Vogel, M. E., ... Schaub, M. (2022). Lessons learned from a long-term irrigation experiment in a dry Scots pine forest: Impacts on traits and functioning. *Ecological Monographs*, 92(2). <https://doi.org/10.1002/ecm.1507>
- Bottero, A., Forrester, D. I., Cailleret, M., Kohnle, U., Gessler, A., Michel, D., Bose, A. K., Bauhus, J., Bugmann, H., Cuntz, M., Gillerot, L., Hanewinkel, M., Lévesque, M., Ryder, J., Sainte-Marie, J., Schwarz, J., Yousefpour, R., Zamora-Pereira, J. C., & Rigling, A. (2021). Growth resistance and resilience of mixed silver fir and Norway spruce forests in central Europe: Contrasting responses to mild and severe droughts. *Global Change Biology*, 27(18), 4403–4419. <https://doi.org/10.1111/gcb.15737>
- Braun, S., de Witte, L. C., & Hopf, S. E. (2020). Auswirkungen des Trockensommers 2018 auf Flächen der Interkantonalen Walddauerbeobachtung. *Schweizerische Zeitschrift Fur Forstwesen*, 171(5), 270–280. <https://doi.org/10.3188/szf.2020.0270>
- Bréda, N., Huc, R., Granier, A., & Dreyer, E. (2006). Temperate forest trees and stands under severe drought: a review of ecophysiological responses, adaptation processes and long-term consequences. *Annals of Forest Science*, 63(6), 625–644. <https://doi.org/10.1051/forest:2006042>
- Brinkmann, N., Eugster, W., Buchmann, N., & Kahmen, A. (2019). Species-specific differences in water uptake depth of mature temperate trees vary with water availability in the soil. *Plant Biology*, 21(1), 71–81. <https://doi.org/10.1111/plb.12907>
- Brodersen, C. R., & McElrone, A. J. (2013). Maintenance of xylem Network Transport Capacity: A Review of Embolism Repair in Vascular Plants. *Frontiers in Plant Science*, 4. <https://doi.org/10.3389/fpls.2013.00108>
- Brodribb, T. J., & Cochard, H. (2009). Hydraulic Failure Defines the Recovery and Point of Death in Water-Stressed Conifers. *Plant Physiology*, 149(1), 575–584. <https://doi.org/10.1104/pp.108.129783>
- Brodribb, T. J., & McAdam, S. A. M. (2013). Abscisic Acid Mediates a Divergence in the Drought Response of Two Conifers . *Plant Physiology*, 162(3), 1370–1377. <https://doi.org/10.1104/pp.113.217877>
- Brodribb, T. J., Powers, J., Cochard, H., & Choat, B. (2020). Hanging by a thread? Forests and drought. *Science*, 368(6488), 261–266. <https://doi.org/10.1126/science.aat7631>
- Brüggemann, N., Gessler, A., Kayler, Z., Keel, S. G., Badeck, F., Barthel, M., Boeckx, P., Buchmann, N., Bruognoli, E., Esperschütz, J., Gavrichkova, O., Ghashghaie, J., Gomez-Casanovas, N., Keitel, C., Knohl, A., Kuptz, D., Palacio, S., Salmon, Y., Uchida, Y., & Bahn, M. (2011). Carbon allocation and carbon isotope fluxes in the plant-soil-atmosphere continuum: a review. *Biogeosciences*, 8(11), 3457–3489. <https://doi.org/10.5194/bg-8-3457-2011>
- Brunn, M., Hafner, B. D., Zwetsloot, M. J., Weikl, F., Pritsch, K., Hikino, K., Ruehr, N. K., Sayer, E. J., & Bauerle, T. L. (2022). Carbon allocation to root exudates is maintained in mature temperate tree species under drought. *New Phytologist*. <https://doi.org/10.1111/nph.18157>

- Brunner, I., Herzog, C., Dawes, M. A., Arend, M., & Sperisen, C. (2015). How tree roots respond to drought. *Frontiers in Plant Science*, 6. <https://doi.org/10.3389/fpls.2015.00547>
- Canarini, A., Schmidt, H., Fuchslueger, L., Martin, V., Herbold, C. W., Zezula, D., Gündler, P., Hasibeder, R., Jecmenica, M., Bahn, M., & Richter, A. (2021). Ecological memory of recurrent drought modifies soil processes via changes in soil microbial community. *Nature Communications*, 12(1), 5308. <https://doi.org/10.1038/s41467-021-25675-4>
- Carminati, A., Zarebanadkouki, M., Kroener, E., Ahmed, M. A., & Holz, M. (2016). Biophysical rhizosphere processes affecting root water uptake. *Annals of Botany*, 118(4), 561–571. <https://doi.org/10.1093/aob/mcw113>
- Chapin, F. S., Schulze, E., & Mooney, H. A. (1990). The Ecology and Economics of Storage in Plants. *Annual Review of Ecology and Systematics*, 21(1), 423–447. <https://doi.org/10.1146/annurev.es.21.110190.002231>
- Chen, H.-J., Bollmark, M., & Eliasson, L. (1996). Evidence that cytokinin controls bud size and branch form in Norway spruce. *Physiologia Plantarum*, 98(3), 612–618. <https://doi.org/10.1111/j.1399-3054.1996.tb05718.x>
- Choat, B., Brodribb, T. J., Brodersen, C. R., Duursma, R. A., López, R., & Medlyn, B. E. (2018). Triggers of tree mortality under drought. *Nature*, 558(7711), 531–539. <https://doi.org/10.1038/s41586-018-0240-x>
- Christmann, A., Grill, E., & Huang, J. (2013). Hydraulic signals in long-distance signaling. *Current Opinion in Plant Biology*, 16(3), 293–300. <https://doi.org/10.1016/j.pbi.2013.02.011>
- Chuste, P.-A., Maillard, P., Bréda, N., Levillain, J., Thirion, E., Wortemann, R., & Massonnet, C. (2020). Sacrificing growth and maintaining a dynamic carbohydrate storage are key processes for promoting beech survival under prolonged drought conditions. *Trees*, 34(2), 381–394. <https://doi.org/10.1007/s00468-019-01923-5>
- Ciais, Ph., Reichstein, M., Viovy, N., Granier, A., Ogée, J., Allard, V., Aubinet, M., Buchmann, N., Bernhofer, Chr., Carrara, A., Chevallier, F., de Noblet, N., Friend, A. D., Friedlingstein, P., Grünwald, T., Heinesch, B., Keronen, P., Knohl, A., Krinner, G., ... Valentini, R. (2005). Europe-wide reduction in primary productivity caused by the heat and drought in 2003. *Nature*, 437(7058), 529–533. <https://doi.org/10.1038/nature03972>
- Cochard, H., Bréda, N., & Granier, A. (1996). Whole tree hydraulic conductance and water loss regulation in *Quercus* during drought: evidence for stomatal control of embolism? *Annales Des Sciences Forestières*, 53(2–3), 197–206. <https://doi.org/10.1051/forest:19960203>
- Cochard, H., Coste, S., Chanson, B., Guehl, J. M., & Nicolini, E. (2005). Hydraulic architecture correlates with bud organogenesis and primary shoot growth in beech (*Fagus sylvatica*). *Tree Physiology*, 25(12), 1545–1552. <https://doi.org/10.1093/treephys/25.12.1545>
- Collins, M., Knutti, R., Arblaster, J., Dufresne, J.-L., Fichet, T., Friedlingstein, P., Gao, X., Gutowski, W. J., Johns, T., Krinner, G., Shongwe, M., Tebaldi, C., Weaver, A. J., &

- Wehner, M. (2013). Long-term Climate Change: Projections, Commitments and Irreversibility Pages 1029 to 1076. In Intergovernmental Panel on Climate Change (Ed.), *Climate Change 2013 - The Physical Science Basis* (pp. 1029–1136). Cambridge University Press. <https://doi.org/10.1017/CBO9781107415324.024>
- Costa, A. C. L., Rowland, L., Oliveira, R. S., Oliveira, A. A. R., Binks, O. J., Salmon, Y., Vasconcelos, S. S., Junior, J. A. S., Ferreira, L. v., Poyatos, R., Mencuccini, M., & Meir, P. (2018). Stand dynamics modulate water cycling and mortality risk in droughted tropical forest. *Global Change Biology*, *24*(1), 249–258. <https://doi.org/10.1111/gcb.13851>
- da Costa, A. C. L., Galbraith, D., Almeida, S., Portela, B. T. T., da Costa, M., de Athaydes Silva Junior, J., Braga, A. P., de Gonçalves, P. H. L., de Oliveira, A. A., Fisher, R., Phillips, O. L., Metcalfe, D. B., Levy, P., & Meir, P. (2010). Effect of 7 yr of experimental drought on vegetation dynamics and biomass storage of an eastern Amazonian rainforest. *New Phytologist*, *187*(3), 579–591. <https://doi.org/10.1111/j.1469-8137.2010.03309.x>
- Dannoura, M., Epron, D., Desalme, D., Massonnet, C., Tsuji, S., Plain, C., Priault, P., & Gérant, D. (2019). The impact of prolonged drought on phloem anatomy and phloem transport in young beech trees. *Tree Physiology*, *39*(2), 201–210. <https://doi.org/10.1093/treephys/tpy070>
- Dawson, T. E., Mambelli, S., Plamboeck, A. H., Templer, P. H., & Tu, K. P. (2002). Stable Isotopes in Plant Ecology. *Annual Review of Ecology and Systematics*, *33*(1), 507–559. <https://doi.org/10.1146/annurev.ecolsys.33.020602.095451>
- Dichio, B., Xiloyannis, C., Sofo, A., & Montanaro, G. (2006). Osmotic regulation in leaves and roots of olive trees during a water deficit and rewatering. *Tree Physiology*, *26*(2), 179–185. <https://doi.org/10.1093/treephys/26.2.179>
- Domec, J.-C., King, J. S., Carmichael, M. J., Overby, A. T., Wortemann, R., Smith, W. K., Miao, G., Noormets, A., & Johnson, D. M. (2021). Aquaporins, and not changes in root structure, provide new insights into physiological responses to drought, flooding, and salinity. *Journal of Experimental Botany*, *72*(12), 4489–4501. <https://doi.org/10.1093/jxb/erab100>
- Duan, H., Wang, D., Wei, X., Huang, G., Fan, H., Zhou, S., Wu, J., Liu, W., Tissue, D. T., & Wan, S. (2020). The decoupling between gas exchange and water potential of *Cinnamomum camphora* seedlings during drought recovery and its relation to ABA accumulation in leaves. *Journal of Plant Ecology*, *13*(6), 683–692. <https://doi.org/10.1093/jpe/rtaa056>
- Duddek, P., Carminati, A., Koebernick, N., Ohmann, L., Lovric, G., Delzon, S., Rodriguez-Dominguez, C. M., King, A., & Ahmed, M. A. (2022). The impact of drought-induced root and root hair shrinkage on root–soil contact. *Plant Physiology*. <https://doi.org/10.1093/plphys/kiac144>
- Encinas-Valero, M., Esteban, R., Hereş, A., Vivas, M., Fakhret, D., Aranjuelo, I., Solla, A., Moreno, G., & Curiel Yuste, J. (2022). Holm oak decline is determined by shifts in fine

- root phenotypic plasticity in response to belowground stress. *New Phytologist*, 235(6), 2237–2251. <https://doi.org/10.1111/nph.18182>
- Epron, D., Bahn, M., Derrien, D., Lattanzi, F. A., Pumpanen, J., Gessler, A., Hogberg, P., Maillard, P., Dannoura, M., Gerant, D., & Buchmann, N. (2012). Pulse-labelling trees to study carbon allocation dynamics: a review of methods, current knowledge and future prospects. *Tree Physiology*, 32(6), 776–798. <https://doi.org/10.1093/treephys/tps057>
- Epron, D., Cabral, O. M. R., Laclau, J.-P., Dannoura, M., Packer, A. P., Plain, C., Battie-Laclau, P., Moreira, M. Z., Trivelin, P. C. O., Bouillet, J.-P., Gérant, D., & Nouvellon, Y. (2016). In situ ¹³CO₂ pulse labelling of field-grown eucalypt trees revealed the effects of potassium nutrition and throughfall exclusion on phloem transport of photosynthetic carbon. *Tree Physiology*, 36(1), 6–21. <https://doi.org/10.1093/treephys/tpv090>
- Erb, K.-H., Fetzl, T., Plutzer, C., Kastner, T., Lauk, C., Mayer, A., Niedertscheider, M., Körner, C., & Haberl, H. (2016). Biomass turnover time in terrestrial ecosystems halved by land use. *Nature Geoscience*, 9(9), 674–678. <https://doi.org/10.1038/ngeo2782>
- FAO and UNEP. (2020). *The State of the World's Forests 2020*. FAO and UNEP. <https://doi.org/10.4060/ca8642en>
- Farquhar, G. D., Buckley, T. N., & Miller, J. M. (2002). Optimal Stomatal Control in Relation to Leaf Area and Nitrogen Content. *Silva Fennica*, 36(3), 625–637.
- Fatichi, S., Leuzinger, S., & Körner, C. (2014). Moving beyond photosynthesis: from carbon source to sink-driven vegetation modeling. *New Phytologist*, 201(4), 1086–1095. <https://doi.org/10.1111/nph.12614>
- Feichtinger, L. M., Eilmann, B., Buchmann, N., & Rigling, A. (2014). Growth adjustments of conifers to drought and to century-long irrigation. *Forest Ecology and Management*, 334, 96–105. <https://doi.org/10.1016/j.foreco.2014.08.008>
- Feichtinger, L. M., Siegwolf, R. T. W., Gessler, A., Buchmann, N., Lévesque, M., & Rigling, A. (2017). Plasticity in gas-exchange physiology of mature Scots pine and European larch drive short- and long-term adjustments to changes in water availability. *Plant, Cell & Environment*, 40(9), 1972–1983. <https://doi.org/10.1111/pce.13008>
- Fitzpatrick, C. R., Copeland, J., Wang, P. W., Guttman, D. S., Kotanen, P. M., & Johnson, M. T. J. (2018). Assembly and ecological function of the root microbiome across angiosperm plant species. *Proceedings of the National Academy of Sciences*, 115(6). <https://doi.org/10.1073/pnas.1717617115>
- Flexas, J., Bota, J., Galmés, J., Medrano, H., & Ribas-Carbó, M. (2006). Keeping a positive carbon balance under adverse conditions: responses of photosynthesis and respiration to water stress. *Physiologia Plantarum*, 127(3), 343–352. <https://doi.org/10.1111/j.1399-3054.2006.00621.x>
- FOREST EUROPE. (2015). *State of Europe's Forests*.
- Forrester, D. I., Tachauer, I. H. H., Annighoefer, P., Barbeito, I., Pretzsch, H., Ruiz-Peinado, R., Stark, H., Vacchiano, G., Zlatanov, T., Chakraborty, T., Saha, S., & Sileshi, G. W. (2017). Generalized biomass and leaf area allometric equations for European tree species

- incorporating stand structure, tree age and climate. *Forest Ecology and Management*, 396, 160–175. <https://doi.org/10.1016/j.foreco.2017.04.011>
- Förster, A., Hertel, D., Werner, R., & Leuschner, C. (2021). Belowground consequences of converting broadleaf to conifer forest: Comparing the fine root systems of European beech and Scots pine. *Forest Ecology and Management*, 496, 119457. <https://doi.org/10.1016/j.foreco.2021.119457>
- Frei, E. R., Gossner, M. M., Vitasse, Y., Queloz, V., Dubach, V., Gessler, A., Ginzler, C., Hagedorn, F., Meusburger, K., Moor, M., Samblàs Vives, E., Rigling, A., Uitentuis, I., von Arx, G., & Wohlgemuth, T. (2022). European beech dieback after premature leaf senescence during the 2018 drought in northern Switzerland. *Plant Biology*. <https://doi.org/10.1111/plb.13467>
- Galiano, L., Timofeeva, G., Saurer, M., Siegwolf, R., Martínez-Vilalta, J., Hommel, R., & Gessler, A. (2017). The fate of recently fixed carbon after drought release: towards unravelling C storage regulation in *Tilia platyphyllos* and *Pinus sylvestris*. *Plant, Cell & Environment*, 40(9), 1711–1724. <https://doi.org/10.1111/pce.12972>
- Gallé, Á., Csiszár, J., Benyó, D., Laskay, G., Leviczky, T., Erdei, L., & Tari, I. (2013). Isohydic and anisohydic strategies of wheat genotypes under osmotic stress: Biosynthesis and function of ABA in stress responses. *Journal of Plant Physiology*, 170(16), 1389–1399. <https://doi.org/10.1016/j.jplph.2013.04.010>
- Gamitzer, U., Schäufele, R., & Schnyder, H. (2009). Observing ¹³C labelling kinetics in CO₂ respired by a temperate grassland ecosystem. *New Phytologist*, 184(2), 376–386. <https://doi.org/10.1111/j.1469-8137.2009.02963.x>
- Gao, D., Joseph, J., Werner, R. A., Brunner, I., Zürcher, A., Hug, C., Wang, A., Zhao, C., Bai, E., Meusburger, K., Gessler, A., & Hagedorn, F. (2021). Drought alters the carbon footprint of trees in soils—tracking the spatio-temporal fate of ¹³C-labelled assimilates in the soil of an old-growth pine forest. *Global Change Biology*, 27(11), 2491–2506. <https://doi.org/10.1111/gcb.15557>
- Gao, J., Zhao, P., Shen, W., Rao, X., & Hu, Y. (2017). Physiological homeostasis and morphological plasticity of two tree species subjected to precipitation seasonal distribution changes. *Perspectives in Plant Ecology, Evolution and Systematics*, 25, 1–19. <https://doi.org/10.1016/j.ppees.2017.01.002>
- García-Fórner, N., Biel, C., Savé, R., & Martínez-Vilalta, J. (2017). Isohydic species are not necessarily more carbon limited than anisohydic species during drought. *Tree Physiology*, 37(4), 441–455. <https://doi.org/10.1093/treephys/tpw109>
- Gartner, K., Nadezhdina, N., Englisch, M., Čermak, J., & Leitgeb, E. (2009). Sap flow of birch and Norway spruce during the European heat and drought in summer 2003. *Forest Ecology and Management*, 258(5), 590–599. <https://doi.org/10.1016/j.foreco.2009.04.028>
- Gaul, D., Hertel, D., Borken, W., Matzner, E., & Leuschner, C. (2008). Effects of experimental drought on the fine root system of mature Norway spruce. *Forest Ecology and Management*, 256(5), 1151–1159. <https://doi.org/10.1016/j.foreco.2008.06.016>

- Gavito, M. E., Jakobsen, I., Mikkelsen, T. N., & Mora, F. (2019). Direct evidence for modulation of photosynthesis by an arbuscular mycorrhiza-induced carbon sink strength. *New Phytologist*, 223(2), 896–907. <https://doi.org/10.1111/nph.15806>
- Gessler, A., Bottero, A., Marshall, J., & Arend, M. (2020). The way back: recovery of trees from drought and its implication for acclimation. *New Phytologist*, 228(6), 1704–1709. <https://doi.org/10.1111/nph.16703>
- Gill, R. A., & Jackson, R. B. (2000). Global patterns of root turnover for terrestrial ecosystems. *New Phytologist*, 147(1), 13–31. <https://doi.org/10.1046/j.1469-8137.2000.00681.x>
- Goisser, M., Geppert, U., Rötzer, T., Paya, A., Huber, A., Kerner, R., Bauerle, T., Pretzsch, H., Pritsch, K., Häberle, K. H., Matyssek, R., & Grams, T. E. E. (2016). Does belowground interaction with *Fagus sylvatica* increase drought susceptibility of photosynthesis and stem growth in *Picea abies*? *Forest Ecology and Management*, 375, 268–278. <https://doi.org/10.1016/j.foreco.2016.05.032>
- Gower, S. T. (2003). Patterns and mechanisms of the forest carbon cycle. *Annual Review of Environment and Resources*, 28, 169–204. <https://doi.org/10.1146/annurev.energy.28.050302.105515>
- Grams, T. E. E., Hesse, B. D., Gebhardt, T., Weigl, F., Rötzer, T., Kovacs, B., Hikino, K., Hafner, B. D., Brunn, M., Bauerle, T., Häberle, K., Pretzsch, H., & Pritsch, K. (2021). The Kroof experiment: realization and efficacy of a recurrent drought experiment plus recovery in a beech/spruce forest. *Ecosphere*, 12(3). <https://doi.org/10.1002/ecs2.3399>
- Grams, T. E. E., Werner, H., Kuptz, D., Ritter, W., Fleischmann, F., Andersen, C. P., & Matyssek, R. (2011). A free-air system for long-term stable carbon isotope labeling of adult forest trees. *Trees*, 25(2), 187–198. <https://doi.org/10.1007/s00468-010-0497-7>
- Granier, A. (1985). Une nouvelle méthode pour la mesure du flux de sève brute dans le tronc des arbres. *Annales Des Sciences Forestières*, 42(2), 193–200. <https://doi.org/10.1051/forest:19850204>
- Granier, A. (1987). Evaluation of transpiration in a Douglas-fir stand by means of sap flow measurements. *Tree Physiology*, 3(4), 309–320. <https://doi.org/10.1093/treephys/3.4.309>
- Grassi, G., & Bagnaresi, U. (2001). Foliar morphological and physiological plasticity in *Picea abies* and *Abies alba* saplings along a natural light gradient. *Tree Physiology*, 21(12–13), 959–967. <https://doi.org/10.1093/treephys/21.12-13.959>
- Grossiord, C., Sevanto, S., Dawson, T. E., Adams, H. D., Collins, A. D., Dickman, L. T., Newman, B. D., Stockton, E. A., & McDowell, N. G. (2017). Warming combined with more extreme precipitation regimes modifies the water sources used by trees. *New Phytologist*, 213(2), 584–596. <https://doi.org/10.1111/nph.14192>
- Häberle, K.-H., Weigt, R., Nikolova, P. S., Reiter, I. M., Cermak, J., Wieser, G., Blaschke, H., Rötzer, T., Pretzsch, H., & Matyssek, R. (2012). Case Study “Kranzberger Forst”: Growth and Defence in European Beech (*Fagus sylvatica* L.) and Norway Spruce (*Picea abies* (L.) Karst.) (pp. 243–271). https://doi.org/10.1007/978-3-642-30645-7_11

- Hagedorn, F., Joseph, J., Peter, M., Luster, J., Pritsch, K., Geppert, U., Kerner, R., Molinier, V., Egli, S., Schaub, M., Liu, J.-F., Li, M., Sever, K., Weiler, M., Siegwolf, R. T. W., Gessler, A., & Arend, M. (2016). Recovery of trees from drought depends on belowground sink control. *Nature Plants*, 2(8), 16111. <https://doi.org/10.1038/nplants.2016.111>
- Hammond, W. M., Williams, A. P., Abatzoglou, J. T., Adams, H. D., Klein, T., López, R., Sáenz-Romero, C., Hartmann, H., Breshears, D. D., & Allen, C. D. (2022). Global field observations of tree die-off reveal hotter-drought fingerprint for Earth's forests. *Nature Communications*, 13(1), 1761. <https://doi.org/10.1038/s41467-022-29289-2>
- Harfouche, A., Meilan, R., & Altman, A. (2014). Molecular and physiological responses to abiotic stress in forest trees and their relevance to tree improvement. *Tree Physiology*, 34(11), 1181–1198. <https://doi.org/10.1093/treephys/tpu012>
- Hart, A. T., Merlin, M., Wiley, E., & Landhäuser, S. M. (2021). Splitting the Difference: Heterogeneous Soil Moisture Availability Affects Aboveground and Belowground Reserve and Mass Allocation in Trembling Aspen. *Frontiers in Plant Science*, 12. <https://doi.org/10.3389/fpls.2021.654159>
- Hartmann, H., Bahn, M., Carbone, M., & Richardson, A. D. (2020). Plant carbon allocation in a changing world – challenges and progress: introduction to a Virtual Issue on carbon allocation. *New Phytologist*, 227(4), 981–988. <https://doi.org/10.1111/nph.16757>
- Hartmann, H., Link, R. M., & Schuldt, B. (2021). A whole-plant perspective of isohydry: stem-level support for leaf-level plant water regulation. *Tree Physiology*, 41(6), 901–905. <https://doi.org/10.1093/treephys/tpab011>
- Hartmann, H., Moura, C. F., Anderegg, W. R. L., Ruehr, N. K., Salmon, Y., Allen, C. D., Arndt, S. K., Breshears, D. D., Davi, H., Galbraith, D., Ruthrof, K. X., Wunder, J., Adams, H. D., Bloemen, J., Cailleret, M., Cobb, R., Gessler, A., Grams, T. E. E., Jansen, S., ... O'Brien, M. (2018). Research frontiers for improving our understanding of drought-induced tree and forest mortality. *New Phytologist*, 218(1), 15–28. <https://doi.org/10.1111/nph.15048>
- Hartmann, H., & Trumbore, S. (2016). Understanding the roles of nonstructural carbohydrates in forest trees – from what we can measure to what we want to know. *New Phytologist*, 211(2), 386–403. <https://doi.org/10.1111/nph.13955>
- Hartmann, H., Ziegler, W., Kolle, O., & Trumbore, S. (2013). Thirst beats hunger – declining hydration during drought prevents carbon starvation in Norway spruce saplings. *New Phytologist*, 200(2), 340–349. <https://doi.org/10.1111/nph.12331>
- Hartmann, H., Ziegler, W., & Trumbore, S. (2013). Lethal drought leads to reduction in nonstructural carbohydrates in Norway spruce tree roots but not in the canopy. *Functional Ecology*, 27(2), 413–427. <https://doi.org/10.1111/1365-2435.12046>
- Helle, G., & Schleser, G. H. (2004). Beyond CO₂-fixation by Rubisco - an interpretation of ¹³C/¹²C variations in tree rings from novel intra-seasonal studies on broad-leaf trees. *Plant, Cell and Environment*, 27(3), 367–380. <https://doi.org/10.1111/j.0016-8025.2003.01159.x>

- Helmisaari, H.-S., Derome, J., Nojd, P., & Kukkola, M. (2007). Fine root biomass in relation to site and stand characteristics in Norway spruce and Scots pine stands. *Tree Physiology*, 27(10), 1493–1504. <https://doi.org/10.1093/treephys/27.10.1493>
- Helmisaari, H.-S., Ostonen, I., Lohmus, K., Derome, J., Lindroos, A.-J., Merila, P., & Nojd, P. (2009). Ectomycorrhizal root tips in relation to site and stand characteristics in Norway spruce and Scots pine stands in boreal forests. *Tree Physiology*, 29(3), 445–456. <https://doi.org/10.1093/treephys/tpn042>
- Hertel, D., Strecker, T., Müller-Haubold, H., & Leuschner, C. (2013). Fine root biomass and dynamics in beech forests across a precipitation gradient - is optimal resource partitioning theory applicable to water-limited mature trees? *Journal of Ecology*, 101(5), 1183–1200. <https://doi.org/10.1111/1365-2745.12124>
- Hesse, B. D. (2021). *Drought response and resilience of water and carbon relations in mature European beech and Norway spruce* [Doctoral thesis]. Technical University of Munich.
- Hesse, B. D., Gebhardt, T., Hafner, B. D., Hikino, K., Reitsam, A., Gigl, M., Dawid, C., Häberle, K.-H., & Grams, T. E. E. (n.d.). *Physiological recovery of tree water relations upon drought release – response of mature beech and spruce after five years of recurrent summer drought (submitted)*.
- Hesse, B. D., Goisser, M., Hartmann, H., & Grams, T. E. E. (2019). Repeated summer drought delays sugar export from the leaf and impairs phloem transport in mature beech. *Tree Physiology*, 39(2), 192–200. <https://doi.org/10.1093/treephys/tpy122>
- Hesse, B. D., Hartmann, H., Rötzer, T., Landhäuser, S. M., Goisser, M., Weigl, F., Pritsch, K., & Grams, T. E. E. (2021). Mature beech and spruce trees under drought – Higher C investment in reproduction at the expense of whole-tree NSC stores. *Environmental and Experimental Botany*, 191, 104615. <https://doi.org/10.1016/j.envexpbot.2021.104615>
- Hodge, A. (2004). The plastic plant: root responses to heterogeneous supplies of nutrients. *New Phytologist*, 162(1), 9–24. <https://doi.org/10.1111/j.1469-8137.2004.01015.x>
- Homolová, L., Lukeš, P., Malenovský, Z., Lhotáková, Z., Kaplan, V., & Hanuš, J. (2013). Measurement methods and variability assessment of the Norway spruce total leaf area: implications for remote sensing. *Trees*, 27(1), 111–121. <https://doi.org/10.1007/s00468-012-0774-8>
- Huang, J., Hammerbacher, A., Gershenzon, J., van Dam, N. M., Sala, A., McDowell, N. G., Chowdhury, S., Gleixner, G., Trumbore, S., & Hartmann, H. (2021). Storage of carbon reserves in spruce trees is prioritized over growth in the face of carbon limitation. *Proceedings of the National Academy of Sciences*, 118(33). <https://doi.org/10.1073/pnas.2023297118>
- Huang, S., Ye, G., Lin, J., Chen, K., Xu, X., Ruan, H., Tan, F., & Chen, H. Y. H. (2018). Autotrophic and heterotrophic soil respiration responds asymmetrically to drought in a subtropical forest in the Southeast China. *Soil Biology and Biochemistry*, 123, 242–249. <https://doi.org/10.1016/j.soilbio.2018.04.029>

- Hudson, P. J., Limousin, J. M., Krofcheck, D. J., Boutz, A. L., Pangle, R. E., Gehres, N., McDowell, N. G., & Pockman, W. T. (2018). Impacts of long-term precipitation manipulation on hydraulic architecture and xylem anatomy of piñon and juniper in Southwest USA. *Plant, Cell & Environment*, *41*(2), 421–435. <https://doi.org/10.1111/pce.13109>
- Ineichen, K., & Wiemken, V. (1992). Changes in the fungus-specific, soluble-carbohydrate pool during rapid and synchronous ectomycorrhiza formation of *Picea abies* with *Pisolithus tinctorius*. *Mycorrhiza*, *2*(1), 1–7. <https://doi.org/10.1007/BF00206277>
- IPCC. (2014). Climate Change 2014, Synthesis Report, Summary for Policymakers. *Contribution of Working Groups I, II and III to the Fifth Assessment Report of the Intergovernmental Panel on Climate Change*.
- IPCC. (2021). Summary for Policymakers. *Climate Change 2021: The Physical Science Basis. Contribution of Working Group I to the Sixth Assessment Report of the Intergovernmental Panel on Climate Change*. <https://doi.org/10.1017/9781009157896.001>
- Jacobs, D. F., Salifu, K. F., & Davis, A. S. (2009). Drought susceptibility and recovery of transplanted *Quercus rubra* seedlings in relation to root system morphology. *Annals of Forest Science*, *66*(5), 504–504. <https://doi.org/10.1051/forest/2009029>
- Jakoby, G., Rog, I., Megidish, S., & Klein, T. (2020). Enhanced root exudation of mature broadleaf and conifer trees in a Mediterranean forest during the dry season. *Tree Physiology*, *40*(11), 1595–1605. <https://doi.org/10.1093/treephys/tpaa092>
- Jiang, P., Meinzer, F. C., Fu, X., Kou, L., Dai, X., & Wang, H. (2021). Trade-offs between xylem water and carbohydrate storage among 24 coexisting subtropical understory shrub species spanning a spectrum of isohydry. *Tree Physiology*, *41*(3), 403–415. <https://doi.org/10.1093/treephys/tpaa138>
- Johnson, D. M., Sherrard, M. E., Domec, J.-C., & Jackson, R. B. (2014). Role of aquaporin activity in regulating deep and shallow root hydraulic conductance during extreme drought. *Trees*, *28*(5), 1323–1331. <https://doi.org/10.1007/s00468-014-1036-8>
- Joseph, J., Gao, D., Backes, B., Bloch, C., Brunner, I., Gleixner, G., Haeni, M., Hartmann, H., Hoch, G., Hug, C., Kahmen, A., Lehmann, M. M., Li, M.-H., Luster, J., Peter, M., Poll, C., Rigling, A., Rissanen, K. A., Ruehr, N. K., ... Gessler, A. (2020). Rhizosphere activity in an old-growth forest reacts rapidly to changes in soil moisture and shapes whole-tree carbon allocation. *Proceedings of the National Academy of Sciences*, *117*(40), 24885–24892. <https://doi.org/10.1073/pnas.2014084117>
- Jump, A. S., Ruiz-Benito, P., Greenwood, S., Allen, C. D., Kitzberger, T., Fensham, R., Martínez-Vilalta, J., & Lloret, F. (2017). Structural overshoot of tree growth with climate variability and the global spectrum of drought-induced forest dieback. *Global Change Biology*, *23*(9), 3742–3757. <https://doi.org/10.1111/gcb.13636>
- Kannenberg, S. A., Novick, K. A., & Phillips, R. P. (2019). Anisohydric behavior linked to persistent hydraulic damage and delayed drought recovery across seven North American tree species. *New Phytologist*, *222*(4), 1862–1872. <https://doi.org/10.1111/nph.15699>

- Kannenbergh, S. A., Schwalm, C. R., & Anderegg, W. R. L. (2020). Ghosts of the past: how drought legacy effects shape forest functioning and carbon cycling. *Ecology Letters*, 23(5), 891–901. <https://doi.org/10.1111/ele.13485>
- Keeling, C. D. (1958). The concentration and isotopic abundances of atmospheric carbon dioxide in rural areas. *Geochimica et Cosmochimica Acta*, 13(4), 322–334. [https://doi.org/10.1016/0016-7037\(58\)90033-4](https://doi.org/10.1016/0016-7037(58)90033-4)
- Keeling, C. D. (1961). The concentration and isotopic abundances of carbon dioxide in rural and marine air. *Geochimica et Cosmochimica Acta*, 24(3–4), 277–298. [https://doi.org/10.1016/0016-7037\(61\)90023-0](https://doi.org/10.1016/0016-7037(61)90023-0)
- Kengdo, S. K., Ahrens, B., Tian, Y., Heinzle, J., Wanek, W., Schindlbacher, A., & Borken, W. (2023). Increase in carbon input by enhanced fine root turnover in a long-term warmed forest soil. *Science of The Total Environment*, 855, 158800. <https://doi.org/10.1016/j.scitotenv.2022.158800>
- Kirfel, K., Leuschner, C., Hertel, D., & Schuldt, B. (2017). Influence of Root Diameter and Soil Depth on the Xylem Anatomy of Fine- to Medium-Sized Roots of Mature Beech Trees in the Top- and Subsoil. *Frontiers in Plant Science*, 8. <https://doi.org/10.3389/fpls.2017.01194>
- Knutzen, F., Dulamsuren, C., Meier, I. C., & Leuschner, C. (2017). Recent Climate Warming-Related Growth Decline Impairs European Beech in the Center of Its Distribution Range. *Ecosystems*, 20(8), 1494–1511. <https://doi.org/10.1007/s10021-017-0128-x>
- Knutzen, F., Meier, I. C., & Leuschner, C. (2015). Does reduced precipitation trigger physiological and morphological drought adaptations in European beech (*Fagus sylvatica* L.)? Comparing provenances across a precipitation gradient. *Tree Physiology*, 35(9), 949–963. <https://doi.org/10.1093/treephys/tpv057>
- Knüver, T., Bär, A., Ganthaler, A., Gebhardt, T., Grams, T. E. E., Häberle, K. -H., Hesse, B. D., Losso, A., Tomedi, I., Mayr, S., & Beikircher, B. (2022). Recovery after long-term summer drought: hydraulic measurements reveal legacy effects in trunks of *Picea abies* but not in *Fagus sylvatica*. *Plant Biology*. <https://doi.org/10.1111/plb.13444>
- Körner, C. (2015). Paradigm shift in plant growth control. *Current Opinion in Plant Biology*, 25, 107–114. <https://doi.org/10.1016/j.pbi.2015.05.003>
- Kramer, R. D., Ishii, H. R., Carter, K. R., Miyazaki, Y., Cavaleri, M. A., Araki, M. G., Azuma, W. A., Inoue, Y., & Hara, C. (2020). Predicting effects of climate change on productivity and persistence of forest trees. *Ecological Research*, 35(4), 562–574. <https://doi.org/10.1111/1440-1703.12127>
- Kuptz, D., Fleischmann, F., Matyssek, R., & Grams, T. E. E. (2011). Seasonal patterns of carbon allocation to respiratory pools in 60-yr-old deciduous (*Fagus sylvatica*) and evergreen (*Picea abies*) trees assessed via whole-tree stable carbon isotope labeling. *New Phytologist*, 191(1), 160–172. <https://doi.org/10.1111/j.1469-8137.2011.03676.x>
- Lanner, R. M. (2017). Primordium initiation drives tree growth. *Annals of Forest Science*, 74(1), 11. <https://doi.org/10.1007/s13595-016-0612-z>

- Lau, J. A., & Lennon, J. T. (2012). Rapid responses of soil microorganisms improve plant fitness in novel environments. *Proceedings of the National Academy of Sciences*, *109*(35), 14058–14062. <https://doi.org/10.1073/pnas.1202319109>
- Lehmann, M. M., Egli, M., Brinkmann, N., Werner, R. A., Saurer, M., & Kahmen, A. (2020). Improving the extraction and purification of leaf and phloem sugars for oxygen isotope analyses. *Rapid Communications in Mass Spectrometry*, *34*(19). <https://doi.org/10.1002/rcm.8854>
- Lehto, T., & Zwiazek, J. J. (2011). Ectomycorrhizas and water relations of trees: a review. *Mycorrhiza*, *21*(2), 71–90. <https://doi.org/10.1007/s00572-010-0348-9>
- Leuschner, C. (2020). Drought response of European beech (*Fagus sylvatica* L.)—A review. *Perspectives in Plant Ecology, Evolution and Systematics*, *47*, 125576. <https://doi.org/10.1016/j.ppees.2020.125576>
- Leuzinger, S., Luo, Y., Beier, C., Dieleman, W., Vicca, S., & Körner, C. (2011). Do global change experiments overestimate impacts on terrestrial ecosystems? *Trends in Ecology & Evolution*, *26*(5), 236–241. <https://doi.org/10.1016/j.tree.2011.02.011>
- Levanic, T., Cater, M., & McDowell, N. G. (2011). Associations between growth, wood anatomy, carbon isotope discrimination and mortality in a *Quercus robur* forest. *Tree Physiology*, *31*(3), 298–308. <https://doi.org/10.1093/treephys/tpq111>
- Li, H., Testerink, C., & Zhang, Y. (2021). How roots and shoots communicate through stressful times. *Trends in Plant Science*, *26*(9), 940–952. <https://doi.org/10.1016/j.tplants.2021.03.005>
- Limousin, J.-M., Bickford, C. P., Dickman, L. T., Pangle, R. E., Hudson, P. J., Boutz, A. L., Gehres, N., Osuna, J. L., Pockman, W. T., & McDowell, N. G. (2013). Regulation and acclimation of leaf gas exchange in a piñon-juniper woodland exposed to three different precipitation regimes. *Plant, Cell & Environment*, *36*(10), 1812–1825. <https://doi.org/10.1111/pce.12089>
- Limousin, J.-M., Longepierre, D., Huc, R., & Rambal, S. (2010). Change in hydraulic traits of Mediterranean *Quercus ilex* subjected to long-term throughfall exclusion. *Tree Physiology*, *30*(8), 1026–1036. <https://doi.org/10.1093/treephys/tpq062>
- Limousin, J.-M., Rambal, S., Ourcival, J. M., Rocheteau, A., Joffre, R., & Rodríguez-Cortina, R. (2009). Long-term transpiration change with rainfall decline in a Mediterranean *Quercus ilex* forest. *Global Change Biology*, *15*(9), 2163–2175. <https://doi.org/10.1111/j.1365-2486.2009.01852.x>
- Limousin, J.-M., Rambal, S., Ourcival, J.-M., Rodríguez-Calcerrada, J., Pérez-Ramos, I. M., Rodríguez-Cortina, R., Misson, L., & Joffre, R. (2012). Morphological and phenological shoot plasticity in a Mediterranean evergreen oak facing long-term increased drought. *Oecologia*, *169*(2), 565–577. <https://doi.org/10.1007/s00442-011-2221-8>
- Liu, D., Ogaya, R., Barbeta, A., Yang, X., & Peñuelas, J. (2015). Contrasting impacts of continuous moderate drought and episodic severe droughts on the aboveground-biomass increment and litterfall of three coexisting Mediterranean woody species. *Global Change Biology*, *21*(11), 4196–4209. <https://doi.org/10.1111/gcb.13029>

- Liu, J., Equiza, M. A., Navarro-Rodenas, A., Lee, S. H., & Zwiazek, J. J. (2014). Hydraulic adjustments in aspen (*Populus tremuloides*) seedlings following defoliation involve root and leaf aquaporins. *Planta*, *240*(3), 553–564. <https://doi.org/10.1007/s00425-014-2106-2>
- Lloret, F., Keeling, E. G., & Sala, A. (2011). Components of tree resilience: effects of successive low-growth episodes in old ponderosa pine forests. *Oikos*, *120*(12), 1909–1920. <https://doi.org/10.1111/j.1600-0706.2011.19372.x>
- Lovisolo, C., Perrone, I., Hartung, W., & Schubert, A. (2008). An abscisic acid-related reduced transpiration promotes gradual embolism repair when grapevines are rehydrated after drought. *New Phytologist*, *180*(3), 642–651. <https://doi.org/10.1111/j.1469-8137.2008.02592.x>
- Lukac, M. (2012). Fine Root Turnover. In *Measuring Roots* (pp. 363–373). Springer Berlin Heidelberg. https://doi.org/10.1007/978-3-642-22067-8_18
- Lützw, M. v., Kögel-Knabner, I., Ekschmitt, K., Matzner, E., Guggenberger, G., Marschner, B., & Flessa, H. (2006). Stabilization of organic matter in temperate soils: mechanisms and their relevance under different soil conditions - a review. *European Journal of Soil Science*, *57*(4), 426–445. <https://doi.org/10.1111/j.1365-2389.2006.00809.x>
- LWF. (2020). *Praxishilfe Klima-Boden Baumartenwahl*.
- Lynch, D. J., Matamala, R., Iversen, C. M., Norby, R. J., & Gonzalez-Meler, M. A. (2013). Stored carbon partly fuels fine-root respiration but is not used for production of new fine roots. *New Phytologist*, *199*(2), 420–430. <https://doi.org/10.1111/nph.12290>
- Ma, Z., Guo, D., Xu, X., Lu, M., Bardgett, R. D., Eissenstat, D. M., McCormack, M. L., & Hedin, L. O. (2018). Evolutionary history resolves global organization of root functional traits. *Nature*, *555*(7694), 94–97. <https://doi.org/10.1038/nature25783>
- Magh, Bonn, Grote, Burzlaff, Pfautsch, & Rennenberg. (2019). Drought Superimposes the Positive Effect of Silver Fir on Water Relations of European Beech in Mature Forest Stands. *Forests*, *10*(10), 897. <https://doi.org/10.3390/f10100897>
- Martinez del Castillo, E., Zang, C. S., Buras, A., Hacket-Pain, A., Esper, J., Serrano-Notivoli, R., Hartl, C., Weigel, R., Klesse, S., Resco de Dios, V., Scharnweber, T., Dorado-Liñán, I., van der Maaten-Theunissen, M., van der Maaten, E., Jump, A., Mikac, S., Banzragch, B.-E., Beck, W., Cavin, L., ... de Luis, M. (2022). Climate-change-driven growth decline of European beech forests. *Communications Biology*, *5*(1), 163. <https://doi.org/10.1038/s42003-022-03107-3>
- Martínez-Vilalta, J., Cochard, H., Mencuccini, M., Sterck, F., Herrero, A., Korhonen, J. F. J., Llorens, P., Nikinmaa, E., Nolè, A., Poyatos, R., Ripullone, F., Sass-Klaassen, U., & Zweifel, R. (2009). Hydraulic adjustment of Scots pine across Europe. *New Phytologist*, *184*(2), 353–364. <https://doi.org/10.1111/j.1469-8137.2009.02954.x>
- Martin-StPaul, N. K., Limousin, J.-M., Vogt-Schilb, H., Rodríguez-Calcerrada, J., Rambal, S., Longepierre, D., & Misson, L. (2013). The temporal response to drought in a Mediterranean evergreen tree: comparing a regional precipitation gradient and a

- throughfall exclusion experiment. *Global Change Biology*, 19(8), 2413–2426.
<https://doi.org/10.1111/gcb.12215>
- Matamala, R., González-Meler, M. A., Jastrow, J. D., Norby, R. J., & Schlesinger, W. H. (2003). Impacts of Fine Root Turnover on Forest NPP and Soil C Sequestration Potential. *Science*, 302(5649), 1385–1387. <https://doi.org/10.1126/science.1089543>
- McCormack, L. M., Adams, T. S., Smithwick, E. A. H., & Eissenstat, D. M. (2014). Variability in root production, phenology, and turnover rate among 12 temperate tree species. *Ecology*, 95(8), 2224–2235. <https://doi.org/10.1890/13-1942.1>
- McDowell, N. G., Allen, C. D., Anderson-Teixeira, K., Aukema, B. H., Bond-Lamberty, B., Chini, L., Clark, J. S., Dietze, M., Grossiord, C., Hanbury-Brown, A., Hurtt, G. C., Jackson, R. B., Johnson, D. J., Kueppers, L., Lichstein, J. W., Ogle, K., Poulter, B., Pugh, T. A. M., Seidl, R., ... Xu, C. (2020). Pervasive shifts in forest dynamics in a changing world. *Science*, 368(6494). <https://doi.org/10.1126/science.aaz9463>
- McDowell, N. G., Sapes, G., Pivovarov, A., Adams, H. D., Allen, C. D., Anderegg, W. R. L., Arend, M., Breshears, D. D., Brodrigg, T., Choat, B., Cochard, H., de Cáceres, M., de Kauwe, M. G., Grossiord, C., Hammond, W. M., Hartmann, H., Hoch, G., Kahmen, A., Klein, T., ... Xu, C. (2022). Mechanisms of woody-plant mortality under rising drought, CO₂ and vapour pressure deficit. *Nature Reviews Earth & Environment*, 3(5), 294–308. <https://doi.org/10.1038/s43017-022-00272-1>
- McDowell, N. G., & Sevanto, S. (2010). The mechanisms of carbon starvation: how, when, or does it even occur at all? *New Phytologist*, 186(2), 264–266. <https://doi.org/10.1111/j.1469-8137.2010.03232.x>
- McDowell, N., Pockman, W. T., Allen, C. D., Breshears, D. D., Cobb, N., Kolb, T., Plaut, J., Sperry, J., West, A., Williams, D. G., & Yezzer, E. A. (2008). Mechanisms of plant survival and mortality during drought: why do some plants survive while others succumb to drought? *New Phytologist*, 178(4), 719–739. <https://doi.org/10.1111/j.1469-8137.2008.02436.x>
- McLean, E. H., Ludwig, M., & Grierson, P. F. (2011). Root hydraulic conductance and aquaporin abundance respond rapidly to partial root-zone drying events in a riparian *Melaleuca* species. *New Phytologist*, 192(3), 664–675. <https://doi.org/10.1111/j.1469-8137.2011.03834.x>
- Meir, P., Metcalfe, D. B., Costa, A. C. L., & Fisher, R. A. (2008). The fate of assimilated carbon during drought: impacts on respiration in Amazon rainforests. *Philosophical Transactions of the Royal Society B: Biological Sciences*, 363(1498), 1849–1855. <https://doi.org/10.1098/rstb.2007.0021>
- Mencuccini, M. (2003). The ecological significance of long-distance water transport: short-term regulation, long-term acclimation and the hydraulic costs of stature across plant life forms. *Plant, Cell & Environment*, 26(1), 163–182. <https://doi.org/10.1046/j.1365-3040.2003.00991.x>
- Mencuccini, M., Rosas, T., Rowland, L., Choat, B., Cornelissen, H., Jansen, S., Kramer, K., Lapenis, A., Manzoni, S., Niinemets, Ü., Reich, P. B., Schrod, F., Soudzilovskaia, N., Wright, I. J., & Martínez-Vilalta, J. (2019). Leaf economics and plant hydraulics drive

- leaf : wood area ratios. *New Phytologist*, 224(4), 1544–1556.
<https://doi.org/10.1111/nph.15998>
- Meusburger, K., Trotsiuk, V., Schmidt-Walter, P., Baltensweiler, A., Brun, P., Bernhard, F., Gharun, M., Habel, R., Hagedorn, F., Köchli, R., Psomas, A., Puhlmann, H., Thimonier, A., Waldner, P., Zimmermann, S., & Walthert, L. (2022). Soil–plant interactions modulated water availability of Swiss forests during the 2015 and 2018 droughts. *Global Change Biology*, 28(20), 5928–5944. <https://doi.org/10.1111/gcb.16332>
- Mitchell, P. J., McAdam, S. A. M., Pinkard, E. A., & Brodribb, T. J. (2016). Significant contribution from foliage-derived ABA in regulating gas exchange in *Pinus radiata*. *Tree Physiology*. <https://doi.org/10.1093/treephys/tpw092>
- Mitchell, P. J., Veneklaas, E. J., Lambers, H., & Burgess, S. S. O. (2008). Leaf water relations during summer water deficit: differential responses in turgor maintenance and variation in leaf structure among different plant communities in south-western Australia. *Plant, Cell & Environment*, 31(12), 1791–1802. <https://doi.org/10.1111/j.1365-3040.2008.01882.x>
- Mohan, J. E., Cowden, C. C., Baas, P., Dawadi, A., Frankson, P. T., Helmick, K., Hughes, E., Khan, S., Lang, A., Machmuller, M., Taylor, M., & Witt, C. A. (2014). Mycorrhizal fungi mediation of terrestrial ecosystem responses to global change: mini-review. *Fungal Ecology*, 10, 3–19. <https://doi.org/10.1016/j.funeco.2014.01.005>
- Montwé, D., Spiecker, H., & Hamann, A. (2014). An experimentally controlled extreme drought in a Norway spruce forest reveals fast hydraulic response and subsequent recovery of growth rates. *Trees*, 28(3), 891–900. <https://doi.org/10.1007/s00468-014-1002-5>
- Morgan, J. M. (1984). Osmoregulation and Water Stress in Higher Plants. *Annual Review of Plant Physiology*, 35(1), 299–319. <https://doi.org/10.1146/annurev.pp.35.060184.001503>
- Moser, B., Kipfer, T., Richter, S., Egli, S., & Wohlgemuth, T. (2015). Drought resistance of *Pinus sylvestris* seedlings conferred by plastic root architecture rather than ectomycorrhizal colonisation. *Annals of Forest Science*, 72(3), 303–309. <https://doi.org/10.1007/s13595-014-0380-6>
- Müller, L. M., & Bahn, M. (2022). Drought legacies and ecosystem responses to subsequent drought. *Global Change Biology*, 28(17), 5086–5103. <https://doi.org/10.1111/gcb.16270>
- Munné-Bosch, S., & Alegre, L. (2004). Die and let live: leaf senescence contributes to plant survival under drought stress. *Functional Plant Biology*, 31(3), 203. <https://doi.org/10.1071/FP03236>
- Nadezhdina, N., Vandegehuchte, M. W., & Steppe, K. (2012). Sap flux density measurements based on the heat field deformation method. *Trees*, 26(5), 1439–1448. <https://doi.org/10.1007/s00468-012-0718-3>
- Nickel, U. T., Weigl, F., Kerner, R., Schäfer, C., Kallenbach, C., Munch, J. C., & Pritsch, K. (2018). Quantitative losses vs. qualitative stability of ectomycorrhizal community responses to 3 years of experimental summer drought in a beech–spruce forest. *Global Change Biology*, 24(2), e560–e576. <https://doi.org/10.1111/gcb.13957>

- Niinemets, Ü. (2010). Responses of forest trees to single and multiple environmental stresses from seedlings to mature plants: Past stress history, stress interactions, tolerance and acclimation. *Forest Ecology and Management*, 260(10), 1623–1639. <https://doi.org/10.1016/j.foreco.2010.07.054>
- Nikolova, P. S., Bauerle, T. L., Häberle, K.-H., Blaschke, H., Brunner, I., & Matyssek, R. (2020). Fine-Root Traits Reveal Contrasting Ecological Strategies in European Beech and Norway Spruce During Extreme Drought. *Frontiers in Plant Science*, 11. <https://doi.org/10.3389/fpls.2020.01211>
- Nikolova, P. S., Raspe, S., Andersen, C. P., Mainiero, R., Blaschke, H., Matyssek, R., & Häberle, K.-H. (2009). Effects of the extreme drought in 2003 on soil respiration in a mixed forest. *European Journal of Forest Research*, 128(2), 87–98. <https://doi.org/10.1007/s10342-008-0218-6>
- Nolan, R. H., Gauthey, A., Losso, A., Medlyn, B. E., Smith, R., Chhajed, S. S., Fuller, K., Song, M., Li, X., Beaumont, L. J., Boer, M. M., Wright, I. J., & Choat, B. (2021). Hydraulic failure and tree size linked with canopy die-back in eucalypt forest during extreme drought. *New Phytologist*, 230(4), 1354–1365. <https://doi.org/10.1111/nph.17298>
- Noormets, A., Epron, D., Domec, J. C., McNulty, S. G., Fox, T., Sun, G., & King, J. S. (2015). Effects of forest management on productivity and carbon sequestration: A review and hypothesis. *Forest Ecology and Management*, 355, 124–140. <https://doi.org/10.1016/j.foreco.2015.05.019>
- Oberhuber, W., Hammerle, A., & Kofler, W. (2015). Tree water status and growth of saplings and mature Norway spruce (*Picea abies*) at a dry distribution limit. *Frontiers in Plant Science*, 6. <https://doi.org/10.3389/fpls.2015.00703>
- Obersteiner, S., & Klein, T. (2022). Closing in on the last frontier: C allocation in the rhizosphere. *Global Change Biology*. <https://doi.org/10.1111/gcb.16432>
- Patzner, K. M. (2004). *The transpiration of trees as a basis for validation and modelling canopy transpiration of stands from a mountainous watershed near the river Ammer*. [Dissertation]. Technical University of Munich.
- Peguero-Pina, J., Mendoza-Herrer, Ó., Gil-Pelegrín, E., & Sancho-Knapik, D. (2018). Cavitation Limits the Recovery of Gas Exchange after Severe Drought Stress in Holm Oak (*Quercus ilex* L.). *Forests*, 9(8), 443. <https://doi.org/10.3390/f9080443>
- Peiffer, M., Bréda, N., Badeau, V., & Granier, A. (2014). Disturbances in European beech water relation during an extreme drought. *Annals of Forest Science*, 71(7), 821–829. <https://doi.org/10.1007/s13595-014-0383-3>
- Peltier, D. M. P., Fell, M., & Ogle, K. (2016). Legacy effects of drought in the southwestern United States: A multi-species synthesis. *Ecological Monographs*, 86(3), 312–326. <https://doi.org/10.1002/ecm.1219>
- Penning de Vries, F. W. T. (1975). The Cost of Maintenance Processes in Plant Cells. *Annals of Botany*, 39(1), 77–92. <https://doi.org/10.1093/oxfordjournals.aob.a084919>

- Peñuelas, J., Canadell, J. G., & Ogaya, R. (2011). Increased water-use efficiency during the 20th century did not translate into enhanced tree growth. *Global Ecology and Biogeography*, 20(4), 597–608. <https://doi.org/10.1111/j.1466-8238.2010.00608.x>
- Petit, G., Zamboni, D., Hesse, B. D., & Häberle, K. (2022). No xylem phenotypic plasticity in mature *Picea abies* and *Fagus sylvatica* trees after five years of throughfall precipitation exclusion. *Global Change Biology*. <https://doi.org/10.1111/gcb.16232>
- Peuke, A. D., Schraml, C., Hartung, W., & Rennenberg, H. (2002). Identification of drought-sensitive beech ecotypes by physiological parameters. *New Phytologist*, 154(2), 373–387. <https://doi.org/10.1046/j.1469-8137.2002.00400.x>
- Phillips, R. P., ERLITZ, Y., Bier, R., & Bernhardt, E. S. (2008). New approach for capturing soluble root exudates in forest soils. *Functional Ecology*, 22(6), 990–999. <https://doi.org/10.1111/j.1365-2435.2008.01495.x>
- Pierce, M., & Raschke, K. (1980). Correlation between loss of turgor and accumulation of abscisic acid in detached leaves. *Planta*, 148(2), 174–182. <https://doi.org/10.1007/BF00386419>
- Poorter, H., & Nagel, O. (2000). The role of biomass allocation in the growth response of plants to different levels of light, CO₂, nutrients and water: a quantitative review. *Functional Plant Biology*, 27(12), 1191. https://doi.org/10.1071/PP99173_CO
- Poorter, H., Niklas, K. J., Reich, P. B., Oleksyn, J., Poot, P., & Mommer, L. (2012). Biomass allocation to leaves, stems and roots: meta-analyses of interspecific variation and environmental control. *New Phytologist*, 193(1), 30–50. <https://doi.org/10.1111/j.1469-8137.2011.03952.x>
- Pou, A., Medrano, H., Tomàs, M., Martorell, S., Ribas-Carbó, M., & Flexas, J. (2012). Anisohydric behaviour in grapevines results in better performance under moderate water stress and recovery than isohydric behaviour. *Plant and Soil*, 359(1–2), 335–349. <https://doi.org/10.1007/s11104-012-1206-7>
- Poyatos, R., Agudé, D., Galiano, L., Mencuccini, M., & Martínez-Vilalta, J. (2013). Drought-induced defoliation and long periods of near-zero gas exchange play a key role in accentuating metabolic decline of Scots pine. *New Phytologist*, 200(2), 388–401. <https://doi.org/10.1111/nph.12278>
- Poyatos, R., Martínez-Vilalta, J., Čermák, J., Ceulemans, R., Granier, A., Irvine, J., Köstner, B., Lagergren, F., Meiresonne, L., Nadezhdina, N., Zimmermann, R., Llorens, P., & Mencuccini, M. (2007). Plasticity in hydraulic architecture of Scots pine across Eurasia. *Oecologia*, 153(2), 245–259. <https://doi.org/10.1007/s00442-007-0740-0>
- Pretsch, H. (2019). *Grundlagen der Waldwachstumsforschung*. Springer Berlin Heidelberg. <https://doi.org/10.1007/978-3-662-58155-1>
- Pretsch, H., Biber, P., Schütze, G., Kemmerer, J., & Uhl, E. (2018). Wood density reduced while wood volume growth accelerated in Central European forests since 1870. *Forest Ecology and Management*, 429, 589–616. <https://doi.org/10.1016/j.foreco.2018.07.045>

- Pretzsch, H., Biber, P., Schütze, G., Uhl, E., & Rötzer, T. (2014). Forest stand growth dynamics in Central Europe have accelerated since 1870. *Nature Communications*, 5(1), 4967. <https://doi.org/10.1038/ncomms5967>
- Pretzsch, H., Grams, T., Häberle, K. H., Pritsch, K., Bauerle, T., & Rötzer, T. (2020). Growth and mortality of Norway spruce and European beech in monospecific and mixed-species stands under natural episodic and experimentally extended drought. Results of the KROOF throughfall exclusion experiment. *Trees*, 34(4), 957–970. <https://doi.org/10.1007/s00468-020-01973-0>
- Pretzsch, H., Rötzer, T., Matyssek, R., Grams, T. E. E., Häberle, K.-H., Pritsch, K., Kerner, R., & Munch, J.-C. (2014). Mixed Norway spruce (*Picea abies* [L.] Karst) and European beech (*Fagus sylvatica* [L.]) stands under drought: from reaction pattern to mechanism. *Trees*, 28(5), 1305–1321. <https://doi.org/10.1007/s00468-014-1035-9>
- Pretzsch, H., Schütze, G., & Uhl, E. (2013). Resistance of European tree species to drought stress in mixed *versus* pure forests: evidence of stress release by inter-specific facilitation. *Plant Biology*, 15(3), 483–495. <https://doi.org/10.1111/j.1438-8677.2012.00670.x>
- Pritzkow, C., Szota, C., Williamson, V., & Arndt, S. K. (2021). Previous drought exposure leads to greater drought resistance in eucalypts through changes in morphology rather than physiology. *Tree Physiology*, 41(7), 1186–1198. <https://doi.org/10.1093/treephys/tpaa176>
- Rehseh, R., Cecilia, A., Zuber, M., Faragó, T., Baumbach, T., Hartmann, H., Jansen, S., Mayr, S., & Ruehr, N. (2020). Drought-Induced Xylem Embolism Limits the Recovery of Leaf Gas Exchange in Scots Pine. *Plant Physiology*, 184(2), 852–864. <https://doi.org/10.1104/pp.20.00407>
- Rehseh, R., Rehseh, S., Gast, A., Jakab, A., Lehmann, M. M., Saurer, M., Gessler, A., & Ruehr, N. K. (2022). Tree allocation dynamics beyond heat and hot drought stress reveal changes in carbon storage, belowground translocation and growth. *New Phytologist*, 233(2), 687–704. <https://doi.org/10.1111/nph.17815>
- Reich, P. B., Walters, M. B., & Ellsworth, D. S. (1997). From tropics to tundra: Global convergence in plant functioning. *Proceedings of the National Academy of Sciences*, 94(25), 13730–13734. <https://doi.org/10.1073/pnas.94.25.13730>
- Reis, F., Magalhães, A. P., Tavares, R. M., Baptista, P., & Lino-Neto, T. (2021). Bacteria could help ectomycorrhizae establishment under climate variations. *Mycorrhiza*, 31(3), 395–401. <https://doi.org/10.1007/s00572-021-01027-4>
- Reiter, I. M. (2004). *Space-related resource investments and gains of adult beech (Fagus sylvatica) and spruce (Picea abies) as a quantification of aboveground competitiveness* [Dissertation]. Technical University of Munich.
- Riederer, M., Kurbasik, K., Steinbrecher, R., & Voss, A. (1988). Surface areas, lengths and volumes of *Picea abies* (L.) Karst. needles: determination, biological variability and effect of environmental factors. *Trees*, 2(3), 165–172. <https://doi.org/10.1007/BF00196021>

- Rodríguez-Calcerrada, J., Rodrigues, A. M., António, C., Perdiguero, P., Pita, P., Collada, C., Li, M., & Gil, L. (2021). Stem metabolism under drought stress – a paradox of increasing respiratory substrates and decreasing respiratory rates. *Physiologia Plantarum*, *172*(2), 391–404. <https://doi.org/10.1111/ppl.13145>
- Rodríguez-Gamir, J., Xue, J., Clearwater, M. J., Meason, D. F., Clinton, P. W., & Domec, J. (2019). Aquaporin regulation in roots controls plant hydraulic conductance, stomatal conductance, and leaf water potential in *Pinus radiata* under water stress. *Plant, Cell & Environment*, *42*(2), 717–729. <https://doi.org/10.1111/pce.13460>
- Rosas, T., Mencuccini, M., Barba, J., Cochard, H., Saura-Mas, S., & Martínez-Vilalta, J. (2019). Adjustments and coordination of hydraulic, leaf and stem traits along a water availability gradient. *New Phytologist*, *223*(2), 632–646. <https://doi.org/10.1111/nph.15684>
- Ruehr, N. K., Grote, R., Mayr, S., & Arneth, A. (2019). Beyond the extreme: recovery of carbon and water relations in woody plants following heat and drought stress. *Tree Physiology*, *39*(8), 1285–1299. <https://doi.org/10.1093/treephys/tpz032>
- Ruehr, N. K., Offermann, C. A., Gessler, A., Winkler, J. B., Ferrio, J. P., Buchmann, N., & Barnard, R. L. (2009). Drought effects on allocation of recent carbon: from beech leaves to soil CO₂ efflux. *New Phytologist*, *184*(4), 950–961. <https://doi.org/10.1111/j.1469-8137.2009.03044.x>
- Sade, N., Gebremedhin, A., & Moshelion, M. (2012). Risk-taking plants. *Plant Signaling & Behavior*, *7*(7), 767–770. <https://doi.org/10.4161/psb.20505>
- Schindlbacher, A., Wunderlich, S., Borcken, W., Kitzler, B., Zechmeister-Boltenstern, S., & Jandl, R. (2012). Soil respiration under climate change: prolonged summer drought offsets soil warming effects. *Global Change Biology*, *18*(7), 2270–2279. <https://doi.org/10.1111/j.1365-2486.2012.02696.x>
- Schiop, S. T., al Hassan, M., Sestras, A. F., Boscaiu, M., Sestras, R. E., & Vicente, O. (2017). Biochemical responses to drought, at the seedling stage, of several Romanian Carpathian populations of Norway spruce (*Picea abies* L. Karst). *Trees*, *31*(5), 1479–1490. <https://doi.org/10.1007/s00468-017-1563-1>
- Schönbeck, L., Gessler, A., Hoch, G., McDowell, N. G., Rigling, A., Schaub, M., & Li, M. (2018). Homeostatic levels of nonstructural carbohydrates after 13 yr of drought and irrigation in *Pinus sylvestris*. *New Phytologist*, *219*(4), 1314–1324. <https://doi.org/10.1111/nph.15224>
- Schönbeck, L., Grossiord, C., Gessler, A., Gisler, J., Meusburger, K., D’Odorico, P., Rigling, A., Salmon, Y., Stocker, B. D., Zweifel, R., & Schaub, M. (2022). Photosynthetic acclimation and sensitivity to short- and long-term environmental changes in a drought-prone forest. *Journal of Experimental Botany*, *73*(8), 2576–2588. <https://doi.org/10.1093/jxb/erac033>
- Schuldt, B., Buras, A., Arend, M., Vitasse, Y., Beierkuhnlein, C., Damm, A., Gharun, M., Grams, T. E. E., Hauck, M., Hajek, P., Hartmann, H., Hiltbrunner, E., Hoch, G., Holloway-Phillips, M., Körner, C., Larysch, E., Lübke, T., Nelson, D. B., Rammig, A., ... Kahmen, A. (2020). A first assessment of the impact of the extreme 2018 summer

- drought on Central European forests. *Basic and Applied Ecology*, 45, 86–103. <https://doi.org/10.1016/j.baae.2020.04.003>
- Schulze, E.-D., Čermák, J., Matyssek, M., Penka, M., Zimmermann, R., Vasíček, F., Gries, W., & Kučera, J. (1985). Canopy transpiration and water fluxes in the xylem of the trunk of *Larix* and *Picea* trees — a comparison of xylem flow, porometer and cuvette measurements. *Oecologia*, 66(4), 475–483. <https://doi.org/10.1007/BF00379337>
- Schwalm, C. R., Anderegg, W. R. L., Michalak, A. M., Fisher, J. B., Biondi, F., Koch, G., Litvak, M., Ogle, K., Shaw, J. D., Wolf, A., Huntzinger, D. N., Schaefer, K., Cook, R., Wei, Y., Fang, Y., Hayes, D., Huang, M., Jain, A., & Tian, H. (2017). Global patterns of drought recovery. *Nature*, 548(7666), 202–205. <https://doi.org/10.1038/nature23021>
- Sevanto, S. (2014). Phloem transport and drought. *Journal of Experimental Botany*, 65(7), 1751–1759. <https://doi.org/10.1093/jxb/ert467>
- Skelton, R. P., Brodribb, T. J., McAdam, S. A. M., & Mitchell, P. J. (2017). Gas exchange recovery following natural drought is rapid unless limited by loss of leaf hydraulic conductance: evidence from an evergreen woodland. *New Phytologist*, 215(4), 1399–1412. <https://doi.org/10.1111/nph.14652>
- Smith, N. G., & Dukes, J. S. (2013). Plant respiration and photosynthesis in global-scale models: incorporating acclimation to temperature and CO₂. *Global Change Biology*, 19(1), 45–63. <https://doi.org/10.1111/j.1365-2486.2012.02797.x>
- Sperlich, D., Barbeta, A., Ogaya, R., Sabaté, S., & Peñuelas, J. (2016). Balance between carbon gain and loss under long-term drought: impacts on foliar respiration and photosynthesis in *Quercus ilex* L. *Journal of Experimental Botany*, 67(3), 821–833. <https://doi.org/10.1093/jxb/erv492>
- Stephenson, N. L., & Mantgem, P. J. (2005). Forest turnover rates follow global and regional patterns of productivity. *Ecology Letters*, 8(5), 524–531. <https://doi.org/10.1111/j.1461-0248.2005.00746.x>
- Sutinen, S., Roitto, M., & Repo, T. (2015). Vegetative buds, needles and shoot growth of Norway spruce are affected by experimentally delayed soil thawing in the field. *Forest Ecology and Management*, 336, 217–223. <https://doi.org/10.1016/j.foreco.2014.10.029>
- Tardieu, F., & Simonneau, T. (1998). Variability among species of stomatal control under fluctuating soil water status and evaporative demand: modelling isohydric and anisohydric behaviours. *Journal of Experimental Botany*, 49(Special), 419–432. https://doi.org/10.1093/jxb/49.Special_Issue.419
- Thalmann, M., & Santelia, D. (2017). Starch as a determinant of plant fitness under abiotic stress. *New Phytologist*, 214(3), 943–951. <https://doi.org/10.1111/nph.14491>
- Tomasella, M., Beikircher, B., Häberle, K.-H., Hesse, B., Kallenbach, C., Matyssek, R., & Mayr, S. (2018). Acclimation of branch and leaf hydraulics in adult *Fagus sylvatica* and *Picea abies* in a forest through-fall exclusion experiment. *Tree Physiology*, 38(2), 198–211. <https://doi.org/10.1093/treephys/tpx140>
- Tombesi, S., Nardini, A., Frioni, T., Soccolini, M., Zadra, C., Farinelli, D., Poni, S., & Palliotti, A. (2015). Stomatal closure is induced by hydraulic signals and maintained by

- ABA in drought-stressed grapevine. *Scientific Reports*, 5(1), 12449.
<https://doi.org/10.1038/srep12449>
- Toreti, A., Masante, D., Acosta Navarro, J., Bavera, D., Cammalleri, C., de Jager, A., di Ciollo, C., Hrast Essenfelder, A., Maetens, W., Magni, D., Mazzeschi, M., Spinoni, J., & de Felice, M. (2022). *Drought in Europe July 2022*. <https://doi.org/10.2760/014884>
- Trugman, A. T., Detto, M., Bartlett, M. K., Medvigy, D., Anderegg, W. R. L., Schwalm, C., Schaffer, B., & Pacala, S. W. (2018). Tree carbon allocation explains forest drought-kill and recovery patterns. *Ecology Letters*, 21(10), 1552–1560.
<https://doi.org/10.1111/ele.13136>
- Tsamir-Rimon, M., Ben-Dor, S., Feldmesser, E., Oppenheimer-Shaanan, Y., David-Schwartz, R., Samach, A., & Klein, T. (2021). Rapid starch degradation in the wood of olive trees under heat and drought is permitted by three stress-specific beta amylases. *New Phytologist*, 229(3), 1398–1414. <https://doi.org/10.1111/nph.16907>
- Urli, M., Porte, A. J., Cochard, H., Guengant, Y., Burlett, R., & Delzon, S. (2013). Xylem embolism threshold for catastrophic hydraulic failure in angiosperm trees. *Tree Physiology*, 33(7), 672–683. <https://doi.org/10.1093/treephys/tpt030>
- Usman, M., Ho-Plágaro, T., Frank, H. E. R., Calvo-Polanco, M., Gaillard, I., Garcia, K., & Zimmermann, S. D. (2021). Mycorrhizal Symbiosis for Better Adaptation of Trees to Abiotic Stress Caused by Climate Change in Temperate and Boreal Forests. *Frontiers in Forests and Global Change*, 4. <https://doi.org/10.3389/ffgc.2021.742392>
- van der Molen, M. K., Dolman, A. J., Ciais, P., Eglin, T., Gobron, N., Law, B. E., Meir, P., Peters, W., Phillips, O. L., Reichstein, M., Chen, T., Dekker, S. C., Doubková, M., Friedl, M. A., Jung, M., van den Hurk, B. J. J. M., de Jeu, R. A. M., Kruijt, B., Ohta, T., ... Wang, G. (2011). Drought and ecosystem carbon cycling. *Agricultural and Forest Meteorology*, 151(7), 765–773. <https://doi.org/10.1016/j.agrformet.2011.01.018>
- Venturas, M. D., Todd, H. N., Trugman, A. T., & Anderegg, W. R. L. (2021). Understanding and predicting forest mortality in the western United States using long-term forest inventory data and modeled hydraulic damage. *New Phytologist*, 230(5), 1896–1910.
<https://doi.org/10.1111/nph.17043>
- Villarino, S. H., Pinto, P., Jackson, R. B., & Piñeiro, G. (2021). Plant rhizodeposition: A key factor for soil organic matter formation in stable fractions. *Science Advances*, 7(16).
<https://doi.org/10.1126/sciadv.abd3176>
- Vilonen, L., Ross, M., & Smith, M. D. (2022). What happens after drought ends: synthesizing terms and definitions. *New Phytologist*. <https://doi.org/10.1111/nph.18137>
- Walthert, L., Ganthaler, A., Mayr, S., Saurer, M., Waldner, P., Walser, M., Zweifel, R., & von Arx, G. (2021). From the comfort zone to crown dieback: Sequence of physiological stress thresholds in mature European beech trees across progressive drought. *Science of The Total Environment*, 753, 141792. <https://doi.org/10.1016/j.scitotenv.2020.141792>
- Wilkinson, S., & Davies, W. J. (2002). ABA-based chemical signalling: the co-ordination of responses to stress in plants. *Plant, Cell & Environment*, 25(2), 195–210.
<https://doi.org/10.1046/j.0016-8025.2001.00824.x>

- Winkler, A., & Oberhuber, W. (2017). Cambial response of Norway spruce to modified carbon availability by phloem girdling. *Tree Physiology*, 37(11), 1527–1535. <https://doi.org/10.1093/treephys/tpx077>
- Woodruff, D. R. (2014). The impacts of water stress on phloem transport in Douglas-fir trees. *Tree Physiology*, 34(1), 5–14. <https://doi.org/10.1093/treephys/tpt106>
- Yandigeri, M. S., Meena, K. K., Singh, D., Malviya, N., Singh, D. P., Solanki, M. K., Yadav, A. K., & Arora, D. K. (2012). Drought-tolerant endophytic actinobacteria promote growth of wheat (*Triticum aestivum*) under water stress conditions. *Plant Growth Regulation*, 68(3), 411–420. <https://doi.org/10.1007/s10725-012-9730-2>
- Yin, J., & Bauerle, T. L. (2017). A global analysis of plant recovery performance from water stress. *Oikos*, 126(10), 1377–1388. <https://doi.org/10.1111/oik.04534>
- Zang, U., Goisser, M., Grams, T. E. E., Haberle, K.-H., Matyssek, R., Matzner, E., & Borken, W. (2014). Fate of recently fixed carbon in European beech (*Fagus sylvatica*) saplings during drought and subsequent recovery. *Tree Physiology*, 34(1), 29–38. <https://doi.org/10.1093/treephys/tpt110>
- Zhou, S.-X., Prentice, I. C., & Medlyn, B. E. (2019). Bridging Drought Experiment and Modeling: Representing the Differential Sensitivities of Leaf Gas Exchange to Drought. *Frontiers in Plant Science*, 9. <https://doi.org/10.3389/fpls.2018.01965>
- Zhu, J., Thimonier, A., Etzold, S., Meusburger, K., Waldner, P., Schmitt, M., Schleppei, P., Schaub, M., Thormann, J.-J., & Lehmann, M. M. (2022). Variation in Leaf Morphological Traits of European Beech and Norway Spruce Over Two Decades in Switzerland. *Frontiers in Forests and Global Change*, 4. <https://doi.org/10.3389/ffgc.2021.778351>
- Zweifel, R., Etzold, S., Sterck, F., Gessler, A., Anfodillo, T., Mencuccini, M., von Arx, G., Lazzarin, M., Haeni, M., Feichtinger, L., Meusburger, K., Knuesel, S., Walthert, L., Salmon, Y., Bose, A. K., Schoenbeck, L., Hug, C., de Girardi, N., Giuggiola, A., ... Rigling, A. (2020). Determinants of legacy effects in pine trees – implications from an irrigation-stop experiment. *New Phytologist*, 227(4), 1081–1096. <https://doi.org/10.1111/nph.16582>
- Zwetsloot, M. J., & Bauerle, T. L. (2021). Repetitive seasonal drought causes substantial species-specific shifts in fine-root longevity and spatio-temporal production patterns in mature temperate forest trees. *New Phytologist*, 231(3), 974–986. <https://doi.org/10.1111/nph.17432>

7. Acknowledgements

First of all, I would like to thank my supervisor, Thorsten E. E. Grams, for giving me the opportunity for this PhD study, and for his generous supports during field work, data interpretation, and revising manuscripts whenever I needed it. I also thank Karin Pritsch for being my great mentor and for invaluable advices.

I thank the members of the ecophysiology, KROOF, and LSAI team: Benjamin D. Hesse and Timo Gebhardt for their support during the field work in Kranzberg even in the night and during weekends, for many invaluable discussions and suggestions; Benjamin D. Hafner for his support and advices especially during the initial phase of my PhD, Jasmin Danzberger for the great cooperation during field work in Kranzberg and Helmholtz Zentrum, for many intensive discussions; Vincent P. Riedel, Karl-Heinz Häberle, Fabian Weigl, Bálint Georg Jákli, Manuela Baumgarten, David Dluhosch, my other co-authors, and the other members of LSAI team for great cooperation and discussion. My thanks also go to Rainer Matyssek and Takayoshi Koike who supervised my bachelor thesis, which became the trigger and the starting point of my research career at the ecophysiology team.

I highly appreciate technical supports during the experiments and data collections. I thank Thomas Feuerbach for his generous support especially for assembling and maintenance of the ^{13}C labeling system even in the night, during weekends and holidays. Many thanks also go to Yessica Stengele, Sepp Heckmair, Barbara Hoffmann, Peter Kuba, Franz Buegger, Horst Bachmeier, Roman Meier, Anna Ullmann, master/bachelor students, and student helpers (Hiwi) for their great support during field works and lab works. I also thank Martina Harnisch and Karin Beerbaum for all the administrative works they did for me.

I acknowledge TUM Graduate School in Weihenstephan, and Deutsche Forschungsgemeinschaft for the financial support, which enabled the project and my PhD study.

Finally, special thanks go to my family for supporting me anytime despite the large physical distance and time difference. I also thank my flatmates and friends in Freising and everywhere in the world for spending great time together.

8. Appendix

- Chapter I (draft)
- Chapter II (submitted)
- Chapter III (published)
- Chapter IV (published)

1 **Title**

2 Physiological and morphological acclimation of mature trees to five years of experimental
3 summer drought at the leaf and crown level

4 **Running Title**

5 Water consumption under repeated drought in mature beech and spruce

6 **List of Authors:**

7 Benjamin D. Hesse^{1*}, Kyohsuke Hikino^{1*}, Timo Gebhardt^{1,2*}, Florian Motte³, Thomas
8 Rötzer³, Fabian Weigl¹, Karin Pritsch⁴, Benjamin D. Hafner⁵, Hans Pretzsch³, Karl-Heinz
9 Häberle⁶, and Thorsten E.E. Grams¹

10 * These authors have contributed equally to this work and share the first authorship

11 **Authors' affiliation**

12 1. Technical University of Munich, School of Life Sciences, Land Surface-Atmosphere
13 Interactions, Hans-Carl-von-Carlowitz Platz 2, 85354 Freising, Germany.

14 2. Technical University of Munich, School of Life Sciences, Forest and Agroforest
15 Systems, Hans-Carl-von-Carlowitz Platz 2, 85354 Freising, Germany.

16 3. Technical University of Munich, School of Life Sciences, Chair for Forest Growth and
17 Yield Science, Hans-Carl-von-Carlowitz-Platz 2, 85354 Freising, Germany.

18 4. Institute of Biochemical Plant Pathology, German Research Center for Environmental
19 Health, Helmholtz Zentrum München, Ingolstaedter Landstr. 1, Neuherberg 85764
20 Germany.

21 5. Cornell University, School of Integrative Plant Science, 236 Tower Road, Ithaca, NY
22 14853, USA

23 6. Technical University of Munich, School of Life Sciences, Chair of Restoration Ecology,
24 Emil-Ramann-Str. 6, 85354 Freising, Germany.

25 **Abstract**

26 As a consequence of the ongoing climate change, global forests have been suffering from severe
27 natural drought, causing immense growth decline and tree mortality. Since frequency and
28 duration of drought events are predicted to increase, ability to acclimate to a long-term and
29 repeated drought is crucial for tree survival. To elucidate long-term physiological and
30 morphological responses of mature Norway spruce (*Picea abies* [L.] KARST.) and European
31 beech (*Fagus sylvatica* L.) to repeated drought, we conducted detailed analyses of leaf and
32 whole-tree level physiology and morphology during five years of experimental summer drought.
33 We thereby measured predawn leaf water potential, leaf gas exchange, sap flow density, whole-
34 tree water consumption, and morphological parameters such as shoot growth and total leaf area.
35 In accordance with the iso- and anisohydric framework, more isohydric spruce reduced their
36 water consumption more strongly than more anisohydric beech, through more drought-sensitive
37 stomatal control as a first drought response. As a long-term response starting from the third
38 drought year, only spruce trees reduced their total leaf area by more than 50% through
39 production of shorter shoots and needles. This response led to a significant decrease in leaf to
40 sapwood area ratio in spruce after the third drought year, which ensures higher water transport
41 capacity per leaf area. Indeed, drought effect on leaf gas exchange and sap flow density became
42 smaller after the reduction of the total leaf area. Thus, under repeated drought, reduction in the
43 total leaf area regulated the leaf and whole-tree physiology in spruce, in addition to the strong
44 stomatal control. However, the reduction of spruce leaf area cannot be quickly reversed, limiting
45 water consumption and carbon uptake even after drought release. Therefore, further studies are
46 needed to elucidate the long-term consequences of the morphological drought acclimation on
47 tree performance under future climate change.

48 **Keywords:**

49

50 **Introduction**

51 Forests cover around 30% of the global terrestrial area and their conditions have direct impacts
52 on global climate and human society (Alkama & Cescatti, 2016; Foley et al., 2005; IPCC, 2019).

53 Trees are exposed to various environmental stress in their lifetime. Recently, global forests have
54 been experiencing immense tree dieback due to severe drought (Allen et al., 2010; Hammond
55 et al., 2022; Hartmann et al., 2018; Schuldt et al., 2020), and the frequency and duration of
56 drought events are predicted to further increase (IPCC, 2021). Thus, tree survival and
57 productivity depend not only on the extent of drought impact on tree function but also on the
58 ability to adjust to prolonged and frequent water-limiting conditions (Limousin et al., 2013).

59 It is well known that drought negatively affects tree function by a decrease in water use, carbon
60 uptake, and growth (Ciais et al., 2005; Hartmann et al., 2018; Peñuelas et al., 2011; Pretzsch,
61 Rötzer, et al., 2014). Partial to complete stomatal closure is one of the first tree reactions to deal
62 with a drought (Choat et al., 2018; Cochard et al., 1996; Limousin et al., 2009). Stomatal
63 behavior is expressed as a continuum associated with the level of isohydry (Allen et al., 2010;
64 Hartmann et al., 2021; Tardieu & Simonneau, 1998). Isohydry species close stomata already at
65 the early phase of drought to maintain midday plant water potential. In contrast, anisohydry
66 species keep stomata longer open, allowing midday water potential to decline. While the early
67 stomatal closure of isohydry species minimizes the risk of hydraulic failure, this response
68 restricts C uptake and may cause a C depletion under a persisting drought. A more anisohydry
69 strategy on the contrary allows plants to continuously assimilate C but at a higher risk of
70 hydraulic failure (McDowell et al., 2008). The different strategies also affect the transport of
71 water within the tree, similarly to the stomatal opening, by a stronger decrease of xylem sap
72 flow density in the sapwood and tree water consumption under drought in more isohydry
73 species than in more anisohydry species (Li et al., 2019). To what extent the single strategies
74 change under repeated drought is not well known, as tree responses to long-term and repeated

75 drought seem to be non-linear due to their adjustment to new environmental conditions (Barbeta
76 et al., 2013; Beier et al., 2012; Feichtinger et al., 2014; Leuzinger et al., 2011; Liu et al., 2015).
77 In addition to the stomatal regulation, morphological and/or anatomical acclimation are to be
78 expected as revealed by greenhouse and field analyses in mostly juvenile plants (e.g. Brodribb
79 et al., 2020; Brunner et al., 2015), whereas the corresponding acclimation of mature trees to
80 repeated drought is hardly studied.

81 Recent observations highlight the importance of leaf morphology and leaf area for controlling
82 water loss, in addition to stomatal control (Adams et al., 2015; Guérin et al., 2018; Limousin et
83 al., 2009; Pritzkow et al., 2021; Schönbeck et al., 2018; Zweifel et al., 2020). Modification in
84 leaf thickness (Flexas et al., 2006; Meier & Leuschner, 2008; Reich et al., 1997) and/or
85 reduction in total leaf area (LA), mostly induced by leaf shedding (Ambrose et al., 2018;
86 Barbeta & Peñuelas, 2016; Galiano et al., 2011; Limousin et al., 2009; Poyatos et al., 2013),
87 can balance the reduced water uptake and transpiration loss under drought (Bréda et al., 2006;
88 Pritzkow et al., 2021; Schönbeck et al., 2018; Trugman et al., 2018). To what extent
89 modifications of the morphology occur in other tree organs (e.g. branch or stem) has rarely been
90 studied under repeated drought (Petit et al., 2022). Barbeta & Peñuelas (2016) suggest that
91 changes in the LA are not necessarily reflected in the sapwood area of the stem (SA), therefore
92 altering the leaf area to sapwood area ratio (LA/SA) (Limousin et al., 2009, 2012; McBranch
93 et al., 2019; Moreno et al., 2021). However, reductions in stem growth under repeated drought
94 (Pretzsch et al., 2020) might additionally affect the LA/SA, to a more stable level as suggested
95 by allometric relationships (Forrester et al., 2017). Yet, a large part of the studies so far was
96 conducted under either short-term/seasonal drought or using precipitation gradient. To date,
97 there are only a few experiments investigating responses of mature trees under a multi-year
98 drought, either with throughfall exclusion (Grossiord et al., 2017; Guérin et al., 2018; Limousin
99 et al., 2009) or after irrigation in naturally dry forests (Bose et al., 2022).

100 In forest ecosystems in Central Europe, Norway spruce (*Picea abies* [L.] KARST.) and
101 European beech (*Fagus sylvatica* L.) are two dominant tree species, accounting for 30% of the
102 forest areas (Pretzsch, Biber, et al., 2014). While spruce deploys a more isohydric strategy and
103 closes stomata earlier (Hartmann et al., 2013; Oberhuber et al., 2015), beech shows a more
104 anisohydric strategy (Leuschner, 2020; Magh et al., 2019), maintaining C assimilation under
105 drought. Although saplings and/or young trees of both species were affected by short-term
106 drought in photosynthesis and transpiration (Gallé & Feller, 2007; Goisser et al., 2013; Kurjak
107 et al., 2012; Střelcová et al., 2013), long-term observations of leaf/tree physiology/morphology
108 and water consumption under prolonged drought are still rare in mature forest stands in central
109 Europe (Oberleitner et al., 2022; Schönbeck et al., 2022).

110 To fill this knowledge gap, the Kranzberg roof (KROOF) project with rainfall exclusion started
111 in 2014 in Kranzberg Forest in Southern Germany (Grams et al., 2021). Both species were
112 subjected to a prolonged drought during entire growing seasons for five consecutive years from
113 2014 to 2018. Taking advantage of this unique precipitation manipulation experiment applying
114 to the two dominant species in Central Europe, we investigated their long-term physiological
115 and morphological responses to a prolonged drought predicted in the future. Given the above
116 mentioned reports and the body of literature, we tested the following hypotheses.

117 [H1] Spruce reduces water consumption more than beech due to stronger stomatal control as a
118 first drought response in line with their more isohydric and anisohydric strategies, respectively.

119 [H2] Under repeated drought, water consumption of both species is reduced not only by
120 stomatal control but also by morphological acclimation.

121 **Materials & Methods**

122 *Experimental Site*

123 This study was conducted in a mixed forest with c. 70-year-old Norway spruce (*P. abies* [L.]
124 KARST.) and c. 90-year-old European beech trees (*F. sylvatica* L.), located in southern
125 Germany/Bavaria (11°39'42"E, 48°25'12"N; 490 m a.s.l.). On this site, a long-term throughfall
126 exclusion experiment (Kranzberg roof project, KROOF) was initiated in 2014, which has been
127 described earlier (Grams et al., 2021, also weather data). Briefly, this experimental site consists
128 of 12 plots (110 - 220 m²) with 4-6 beech trees on one side and 4-6 spruce trees on the other
129 side of each plot. In 2010, all plots were trenched to 1 m of soil depth to prevent trees from
130 taking up the water outside the plots (Pretzsch, Rötzer, et al., 2014). Six plots are equipped with
131 roofs underneath the canopy to exclude the throughfall of precipitation (throughfall exclusion
132 plots, TE) and the other six plots are without roofs and defined as control plots (CO). Both tree
133 species in the TE plots were exposed to complete throughfall exclusion during the entire
134 growing seasons for five consecutive years from 2014 to 2018. The roofs were kept open during
135 precipitation events after the growing season until next spring. A canopy crane next to the plots
136 allowed detailed analyses of physiology and morphology in the canopy.

137 *Measurement of volumetric soil water content and predawn leaf water potential*

138 Soil moisture was recorded weekly using Time Domain Reflectometry (TDR100, Campbell
139 Scientific, Logan, CT, USA). The sensors are buried at three positions per plot in four depths:
140 0–7 cm, 10–30 cm, 30–50 cm, and 50–70 cm (for details see Grams et al. 2021). Relative
141 extractable water (REW) was calculated using soil water content at saturation (Hesse et al.,
142 2019) and permanent wilting point (Grams et al., 2021). Predawn leaf water potential (Ψ_{PD} in
143 MPa) of sun-exposed twigs was assessed on sunny days in July/August before sunrise (3 am –
144 5 am CET) with a Scholander pressure bomb (mod. 1505D, PMS Instrument Co., Albany, OR,
145 USA) on 6 to 8 individuals per species and treatment.

146 *Measurement of mean daily xylem sap flow density*

147 Xylem sap flow density per unit sapwood area was measured with Granier-type heat dissipation
148 sensors (Granier, 1987) in 10 min intervals. At breast height, sap flow was measured in the outer
149 xylem sapwood (0-2cm depth) with two sensors (north and south exposure). Data from both
150 sensors were averaged and the mean sap flow density per day and tree was calculated (u_{daily} in
151 $\text{L dm}^{-2} \text{ d}^{-1}$). Sap flow density was measured from April to November in spruce and from May
152 to October in beech for all years and in 8 to 10 individuals per species and treatment.

153 *Calculation of the annual whole-tree water use*

154 Whole tree water consumption was calculated by the xylem sapflow density profiles measured
155 on 4-6 trees per species and treatment of the same experiment (Gebhardt et al., submitted). U_{daily}
156 data were weighted in accordance with the xylem sap flow profile for each 1 cm ring of sapwood
157 (e.g. 0-1 cm, 1-2, ..., 7-8 cm), multiplied with the respective sapwood area annulus and summed
158 up over all 8 cm to calculate the whole tree daily water consumption (in L). For the measured
159 trees the conducting sapwood depth has been shown to be around 8 cm (Gebhardt et al.,
160 submitted) and did not change due to the five years of the recurrent drought event.

161 *Measurements of leaf gas exchange rates*

162 Light saturated gas exchange rates at 400 ppm CO_2 (A_{sat}) and stomatal conductance to water
163 vapor (g_s) were determined on sun-exposed twigs using the open gas exchange system LI-6800
164 and LI-6400 (Li-Cor Inc., Lincoln, NE, USA). We limited the measurement time between
165 around 9 and 15 (CET). For beech, we selected 3-5 intact sun-exposed leaves from each tree.
166 For spruce, 2-3 twigs with one-year-old needles per tree were randomly chosen. In TE, however,
167 annual branch growth was not always sufficiently long to cover the gas exchange chamber, so
168 needles from the previous years sometimes had to be taken into account. During the
169 measurements, we set the light intensity (PPFD) to $1500 \mu\text{mol m}^{-2} \text{ s}^{-1}$ to saturate CO_2 uptake

170 and kept the leaf temperature at 25 °C. The relative humidity was set around 60-65%. Gas
171 exchange measurements were performed on 6 to 8 individuals per species and treatment.

172 Needles of spruce used for the gas exchange measurements were collected after each growing
173 season and immediately scanned (Epson Perfection 4990 Photo, Epson Deutschland GmbH,
174 Meerbusch, Germany). The projected leaf area was determined using software Image J (version
175 1.53a, National Institute of Health, USA), which was then multiplied by a factor of 3.2 to
176 calculate the total leaf area (Goisser et al., 2016; Homolová et al., 2013).

177 *Measurements of specific leaf area and shoot length growth*

178 Specific leaf area (SLA in cm² g⁻¹), and shoot length growth were recorded annually for both
179 species. For SLA, 5-10 beech leaves or c. 150 spruce needles in sun crowns were harvested,
180 scanned (Epson Perfection 4990 Photo), dried for 72 h at 64 °C, and weighed. The projected
181 leaf area was determined using software Image J. The leaf size of beech trees was thereby also
182 recorded.

183 For shoot length growth, 4-6 branches per tree in sun crowns were randomly selected and
184 measured. For spruce, needle length (mm) and density (n cm⁻¹) were additionally measured in
185 sun crowns. Needle length was recorded with randomly selected 4-6 needles from different
186 branches. Needle density was determined by counting the needles and shoot length. All
187 measurements were performed on 6 to 8 trees per species and treatment.

188 *Estimation of leaf area*

189 *Spruce*

190 The leaf area of spruce was calculated for all years on 3 (for CO) and 6 (for TE) trees (see
191 Gebhardt et al., (submitted) for details). Briefly, total number of needles of each needle age (N_n)
192 was calculated using field data, separately for sun and shade crowns.

$$193 \quad N_n = N_s \times L_b \times L_s \times D,$$

194 where N_s represents the number of shoots of each needle age (in $n \text{ cm}^{-1}$ needled branch length),
 195 L_b the total length of the needled branches (in cm), L_s the length of each shoot (in cm), and D
 196 the needle density in each shoot (in $n \text{ cm}^{-1}$). Then, the total leaf area of each needle age (A_n in
 197 m^2) was calculated using needle length (L_n in mm) following Riederer et al. (1988).

$$198 \quad A_n = \frac{N_n \times (3.279 \times L_n - 16.31)}{1000000} \text{ (for current year needles)}$$

$$199 \quad A_n = \frac{N_n \times (4.440 \times L_n - 24.78)}{1000000} \text{ (for older needles)}$$

200 Finally, A_n was summed up to determine the total leaf area (LA).

201 *Beech*

202 To estimate the total leaf biomass of beech trees, litter bags were equipped below the canopy
 203 base in two positions per plot (4 plots per treatment), in the middle of spruce and beech tree
 204 groups. Five litter bags (0.25 m^2 each) were arranged in each tree group and they were collected
 205 every 1 - 4 months. The collected beech leaves were sorted, dried and weighed. Beech leaves
 206 found in the bags below the spruce tree groups were considered to derive from the beech trees
 207 in the same plot. We calculated the mean dry leaf biomass per bag/plot, reflecting the leaf
 208 biomass per 0.25 m^2 projected canopy area. The projected canopy area (CA) of each tree was
 209 estimated using the mean canopy radius (CR_{mean}), calculated from eight canopy radii as
 210 followed (Pretzsch, 2019).

$$211 \quad CR_{mean} = \sqrt{\frac{CR_i^2 + CR_{ii}^2 + CR_{iii}^2 + CR_{iv}^2 + CR_v^2 + CR_{vi}^2 + CR_{vii}^2 + CR_{viii}^2}{8}}$$

212 where CR_N is the eight canopy radii measured on site.

213 Then, the projected canopy area (CA) was calculated:

$$214 \quad CA = \pi * CR_{mean}^2$$

215 Mean dry leaf biomass per litterbag was then extrapolated to the mean CA of all trees in each
216 plot and converted to leaf area using SLA determined above.

217 *Statistics*

218 Data were analyzed using R (version 4.0.3) in R studio (version 1.3.1093). Ψ_{PD} , annual water
219 consumption, leaf gas exchange, and morphology were tested with a linear mixed model using
220 the year (2013-2018) and the treatment (CO and TE) as fixed and the tree number and the plot
221 as a random effect (package: nlme, version: 3.1-151). Normality of the residuals (Shapiro test)
222 and homogeneity of variances (Levene test) was tested for every model. If any fixed factor was
223 significant, post-hoc test with Tukey correction (package: lsmeans, version: 2.30-0) was
224 performed. The relationship between U_{daily} and Ψ_{PD} was tested with a linear regression after
225 exponential transformation of Ψ_{PD} . All the errors in the text and graphics refer to the standard
226 error of the mean (SE) unless otherwise noted.

227 **Results**

228 *Relative extractable water (REW) and predawn leaf water potential (Ψ_{PD})*

229 Relative extractable water (REW) averaged over 0-70 cm soil depths significantly decreased
230 through throughfall exclusion already in the first drought year 2014 (Fig 1a). Mean REW under
231 TE trees between April and September were 24.2 ± 0.9 , 13.0 ± 0.4 , 18.9 ± 0.5 , 26.0 ± 0.7 , and
232 $18 \pm 0.6\%$ in 2014, 2015, 2016, 2017, and 2018, which were all significantly lower than that
233 under CO trees (38.1 ± 0.7 , 43.4 ± 0.7 , 51.6 ± 0.6 , 43.3 ± 0.6 , and $40.2 \pm 0.6\%$, respectively).
234 In the first drought year (2014), Ψ_{PD} of TE beech (-0.62 ± 0.02 MPa) was only slightly lower
235 than those of CO (-0.44 ± 0.02 MPa, Fig. 1b). Ψ_{PD} of TE beech significantly decreased in the
236 second drought year 2015 to -1.28 ± 0.06 MPa, compared to the CO beech with -0.80 ± 0.05
237 MPa. In 2016, Ψ_{PD} of TE beech remained significantly (2016, with -0.67 ± 0.02 MPa) and in

238 2018 insignificantly (-0.54 ± 0.06 MPa) lower than that of CO beech (2016: -0.35 ± 0.02 MPa,
239 2018: -0.41 ± 0.02 MPa).

240 In contrast, TE spruce already significantly lowered their Ψ_{PD} in the first drought year 2014 to
241 -1.39 ± 0.05 MPa compared to CO spruce with -0.89 ± 0.06 MPa (Fig. 1c). In the second
242 drought year, the difference between treatments became larger (CO: -0.96 ± 0.04 , TE: $-1.60 \pm$
243 0.05 MPa). In 2016 and 2018, Ψ_{PD} of TE spruce remained significantly lower (-0.94 ± 0.06 and
244 -0.89 ± 0.07 MPa) than that of CO spruce with -0.56 ± 0.02 and -0.58 ± 0.04 MPa.

245 *Annual whole-tree water use*

246 Annual whole-tree water use of spruce trees was more strongly reduced under drought than that
247 of beech (Fig. 2). TE spruce already significantly reduced their water use in 2014 to 1147 ± 146
248 $L\ year^{-1}$, by more than 60% compared to CO spruce with $3065 \pm 456\ L\ year^{-1}$. In the following
249 drought years, water use of TE spruce remained rather constant (895 ± 108 , 933 ± 123 , and
250 $1203 \pm 173\ L\ year^{-1}$ in 2015, 2016, and 2018) and significantly lower than that of CO spruce
251 (2942 ± 451 , 3290 ± 335 , and $3342 \pm 373\ L\ year^{-1}$, respectively). In contrast, TE beech only
252 slightly reduced their annual water use throughout the drought years by 10-35% (not
253 significant). TE beech consumed 3366 ± 542 , 3849 ± 671 , 5324 ± 1336 , and 4411 ± 803 in 2014,
254 2015, 2016, and 2018, which was slightly lower than the water use of CO beech (3946 ± 574 ,
255 5874 ± 849 , 6582 ± 1129 , and 4828 ± 763 , respectively).

256 *Stomatal conductance and assimilation rate at the leaf level*

257 The stronger drought effect on annual water use of spruce compared to beech can be first
258 explained by the leaf-level physiology. In the first drought year (2014), TE beech significantly
259 lowered light-saturated assimilation rates (A_{sat}) and stomatal conductance (g_s) (TE: 10.9 ± 0.8
260 $\mu mol\ m^{-2}\ s^{-1}$ and $122 \pm 12\ mmol\ m^{-2}\ s^{-1}$, Fig. 3) by 19% and 36% compared to CO beech (CO:
261 $13.3 \pm 0.5\ \mu mol\ m^{-2}\ s^{-1}$ and $192 \pm 16\ mmol\ m^{-2}\ s^{-1}$). In the second drought year (2015), these

262 decreases under drought became larger by 36% (CO: 9.5 ± 0.5 and TE: $6.1 \pm 0.5 \mu\text{mol m m}^{-2} \text{s}^{-1}$) and 49% (CO: 97 ± 8 and TE: $50 \pm 5 \text{ mmol m}^{-2} \text{s}^{-1}$), respectively. After TE beech showed the
263 minimum A_{sat} and g_s in 2015, both parameters increased close to the level of CO trees, reflected
264 by the non-significant treatment effect in 2017 and 2018. Compared to beech, spruce exhibited
265 a larger drought effect. Drought treatment significantly reduced A_{sat} and g_s of TE spruce in the
266 first two drought years by up to 85% (A_{sat} : -60% in 2014 and -83% in 2015, g_s : -66% in 2014
267 and -84% in 2015). In the fifth drought year (2018), the differences between CO and TE spruce
268 became smaller (A_{sat} : -55%, g_s : -63%), although they were still significant.
269

270 *Xylem sap flow density at outer 2 cm sapwood*

271 Similar trend was also observed in the xylem sap flow density. In TE beech in 2014, annual
272 average of mean sap flow density per day at outer 2cm sapwood (u_{daily}) was $5.36 \pm 0.09 \text{ L dm}^{-2} \text{ d}^{-1}$,
273 which was only slightly lower than that of CO beech with $6.29 \pm 0.08 \text{ L dm}^{-2} \text{ d}^{-1}$ (Table 1,
274 for the detailed course of u_{daily} , see Fig. S1). In the following drought years, TE beech
275 continuously but insignificantly showed lower annual average of u_{daily} (5.90 ± 0.08 , 7.98 ± 0.10 ,
276 and $6.96 \pm 0.08 \text{ L dm}^{-2} \text{ d}^{-1}$ in 2015, 2016, and 2018) by 10-30% than CO beech with $9.12 \pm$
277 0.12 , 10.18 ± 0.15 , and $7.69 \pm 0.09 \text{ L dm}^{-2} \text{ d}^{-1}$, respectively. In contrast, u_{daily} of spruce was
278 significantly reduced (Table 1). Already in the first drought year in 2014, annual average of
279 u_{daily} was $1.35 \pm 0.03 \text{ L dm}^{-2} \text{ d}^{-1}$ in TE spruce, which was 60% lower than that of CO spruce
280 with $3.30 \pm 0.05 \text{ L dm}^{-2} \text{ d}^{-1}$. In the following drought years, u_{daily} of TE spruce remained
281 significantly lower by up to 65% reduction (1.11 ± 0.02 and 1.43 ± 0.03 in 2015 and 2016)
282 compared to that of CO spruce (3.15 ± 0.05 and 3.58 ± 0.05 , respectively). However, the
283 difference between treatment became smaller in the last drought year 2018 (1.71 ± 0.03 in TE
284 and $3.48 \pm 0.04 \text{ L dm}^{-2} \text{ d}^{-1}$ in CO).

285 Furthermore, u_{daily} was positively correlated with Ψ_{PD} in both species (Fig. 4). After the
286 exponential transformation of Ψ_{PD} , spruce showed a steeper slope (12.7) and a smaller intercept

287 (-1.9) compared to beech with 12.2 and 3.2, respectively. Thus, spruce showed more stronger
288 decrease of sap flow density with decreasing Ψ_{PD} .

289 *Morphology at the branch and leaf-level*

290 *Branch length growth*

291 Before the onset of the drought treatment in 2013, later CO and TE trees of beech showed
292 similar shoot length growth (CO: 27.8 ± 1.9 cm, TE: 31.1 ± 2.1 cm, data not shown), which
293 remained similar in the first drought year (2014, Fig. 5a). Drought effect was observed after the
294 second drought year (2015). TE beech significantly reduced shoot length growth by 58% (CO:
295 30.5 ± 2.9 cm, TE: 17.7 ± 1.6 cm). In the following three drought years, TE beech remained
296 significantly lower with similar relative reductions (13.3 ± 1.1 , 11.8 ± 1.5 , and 15.8 ± 3.0 cm)
297 than CO beech (29.0 ± 1.8 , 35.9 ± 0.9 , and 27.1 ± 2.1 cm).

298 Similarly to beech, spruce showed the first drought effect in the second drought year (2015,
299 Fig. 5b) with 40% lower length growth (8.0 ± 1.4 cm) than that of CO spruce (13.6 ± 1.0 cm).
300 During the following three drought years, shoot length growth of TE spruce remained
301 significantly smaller (4.2 ± 0.9 , 5.4 ± 0.8 and 7.3 ± 0.8 cm) than that of CO spruce (13.9 ± 0.9 ,
302 17.8 ± 1.4 and 14.1 ± 1.1 cm).

303 *Leaf morphology*

304 Leaf size was similar between treatments in the second and fifth drought years (Fig. 5c). In
305 2016, TE beech had significantly smaller leaves with 13 ± 1 cm² than CO beech with 19 ± 1
306 cm². SLA of beech was not affected by drought treatments, although the values varied among
307 years (112 ± 4 and 117 ± 3 cm² g⁻¹ in 2015, 88 ± 2 and 94 ± 4 cm² g⁻¹ in 2016, 102 ± 4 and 106
308 ± 8 cm² g⁻¹ in 2018, for CO and TE, respectively, Fig S2a).

309 Similarly, spruce did not change SLA throughout the drought years, although the TE spruce
310 showed insignificantly higher SLA in 2015 (32.5 ± 2.6 cm² g⁻¹) than CO spruce (29.0 ± 0.4 cm²

311 g^{-1} , Fig. S2b). In the other years, SLA varied between 27 and 32 $\text{cm}^2 \text{g}^{-1}$ in both treatments. In
312 contrast, needle lengths of TE spruce significantly decreased in the second drought year (9 ± 1
313 mm) and remained significantly smaller in the following drought years (10 ± 1 , 11 ± 1 and 11
314 ± 1 mm in 2016, 2017 and 2018) than those of CO spruce (remained constant around 15 ± 1
315 mm, Fig 5d).

316 *Total leaf area of beech*

317 LA of beech estimated from litterbag data indicates no significant reduction (Fig. 5e), although
318 TE beech produced a slightly smaller LA each year (123 ± 37 , 129 ± 29 , and $111 \pm 49 \text{ m}^2 \text{ tree}^{-1}$
319 1 in 2015, 2016, and 2017), compared to CO beech with 171 ± 43 , 151 ± 38 , and $153 \pm 42 \text{ m}^2$
320 tree^{-1} , respectively.

321 *Total leaf area of spruce*

322 Modification in leaf and branch growth led to a significant reduction in the total leaf area (LA,
323 Fig. 5f). In the first drought year, the total leaf area of TE spruce trees was $468 \pm 54 \text{ m}^2 \text{ tree}^{-1}$
324 which was similar to that of CO trees with $447 \pm 146 \text{ m}^2 \text{ tree}^{-1}$. However, in the third drought
325 year, TE spruce trees started to reduce their total leaf area ($277 \pm 32 \text{ m}^2 \text{ tree}^{-1}$) due to smaller
326 shoot and needle length. Then, the total leaf area of TE trees remained significantly by 60-70%
327 lower with 188 ± 30 and $172 \pm 32 \text{ m}^2 \text{ tree}^{-1}$ in 2017 and 2018 compared to that of CO trees with
328 458 ± 136 and $501 \pm 139 \text{ m}^2 \text{ tree}^{-1}$.

329 **Discussion**

330 *Spruce reduced water consumption more than beech under repeated drought through stronger* 331 *stomatal regulation as a first drought response*

332 During the drought period, relative extractable water (REW) was significantly lower under TE
333 trees compared to CO trees (Fig 1). Accordingly, TE trees of both species experienced a
334 predawn leaf water potential of as low as -1.8 MPa (Fig. 1), i.e. high water stress according to

335 Walthert et al. (2021). Compared to beech, spruce trees reduced their water consumption more
336 strongly under repeated drought (Fig. 2), confirming H1 that spruce would show stronger
337 drought effect. These responses are in line with the different water management strategies
338 between more anisohydric beech and more isohydric spruce, mostly determined with young
339 trees (Hartmann et al., 2021). As a first reaction to the drought, both species regulated stomatal
340 opening (Fig. 3) and reduced sap flow density (Table 1, Fig. S1), which is in line with previous
341 reports under seasonal drought in beech (Lüttschwager & Jochheim, 2020; Nalevanková et al.,
342 2020; Peiffer et al., 2014) and spruce forests (Baumgarten et al., 2019; Gartner et al., 2009;
343 Lagergren & Lindroth, 2002). Compared to the decrease in beech by 20-50% (A_{sat} , g_s , and
344 U_{daily}), the drought effect on spruce was more severe (60-85%). The more isohydric response
345 of spruce trees is further supported by the steeper slope of the relationship between U_{daily} and
346 Ψ_{PD} (Fig. 4). Therefore, in the first drought years, water consumption of both species are mainly
347 regulated by stomatal control as a short-term drought response, with a stronger water regulation
348 in spruce at the leaf level reflecting more isohydric strategy.

349 *Only spruce reduced total leaf area under repeated drought as a long-term drought response,*
350 *increasing water consumption per leaf area*

351 Under a long-term drought, leaf morphology plays an important role to balance water uptake
352 and loss, in addition to the stomatal control (Limousin et al., 2009). Thicker leaves and smaller
353 leaf area can improve turgor maintenance (Mitchell et al., 2008), increase A_{sat} and g_s per unit
354 leaf area (Flexas et al., 2006; Mencuccini & Comstock, 1999; Reich et al., 1997), and
355 simultaneously reduce water loss (Bert et al., 2021). However, neither of the species
356 significantly changed SLA throughout the drought period (Fig. S2), thus no acclimation through
357 leaf quality under the repeated drought, similar to the previous observations on saplings/young
358 trees (Knutzen et al., 2015; Raison et al., 1992) and mature trees (Dobbertin et al., 2010; Martin-
359 StPaul et al., 2013) including other species. Similarly, TE beech did not significantly modify

360 their leaf size (Fig 5c, except for leaf size in 2016, which can be explained by the severe natural
361 drought in 2015 in addition to the drought treatment) or LA (Fig 5e), rejecting H2 for beech
362 that morphological changes would regulate water consumption under repeated drought.
363 Furthermore, the branches of the TE beech became significantly shorter under the repeated
364 drought (Fig. 5a), leading to a smaller crown size (Jacobs et al., 2021). As a result, beech trees
365 invested more carbon to the leaf area rather than to the branch biomass (Petit et al., 2022).
366 During the drought, beech trees continued their root production to compensate for root mortality
367 (Nikolova et al., 2020; Zwetsloot & Bauerle, 2021), maintaining their water uptake capacity.
368 To supply this belowground carbon sink, carbon allocation was possibly shifted from branch to
369 fine root growth, as widely observed in saplings during drought (see review by Poorter et al.,
370 2012), without any strong reduction in the leaf production.

371 In contrast, TE spruce significantly decreased needle and shoot length (Fig 5b,d), leading to a
372 strong reduction in LA (Fig. 5f) and lower crown transparency (Jacobs et al., 2021). Since
373 spruce needle biomass collected by litterbags underneath the canopy did not differ between
374 treatments (data not shown), the reduction in LA was mainly caused by the production of shorter
375 needles and shoots under repeated drought rather than leaf shedding, in contrast to recent
376 observations in other species (Ambrose et al., 2018; Barbeta & Peñuelas, 2016). This is likely
377 because the Ψ_{PD} of TE spruce throughout the drought years was higher than the water potential
378 of c. -2.1 MPa causing a 50% loss of conductivity in end-twigs as determined for the same
379 spruce trees (Tomasella et al., 2018). In contrast to leaf shedding as a quick response to a severe
380 drought, the observed decrease in LA through morphological changes started in the third
381 drought year. Therefore, the water consumption of spruce in the first two drought years was
382 controlled mainly through stomatal regulation, and after the third drought year additionally
383 through smaller LA, to balance water loss with the strong decrease in water uptake due to
384 reduced fine root growth (Zwetsloot & Bauerle, 2021). Leaf to sapwood area ratio (LA/SA) of

385 spruce branches was not modified under the present drought (Petit et al., 2022) in contrast to
386 previous reports from other long-term drought experiments (Hudson et al., 2018; Limousin et
387 al., 2012; Martin-StPaul et al., 2013). However, the strong reduction in the whole-tree LA
388 together with the unaffected conducting sapwood depth (Gebhardt et al., submitted) led to a
389 significant decrease in LA/SA at the whole-tree level, ensuring greater water transport capacity
390 per leaf area (McDowell & Allen, 2015). Furthermore, despite the loss of the LA (by > 50%)
391 after the third drought year, the water consumption of TE spruce remained at the similar low
392 level throughout the five drought years, rejecting H2 that total water consumption would be
393 additionally regulated by morphological changes. The maintained water consumption despite
394 the loss of transpiring LA indicates an increased water consumption per leaf area, which is
395 supported by smaller differences in U_{daily} and g_s between CO and TE trees in the last drought
396 years compared to the first two years (Fig. 3, Table 1). Therefore, under repeated drought, not
397 only a strong stomatal control as a short-term response but the reduction in the total leaf area
398 as a long-term response plays a significant role for the leaf and whole-tree level physiology of
399 spruce trees.

400 **Conclusion**

401 This study reveals physiological and morphological acclimation of mature beech and spruce
402 trees to deal with five years of complete exclusion of growing season precipitation. Under the
403 same drought treatment, beech trees regulated water consumption only by stomatal control,
404 whereas spruce trees showed stronger stomatal regulation as a short-term and the reduction in
405 total leaf area as a long-term response. Compared to the sole stomatal control of beech,
406 reduction in water consumption and associated C uptake of spruce through the reduction in the
407 total leaf area can last for years even after drought release, causing drought legacy effect on tree
408 productivity. Furthermore, consequences of the observed morphological responses likely differ
409 between deciduous and evergreen trees, since the former can produce new leaves in the next

410 growing seasons while the latter keep older leaves for years. Under increasing frequency and
411 duration of drought, trees most likely experience further drought events in the near future.
412 Therefore, it is strikingly important to understand how the short- and long-term responses to
413 the previous drought affect tree performances under the next drought.

414 **Acknowledgements**

415 **References**

- 416 Adams, H. D., Collins, A. D., Briggs, S. P., Vennetier, M., Dickman, L. T., Sevanto, S. A.,
417 Garcia-Forner, N., Powers, H. H., & McDowell, N. G. (2015). Experimental drought and
418 heat can delay phenological development and reduce foliar and shoot growth in semiarid
419 trees. *Global Change Biology*, *21*(11), 4210–4220. <https://doi.org/10.1111/gcb.13030>
- 420 Alkama, R., & Cescatti, A. (2016). Biophysical climate impacts of recent changes in global
421 forest cover. *Science*, *351*(6273), 600–604. <https://doi.org/10.1126/science.aac8083>
- 422 Allen, C. D., Macalady, A. K., Chenchouni, H., Bachelet, D., McDowell, N., Vennetier, M.,
423 Kitzberger, T., Rigling, A., Breshears, D. D., Hogg, E. H. (Ted), Gonzalez, P., Fensham,
424 R., Zhang, Z., Castro, J., Demidova, N., Lim, J.-H., Allard, G., Running, S. W., Semerci,
425 A., & Cobb, N. (2010). A global overview of drought and heat-induced tree mortality
426 reveals emerging climate change risks for forests. *Forest Ecology and Management*,
427 *259*(4), 660–684. <https://doi.org/10.1016/j.foreco.2009.09.001>
- 428 Ambrose, A. R., Baxter, W. L., Martin, R. E., Francis, E., Asner, G. P., Nydick, K. R., & Dawson,
429 T. E. (2018). Leaf- and crown-level adjustments help giant sequoias maintain favorable
430 water status during severe drought. *Forest Ecology and Management*, *419–420*, 257–267.
431 <https://doi.org/10.1016/j.foreco.2018.01.012>

- 432 Barbeta, A., Ogaya, R., & Peñuelas, J. (2013). Dampening effects of long-term experimental
433 drought on growth and mortality rates of a Holm oak forest. *Global Change Biology*,
434 *19*(10), 3133–3144. <https://doi.org/10.1111/gcb.12269>
- 435 Barbeta, A., & Peñuelas, J. (2016). Sequence of plant responses to droughts of different
436 timescales: lessons from holm oak (*Quercus ilex*) forests. *Plant Ecology & Diversity*,
437 *9*(4), 321–338. <https://doi.org/10.1080/17550874.2016.1212288>
- 438 Baumgarten, M., Hesse, B. D., Augustaitienė, I., Marozas, V., Mozgeris, G., Byčenkienė, S.,
439 Mordas, G., Pivoras, A., Pivoras, G., Juonytė, D., Ulevičius, V., Augustaitis, A., &
440 Matyssek, R. (2019). Responses of species-specific sap flux, transpiration and water use
441 efficiency of pine, spruce and birch trees to temporarily moderate dry periods in mixed
442 forests at a dry and wet forest site in the hemi-boreal zone. *Journal of Agricultural*
443 *Meteorology*, *75*(1), 13–29. <https://doi.org/10.2480/agrmet.D-18-00008>
- 444 Beier, C., Beierkuhnlein, C., Wohlgemuth, T., Penuelas, J., Emmett, B., Körner, C., de Boeck,
445 H., Christensen, J. H., Leuzinger, S., Janssens, I. A., & Hansen, K. (2012). Precipitation
446 manipulation experiments - challenges and recommendations for the future. *Ecology*
447 *Letters*, *15*(8), 899–911. <https://doi.org/10.1111/j.1461-0248.2012.01793.x>
- 448 Bert, D., le Provost, G., Delzon, S., Plomion, C., & Gion, J.-M. (2021). Higher needle anatomic
449 plasticity is related to better water-use efficiency and higher resistance to embolism in fast-
450 growing *Pinus pinaster* families under water scarcity. *Trees*, *35*(1), 287–306.
451 <https://doi.org/10.1007/s00468-020-02034-2>
- 452 Bose, A. K., Rigling, A., Gessler, A., Hagedorn, F., Brunner, I., Feichtinger, L., Bigler, C., Egli,
453 S., Etzold, S., Gossner, M. M., Guidi, C., Lévesque, M., Meusburger, K., Peter, M., Saurer,
454 M., Scherrer, D., Schleppi, P., Schönbeck, L., Vogel, M. E., ... Schaub, M. (2022). Lessons
455 learned from a long-term irrigation experiment in a dry Scots pine forest: Impacts on traits
456 and functioning. *Ecological Monographs*, *92*(2). <https://doi.org/10.1002/ecm.1507>

457 Bréda, N., Huc, R., Granier, A., & Dreyer, E. (2006). Temperate forest trees and stands under
458 severe drought: a review of ecophysiological responses, adaptation processes and long-
459 term consequences. *Annals of Forest Science*, 63(6), 625–644.
460 <https://doi.org/10.1051/forest:2006042>

461 Brodribb, T. J., Powers, J., Cochard, H., & Choat, B. (2020). Hanging by a thread? Forests and
462 drought. *Science*, 368(6488), 261–266. <https://doi.org/10.1126/science.aat7631>

463 Brunner, I., Herzog, C., Dawes, M. A., Arend, M., & Sperisen, C. (2015). How tree roots
464 respond to drought. *Frontiers in Plant Science*, 6. <https://doi.org/10.3389/fpls.2015.00547>

465 Choat, B., Brodribb, T. J., Brodersen, C. R., Duursma, R. A., López, R., & Medlyn, B. E. (2018).
466 Triggers of tree mortality under drought. *Nature*, 558(7711), 531–539.
467 <https://doi.org/10.1038/s41586-018-0240-x>

468 Ciais, Ph., Reichstein, M., Viovy, N., Granier, A., Ogée, J., Allard, V., Aubinet, M., Buchmann,
469 N., Bernhofer, Chr., Carrara, A., Chevallier, F., de Noblet, N., Friend, A. D., Friedlingstein,
470 P., Grünwald, T., Heinesch, B., Keronen, P., Knohl, A., Krinner, G., ... Valentini, R. (2005).
471 Europe-wide reduction in primary productivity caused by the heat and drought in 2003.
472 *Nature*, 437(7058), 529–533. <https://doi.org/10.1038/nature03972>

473 Cochard, H., Bréda, N., & Granier, A. (1996). Whole tree hydraulic conductance and water loss
474 regulation in *Quercus* during drought: evidence for stomatal control of embolism? *Annales*
475 *Des Sciences Forestières*, 53(2–3), 197–206. <https://doi.org/10.1051/forest:19960203>

476 Dobbertin, M., Eilmann, B., Bleuler, P., Giuggiola, A., Graf Pannatier, E., Landolt, W., Schleppei,
477 P., & Rigling, A. (2010). Effect of irrigation on needle morphology, shoot and stem growth
478 in a drought-exposed *Pinus sylvestris* forest. *Tree Physiology*, 30(3), 346–360.
479 <https://doi.org/10.1093/treephys/tpp123>

- 480 Feichtinger, L. M., Eilmann, B., Buchmann, N., & Rigling, A. (2014). Growth adjustments of
481 conifers to drought and to century-long irrigation. *Forest Ecology and Management*, 334,
482 96–105. <https://doi.org/10.1016/j.foreco.2014.08.008>
- 483 Flexas, J., Bota, J., Galmés, J., Medrano, H., & Ribas-Carbó, M. (2006). Keeping a positive
484 carbon balance under adverse conditions: responses of photosynthesis and respiration to
485 water stress. *Physiologia Plantarum*, 127(3), 343–352. <https://doi.org/10.1111/j.1399-3054.2006.00621.x>
- 487 Foley, J. A., DeFries, R., Asner, G. P., Barford, C., Bonan, G., Carpenter, S. R., Chapin, F. S.,
488 Coe, M. T., Daily, G. C., Gibbs, H. K., Helkowski, J. H., Holloway, T., Howard, E. A.,
489 Kucharik, C. J., Monfreda, C., Patz, J. A., Prentice, I. C., Ramankutty, N., & Snyder, P. K.
490 (2005). Global Consequences of Land Use. *Science*, 309(5734), 570–574.
491 <https://doi.org/10.1126/science.1111772>
- 492 Forrester, D. I., Tachauer, I. H. H., Annighoefer, P., Barbeito, I., Pretzsch, H., Ruiz-Peinado, R.,
493 Stark, H., Vacchiano, G., Zlatanov, T., Chakraborty, T., Saha, S., & Sileshi, G. W. (2017).
494 Generalized biomass and leaf area allometric equations for European tree species
495 incorporating stand structure, tree age and climate. *Forest Ecology and Management*, 396,
496 160–175. <https://doi.org/10.1016/j.foreco.2017.04.011>
- 497 Galiano, L., Martínez-Vilalta, J., & Lloret, F. (2011). Carbon reserves and canopy defoliation
498 determine the recovery of Scots pine 4 yr after a drought episode. *New Phytologist*,
499 190(3), 750–759. <https://doi.org/10.1111/j.1469-8137.2010.03628.x>
- 500 Gallé, A., & Feller, U. (2007). Changes of photosynthetic traits in beech saplings (*Fagus*
501 *sylvatica*) under severe drought stress and during recovery. *Physiologia Plantarum*, 131(3),
502 412–421. <https://doi.org/10.1111/j.1399-3054.2007.00972.x>

503 Gartner, K., Nadezhdina, N., Englisch, M., Čermak, J., & Leitgeb, E. (2009). Sap flow of birch
504 and Norway spruce during the European heat and drought in summer 2003. *Forest Ecology
505 and Management*, 258(5), 590–599. <https://doi.org/10.1016/j.foreco.2009.04.028>

506 Gebhardt, T., Hesse, B. D., Hikino, K., Kolovrat, K., Hafner, B. D., Grams, T. E. E., & Häberle,
507 K.-H. (n.d.). *Repeated summer drought changes the radial xylem sapflow profile in mature
508 Picea abies (L.) Karst. (submitted).*

509 Goisser, M., Geppert, U., Rötzer, T., Paya, A., Huber, A., Kerner, R., Bauerle, T., Pretzsch, H.,
510 Pritsch, K., Häberle, K. H., Matyssek, R., & Grams, T. E. E. (2016). Does belowground
511 interaction with *Fagus sylvatica* increase drought susceptibility of photosynthesis and stem
512 growth in *Picea abies*? *Forest Ecology and Management*, 375, 268–278.
513 <https://doi.org/10.1016/j.foreco.2016.05.032>

514 Goisser, M., Zang, U., Matzner, E., Borke, W., Häberle, K.-H., & Matyssek, R. (2013). Growth
515 of juvenile beech (*Fagus sylvatica* L.) upon transplant into a wind-opened spruce stand of
516 heterogeneous light and water conditions. *Forest Ecology and Management*, 310, 110–119.
517 <https://doi.org/10.1016/j.foreco.2013.08.006>

518 Grams, T. E. E., Hesse, B. D., Gebhardt, T., Weigl, F., Rötzer, T., Kovacs, B., Hikino, K., Hafner,
519 B. D., Brunn, M., Bauerle, T., Häberle, K., Pretzsch, H., & Pritsch, K. (2021). The Kroof
520 experiment: realization and efficacy of a recurrent drought experiment plus recovery in a
521 beech/spruce forest. *Ecosphere*, 12(3). <https://doi.org/10.1002/ecs2.3399>

522 Granier, A. (1987). Evaluation of transpiration in a Douglas-fir stand by means of sap flow
523 measurements. *Tree Physiology*, 3(4), 309–320. <https://doi.org/10.1093/treephys/3.4.309>

524 Grossiord, C., Sevanto, S., Dawson, T. E., Adams, H. D., Collins, A. D., Dickman, L. T.,
525 Newman, B. D., Stockton, E. A., & McDowell, N. G. (2017). Warming combined with

526 more extreme precipitation regimes modifies the water sources used by trees. *New*
527 *Phytologist*, 213(2), 584–596. <https://doi.org/10.1111/nph.14192>

528 Guérin, M., Martin-Benito, D., Arx, G., Andreu-Hayles, L., Griffin, K. L., Hamdan, R.,
529 McDowell, N. G., Muscarella, R., Pockman, W., & Gentine, P. (2018). Interannual
530 variations in needle and sapwood traits of *Pinus edulis* branches under an experimental
531 drought. *Ecology and Evolution*, 8(3), 1655–1672. <https://doi.org/10.1002/ece3.3743>

532 Hammond, W. M., Williams, A. P., Abatzoglou, J. T., Adams, H. D., Klein, T., López, R., Sáenz-
533 Romero, C., Hartmann, H., Breshears, D. D., & Allen, C. D. (2022). Global field
534 observations of tree die-off reveal hotter-drought fingerprint for Earth’s forests. *Nature*
535 *Communications*, 13(1), 1761. <https://doi.org/10.1038/s41467-022-29289-2>

536 Hartmann, H., Link, R. M., & Schuldt, B. (2021). A whole-plant perspective of isohydry: stem-
537 level support for leaf-level plant water regulation. *Tree Physiology*, 41(6), 901–905.
538 <https://doi.org/10.1093/treephys/tpab011>

539 Hartmann, H., Moura, C. F., Anderegg, W. R. L., Ruehr, N. K., Salmon, Y., Allen, C. D., Arndt,
540 S. K., Breshears, D. D., Davi, H., Galbraith, D., Ruthrof, K. X., Wunder, J., Adams, H. D.,
541 Bloemen, J., Cailleret, M., Cobb, R., Gessler, A., Grams, T. E. E., Jansen, S., ... O’Brien,
542 M. (2018). Research frontiers for improving our understanding of drought-induced tree
543 and forest mortality. *New Phytologist*, 218(1), 15–28. <https://doi.org/10.1111/nph.15048>

544 Hartmann, H., Ziegler, W., Kolle, O., & Trumbore, S. (2013). Thirst beats hunger – declining
545 hydration during drought prevents carbon starvation in Norway spruce saplings. *New*
546 *Phytologist*, 200(2), 340–349. <https://doi.org/10.1111/nph.12331>

547 Hesse, B. D., Goisser, M., Hartmann, H., & Grams, T. E. E. (2019). Repeated summer drought
548 delays sugar export from the leaf and impairs phloem transport in mature beech. *Tree*
549 *Physiology*, 39(2), 192–200. <https://doi.org/10.1093/treephys/tpy122>

550 Homolová, L., Lukeš, P., Malenovský, Z., Lhotáková, Z., Kaplan, V., & Hanuš, J. (2013).
551 Measurement methods and variability assessment of the Norway spruce total leaf area:
552 implications for remote sensing. *Trees*, 27(1), 111–121. [https://doi.org/10.1007/s00468-](https://doi.org/10.1007/s00468-012-0774-8)
553 012-0774-8

554 Hudson, P. J., Limousin, J. M., Krofcheck, D. J., Boutz, A. L., Pangle, R. E., Gehres, N.,
555 McDowell, N. G., & Pockman, W. T. (2018). Impacts of long-term precipitation
556 manipulation on hydraulic architecture and xylem anatomy of piñon and juniper in
557 Southwest USA. *Plant, Cell & Environment*, 41(2), 421–435.
558 <https://doi.org/10.1111/pce.13109>

559 IPCC. (2019). *Climate Change and Land: an IPCC special report on climate change,*
560 *desertification, land degradation, sustainable land management, food security, and*
561 *greenhouse gas fluxes in terrestrial ecosystems. [P.R. Shukla, J. Skea, E. Calvo Buendia,*
562 *V. Masson-Delmotte, H.-O. Pörtner, D. C. Roberts, P. Zhai, R. Slade, S. Connors, R. van*
563 *Diemen, M. Ferrat, E. Haughey, S. Luz, S. Neogi, M. Pathak, J. Petzold, J. Portugal*
564 *Pereira, P. Vyas, E. Huntley, K. Kissick, M. Belkacemi, J. Malley, (eds.)]. In press.*

565 IPCC. (2021). Summary for Policymakers. *Climate Change 2021: The Physical Science*
566 *Basis. Contribution of Working Group I to the Sixth Assessment Report of the*
567 *Intergovernmental Panel on Climate Change.*
568 <https://doi.org/10.1017/9781009157896.001>

569 Jacobs, M., Rais, A., & Pretzsch, H. (2021). How drought stress becomes visible upon detecting
570 tree shape using terrestrial laser scanning (TLS). *Forest Ecology and Management*, 489,
571 118975. <https://doi.org/10.1016/j.foreco.2021.118975>

572 Knutzen, F., Meier, I. C., & Leuschner, C. (2015). Does reduced precipitation trigger
573 physiological and morphological drought adaptations in European beech (*Fagus sylvatica*

574 L.)? Comparing provenances across a precipitation gradient. *Tree Physiology*, 35(9), 949–
575 963. <https://doi.org/10.1093/treephys/tpv057>

576 Kurjak, D., Štrelcová, K., Ditmarová, L., Priwitzer, T., Kmet', J., Homolák, M., & Pichler, V.
577 (2012). Physiological response of irrigated and non-irrigated Norway spruce trees as a
578 consequence of drought in field conditions. *European Journal of Forest Research*, 131(6),
579 1737–1746. <https://doi.org/10.1007/s10342-012-0611-z>

580 Lagergren, F., & Lindroth, A. (2002). Transpiration response to soil moisture in pine and spruce
581 trees in Sweden. *Agricultural and Forest Meteorology*, 112(2), 67–85.
582 [https://doi.org/10.1016/S0168-1923\(02\)00060-6](https://doi.org/10.1016/S0168-1923(02)00060-6)

583 Leuschner, C. (2020). Drought response of European beech (*Fagus sylvatica* L.)—A review.
584 *Perspectives in Plant Ecology, Evolution and Systematics*, 47, 125576.
585 <https://doi.org/10.1016/j.ppees.2020.125576>

586 Leuzinger, S., Luo, Y., Beier, C., Dieleman, W., Vicca, S., & Körner, C. (2011). Do global
587 change experiments overestimate impacts on terrestrial ecosystems? *Trends in Ecology &*
588 *Evolution*, 26(5), 236–241. <https://doi.org/10.1016/j.tree.2011.02.011>

589 Li, X., Blackman, C. J., Peters, J. M. R., Choat, B., Rymer, P. D., Medlyn, B. E., & Tissue, D.
590 T. (2019). More than iso/anisohydry: Hydroscares integrate plant water use and drought
591 tolerance traits in 10 eucalypt species from contrasting climates. *Functional Ecology*,
592 33(6), 1035–1049. <https://doi.org/10.1111/1365-2435.13320>

593 Limousin, J.-M., Bickford, C. P., Dickman, L. T., Pangle, R. E., Hudson, P. J., Boutz, A. L.,
594 Gehres, N., Osuna, J. L., Pockman, W. T., & McDowell, N. G. (2013). Regulation and
595 acclimation of leaf gas exchange in a piñon-juniper woodland exposed to three different
596 precipitation regimes. *Plant, Cell & Environment*, 36(10), 1812–1825.
597 <https://doi.org/10.1111/pce.12089>

598 Limousin, J.-M., Rambal, S., Ourcival, J. M., Rocheteau, A., Joffre, R., & Rodriguez-Cortina,
599 R. (2009). Long-term transpiration change with rainfall decline in a Mediterranean
600 *Quercus ilex* forest. *Global Change Biology*, 15(9), 2163–2175.
601 <https://doi.org/10.1111/j.1365-2486.2009.01852.x>

602 Limousin, J.-M., Rambal, S., Ourcival, J.-M., Rodríguez-Calcerrada, J., Pérez-Ramos, I. M.,
603 Rodríguez-Cortina, R., Misson, L., & Joffre, R. (2012). Morphological and phenological
604 shoot plasticity in a Mediterranean evergreen oak facing long-term increased drought.
605 *Oecologia*, 169(2), 565–577. <https://doi.org/10.1007/s00442-011-2221-8>

606 Liu, D., Ogaya, R., Barbeta, A., Yang, X., & Peñuelas, J. (2015). Contrasting impacts of
607 continuous moderate drought and episodic severe droughts on the aboveground-biomass
608 increment and litterfall of three coexisting Mediterranean woody species. *Global Change
609 Biology*, 21(11), 4196–4209. <https://doi.org/10.1111/gcb.13029>

610 Lüttschwager, D., & Jochheim, H. (2020). Drought Primarily Reduces Canopy Transpiration of
611 Exposed Beech Trees and Decreases the Share of Water Uptake from Deeper Soil Layers.
612 *Forests*, 11(5), 537. <https://doi.org/10.3390/f11050537>

613 Magh, Bonn, Grote, Burzlaff, Pfautsch, & Rennenberg. (2019). Drought Superimposes the
614 Positive Effect of Silver Fir on Water Relations of European Beech in Mature Forest Stands.
615 *Forests*, 10(10), 897. <https://doi.org/10.3390/f10100897>

616 Martin-StPaul, N. K., Limousin, J.-M., Vogt-Schilb, H., Rodríguez-Calcerrada, J., Rambal, S.,
617 Longepierre, D., & Misson, L. (2013). The temporal response to drought in a
618 Mediterranean evergreen tree: comparing a regional precipitation gradient and a
619 throughfall exclusion experiment. *Global Change Biology*, 19(8), 2413–2426.
620 <https://doi.org/10.1111/gcb.12215>

621 McBranch, N. A., Grossiord, C., Adams, H., Borrego, I., Collins, A. D., Dickman, T., Ryan, M.,
622 Sevanto, S., & McDowell, N. G. (2019). Lack of acclimation of leaf area:sapwood area
623 ratios in piñon pine and juniper in response to precipitation reduction and warming. *Tree*
624 *Physiology*, 39(1), 135–142. <https://doi.org/10.1093/treephys/tpy066>

625 McDowell, N. G., & Allen, C. D. (2015). Darcy’s law predicts widespread forest mortality
626 under climate warming. *Nature Climate Change*, 5(7), 669–672.
627 <https://doi.org/10.1038/nclimate2641>

628 McDowell, N., Pockman, W. T., Allen, C. D., Breshears, D. D., Cobb, N., Kolb, T., Plaut, J.,
629 Sperry, J., West, A., Williams, D. G., & Yezzer, E. A. (2008). Mechanisms of plant survival
630 and mortality during drought: why do some plants survive while others succumb to
631 drought? *New Phytologist*, 178(4), 719–739. [https://doi.org/10.1111/j.1469-](https://doi.org/10.1111/j.1469-8137.2008.02436.x)
632 [8137.2008.02436.x](https://doi.org/10.1111/j.1469-8137.2008.02436.x)

633 Meier, I. C., & Leuschner, C. (2008). Leaf Size and Leaf Area Index in *Fagus sylvatica* Forests:
634 Competing Effects of Precipitation, Temperature, and Nitrogen Availability. *Ecosystems*,
635 11(5), 655–669. <https://doi.org/10.1007/s10021-008-9135-2>

636 Mencuccini, M., & Comstock, J. (1999). Variability in hydraulic architecture and gas exchange
637 of common bean (*Phaseolus vulgaris*) cultivars under well-watered conditions:
638 interactions with leaf size. *Functional Plant Biology*, 26(2), 115.
639 <https://doi.org/10.1071/PP98137>

640 Mitchell, P. J., Veneklaas, E. J., Lambers, H., & Burgess, S. S. O. (2008). Leaf water relations
641 during summer water deficit: differential responses in turgor maintenance and variation in
642 leaf structure among different plant communities in south-western Australia. *Plant, Cell*
643 *& Environment*, 31(12), 1791–1802. <https://doi.org/10.1111/j.1365-3040.2008.01882.x>

644 Moreno, M., Simioni, G., Cailleret, M., Ruffault, J., Badel, E., Carrière, S., Davi, H., Gavinet,
645 J., Huc, R., Limousin, J.-M., Marloie, O., Martin, L., Rodríguez-Calcerrada, J., Vennetier,
646 M., & Martin-StPaul, N. (2021). Consistently lower sap velocity and growth over nine
647 years of rainfall exclusion in a Mediterranean mixed pine-oak forest. *Agricultural and*
648 *Forest Meteorology*, 308–309, 108472. <https://doi.org/10.1016/j.agrformet.2021.108472>

649 Nalevanková, P., Sitková, Z., Kučera, J., & Střelcová, K. (2020). Impact of Water Deficit on
650 Seasonal and Diurnal Dynamics of European Beech Transpiration and Time-Lag Effect
651 between Stand Transpiration and Environmental Drivers. *Water*, 12(12), 3437.
652 <https://doi.org/10.3390/w12123437>

653 Nikolova, P. S., Bauerle, T. L., Häberle, K.-H., Blaschke, H., Brunner, I., & Matyssek, R. (2020).
654 Fine-Root Traits Reveal Contrasting Ecological Strategies in European Beech and Norway
655 Spruce During Extreme Drought. *Frontiers in Plant Science*, 11.
656 <https://doi.org/10.3389/fpls.2020.01211>

657 Oberhuber, W., Hammerle, A., & Kofler, W. (2015). Tree water status and growth of saplings
658 and mature Norway spruce (*Picea abies*) at a dry distribution limit. *Frontiers in Plant*
659 *Science*, 6. <https://doi.org/10.3389/fpls.2015.00703>

660 Oberleitner, F., Hartmann, H., Hasibeder, R., Huang, J., Losso, A., Mayr, S., Oberhuber, W.,
661 Wieser, G., & Bahn, M. (2022). Amplifying effects of recurrent drought on the dynamics
662 of tree growth and water use in a subalpine forest. *Plant, Cell & Environment*, 45(9), 2617–
663 2635. <https://doi.org/10.1111/pce.14369>

664 Peiffer, M., Bréda, N., Badeau, V., & Granier, A. (2014). Disturbances in European beech water
665 relation during an extreme drought. *Annals of Forest Science*, 71(7), 821–829.
666 <https://doi.org/10.1007/s13595-014-0383-3>

667 Peñuelas, J., Canadell, J. G., & Ogaya, R. (2011). Increased water-use efficiency during the
668 20th century did not translate into enhanced tree growth. *Global Ecology and*
669 *Biogeography*, 20(4), 597–608. <https://doi.org/10.1111/j.1466-8238.2010.00608.x>

670 Petit, G., Zamboni, D., Hesse, B. D., & Häberle, K. (2022). No xylem phenotypic plasticity in
671 mature *Picea abies* and *Fagus sylvatica* trees after five years of throughfall precipitation
672 exclusion. *Global Change Biology*. <https://doi.org/10.1111/gcb.16232>

673 Poorter, H., Niklas, K. J., Reich, P. B., Oleksyn, J., Poot, P., & Mommer, L. (2012). Biomass
674 allocation to leaves, stems and roots: meta-analyses of interspecific variation and
675 environmental control. *New Phytologist*, 193(1), 30–50. [https://doi.org/10.1111/j.1469-](https://doi.org/10.1111/j.1469-8137.2011.03952.x)
676 [8137.2011.03952.x](https://doi.org/10.1111/j.1469-8137.2011.03952.x)

677 Poyatos, R., Aguadé, D., Galiano, L., Mencuccini, M., & Martínez-Vilalta, J. (2013). Drought-
678 induced defoliation and long periods of near-zero gas exchange play a key role in
679 accentuating metabolic decline of Scots pine. *New Phytologist*, 200(2), 388–401.
680 <https://doi.org/10.1111/nph.12278>

681 Pretzsch, H. (2019). *Grundlagen der Waldwachstumsforschung*. Springer Berlin Heidelberg.
682 <https://doi.org/10.1007/978-3-662-58155-1>

683 Pretzsch, H., Biber, P., Schütze, G., Uhl, E., & Rötzer, T. (2014). Forest stand growth dynamics
684 in Central Europe have accelerated since 1870. *Nature Communications*, 5(1), 4967.
685 <https://doi.org/10.1038/ncomms5967>

686 Pretzsch, H., Grams, T., Häberle, K. H., Pritsch, K., Bauerle, T., & Rötzer, T. (2020). Growth
687 and mortality of Norway spruce and European beech in monospecific and mixed-species
688 stands under natural episodic and experimentally extended drought. Results of the KROOF
689 throughfall exclusion experiment. *Trees*, 34(4), 957–970. [https://doi.org/10.1007/s00468-](https://doi.org/10.1007/s00468-020-01973-0)
690 [020-01973-0](https://doi.org/10.1007/s00468-020-01973-0)

691 Pretzsch, H., Rötzer, T., Matyssek, R., Grams, T. E. E., Häberle, K.-H., Pritsch, K., Kerner, R.,
692 & Munch, J.-C. (2014). Mixed Norway spruce (*Picea abies* [L.] Karst) and European beech
693 (*Fagus sylvatica* [L.]) stands under drought: from reaction pattern to mechanism. *Trees*,
694 28(5), 1305–1321. <https://doi.org/10.1007/s00468-014-1035-9>

695 Pritzkow, C., Szota, C., Williamson, V., & Arndt, S. K. (2021). Previous drought exposure leads
696 to greater drought resistance in eucalypts through changes in morphology rather than
697 physiology. *Tree Physiology*, 41(7), 1186–1198. <https://doi.org/10.1093/treephys/tpaa176>

698 Raison, R. J., Myers, B. J., & Benson, M. L. (1992). Dynamics of *Pinus radiata* foliage in
699 relation to water and nitrogen stress: I. Needle production and properties. *Forest Ecology*
700 *and Management*, 52(1–4), 139–158. [https://doi.org/10.1016/0378-1127\(92\)90499-Y](https://doi.org/10.1016/0378-1127(92)90499-Y)

701 Reich, P. B., Walters, M. B., & Ellsworth, D. S. (1997). From tropics to tundra: Global
702 convergence in plant functioning. *Proceedings of the National Academy of Sciences*,
703 94(25), 13730–13734. <https://doi.org/10.1073/pnas.94.25.13730>

704 Riederer, M., Kurbasik, K., Steinbrecher, R., & Voss, A. (1988). Surface areas, lengths and
705 volumes of *Picea abies* (L.) Karst. needles: determination, biological variability and effect
706 of environmental factors. *Trees*, 2(3). <https://doi.org/10.1007/BF00196021>

707 Schönbeck, L., Gessler, A., Hoch, G., McDowell, N. G., Rigling, A., Schaub, M., & Li, M.
708 (2018). Homeostatic levels of nonstructural carbohydrates after 13 yr of drought and
709 irrigation in *Pinus sylvestris*. *New Phytologist*, 219(4), 1314–1324.
710 <https://doi.org/10.1111/nph.15224>

711 Schönbeck, L., Grossiord, C., Gessler, A., Gisler, J., Meusburger, K., D’Odorico, P., Rigling,
712 A., Salmon, Y., Stocker, B. D., Zweifel, R., & Schaub, M. (2022). Photosynthetic
713 acclimation and sensitivity to short- and long-term environmental changes in a drought-

714 prone forest. *Journal of Experimental Botany*, 73(8), 2576–2588.
715 <https://doi.org/10.1093/jxb/erac033>

716 Schuldt, B., Buras, A., Arend, M., Vitasse, Y., Beierkuhnlein, C., Damm, A., Gharun, M., Grams,
717 T. E. E., Hauck, M., Hajek, P., Hartmann, H., Hiltbrunner, E., Hoch, G., Holloway-Phillips,
718 M., Körner, C., Larysch, E., Lübbe, T., Nelson, D. B., Rammig, A., ... Kahmen, A. (2020).
719 A first assessment of the impact of the extreme 2018 summer drought on Central European
720 forests. *Basic and Applied Ecology*, 45, 86–103.
721 <https://doi.org/10.1016/j.baae.2020.04.003>

722 Střelcová, K., Kurjak, D., Leštianska, A., Kovalčíková, D., Ditmarová, L., Škvarenina, J., &
723 Ahmed, Y. A.-R. (2013). Differences in transpiration of Norway spruce drought stressed
724 trees and trees well supplied with water. *Biologia*, 68(6), 1118–1122.
725 <https://doi.org/10.2478/s11756-013-0257-4>

726 Tardieu, F., & Simonneau, T. (1998). Variability among species of stomatal control under
727 fluctuating soil water status and evaporative demand: modelling isohydric and anisohydric
728 behaviours. *Journal of Experimental Botany*, 49(Special), 419–432.
729 https://doi.org/10.1093/jxb/49.Special_Issue.419

730 Tomasella, M., Beikircher, B., Häberle, K.-H., Hesse, B., Kallenbach, C., Matyssek, R., & Mayr,
731 S. (2018). Acclimation of branch and leaf hydraulics in adult *Fagus sylvatica* and *Picea*
732 *abies* in a forest through-fall exclusion experiment. *Tree Physiology*, 38(2), 198–211.
733 <https://doi.org/10.1093/treephys/tpx140>

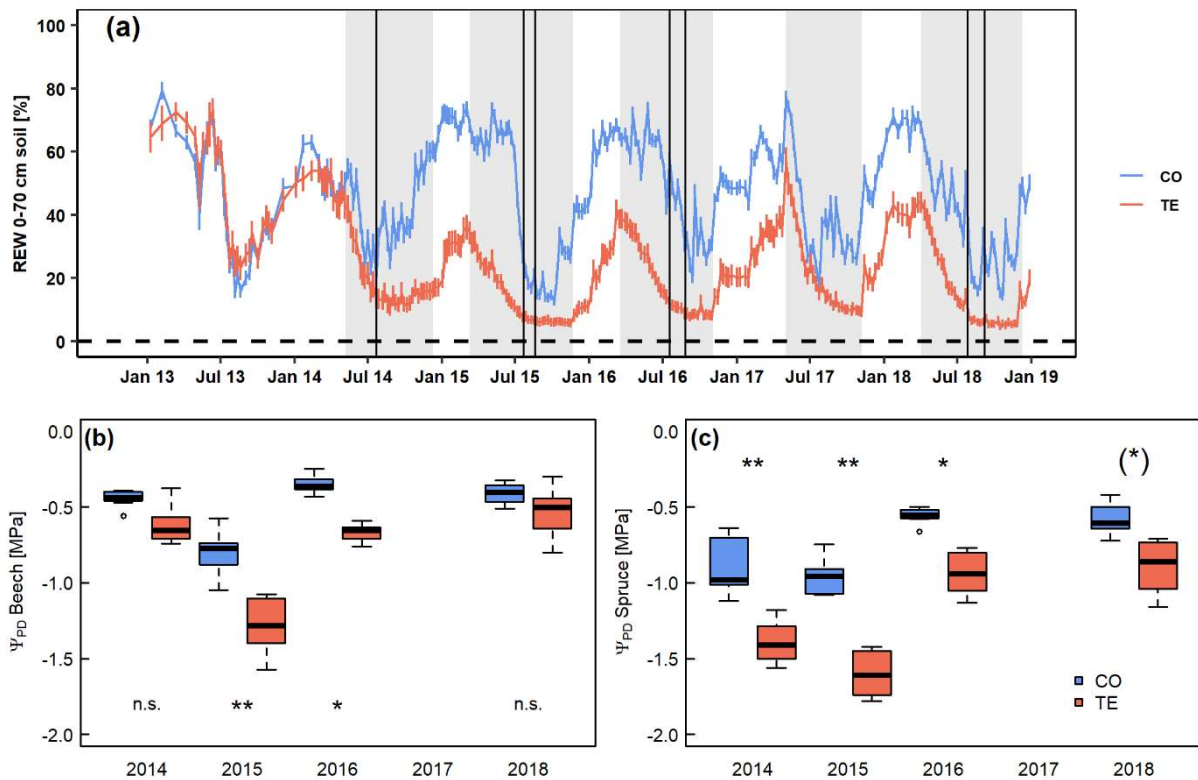
734 Trugman, A. T., Detto, M., Bartlett, M. K., Medvigy, D., Anderegg, W. R. L., Schwalm, C.,
735 Schaffer, B., & Pacala, S. W. (2018). Tree carbon allocation explains forest drought-kill
736 and recovery patterns. *Ecology Letters*, 21(10), 1552–1560.
737 <https://doi.org/10.1111/ele.13136>

738 Walthert, L., Ganthaler, A., Mayr, S., Saurer, M., Waldner, P., Walser, M., Zweifel, R., & von
739 Arx, G. (2021). From the comfort zone to crown dieback: Sequence of physiological stress
740 thresholds in mature European beech trees across progressive drought. *Science of The Total*
741 *Environment*, 753, 141792. <https://doi.org/10.1016/j.scitotenv.2020.141792>

742 Zweifel, R., Etzold, S., Sterck, F., Gessler, A., Anfodillo, T., Mencuccini, M., von Arx, G.,
743 Lazzarin, M., Haeni, M., Feichtinger, L., Meusburger, K., Knuesel, S., Walthert, L.,
744 Salmon, Y., Bose, A. K., Schoenbeck, L., Hug, C., de Girardi, N., Giuggiola, A., ... Rigling,
745 A. (2020). Determinants of legacy effects in pine trees – implications from an irrigation-
746 stop experiment. *New Phytologist*, 227(4), 1081–1096. <https://doi.org/10.1111/nph.16582>

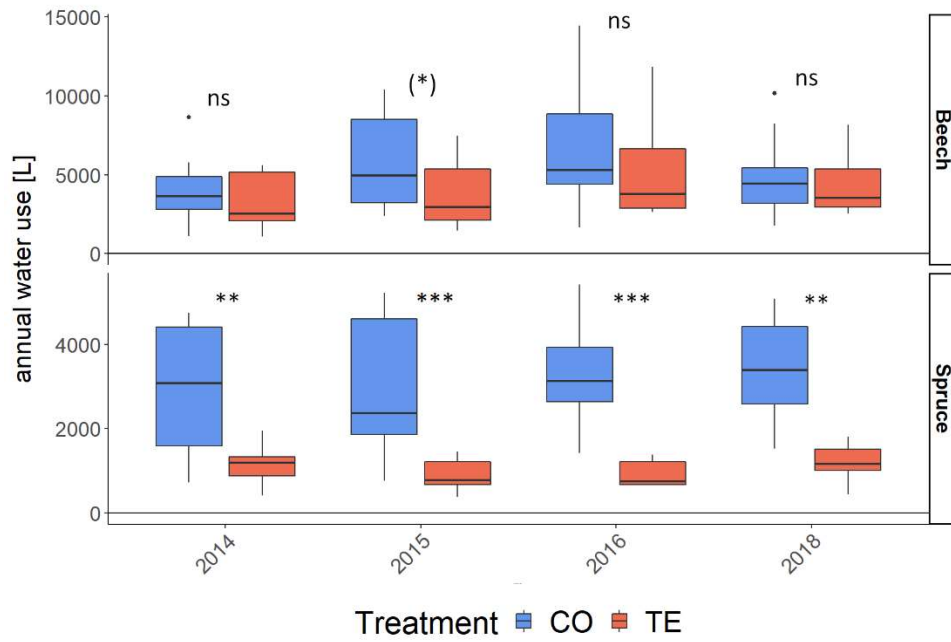
747 Zwetsloot, M. J., & Bauerle, T. L. (2021). Repetitive seasonal drought causes substantial
748 species-specific shifts in fine-root longevity and spatio-temporal production patterns in
749 mature temperate forest trees. *New Phytologist*, 231(3), 974–986.
750 <https://doi.org/10.1111/nph.17432>

751



753

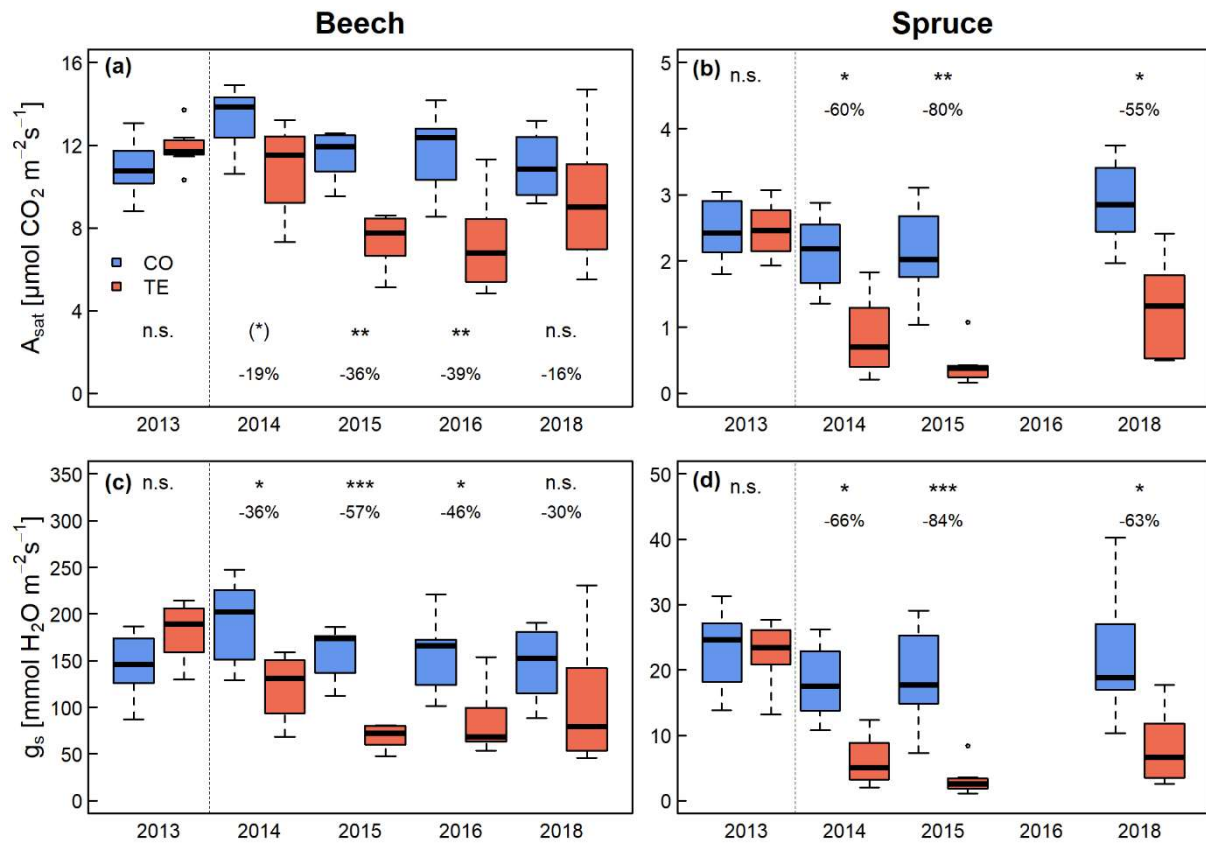
754 *Fig. 1: Relative extractable water (REW) averaged over 0-70 cm soil depth (a), predawn leaf*
 755 *water potential (Ψ_{PD}) of beech (b) and spruce (c) during the experiments in control (CO, blue)*
 756 *and throughfall exclusion (TE, red) plots. Vertical black lines in display the timing of the*
 757 *measurements of leaf physiology (i.e. predawn leaf water potential, leaf gas exchange). Ψ_{PD} of*
 758 *2015, 2016, and 2018 are average of two measurements conducted in July and August. Shaded*
 759 *area in indicates the period when the roof were closed. Asterisks indicate significant results*
 760 *based on linea-mixed model comparing CO and TE trees, **, $p < 0.01$; *, $p < 0.05$; (*), $p <$*
 761 *0.1; n.s., not significant.*



762

763 *Fig. 2: Annual water use (in L) of beech and spruce trees in control (CO) and throughfall*
 764 *exclusion (TE) plots. Asterisks indicate significant results based on linea-mixed model*
 765 *comparing CO and TE trees, ***, $p < 0.001$; **, $p < 0.01$; (*), $p < 0.1$; n.s., not significant.*

766

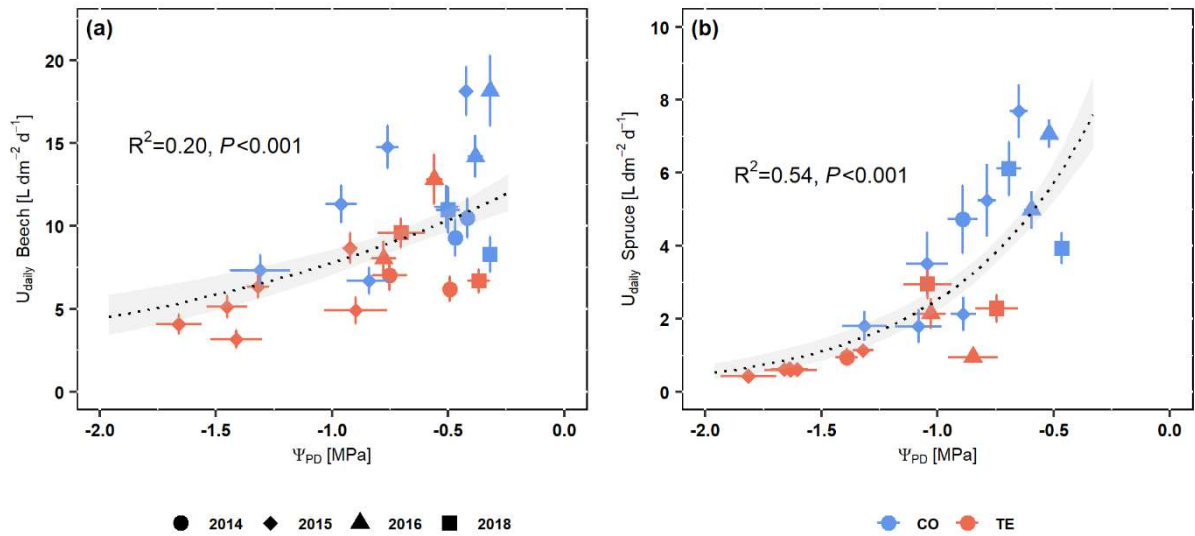


767

768 *Fig. 3: Light-saturated CO₂ assimilation rates (A_{sat}), Stomatal conductance to water vapour*
 769 *(g_s), of control (CO, blue) and throughfall exclusion (TE, red) beech (left) and spruce (right)*
 770 *trees. The drought treatment started in 2014 growing season. Asterisks indicate significant*
 771 *results based on linea-mixed model comparing CO and TE trees, ***, $p < 0.001$; **, $p < 0.01$;*
 772 **, $p < 0.05$; (*), $p < 0.1$; n.s., not significant. Numbers give relative reduction in TE trees*
 773 *compared to CO trees.*

774

775



776

777 *Fig. 4: Correlation between mean sap flow density per day at outer 2cm sapwood (u_{daily}) and*
 778 *predawn leaf water potential (Ψ_{PD}) in beech (a) and spruce (b) trees. Both treatments*
 779 *(control; CO and throughfall exclusion; TE) and all years are fitted together for each species,*
 780 *with a linear regression after exponential transformation of Ψ_{PD} . The dotted curves and the*
 781 *gray area display the prediction of the power function and its 95% confidence interval.*

782

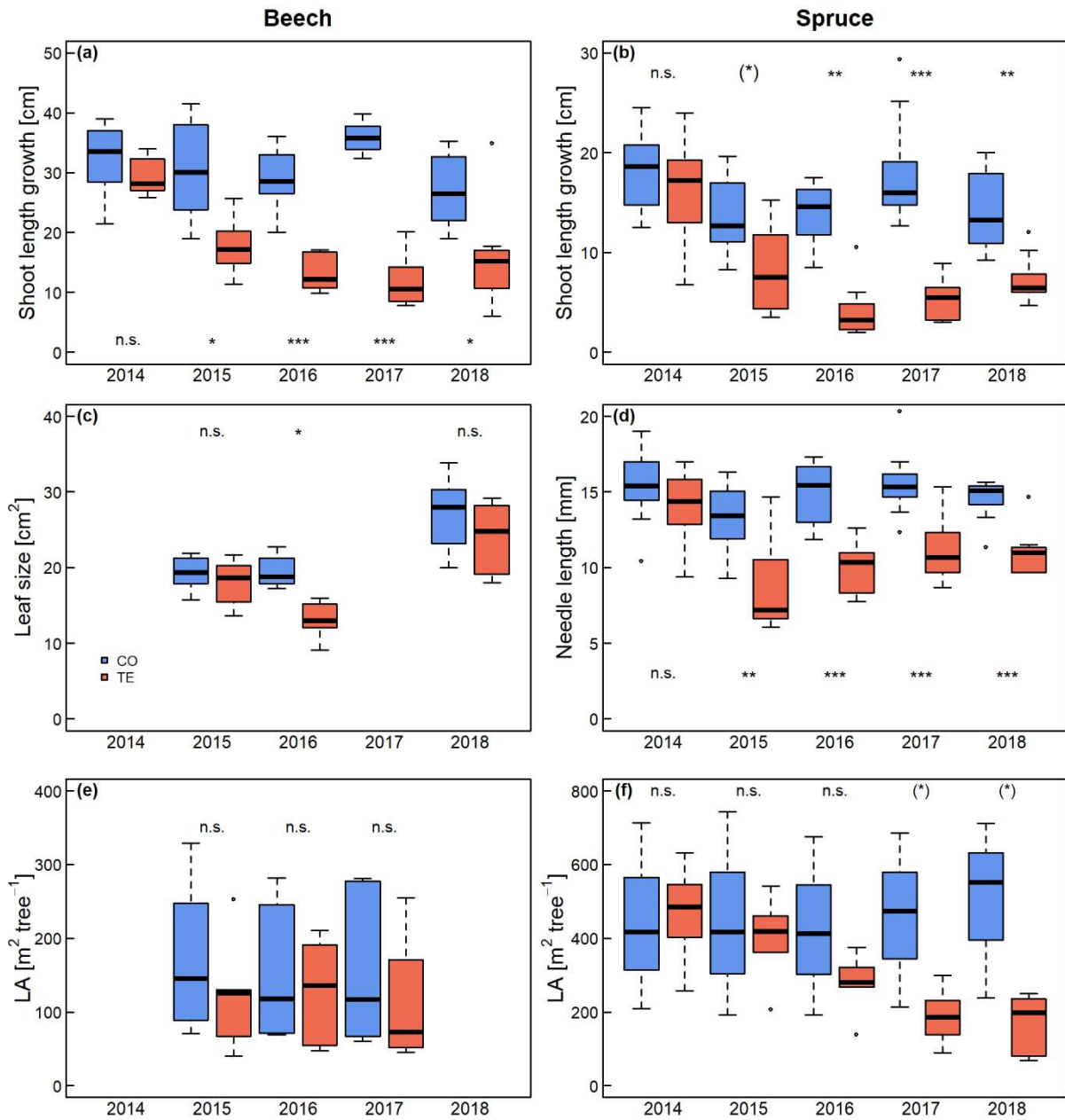
783

784

785

786

787



788

789 *Fig. 5: Shoot length growth (a,b), leaf size (c), needle length (d), and total leaf area (LA, e,f) of*
 790 *control (CO, blue) and throughfall exclusion (TE, red) beech (left) and spruce (right) trees.*
 791 *Asterisks indicate significant results based on linea-mixed model comparing CO and TE trees,*
 792 ****, $p < 0.001$; **, $p < 0.01$; *, $p < 0.05$; (*), $p < 0.1$; n.s., not significant.*

793

794

795

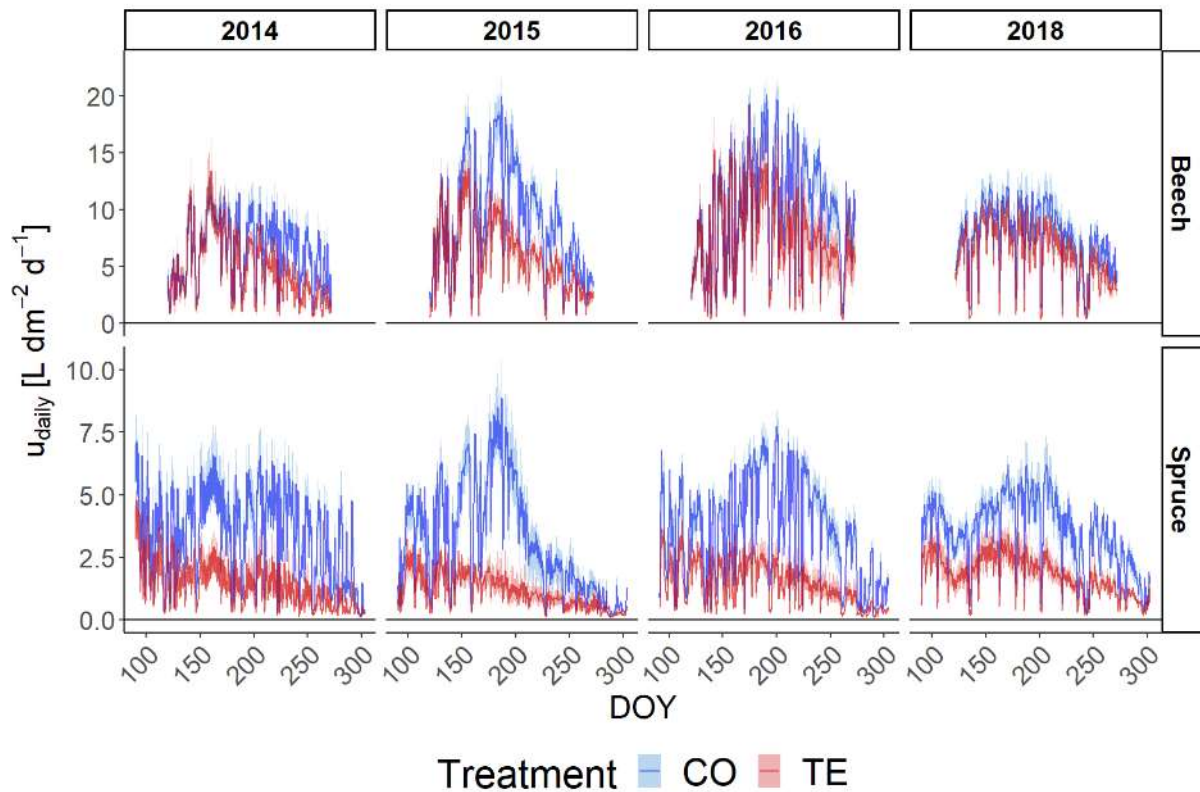
796

797 **Tables**

798 *Table 1: Annual mean of the sap flow density per day at outer 2cm sapwood (u_{daily}) in control*
 799 *(CO) and throughfall exclusion (TE) beech and spruce trees, given in mean(SE). Asterisks*
 800 *indicate significant results based on linea-mixed model comparing CO and TE trees, ***, $p <$*
 801 *0.001; **, $p < 0.01$; (*), $p < 0.1$. The detailed course of u_{daily} is displayed in Fig. S1.*

		2014	2015	2016	2018
Annual mean	beech	CO 6.29(0.08)	9.12(0.12)	10.18(0.15)	7.69(0.09)
		TE 5.36(0.09)	5.90(0.08) (*)	7.87(0.10)	6.96(0.08)
u_{daily} (L dm ⁻² d ⁻¹)	spruce	CO 3.30(0.05)	3.15(0.05)	3.58(0.05)	3.48(0.04)
		TE 1.35(0.03)**	1.11(0.02)***	1.43(0.03)***	1.71(0.03)**

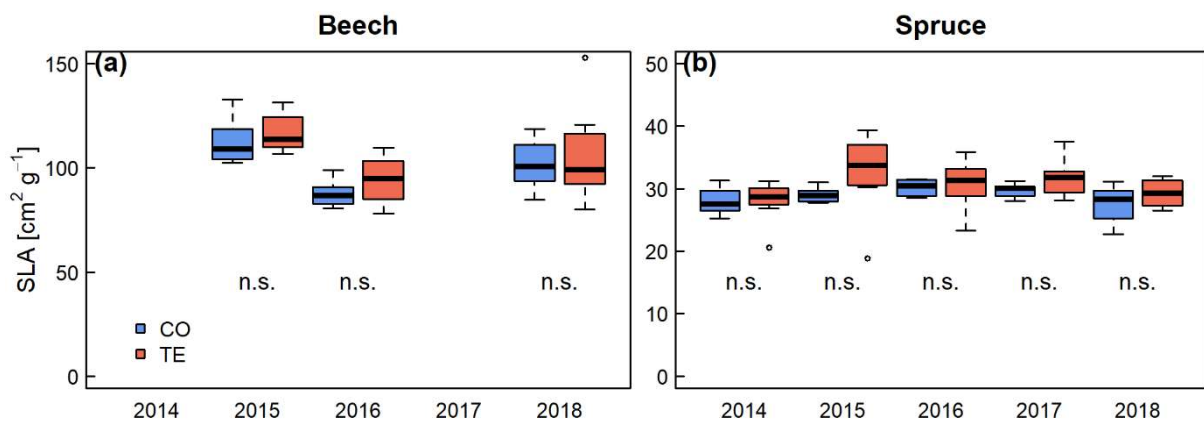
802



804

805 *Fig. S 1: Course of the sap flow density per day at outer 2cm sapwood (u_{daily}) in control (CO,*
 806 *blue) and throughfall exclusion (TE, red) beech (top) and spruce (bottom) trees. DOY gives day*
 807 *of year.*

808



809

810 *Fig. S 2: Specific leaf area (SLA) of control (CO, blue) and throughfall exclusion (TE, red)*
 811 *beech (a, left) and spruce (b, right) trees. “n.s.” indicates no significant results based on linea-*
 812 *mixed model comparing CO and TE trees.*

1 **Title**

2 Repeated summer drought changes the radial xylem sapflow profile in mature *Picea abies* (L.)
3 Karst.

4 **Running head**

5 Drought alters radial sap flow profile in mature spruce

6 **Authors names:**

7 Timo Gebhardt^{1,2†}, Benjamin D. Hesse^{2†}, Kyohsuke Hikino², Katarina Kolovrat², Benjamin D.
8 Hafner³, Thorsten E.E. Grams², Karl-Heinz Häberle⁴

9 **Authors' affiliation**

10 1- Technical University of Munich, School of Life Sciences, Forest and Agroforest
11 Systems, Hans-Carl-von-Carlowitz Platz 2, 85354 Freising, Germany.

12 2- Technical University of Munich, School of Life Sciences, Land Surface-Atmosphere
13 Interactions, Hans-Carl-von-Carlowitz Platz 2, 85354 Freising, Germany.

14 3- Cornell University, School of Integrative Plant Science, 236 Tower Road, Ithaca, NY
15 14853, USA.

16 4- Technical University of Munich, School of Life Sciences, Chair of Restoration Ecology,
17 Emil-Ramann-Str. 6, 85354 Freising, Germany.

18 † - Equally contributing authors

19 **ORCID**

20 Timo Gebhardt - <https://orcid.org/0000-0003-0047-5949>

21 Benjamin Hesse - <https://orcid.org/0000-0003-1113-9801>

22 Thorsten E.E. Grams - <https://orcid.org/0000-0002-4355-8827>

23 Karl-Heinz Häberle - <https://orcid.org/0000-0001-7946-7305>

24

25 **Corresponding author**

26 Timo Gebhardt (timo.gebhardt@tum.de)

27 **Keywords**

28 water transport, drought, recovery, leaf area, European beech, Norway spruce

29 **Dedication**

30 Dedicated to our late colleague and friend Jan Čermák, who inspired and improved research
31 about water transport and sap flow techniques over decades.

32 **Highlights**

- 33 • Radial xylem sap flow profiles are rarely studied, especially under abiotic stress.
- 34 • A beech/spruce forest was exposed to repeated seasonal drought and recovery.
- 35 • HFD and TD type sensors were applied to measure the xylem sap flow density profile.
- 36 • Repeated drought reduced the xylem sap flow profile in spruce but not of beech.
- 37 • Radial sap flow profiles are altered by drought-induced leaf area reductions.

38 **Abstract**

39 Water consumption of trees is one of the most important processes connected to their survival
40 under ongoing climate change and extreme events such as drought. Radial profiles of xylem
41 sap flow density are an integral component to quantify the water transport for the level of an
42 individual tree and that of ecosystems. However, knowledge of such radial profiles, in particular
43 under stress, is very scarce. Here we show the radial profile of the xylem sap flow density in
44 mature European beech (*Fagus sylvatica* L) and Norway spruce (*Picea abies* (L) Karst.) under
45 repeated summer drought induced by throughfall exclusion (TE) and subsequent recovery
46 compared to untreated control trees (CO). We measured xylem sap flow density (u_{daily} in L dm^{-2}
47 d^{-1}) down to 8 cm sapwood depth at breast height using two different approaches, a thermal
48 dissipation system and the heat field deformation method. In beech, repeated throughfall
49 exclusion did not affect the radial xylem sap flow profile. However, in spruce, u_{daily} was strongly
50 reduced across the profile under repeated drought, changing the profile from a linear to a
51 logarithmic regression. Even two years after drought release, the xylem sap flow profile did not
52 fully recover in TE spruce. The reduction of u_{daily} along the radial profile was accompanied by
53 a reduction of the leaf area in TE spruce by c. 50%, while sapwood depth remained constant.
54 The reduction of the xylem sap flow density along the profile reduced the calculated water
55 consumption of TE spruce trees by more than 33% compared to CO trees, also after drought
56 release. The impact of stressors such as repeated drought on the xylem sap flow density across
57 the radial profile and its consequences for trees' and stands' water consumption needs to be
58 addressed in more detail to minimize uncertainties in quantifying ecosystem water cycles.

59 1. Introduction

60 The past decade with the drought years of 2015, 2018 and 2019 in Central Europe revealed
61 strikingly the consequences of severe and especially repeated drought/heat events for forest
62 ecosystems (Schuldt et al., 2020). Nevertheless, responses of the water balance on tree-level
63 and forest stands to such repeated drought events and subsequent recovery are poorly
64 understood (Ruehr et al., 2019). Xylem sap flow density measurements are an important tool
65 for assessing whole-tree water consumption and budgeting forest ecosystem water balances
66 (Gebhardt et al., 2014; Nadezhdina et al., 2012; Matyssek et al. 2009). Moreover, the estimation
67 of the water consumption of trees and forest ecosystems is a crucial part of many process-based
68 models, especially under severe drought events and during subsequent recovery (Morales et al.,
69 2007). Xylem sap flow density measurements are not only helpful in estimating the effects of
70 abiotic stresses (e.g. drought or heat events) on tree water consumption (Lu et al., 2000) but on
71 a larger scale also in estimating water and carbon fluxes of whole forest stands or ecosystems
72 (Poyatos et al., 2021). When calculating the whole-tree water consumption, the decrease in
73 sapflow density along the sapwood profile needs to be considered. However many studies
74 assume a homogenous flow throughout the xylem (see lit. survey in Berdanier et al., 2016;
75 Čermák and Nadezhdina, 1998) and therefore overestimate the actual water consumption.
76 Within the last decades, only a limited number of xylem sap flow profiles of a few species have
77 been published (e.g. Delzon et al., 2004; Fernández et al., 2008; Korakaki and Fotelli, 2021; Lu
78 et al., 2000; Phillips et al., 1996). As with other species, the highest xylem sap flow density was
79 observed in Norway spruce and European beech in the outer cm of the sapwood, with a linear
80 decrease in the flow towards the inner part (Figure 1a), probably due to a decreasing hydraulic
81 conductivity with sapwood depth (Čermák and Nadezhdina, 1998; Gebauer et al., 2008).

82 The radial profile can differ between tree species according to xylem anatomy (Berdanier et al.,
83 2016; Gebauer et al., 2008), age or in response to the atmospheric water demand characterized
84 by VPD (vapor pressure deficit) and/or radiation (Figure 1b, Čermák et al., 2008; Ford et al.,
85 2004b, 2004a; Lüttschwager and Remus, 2007; Nadezhdina et al., 2007). Under drought, trees
86 close their stomata (Grossiord et al., 2020) and reduce xylem sap flow density, primarily in the
87 outer part of the conducting sapwood area as observed for example in *Pinus sylvestris* (L)
88 (Čermák et al., 2008; Nadezhdina et al., 2007). Therefore, the decrease of the sap flow density
89 from the outer to the inner sapwood is flattened (decrease in the slope, see red line in Figure
90 1c). Such a flattening in response to drought may be caused by i) changes in water uptake from
91 different soil depths (Čermák et al., 2008; Nadezhdina et al., 2007), ii) changes in the
92 conducting sapwood depth (Čermák and Nadezhdina, 1998; Köstner et al., 2002; McDowell et

93 al., 2002) or iii) in dependence of the canopy area mostly affected by drought (upper (sun) vs.
94 lower (shade) crown, Spicer and Gartner, 2001; Wullschleger and King, 2000). The opposite
95 response, a steepened profile (increase in slope) seems to occur in periods with low VPD
96 (Figure 1b, Ford et al., 2004a, 2004b). However, to our knowledge, no studies have been
97 conducted on changes in the radial profile of sap flow density under repeated drought. In
98 addition to immediate physiological responses, repeated drought can cause morphological
99 changes to trees such as fine root- and stem growth, as well as anatomical acclimation (Pretzsch
100 et al., 2020; Tyree et al., 1993). The influence of morphological tree reactions to repeated
101 drought on the xylem sap flow profile is to our knowledge unknown.

102 To fill this gap, we took advantage of a long-term throughfall-exclusion experiment in the south
103 of Germany (Kranzberg forest roof experiment, (KROOF, Grams et al., 2021). In this five-year
104 drought experiment, a strong reduction in stem growth increment was found for European beech
105 and Norway spruce (Pretzsch et al., 2020) as well as a reduced abundance of fine roots
106 (Zwetsloot and Bauerle, 2021) and ectomycorrhizal communities (Nickel et al., 2018). We
107 assessed the xylem sap flow density along the radial profile in stems of repeatedly drought-
108 stressed mature trees of Norway spruce and European beech to test the following hypothesis:

109 H1: Repeated drought reduces the sapflow density in the outer sapwood and this decreases the
110 slope of the sap flow profile along sapwood depth (see red line in Figure 1c).

111 H2: Radial profile of sap flow density recovers after drought release.

112 **2. Material and Methods**

113 **2.1 Experimental site and design**

114 The KROOF experiment is located in Kranzberg Forest near Freising in south-east Germany
115 (11°39'42"E, 48°25'12"N). The tree stand is composed of Norway spruce (*Picea abies* (L)
116 Karst.) and European beech (*Fagus sylvatica* L), planted in 1951 ± 2 AD and 1931 ± 4 AD,
117 respectively (Pretzsch et al., 2014). With a luvisol soil originating from a loess layer above
118 tertiary sediments and an average precipitation of 750-800 mm a⁻¹ there is a good water
119 availability given at the site (for details see Grams et al. 2021). From 2014 to 2018 the KROOF
120 experiment ("phase I") focused on the effects of repeated summer drought. Drought was
121 generated via a throughfall-exclusion system (TE), which held off the precipitation during the
122 growing season from 6 experimental plots with 3 to 7 trees of each species. For comparison, 6
123 untreated control plots (CO, Grams et al. 2021) were established next to the TE plots. In the

124 second half of 2019 the KROOF experiment “phase II” started with a controlled watering of
125 the TE plots to the soil moisture level of the CO plots (Grams et al. 2021).

126 2.2 Climatic conditions and soil water content at the experimental site

127 Air temperature (T in °C), vapor pressure deficit (VPD in kPa), solar global radiation (Rad in
128 W m^{-2}) and daily precipitation (Precip in mm) were measured daily on site above the canopy
129 on a scaffolding tower and are presented here as the mean values of the growing season (April-
130 September).

131 Plant available water (PAW in vol.-%, volume of water per volume of soil) was calculated
132 weekly from the soil water content for 0 to 70 cm soil depth measured via time domain
133 reflectometry sensors (TDR100 and TDR200, Campbell Scientific, Logan, USA) and the
134 permanent wilting points at the experimental site from Grams et al. (2021).

135 2.3 Xylem sap flow density profile at diameter at breast height

136 Sap flow density per unit sapwood area at breast height was measured using two methods,
137 thermal dissipation (TD) (Granier, 1987, 1985) and heat field deformation (HFD) (Nadezhdina
138 et al., 2012) in 10 min intervals. In summer 2019, TD-sensors were installed on three to four
139 trees per species and treatment at three sapwood depths, i.e. 0-2 cm, 2-4 cm and 4-6 cm from
140 the cambium and the mean sap flow density per day and tree was calculated (u_{daily} in $\text{L dm}^{-2} \text{d}^{-1}$).
141 HFD sensors (measurement points: 0.5, 1.5, 2.5, 3.5, 4.5, 5.5, 6.5 and 7.5 cm xylem depth)
142 were installed on four to five trees per species and treatment in 2016, 2020 and 2021. Evaluation
143 of HFD data was done with the Sap Flow Tool (ICT International, Armidale, NSW, Australia,
144 version 1.5) and followed the suggestion of Nadezhdina (2018) and Nadezhdina et al. (2012).
145 The relative proportions of the xylem sap flow profile (u_{depth_x} in %, with x symbolizing the
146 depth in the sapwood xylem) were calculated in relation to the outermost sensor point (HFD:
147 0.5 cm and TD: 0-2 cm) for each tree individually. Every tree was measured at least for two
148 consecutive weeks between June and September and days with rainfall (i.e. no sap flow) were
149 excluded from further analysis.

150 2.4 Number of tree rings in the outer xylem sapwood

151 To estimate the age of the conducting xylem along the sapflow profile the number of tree rings
152 in the sapwood was counted on wood cores taken in 2019 at dbh. Cores were extracted to a
153 depth of 8 cm and divided into 8 segments of 1 cm length each, to match the measurement
154 points of the HFD method.

155 2.5 Leaf area of spruce under repeated drought

156 Total leaf area (LA m² tree⁻¹) was estimated from three CO and six TE spruce trees (see
157 supporting Material and Methods and Figure S1 for details). Briefly, for each tree, the total
158 number of needles of each needle age was calculated separately for sun and shade crowns using
159 field data collected in late summer 2020:

$$160 \quad N_n = N_s \times L_b \times L_s \times D$$

161 where N_s gives the number of shoots of each needle age (in n cm⁻¹ needled branch length), L_b
162 the total length of the needled branches (in cm), L_s the length of each shoot (in cm), and D the
163 needle density in each shoot (in n cm⁻¹). Then, the total leaf area of each needle age (A_n in m²)
164 was calculated using needle length (L_n in mm) following Riederer et al. (1988).

$$165 \quad A_n = \frac{N_n \times (3.279 \times L_n - 16.31)}{1000000} \text{ (for current year needles)}$$

$$166 \quad A_n = \frac{N_n \times (4.440 \times L_n - 24.78)}{1000000} \text{ (for older needles)}$$

167 Finally, the surface area of each needle age was summed up to determine the total leaf area
168 (LA) of each tree in 2020. Based on the data of 2020, we retrospectively calculated annual LA
169 between 2014 and 2019 and for 2021.

170 2.6 Statistical analysis

171 Statistical differences in the data between treatments and species were analyzed using R
172 (version: 3.6, R Development Core Team 2008) in RStudio (version 1.2.1335, RStudio Team
173 2015). Data were tested for homogeneity of variances (Levene test) and the residuals of every
174 model were tested for normality (QQ-Plot). For differences in the sapflow profile and the
175 number of tree rings between years, species and treatments we calculated a linear mixed effect
176 model ('lme' function) using the tree individual as a random effect (package: nlme, version:
177 3.1-137). The method (TD vs. HFD) did not show any significant influence on the xylem sap
178 flow profile ($p > 0.05$) and was therefore excluded from the analysis. If the mixed effect model
179 showed significant effects, we made a posthoc test using the 'emmeans' function with Tukey
180 correction (package: emmeans, version: 1.3.1). Data were plotted with the 'ggplot2' package
181 (version: 3.5.2) and data are given in the text as the mean \pm 1SD.

182 **3 Results**

183 3.1 Climatic conditions and soil water content on the experimental site

184 The overall mean temperature for the four growing seasons with measurements of the radial
185 sap flow profile was 16.1 ± 4.0 °C, with 2016 (17.8 ± 4.0 °C) being the warmest and 2021 the
186 coldest year (14.2 ± 4.8 °C, Table 1). Vapor pressure deficit was similar for all four growing
187 seasons (mean value: 0.54 ± 0.19 kPa) but slightly higher in 2019 (0.66 ± 0.26 kPa, Table 1).
188 The average global solar radiation was very similar in 2019 and 2020 (mean value: 335 ± 59 W
189 m^{-2}) and almost 30% lower in 2016 (216 ± 29 W m^{-2}) and 45% lower in 2021 (186 ± 31 W m^{-2} ,
190 Table 1). Precipitation during the growing season was similar for 2016 and 2020 (mean value:
191 468.5 mm), but slightly lower in 2019 (406.1 mm) and much higher in 2021 (601.4 mm, Table
192 1).

193 The PAW averaged over the top 70 cm of the soil was significantly lower in TE compared to
194 CO in the growing seasons of 2016 (CO: 14.1 ± 0.8 vol.-% and TE: 4.7 ± 0.4 vol.-%) and 2019
195 before the re-watering (CO: 13.4 ± 0.4 vol.-% and TE: 6.7 ± 0.3 vol.-%). In 2020, TE showed
196 relatively higher PAW values (CO: 10.8 ± 0.6 vol.-% and TE: 14.2 ± 0.4 vol.-%), similar to CO
197 values of 2016 and 2019 (Table 1) and in 2021 both treatments showed the highest, very similar
198 values (CO: 18.2 ± 0.6 vol.-% and TE: 17.4 ± 0.4 vol.-%).

199 3.2 Sap flow density profile

200 In beech, no differences between CO and TE trees in the relative xylem sapflow density across
201 the sapwood depth were found (Figure 2) and the profiles of the years did not differ significantly
202 ($p > 0.05$). In 2016 and 2019, both treatments showed a linear reduction in their sap flow profile
203 from the cambium to c. 7.5 cm sapwood depth (R^2 for CO: 0.887 and TE: 0.804), resulting in a
204 reduction of about 10 % per 1 cm sapwood depth in relation to the sap flow density in 1 cm
205 depth for each centimeter sapwood depth for both years combined (Figure 2).

206 The sapflow profiles in CO spruce were very similar over all four years of examination,
207 showing combined a linear decrease (R^2 : 0.920) of about 14% for each cm sapwood, down to
208 almost 0 % sap flow density in 7.5 cm depth in relation to the value at 1 cm depth (Figure 3).
209 For TE spruce, the flow in 7.5 cm depth was also close to 0, however, the decrease in relative
210 xylem sapflow density followed a logarithmic function (R^2 : 0.926, Figure 3). This resulted in
211 significantly reduced relative xylem sapflow density across the radial profile compared to CO
212 trees (P-value < 0.001). Especially for the sapwood depth between 2 to 5 cm, relative sapflow
213 in the TE profile was significantly lower than in the CO profile (Figure 3). Additionally, there

214 was no difference in spruce between the profile of drought years (2016 & 2019) and recovering
215 years (2020 & 2021).

216 In contrast to the sapflow profile, the absolute xylem sapflow density of TE in the outermost
217 part of the sapwood differed significantly between the drought years and after recovery. In
218 2016, the absolute xylem sap flow density in 0-2 cm sapwood depth was significantly reduced
219 by about 60 % ($p < 0.05$) in TE ($2.86 \pm 1.03 \text{ L dm}^{-2} \text{ d}^{-1}$) compared to CO spruce trees ($7.12 \pm$
220 $1.76 \text{ L dm}^{-2} \text{ d}^{-1}$, Figure 4). In 2021, after two years of recovery, TE and CO spruce trees showed
221 similar u_{daily} (overall mean: $6.02 \pm 1.91 \text{ L dm}^{-2} \text{ d}^{-1}$), indicating a full recovery in the outermost
222 xylem sapwood (Figure 4).

223 3.3 Number of tree rings in the xylem sapwood

224 In beech, over the outermost 8 cm of sapwood, no significant differences were found in the
225 number of tree rings (CO: 39.0 ± 10.9 and TE 46.9 ± 9.4). The slightly higher number of tree
226 rings in TE beech was mostly due to a higher number of rings in the outermost cm of sapwood
227 in TE (12.2 ± 3.9) than in CO trees (7.8 ± 3.5 , $p < 0.1$, Table 2). For spruce, a similar pattern
228 was found with CO (33.2 ± 4.3) and TE (34.0 ± 7.0) having a very similar number of tree rings,
229 yet there were significantly more tree rings in TE (9.3 ± 1.7) compared to CO (6.8 ± 1.5 , p -
230 value < 0.05 , Table 2) in the outermost sapwood cm. Overall, the number of tree rings per depth
231 sapwood increased in TE trees in both species in the outer/younger parts of the xylem,
232 corresponding to the drought period of 2014-2019.

233 3.4 Leaf area of spruce

234 During the early drought (2014 to 2015), the leaf area was similar between CO and TE spruce
235 trees (mean values over both treatments: $440 \pm 163 \text{ m}^2 \text{ tree}^{-1}$, Figure 5). During the 3rd to 5th
236 drought year (2016 to 2019) the leaf area was about half in the TE ($212 \pm 86 \text{ m}^2 \text{ tree}^{-1}$) treatment
237 compared to CO ($461 \pm 210 \text{ m}^2 \text{ tree}^{-1}$), which remained in the recovery period (2020 to 2021;
238 mean values for 2020 to 2021 of CO: $492 \pm 186 \text{ m}^2 \text{ tree}^{-1}$ and TE $186 \pm 82 \text{ m}^2 \text{ tree}^{-1}$, Figure 5).

239 **4 Discussion**

240 In contrast to H1 with a proposed decrease of the slope of the profile, we found an increase of
241 the slope across the radial xylem sap flow profile due to repeated drought in spruce and no
242 changes in beech. Therefore H1 cannot be accepted for both species. As the pattern of the xylem
243 sap flow profile was not altered under repeated drought in beech, H2 for beech could not be
244 answered. However, for spruce, the slope of the xylem sap flow profile did not recover after
245 drought release and therefore H2 was rejected for spruce.

246 Despite the clear physiological responses of beech to the repeated drought (Grams et al., 2021;
247 Hesse et al., 2019; Tomasella et al., 2018), no alterations in the xylem sap flow radial profile
248 were found. While TE beech trees received the same throughfall exclusion treatment as TE
249 spruce, the implications seemed to be less harsh for beech than for spruce with weaker
250 morphological responses in stem growth (Pretzsch et al., 2020), roots (Grams et al., 2021) or
251 crown architecture (Jacobs et al., 2021). However, the drought did not affect the wood anatomy
252 of both species as the conduit characteristics were not different between TE and CO on the
253 branch level (Petit et al., 2022). Furthermore, for both species, the conducting sapwood depth
254 was not decreasing under drought but integrated over the last 30 to 50 tree rings (i.e. 8 cm).
255 Therefore, the reductions in stem growth over the last 5 years of experimental drought did not
256 reduce the depth of the radial xylem sap flow profile significantly. For beech, altogether drought
257 impact was not strong enough to cause a change in the xylem sapflow profile, potentially this
258 is related to the more anisohydric strategy (drought tolerance) of beech (Leuschner, 2020). On
259 the other side, despite the strong physiological response to the drought of spruce with the
260 reduction of the absolute sapflow density in the outer part of the xylem (Figure 1c and 4), the
261 change of the relative radial sapflow profile was inverse to other drought studies (Fi. 1c; Čermák
262 et al., 2008; Nadezhdina et al., 2007). Therefore, under repeated drought, changes in the radial
263 sapflow profile in the spruce trees were probably not driven by physiological (e.g. stomatal
264 closure) or cellular anatomical (e.g. conduit size) drought reactions, but related to
265 morphological changes at the organ level (e.g. roots or leaves). This is further supported by the
266 missing recovery of the profile in spruce, but a full recovery of xylem sap flow density in the
267 outermost two centimeters (Figure 4, Hesse et al submitted, Knüver et al 2022).

268 Such morphological responses under drought included a strong decrease in fine root growth
269 (Zwetsloot and Bauerle, 2021) as well as a reduction in twig growth and leaf area in spruce
270 (Figure 5, Jacobs et al., 2021; Tomasella et al., 2018). Since TE spruce had only half the leaf
271 area of CO trees with ongoing drought and did not recover after drought release (Figure 5), the
272 overall water demand per tree was strongly reduced. Furthermore, the reduced leaf area at
273 increased soil water availability in TE plots after drought release (Table 1) suggests that the
274 radial profile was strongly related to the overall tree water demand. Therefore, either conduit
275 capacity in older xylem tissue may have been down-regulated (Dietrich et al., 2018) or older
276 conduits were partially abandoned (e.g. through embolism or early heartwood formation,
277 Lüttschwager and Remus, 2007). With the observed (partial) canopy dieback of forests due to
278 climate extremes, e.g. in 2018/19 in Central Europe (Schuldt et al., 2020), also the water
279 demand and therefore the xylem sap flow density along the profile might be reduced.

280 Altogether, not only do climatic factors (e.g. VPD) define the water demand of a tree and
281 therefore shape the xylem sap flow profile (Figure 1b) but additionally, tree morphology (e.g.
282 leaf area) needs to be considered.

283 Measurements of the leaf area of trees are challenging and therefore often existing correlations
284 between leaf area (LA) and stem diameter (as a proxy for sapwood area (SA)) are used to
285 estimate the leaf area of trees (Swenson and Enquist, 2008; Vertessy et al., 1995, Forrester et
286 al. 2017). It has been shown, that the LA/SA ratio can change with tree height, tree age, and
287 tree species (Köstner et al., 2002; McDowell et al., 2002), and decreases due to repeated
288 summer droughts as shown in this study (c.50%). A decrease in LA/SA ratio also has been
289 observed in other long-term drought experiments with mature trees at the branch level (Hudson
290 et al., 2018; Limousin et al., 2012; Martin-Stpaul et al., 2013) and at the whole-tree level
291 (Limousin et al., 2012; McBranch et al., 2018; Moreno et al., 2021). However, here we show
292 additionally a change of the xylem sap flow profile by the reduced LA, indicating a reduction
293 in the whole tree water consumption, independent of the conducting sapwood area. Therefore,
294 such profile measurements should be included not only in experimental but also stronger in
295 process-based modeling approaches. In the present example, the whole-tree water consumption
296 of drought-stressed spruce would be overestimated by about $33.9 \pm 1.5 \%$, if the unaffected
297 profile of control trees was used. In our case, this would lead to an underestimation of water
298 consumption between 370 ± 149 L under repeated drought and 814 ± 453 L per tree and growing
299 season after one year of recovery.

300 Especially in modeling approaches regarding the water balance of whole forest stands or
301 ecosystems (e.g. Kucharik et al. 2000, Gerten et al. 2004, Tang et al. 2015), such uncertainties
302 can lead to fatal misjudgments of ecosystem performances under climate change scenarios
303 (Krause et al., 2018; Oberpriller et al., 2021; Zaehle et al., 2005). A decreased water
304 consumption would not only impact the water balance but also the modeled carbon balance of
305 trees and following growth processes, as transpiration and CO₂ uptake are highly dependent in
306 plants (Zaehle et al., 2005). Besides whole tree water consumption, xylem sap flow
307 measurements can express the overall canopy conductance and therefore the CO₂ uptake of a
308 tree can be estimated (Köstner et al., 1992; Nadezhdina et al., 2012; Poyatos et al., 2021). Xylem
309 sap flow density coupled with radial profile measurements is, therefore, an important tool for
310 assessing the water balance of trees, especially under currently proceeding climate change and
311 increasing abiotic and biotic stressors.

312 **Acknowledgments**

313 We would like to thank Thomas Feuerbach for the technical support and Sepp Heckmair, Peter
314 Kuba and Christian Kallenbach for help during sampling.

315 **Funding**

316 BDH was founded by a doctoral scholarship from the German Federal Environmental
317 Foundation (DBU). The research site is owned by Bayerische Staatsforsten who gave us free
318 access and allowed the experimental setup. We highly appreciate the funding of the project by
319 the German Research Foundation (DFG, GR 1881/5-1, MA1763/7-1) and by the Bavarian State
320 Ministries of the Environment and Consumer Protection as well as Food, Agriculture and
321 Forestry (BayKROOF, W047/Kroof II).

322 **Bibliography**

323 Berdanier, A.B., Miniati, C.F., Clark, J.S., 2016. Predictive models for radial sap flux variation
324 in coniferous, diffuse-porous and ring-porous temperate trees. *Tree Physiol.* 36, 932–941.
325 <https://doi.org/10.1093/treephys/tpw027>

326 Čermák, J., Nadezhdina, N., 1998. Sapwood as the scaling parameter - defining according to
327 xylem water content or radial pattern of sap flow? *Ann. For. Sci.* 509–521.

328 Čermák, J., Nadezhdina, N., Meiresonne, L., Ceulemans, R., 2008. Scots pine root distribution
329 derived from radial sap flow patterns in stems of large leaning trees. *Plant Soil* 305, 61–
330 75. <https://doi.org/10.1007/s11104-007-9433-z>

331 Delzon, S., Sartore, M., Granier, A., Loustau, D., 2004. Radial profiles of sap flow with
332 increasing tree size in maritime pine. *Tree Physiol.* 24, 1285–1293.
333 <https://doi.org/10.1093/treephys/24.11.1285>

334 Dietrich, L., Hoch, G., Kahmen, A., Körner, C., 2018. Losing half the conductive area hardly
335 impacts the water status of mature trees. *Sci. Rep.* 8, 1–9. <https://doi.org/10.1038/s41598-018-33465-0>

337 Fernández, J.E., Green, S.R., Caspari, H.W., Diaz-Espejo, A., Cuevas, M. V., 2008. The use of
338 sap flow measurements for scheduling irrigation in olive, apple and Asian pear trees and
339 in grapevines. *Plant Soil* 305, 91–104. <https://doi.org/10.1007/s11104-007-9348-8>

340 Ford, C.R., Goranson, C.E., Mitchell, R.J., Will, R.E., Teskey, R.O., 2004a. Diurnal and
341 seasonal variability in the radial distribution of sap flow: Predicting total stem flow in
342 *Pinus taeda* trees. *Tree Physiol.* 24, 941–950. <https://doi.org/10.1093/treephys/24.9.951>

- 343 Ford, C.R., McGuire, M.A., Mitchell, R.J., Teskey, R.O., 2004b. Assessing variation in the
344 radial profile of sap flux density in Pinus species and its effect on daily water use. *Tree*
345 *Physiol.* 24, 241–249. <https://doi.org/10.1093/treephys/24.3.241>
- 346 Gebauer, T., Horna, V., Leuschner, C., 2008. Variability in radial sap flux density patterns and
347 sapwood area among seven co-occurring temperate broad-leaved tree species. *Tree*
348 *Physiol.* 28, 1821–1830. <https://doi.org/10.1093/treephys/28.12.1821>
- 349 Gebhardt, T., Häberle, K.H., Matyssek, R., Schulz, C., Ammer, C., 2014. The more, the better?
350 Water relations of Norway spruce stands after progressive thinning. *Agric. For. Meteorol.*
351 197, 235–243. <https://doi.org/10.1016/j.agrformet.2014.05.013>
- 352 Gerten, D., Schaphoff, S., Haberlandt, U., Lucht, W., Sitch, S., 2004. Terrestrial vegetation and
353 water balance - Hydrological evaluation of a dynamic global vegetation model. *J. Hydrol.*
354 286, 249–270. <https://doi.org/10.1016/j.jhydrol.2003.09.029>
- 355 Grams, T.E.E., Hesse, B.D., Gebhardt, T., Weigl, F., Rötzer, T., Kovacs, B., Hikino, K., Hafner,
356 B.D., Brunn, M., Bauerle, T.L., Häberle, K.-H., Pretzsch, H., Pritsch, K., 2021. The Kroof
357 experiment: realization and efficacy of a recurrent drought experiment plus recovery in a
358 beech/spruce forest. *Ecosphere* 12. <https://doi.org/10.1002/ecs2.3399>
- 359 Granier, A., 1987. Evaluation of transpiration in a Douglas-fir stand by means of sap flow
360 measurements. *Tree Physiol.* 3, 309–320. <https://doi.org/10.1093/treephys/3.4.309>
- 361 Granier, A., 1985. Une nouvelle méthode pour la mesure du flux de sève brute dans le tronc
362 des arbres. *Ann. For. Sci.* 3, 247–255. <https://doi.org/10.1007/BF00117583>
- 363 Grossiord, C., Buckley, T.N., Cernusak, L.A., Novick, K.A., Poulter, B., Siegwolf, R.T.W.,
364 Sperry, J.S., McDowell, N.G., 2020. Plant responses to rising vapor pressure deficit. *New*
365 *Phytol.* 226, 1550–1566. <https://doi.org/10.1111/nph.16485>
- 366 Hesse, B.D., Goisser, M., Hartmann, H., Grams, T.E.E., 2019. Repeated summer drought delays
367 sugar export from the leaf and impairs phloem transport in mature beech. *Tree Physiol.*
368 39, 192–200. <https://doi.org/10.11821/dlxb201802008>
- 369 Hudson, P.J., Limousin, J.M., Krofcheck, D.J., Boutz, A.L., Pangle, R.E., Gehres, N.,
370 McDowell, N.G., Pockman, W.T., 2018. Impacts of long-term precipitation manipulation
371 on hydraulic architecture and xylem anatomy of piñon and juniper in Southwest USA.
372 *Plant Cell Environ.* 41, 421–435. <https://doi.org/10.1111/pce.13109>

- 373 Jacobs, M., Rais, A., Pretzsch, H., 2021. How drought stress becomes visible upon detecting
374 tree shape using terrestrial laser scanning (TLS). *For. Ecol. Manage.* 489, 118975.
375 <https://doi.org/10.1016/j.foreco.2021.118975>
- 376 Korakaki, E., Fotelli, M.N., 2021. Sap flow in aleppo pine in Greece in relation to sapwood
377 radial gradient, temporal and climatic variability. *Forests* 12, 1–16.
378 <https://doi.org/10.3390/f12010002>
- 379 Köstner, B., Falge, E., Tenhunen, J.D., 2002. Age-related effects on leaf area/sapwood area
380 relationships, canopy transpiration and carbon gain of Norway spruce stands (*Picea abies*)
381 in the Fichtelgebirge, Germany. *Tree Physiol.* 22, 567–574.
382 <https://doi.org/10.1093/treephys/22.8.567>
- 383 Köstner, B.M.M., Schulze, E.D., Kelliher, F.M., Hollinger, D.Y., Byers, J.N., Hunt, J.E.,
384 McSeveny, T.M., Meserth, R., Weir, P.L., 1992. Transpiration and canopy conductance in
385 a pristine broad-leaved forest of *Nothofagus*: an analysis of xylem sap flow and eddy
386 correlation measurements. *Oecologia* 91, 350–359. <https://doi.org/10.1007/BF00317623>
- 387 Krause, A., Pugh, T.A.M., Bayer, A.D., Li, W., Leung, F., Bondeau, A., Doelman, J.C.,
388 Humpenöder, F., Anthoni, P., Bodirsky, B.L., Ciais, P., Müller, C., Murray-Tortarolo, G.,
389 Olin, S., Popp, A., Sitch, S., Stehfest, E., Arneth, A., 2018. Large uncertainty in carbon
390 uptake potential of land-based climate-change mitigation efforts. *Glob. Chang. Biol.* 24,
391 3025–3038. <https://doi.org/10.1111/gcb.14144>
- 392 Kucharik, C.J., Foley, J.A., Déliire, C., Fisher, V.A., Coe, M.T., Lenters, J.D., Young-Moiling,
393 C., Ramankutty, N., Norman, J.M., Gower, S.T., 2000. Testing the performance of a
394 dynamic global ecosystem model: Water balance, carbon balance, and vegetation
395 structure. *Global Biogeochem. Cycles* 14, 795–825.
396 <https://doi.org/10.1029/1999GB001138>
- 397 Leuschner, C., 2020. Drought response of European beech (*Fagus sylvatica* L.)—A review.
398 *Perspect. Plant Ecol. Evol. Syst.* 47.
- 399 Limousin, J.M., Rambal, S., Ourcival, J.M., Rodríguez-Calcerrada, J., Pérez-Ramos, I.M.,
400 Rodríguez-Cortina, R., Misson, L., Joffre, R., 2012. Morphological and phenological
401 shoot plasticity in a Mediterranean evergreen oak facing long-term increased drought.
402 *Oecologia* 169, 565–577. <https://doi.org/10.1007/s00442-011-2221-8>
- 403 Lu, P., Müller, W.J., Chacko, E.K., 2000. Spatial variations in xylem sap flux density in the

404 trunk of orchard-grown, mature mango trees under changing soil water conditions. *Tree*
405 *Physiol.* 20, 683–692. <https://doi.org/10.1093/treephys/20.10.683>

406 Lüttschwager, D., Remus, R., 2007. Radial distribution of sap flux density in trunks of a mature
407 beech stand. *Ann. For. Sci.* 64, 431–438. <https://doi.org/10.1051/forest:2007020>

408 Martin-Stpaul, N.K., Limousin, J.M., Vogt-Schilb, H., Rodríguez-Calcerrada, J., Rambal, S.,
409 Longepierre, D., Misson, L., 2013. The temporal response to drought in a Mediterranean
410 evergreen tree: Comparing a regional precipitation gradient and a throughfall exclusion
411 experiment. *Glob. Chang. Biol.* 19, 2413–2426. <https://doi.org/10.1111/gcb.12215>

412 McBranch, N.A., Grossiord, C., Adams, H., Borrego, I., Collins, A.D., Dickman, T., Ryan, M.,
413 Sevanto, S., McDowell, N.G., 2018. Lack of acclimation of leaf area:sapwood area ratios
414 in piñon pine and juniper in response to precipitation reduction and warming. *Tree Physiol.*
415 39, 135–142. <https://doi.org/10.1093/treephys/tpy066>

416 McDowell, N., Barnard, H., Bond, B.J., Hinckley, T., Hubbard, R.M., Ishii, H., Köstner, B.,
417 Magnani, F., Marshall, J.D., Meinzer, F.C., Phillips, N., Ryan, M.G., Whitehead, D., 2002.
418 The relationship between tree height and leaf area: Sapwood area ratio. *Oecologia* 132,
419 12–20. <https://doi.org/10.1007/s00442-002-0904-x>

420 Morales, P., Hickler, T., Rowell, D.P., Smith, B., Sykes, M.T., 2007. Changes in European
421 ecosystem productivity and carbon balance driven by regional climate model output. *Glob.*
422 *Chang. Biol.* 13, 108–122. <https://doi.org/10.1111/j.1365-2486.2006.01289.x>

423 Moreno, M., Simioni, G., Cailleret, M., Ruffault, J., Badel, E., Carrière, S., Davi, H., Gavinet,
424 J., Huc, R., Limousin, J.M., Marloie, O., Martin, L., Rodríguez-Calcerrada, J., Vennetier,
425 M., Martin-StPaul, N., 2021. Consistently lower sap velocity and growth over nine years
426 of rainfall exclusion in a Mediterranean mixed pine-oak forest. *Agric. For. Meteorol.* 308–
427 309. <https://doi.org/10.1016/j.agrformet.2021.108472>

428 Nadezhdina, N., 2018. Revisiting the heat field deformation (HFD) method for measuring sap
429 flow. *IForest* 11, 118–130. <https://doi.org/10.3832/ifor2381-011>

430 Nadezhdina, N., Cermak, J., Meiresonne, L., Ceulemans, R., 2007. Transpiration of Scots pine
431 in Flanders growing on soil with irregular substratum. *For. Ecol. Manage.* 243, 1–9.
432 <https://doi.org/10.1016/j.foreco.2007.01.089>

433 Nadezhdina, N., Vandegehuchte, M.W., Steppe, K., 2012. Sap flux density measurements
434 based on the heat field deformation method. *Trees - Struct. Funct.* 26, 1439–1448.

- 435 <https://doi.org/10.1007/s00468-012-0718-3>
- 436 Nickel, U.T., Weikl, F., Kerner, R., Schäfer, C., Kallenbach, C., Munch, J.C., Pritsch, K., 2018.
437 Quantitative losses vs. qualitative stability of ectomycorrhizal community responses to
438 3 years of experimental summer drought in a beech–spruce forest. *Glob. Chang. Biol.* 24,
439 e560–e576. <https://doi.org/10.1111/gcb.13957>
- 440 Oberpriller, J., Herschlein, C., Anthoni, P., Arneth, A., Krause, A., Lindeskog, M., Olin, S.,
441 Hartig, F., 2021. Climate and parameter sensitivity and induced uncertainties in carbon
442 stock projections for European forests (using LPJ-GUESS 4.0). *Geosci. Model Dev.*
443 Discuss. preprint.
- 444 Patzner, K.M., 2004. Die Transpiration von Waldbäumen als Grundlage der Validierung und
445 Modellierung der Bestandestranspiration in einem Wassereinzugsgebiet des Flusses ‘
446 Ammer’. Technische Universität München.
- 447 Petit, G., Zamboni, D., Hesse, B.D., Häberle, K.-H., 2022. No xylem phenotypic plasticity in
448 mature *Picea abies* and *Fagus sylvatica* trees after five years of throughfall precipitation
449 exclusion. *Glob. Chang. Biol.* Accepted. <https://doi.org/10.1111/gcb.16232>
- 450 Phillips, N., Oren, R., Zimmermann, R., 1996. Radial patterns of xylem sap flow in non-,
451 diffuse- and ring-porous tree species. *Plant, Cell Environ.* 19, 983–990.
452 <https://doi.org/10.1111/j.1365-3040.1996.tb00463.x>
- 453 Poyatos, R., Granda, V., Flo, V., Adams, M.A., Adorján, B., Aguadé, D., Aidar, M.P.M., Allen,
454 S., Alvarado-Barrientos, M.S., Anderson-Teixeira, K.J., Aparecido, L.M., Arain, M.A.,
455 Aranda, I., Asbjornsen, H., Baxter, R., Beamesderfer, E., Berry, Z.C., Berveiller, D.,
456 Blakely, B., Boggs, J., Bohrer, G., Bolstad, P. V., Bonal, D., Bracho, R., Brito, P., Brodeur,
457 J., Casanoves, F., Chave, J., Chen, H., Cisneros, C., Clark, K., Cremonese, E., Dang, H.,
458 David, J.S., David, T.S., Delpierre, N., Desai, A.R., Do, F.C., Dohnal, M., Domec, J.-C.,
459 Dzikiti, S., Edgar, C., Eichstaedt, R., El-Madany, T.S., Elbers, J., Eller, C.B., Euskirchen,
460 E.S., Ewers, B., Fonti, P., Forner, A., Forrester, D.I., Freitas, H.C., Galvagno, M., Garcia-
461 Tejera, O., Ghimire, C.P., Gimeno, T.E., Grace, J., Granier, A., Griebel, A., Guangyu, Y.,
462 Gush, M.B., Hanson, P.J., Hasselquist, N.J., Heinrich, I., Hernandez-Santana, V.,
463 Herrmann, V., Hölttä, T., Holwerda, F., Irvine, J., Ayutthaya, S.I.N., Jarvis, P.G.,
464 Jochheim, H., Joly, C.A., Kaplick, J., Kim, H.S., Klemedtsson, L., Kropp, H., Lagergren,
465 F., Lane, P., Lang, P., Lapenas, A., Lechuga, V., Lee, M., Leuschner, C., Limousin, J.-M.,
466 Linares, J.C., Linderson, M.-L., Lindroth, A., Llorens, P., López-Bernal, Á., Loranty,

467 M.M., Lüttschwager, D., Macinnis-Ng, C., Maréchaux, I., Martin, T.A., Matheny, A.,
468 McDowell, N., McMahon, S., Meir, P., Mészáros, I., Migliavacca, M., Mitchell, P.,
469 Mölder, M., Montagnani, L., Moore, G.W., Nakada, R., Niu, F., Nolan, R.H., Norby, R.,
470 Novick, K., Oberhuber, W., Obojes, N., Oishi, A.C., Oliveira, R.S., Oren, R., Ourciva, J.-
471 M., Paljakka, T., Perez-Priego, O., Peri, P.L., Peters, R.L., Pfautsch, S., Pockman, W.T.,
472 Preisler, Y., Rascher, K., Robinson, G., Rocha, H., Rocheteau, A., Röhl, A., Rosado,
473 B.H.P., Rowland, L., Rubtsov, A. V., Sabaté, S., Salmon, Y., Salomón, R.L., Sánchez-
474 Costa, E., Schäfer, K.V.R., Schuldt, B., Shashkin, A., Stahl, C., Stojanovi'c, M., Suárez,
475 J.C., Sun, G., Szatniewska, J., Tatarinov, F., Tesař, M., Thomas, F.M., Tor-ngern, P.,
476 Urban, J., Valladares, F., Tol, C. van der, Meerveld, I. van, Varlagin, A., Voigt, H.,
477 Warren, J., Werner, C., Werner, W., Wieser, G., Wingate, L., Wullschleger, S., Yi, K.,
478 Zweifel, R., Steppe, K., Mencuccini, M., Martínez-Vilalta, J., 2021. Global transpiration
479 data from sap flow measurements : the SAPFLUXNET database. *Earth Syst. Sci. Data* 13,
480 2607–2649.

481 Pretzsch, H., Grams, T., Häberle, K.H., Pritsch, K., Bauerle, T., Rötzer, T., 2020. Growth and
482 mortality of Norway spruce and European beech in monospecific and mixed-species
483 stands under natural episodic and experimentally extended drought. Results of the KROOF
484 throughfall exclusion experiment. *Trees - Struct. Funct.* 34, 957–970.
485 <https://doi.org/10.1007/s00468-020-01973-0>

486 Pretzsch, H., Rötzer, T., Matyssek, R., Grams, T.E.E., Häberle, K.H., Pritsch, K., Kerner, R.,
487 Munch, J.C., 2014. Mixed Norway spruce (*Picea abies* [L.] Karst) and European beech
488 (*Fagus sylvatica* [L.]) stands under drought: from reaction pattern to mechanism. *Trees -*
489 *Struct. Funct.* 28, 1305–1321. <https://doi.org/10.1007/s00468-014-1035-9>

490 R Development Core Team, 2008. R: A language and environment for statistical computing.
491 <http://www.R-project.org>.

492 Riederer, M., Kurbasik, K., Steinbrecher, R., Voss, A., 1988. Surface areas, lengths and
493 volumes of *Picea abies* (L.) Karst. needles: determination, biological variability and effect
494 of environmental factors. *Trees* 2, 165–172. <https://doi.org/10.1007/BF00196021>

495 RStudio Team, 2015. RStudio: Integrated Development for R. <http://www.rstudio.com/>.

496 Ruehr, N.K., Grote, R., Mayr, S., Arneth, A., 2019. Beyond the extreme: recovery of carbon
497 and water relations in woody plants following heat and drought stress. *Tree Physiol.* 39,
498 1285–1299. <https://doi.org/10.1093/treephys/tpz032>

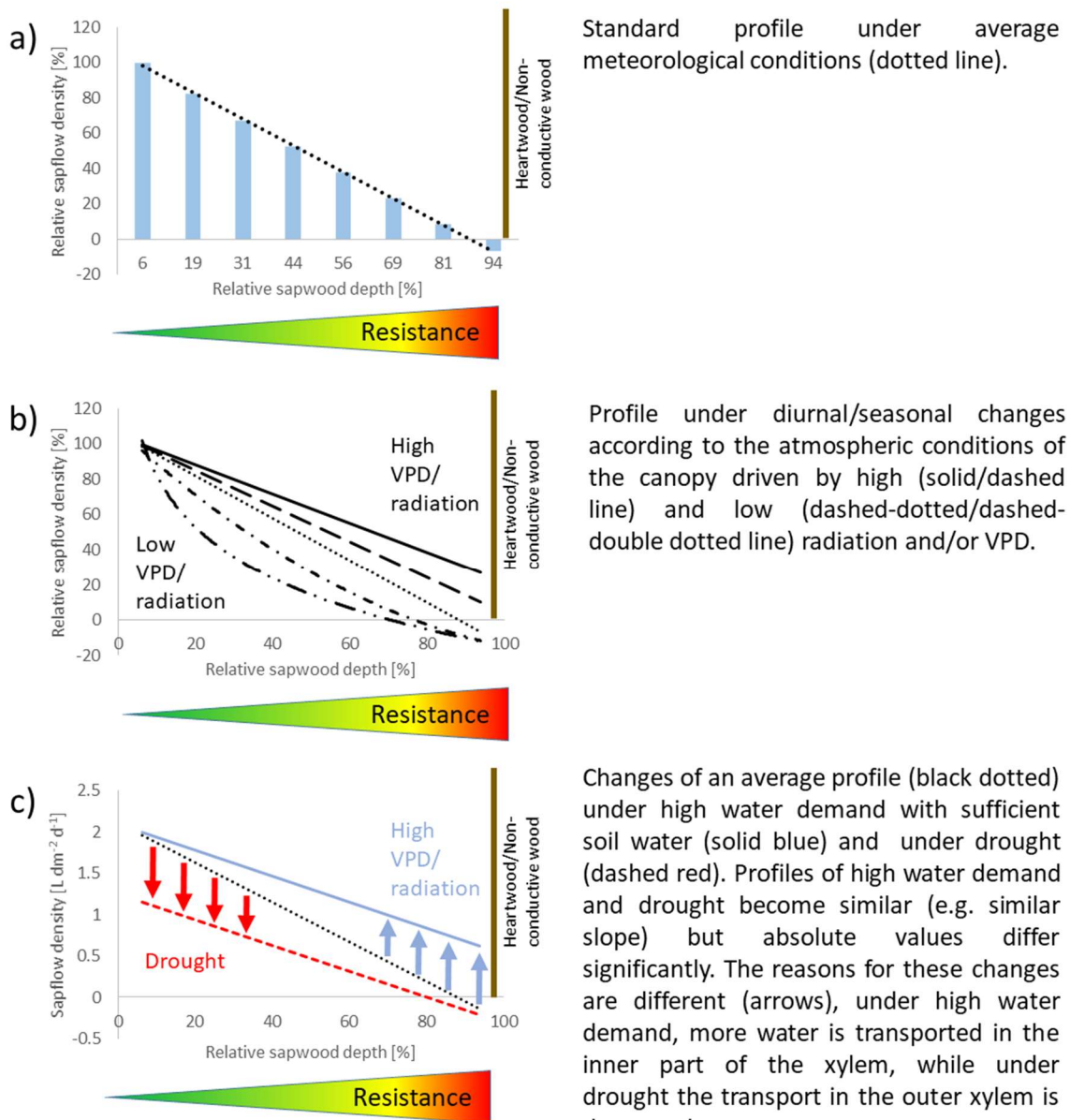
- 499 Schuldt, B., Buras, A., Arend, M., Vitasse, Y., Beierkuhnlein, C., Damm, A., Gharun, M.,
500 Grams, T.E.E., Hauck, M., Hajek, P., Hartmann, H., Hilbrunner, E., Hoch, G., Holloway-
501 Phillips, M., Körner, C., Larysch, E., Lübbe, T., Nelson, D.B., Rammig, A., Rigling, A.,
502 Rose, L., Ruehr, N.K., Schumann, K., Weiser, F., Werner, C., Wohlgemuth, T., Zang,
503 C.S., Kahmen, A., 2020. A first assessment of the impact of the extreme 2018 summer
504 drought on Central European forests. *Basic Appl. Ecol.* 45, 86–103.
- 505 Spicer, R., Gartner, B.L., 2001. The effects of cambial age and position within the stem on
506 specific conductivity in Douglas-fir (*Pseudotsuga menziesii*) sapwood. *Trees - Struct.*
507 *Funct.* 15, 222–229. <https://doi.org/10.1007/s004680100093>
- 508 Swenson, N.G., Enquist, B.J., 2008. The relationship between stem and branch wood specific
509 gravity and the ability of each measure to predict leaf area. *Am. J. Bot.* 95, 516–519.
510 <https://doi.org/10.3732/ajb.95.4.516>
- 511 Tang, J., Miller, P.A., Crill, P.M., Olin, S., Pilesjö, P., 2015. Investigating the influence of two
512 different flow routing algorithms on soil-water-vegetation interactions using the dynamic
513 ecosystem model LPJ-GUESS. *Ecohydrology* 8, 570–583.
514 <https://doi.org/10.1002/eco.1526>
- 515 Tomasella, M., Beikircher, B., Häberle, K.-H., Hesse, B., Kallenbach, C., Matyssek, R., Mayr,
516 S., 2018. Acclimation of branch and leaf hydraulics in adult *Fagus sylvatica* and *Picea*
517 *abies* in a forest through-fall exclusion experiment. *Tree Physiol.* 1–14.
518 <https://doi.org/10.1093/treephys/tpx140>
- 519 Tyree, M.T., Cochard, H., Cruiziat, P., Sinclair, R. B., Ameglio, T., 1993. Drought-induced leaf
520 shedding in walnut: evidence for vulnerability segmentation. *Plant. Cell Environ.* 16, 879–
521 882. <https://doi.org/10.1111/j.1365-3040.1993.tb00511.x>
- 522 Vertessy, R.A., Benyon, R.G., O’Sullivan, S.K., Gribben, P.R., 1995. Relationships between
523 stem diameter, sapwood area, leaf area and transpiration in a young mountain ash forest.
524 *Tree Physiol.* 15, 559–567. <https://doi.org/10.1093/treephys/15.9.559>
- 525 Wullschleger, S.D., King, A.W., 2000. Radial variation in sap velocity as a function of stem
526 diameter and sapwood thickness in yellow-poplar trees. *Tree Physiol.* 20, 511–518.
527 <https://doi.org/10.1093/treephys/20.8.511>
- 528 Zaehle, S., Sitch, S., Smith, B., Hatterman, F., 2005. Effects of parameter uncertainties on the
529 modeling of terrestrial biosphere dynamics. *Global Biogeochem. Cycles* 19, 1–16.

530 <https://doi.org/10.1029/2004GB002395>

531 Zwetsloot, M.J., Bauerle, T.L., 2021. Repetitive seasonal drought causes substantial species-
532 specific shifts in fine-root longevity and spatio-temporal production patterns in mature
533 temperate forest trees. *New Phytol.* <https://doi.org/10.1111/nph.17432>

534

535 **Figures**



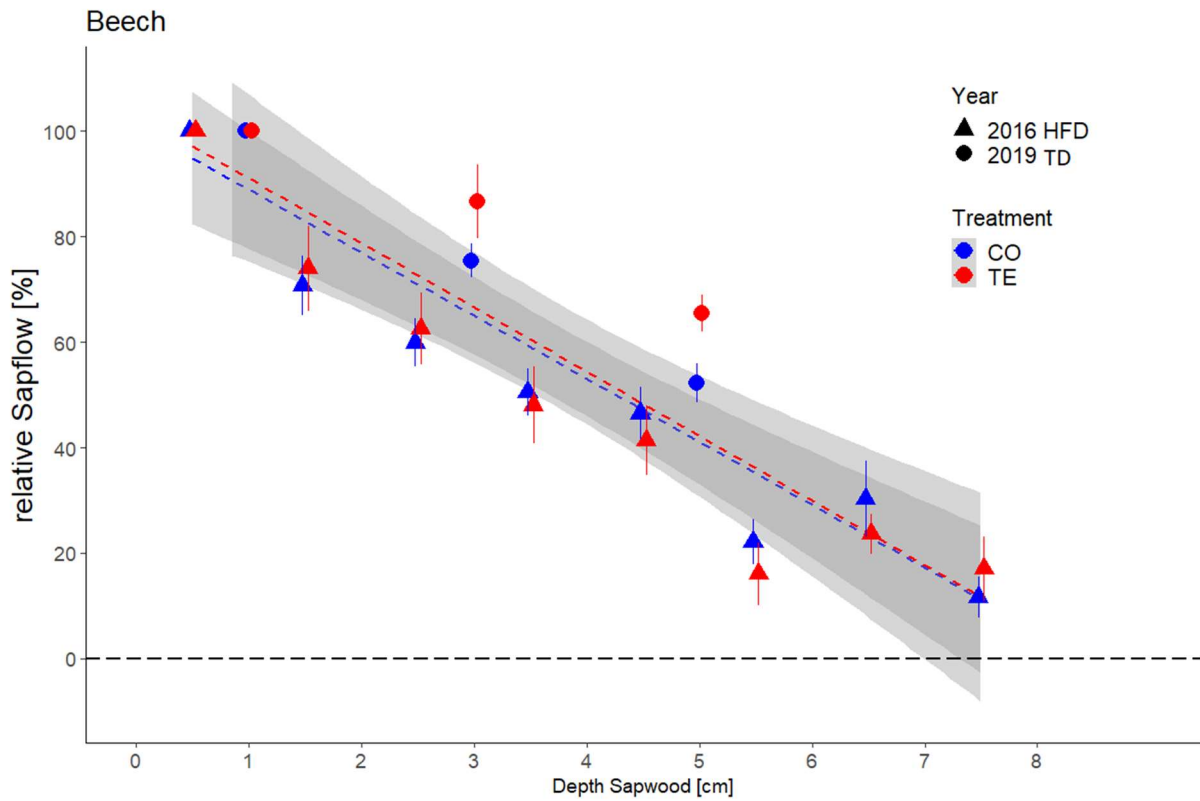
536

537 *Figure 1: Simplified concept figure of the radial xylem sap flow profile under well-watered and average*
538 *climatic conditions (a), alterations in the radial profile due to changes in the water demand of the tree*
539 *driven by climatic factors (e.g. VPD and/or radiation, b) and potential changes of the xylem sap flow*
540 *profile under high atmospheric water demand VPD with high water availability (blue) and during a*

541 single drought period (red, c). Figures follow the framework and suggestions of Čermák et al., 2008;
542 Ford et al., 2004b, 2004a; Lüttschwager and Remus, 2007; Nadezhdina et al., 2007.

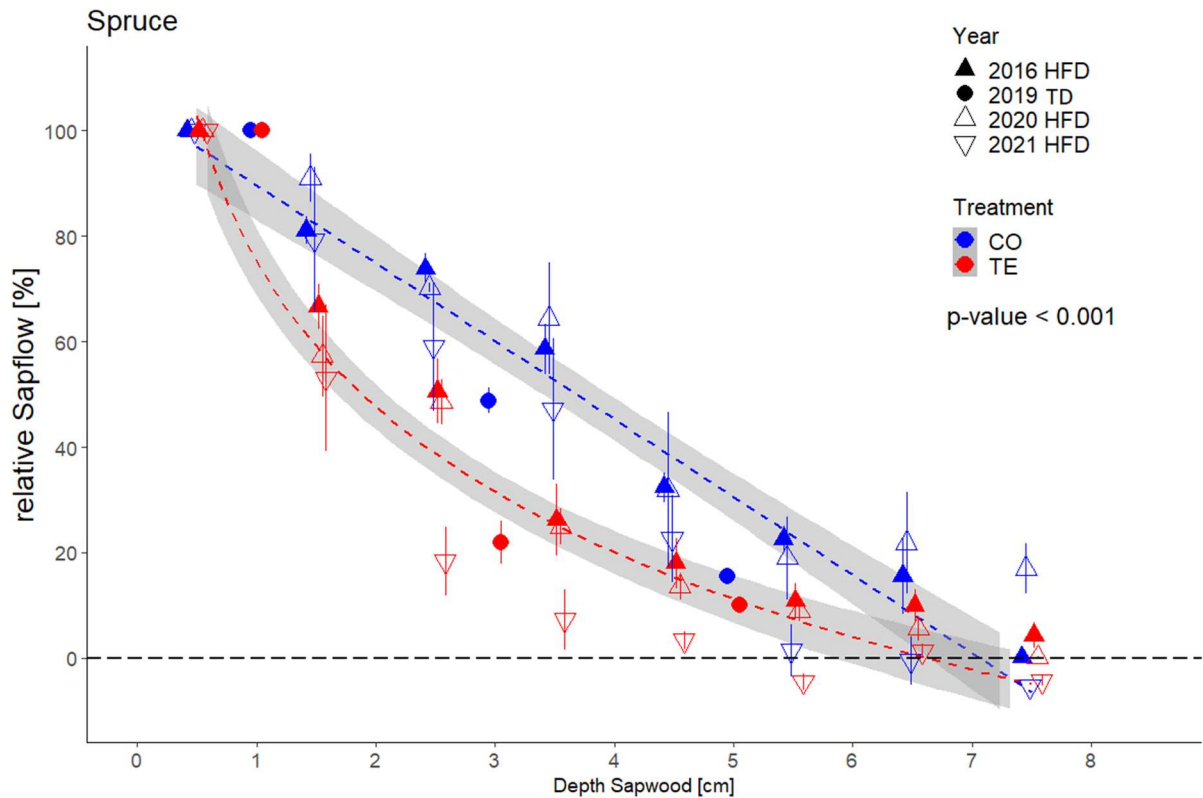
543

544



545

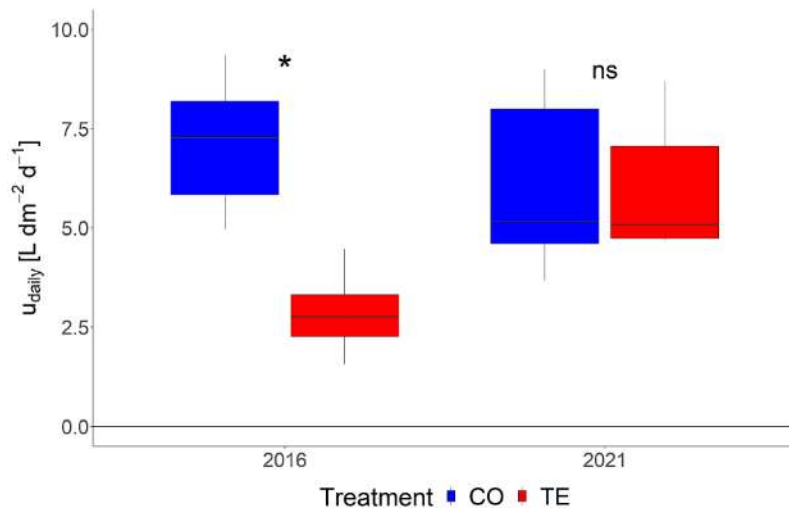
546 Figure 2: Xylem sap flow density profile of beech, with the relative sap flow density in relation to the
547 sap flow of 1cm depth, of 2016 (triangles) and 2019 (circles) for control (CO, blue) and throughfall-
548 exclusion (TE, red). Dashed lines show the linear regression and gray areas the 95% confidence
549 interval. Data are shown as the mean \pm ISE.



550

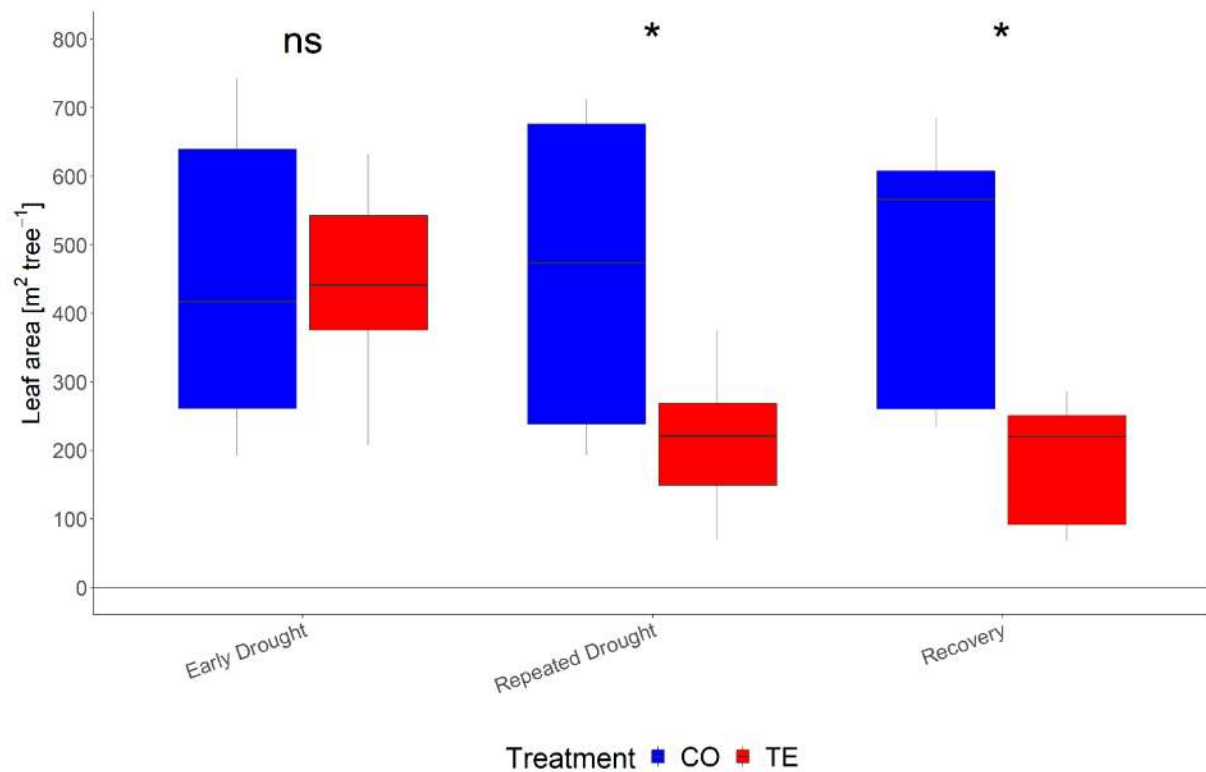
551 *Figure 3: Xylem sap flow density profile of spruce, with the relative sap flow density in relation to the*
 552 *sap flow of 1cm depth, in 2016 (closed triangles), 2019 (circles), 2020 (open triangles) and 2021 (open*
 553 *reverse triangle) for control (CO, blue) and throughfall-exclusion (TE, red). Dashed lines show the*
 554 *linear (CO)/logarithmic (TE) regression and gray areas the 95% confidence interval. Data are shown*
 555 *as the mean ± ISE.*

556



557

558 *Figure 4: Mean absolute daily xylem sap flow density in the outermost sapwood segment measured with*
 559 *HFD in 2016 and 2021 in spruce shown for control (CO in blue) and throughfall-exclusion (TE in red)*
 560 *by boxplots. Asterisks indicate significant differences between CO and TE within each year with ns =*
 561 *p-value > 0.05 and * = p-value < 0.05.*



562

563 *Figure 5: Leaf area of spruce per tree (LA in m² tree⁻¹) during the early drought (2014 to 2015), repeated*
 564 *drought (2016 to 2018) and watering phase (2019 to 2021) shown for control (CO in blue) and*
 565 *throughfall-exclusion (TE in red) by boxplots. Asterisks indicate significant differences between CO and*
 566 *TE within each year with ns = p-value > 0.05 and * = p-value < 0.05.*

567

568

569

570

571

572

573

574

575

576 **Tables**

577 *Table 1: Plant available water (vol.-%) in the soil of CO and TE plots for 0 to 70 cm soil depth during*
 578 *the measurement periods in 2016, 2019, 2020 and 2021. (***) = P-value < 0.001 and ns = P-value >*
 579 *0.05 between CO and TE for each year respectively). Data are shown as the mean ± 1SE.*

PAW [vol.-%]	2016	2019	2020	2021
CO	14.1 ± 0.8 ***	13.4 ± 0.4 ***	10.8 ± 0.6 ***	18.2 ± 0.6 ns
TE	4.7 ± 0.4 ***	6.7 ± 0.3 ***	14.2 ± 0.4 ***	17.4 ± 0.4 ns
Temp [°C]	17.8 ± 4.0	16.8 ± 4.0	15.5 ± 3.2	14.2 ± 4.8
VPD [kPa]	0.50 ± 0.12	0.66 ± 0.26	0.54 ± 0.17	0.48 ± 0.17
Rad [W m ⁻²]	216 ± 29	336 ± 69	334 ± 55	186 ± 31
Precip [mm]	461	406	476	601

580

581

582 *Table 2: Number of tree rings per cm sapwood depth and the sum of tree rings (0 to 8 cm depth) of*
 583 *beech and spruce for control (CO) and throughfall-exclusion trees (TE). Symbols indicate intraspecific*
 584 *significant differences of the same depth between CO and TE (• = P-value < 0.1 and * = P-value <*
 585 *0.05). Data are shown as the mean ± 1SE.*

Depth [cm]		0-1	1-2	2-3	3-4	4-5	5-6	6-7	7-8	Sum
Beech	CO	7.8 ±	7.0 ±	4.1 ±	4.3 ±	3.9 ±	4.0 ±	4.1 ±	3.8 ±	39.0 ±
		3.5 •	2.9	1.4	1.0	1.1	1.2	1.3	0.7	10.9
	TE	12.2 ±	6.2 ±	5.1 ±	4.3 ±	5.3 ±	5.0 ±	4.6 ±	4.4 ±	46.9 ±
		3.9 •	1.3	0.8	1.0	1.5	1.1	1.3	0.9	9.4
Spruce	CO	6.8 ±	4.5 ±	4.4 ±	4.5 ±	3.7 ±	3.3 ±	2.8 ±	3.1 ±	33.2 ±
		1.5 *	0.8	1.1	0.9	1.0	0.6	0.7	0.4	4.3
	TE	9.3 ±	4.5 ±	4.7 ±	3.8 ±	2.9 ±	3.1 ±	3.0 ±	2.8 ±	34.0 ±
		1.7 *	1.7	1.3	1.7	0.8	0.7	0.5	0.7	7.0

586

587 **Supporting information**

588 Total leaf area (LA m² tree⁻¹) was estimated from three CO and six TE spruce trees. First, in
 589 late summer 2020, we counted the number of branches in the sun and the shade crown for each
 590 tree. Then, the number of shoots of each needle age (N_s, in n cm⁻¹ needled branch length) was
 591 counted on one representative branch in the middle of the sun crown (at c. 5 m from the top)
 592 and one representative branch in the middle of the shade crown (red lines in figure S1a & b).
 593 For the chosen two branches and one additional branch at the bottom of the sun crown (orange

594 lines in figure S1a & b) we measured the length of the needled part (green area in figure S1a &
 595 b) and the needleless part (white area in figure S1a & b). Then, the total length of the needled
 596 branches (L_b in cm) was estimated for sun and shade crowns using the total number of branches.
 597 For sun crowns, we assumed a linear increase of both needled and needleless parts towards the
 598 bottom of the sun crowns as observed on-site (Figure S1a). For shade crowns, we observed a
 599 constant length of needled and needleless parts of all branches (Figure S1a). Subsequently, the
 600 total number of needles of each needle age (N_n , separated into sun/shade crown) was calculated
 601 with N_s , L_b , length of each shoot (L_s in cm, measured for sun and shade crowns, unpublished
 602 data), and needle density in each shoot (D in $n\text{ cm}^{-1}$, measured for each tree for sun and shade
 603 crowns, unpublished data):

$$604 \quad N_n = N_s \times L_b \times L_s \times D$$

605 Then, the total leaf area of each needle age (A_n in m^2) was calculated using needle length (L_n
 606 in mm, measured for sun and shade crowns) following Riederer et al. (1988):

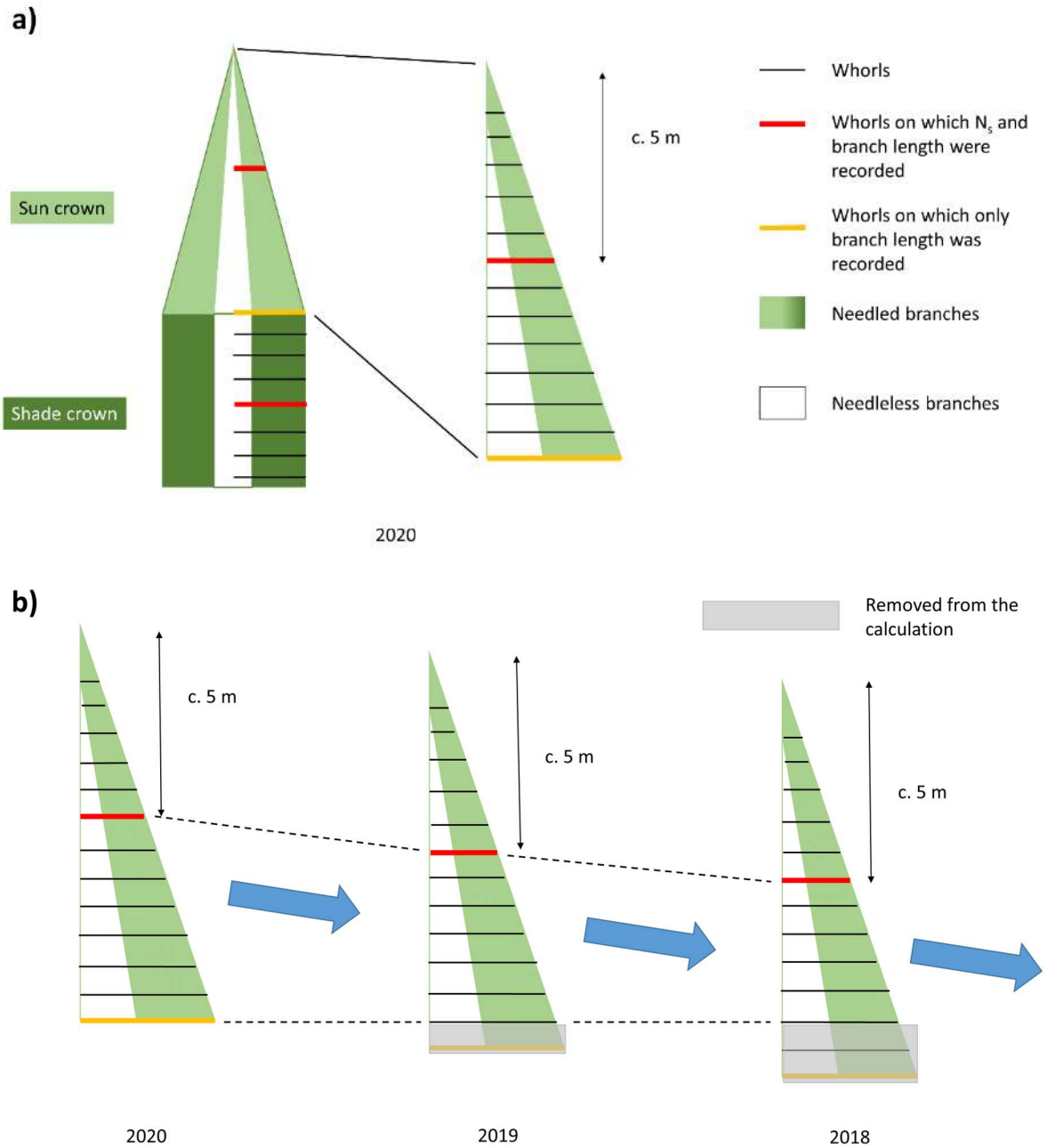
$$607 \quad A_n = \frac{N_n \times (3.279 \times L_n - 16.31)}{1000000} \text{ (for current year needles)}$$

$$608 \quad A_n = \frac{N_n \times (4.440 \times L_n - 24.78)}{1000000} \text{ (for older needles)}$$

609 For the surface area of shade needles, A_n was multiplied with a factor ($2.32/3.25 = 0.71$) to
 610 account for the different leaf thickness between sun and shade needles, determined earlier for
 611 the spruce trees on the experimental site (Patzner, 2004). Finally, the surface area of each needle
 612 age was summed up to determine the total leaf area (LA) of each tree in 2020.

613 Based on the data for 2020, we retrospectively calculated annual LA between 2014 and 2019
 614 and for 2021, making the following four assumptions: 1) N_s in sun crowns remained constant
 615 if a branch at the same distance from the top would be assessed every year (red line in Figure
 616 S1b). In this case, the lowest whorl at the bottom of the sun crown (three to four branches) is
 617 removed from the calculation of L_b every year. 2) The needle age distribution remains constant
 618 throughout the calculation period. 3) For shade crowns, N_s and the number of branches remain
 619 constant throughout the calculation period. 4) Since L_s , D , and L_n of shoots older than 2013
 620 could not be recorded, we averaged the values of 2013-2020 for CO spruce and used the values
 621 of 2013 for TE spruce, since drought effects were observed after 2014 in TE trees.

622 The calculated LA of CO trees in each year (2014-2021) corresponded to values ($p > 0.9$)
 623 estimated with a site-specific allometric relationship between dbh and LA determined by
 624 Patzner (2004) after whole-tree harvests.












625

626 *Figure S 1: Additional information for the calculation of the total leaf area of spruce*

RESEARCH ARTICLE

High resilience of carbon transport in long-term drought-stressed mature Norway spruce trees within 2 weeks after drought release

Kyohsuke Hikino¹  | Jasmin Danzberger² | Vincent P. Riedel¹  | Romy Rehschuh³  | Nadine K. Ruehr³  | Benjamin D. Hesse¹  | Marco M. Lehmann⁴  | Franz Buegger²  | Fabian Weikl^{1,2}  | Karin Pritsch²  | Thorsten E. E. Grams¹ 

¹Technical University of Munich (TUM), TUM School of Life Sciences, Land Surface-Atmosphere Interactions, Ecophysiology of Plants, Freising, Germany

²Helmholtz Zentrum München – German Research Center for Environmental Health (GmbH), Institute of Biochemical Plant Pathology, Neuherberg, Germany

³Karlsruhe Institute of Technology, Institute of Meteorology and Climate Research—Atmospheric Environmental Research (KIT/IMK-IFU), Garmisch-Partenkirchen, Germany

⁴Swiss Federal Institute for Forest, Snow and Landscape Research (WSL), Forest Dynamics, Birmensdorf, Switzerland

Correspondence

Kyohsuke Hikino, Technical University of Munich (TUM), TUM School of Life Sciences, Professorship for Land Surface-Atmosphere Interactions, Ecophysiology of Plants, Hans-Carl-von-Carlowitz Platz 2, 85354 Freising, Germany.
Email: kyohsuke.hikino@tum.de

Present address

Vincent P. Riedel, University of Würzburg, Julius-von-Sachs-Institute of Biological Sciences, Ecophysiology and Vegetation Ecology, Würzburg, Germany

Funding information

Deutsche Forschungsgemeinschaft, Grant/Award Number: GR 1881/5-1, MA1763/10-1, PR292/22-1, PR555/2-1 and RU 1657/2-1; Deutsche Bundesstiftung Umwelt, Grant/Award Number: AZ 20018/535; Schweizerischer Nationalfonds zur Förderung der Wissenschaftlichen Forschung, Grant/Award Number: 179978; Bavarian State Ministries of the Environment and Consumer Protection as well as Food, Agriculture and Forestry, Grant/Award Number: W047/Kroof II

Abstract

Under ongoing global climate change, drought periods are predicted to increase in frequency and intensity in the future. Under these circumstances, it is crucial for tree's survival to recover their restricted functionalities quickly after drought release. To elucidate the recovery of carbon (C) transport rates in c. 70-year-old Norway spruce (*Picea abies* [L.] KARST.) after 5 years of recurrent summer droughts, we conducted a continuous whole-tree ¹³C labeling experiment in parallel with watering. We determined the arrival time of current photoassimilates in major C sinks by tracing the ¹³C label in stem and soil CO₂ efflux, and tips of living fine roots. In the first week after watering, aboveground C transport rates (CTR) from crown to trunk base were still 50% lower in previously drought-stressed trees (0.16 ± 0.01 m h⁻¹) compared to controls (0.30 ± 0.06 m h⁻¹). Conversely, CTR below ground, that is, from the trunk base to soil CO₂ efflux were already similar between treatments (c. 0.03 m h⁻¹). Two weeks after watering, aboveground C transport of previously drought-stressed trees recovered to the level of the controls. Furthermore, regrowth of water-absorbing fine roots upon watering was supported by faster incorporation of ¹³C label in previously drought-stressed (within 12 ± 10 h upon arrival at trunk base) compared to control trees (73 ± 10 h). Thus, the whole-tree C transport system from the crown to soil CO₂ efflux fully recovered within 2 weeks after drought release, and hence showed high resilience to recurrent summer droughts in mature Norway spruce forests. This high resilience of the C transport system is an important prerequisite for the recovery of other tree functionalities and productivity.

This is an open access article under the terms of the Creative Commons Attribution License, which permits use, distribution and reproduction in any medium, provided the original work is properly cited.

© 2021 The Authors. *Global Change Biology* published by John Wiley & Sons Ltd.

KEYWORDS

¹³C labeling, climate change, forest ecosystem, phloem, photosynthesis, *Picea abies*, recovery, soil CO₂ efflux, stem CO₂ efflux, watering

1 | INTRODUCTION

Global climate change has been causing significant and mostly negative impacts on forest ecosystem carbon (C) cycling such as reduced productivity (Ciais et al., 2005; Collins et al., 2013). Drought is one of the most influential drivers of tree mortality (Allen et al., 2010; 2015; McDowell et al., 2008; van Mantgem et al., 2009) and it is predicted to occur more frequently and for longer durations in the future (IPCC, 2007, 2014). Under these circumstances, tree survival primarily depends on the extent to which tree functionality is impaired by drought (i.e., resistance, Lloret et al., 2011). After drought release, it is then crucial that surviving trees recover their limited functionality back to pre-drought levels (i.e., resilience, Lloret et al., 2011). Since drought release typically causes a high C demand for repair and growth particularly in belowground sinks (Gao et al., 2021; Hagedorn et al., 2016; Joseph et al., 2020), C transport from leaves to sink organs is an important process for tree recovery (Ruehr et al., 2019). C assimilates are transported from the crown via the phloem to various above- and belowground C sinks (Lemoine et al., 2013; Salmon et al., 2019). Recent studies revealed that saplings (Barthel et al., 2011; Ruehr et al., 2009; Zang et al., 2014), young trees (Dannoura et al., 2019; Epron et al., 2016), and mature trees (Gao et al., 2021; Hesse et al., 2019; Wang et al., 2021) restricted transport of current photoassimilates under drought, thereby reducing the C supply to sinks. Upon drought release, C limitation in sink tissues can occur if the C transport would not recover fast enough to meet the sink demands (Hartmann et al., 2013; Hartmann et al., 2013; Sevanto, 2014; Winkler & Oberhuber, 2017), but knowledge on mature trees is scarce (Gao et al., 2021).

There are two main causes restricting transport of current photoassimilates from the crown along the stem to belowground C sinks under drought (Salmon et al., 2019). First, water limitation delays the export of sugars from leaves, increasing the mean residence time (MRT) of photoassimilates in leaves (Dannoura et al., 2019; Epron et al., 2012; Hesse et al., 2019; Ruehr et al., 2009). This is caused by accumulation of osmolytes, and/or production of secondary metabolites and volatile compounds (Epron & Dreyer, 1996; Ruehr et al., 2009; Salmon et al., 2019). Second, the phloem transport velocity can be reduced through increased phloem viscosity (Epron et al., 2016; Hesse et al., 2019; Sevanto, 2014, 2018; Woodruff, 2014), lower C source/sink strength (Lemoine et al., 2013; Ryan & Asao, 2014; Sevanto, 2014), and smaller phloem conduit diameter (Dannoura et al., 2019; Woodruff, 2014). Increased phloem viscosity is a result of water limitation in the xylem, as the xylem supplies the nearby phloem with water (Hölttä et al., 2006, 2009). Lower C source/sink strength (e.g., photosynthesis rates and stem/soil CO₂ efflux rates) limits sugar loading/unloading processes between C source/sink and phloem. This hinders the osmotic regulation in

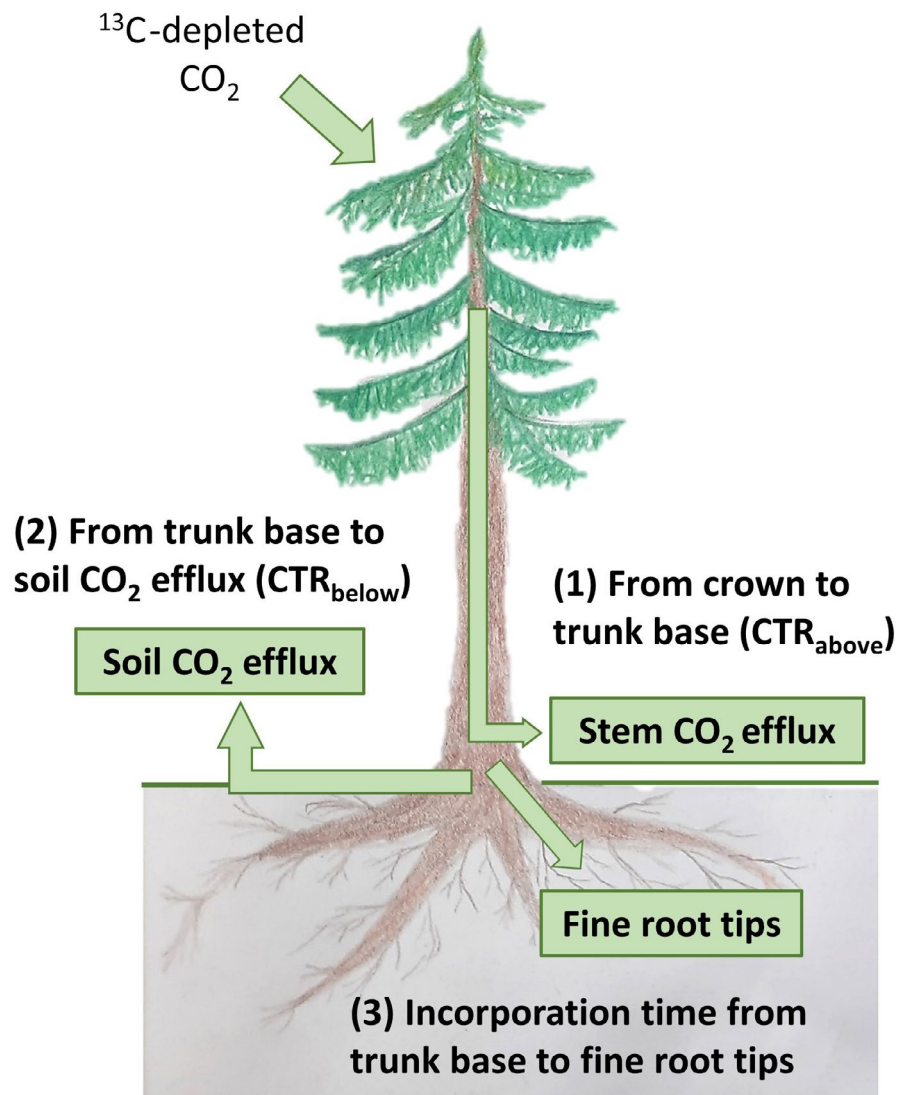
phloem and thus limits water exchange between phloem and xylem. Smaller phloem conduit diameter is caused by restricted cell expansion due to turgor reduction usually under severe drought (Hsiao, 1973), thereby reducing phloem conductivity.

Recovery of C transport depends on the restricting mechanisms. MRT of leaf sugars decreases after drought release within days (Zang et al., 2014). Drought release increases plant water potential and water availability in the xylem, typically followed by increased C source and sink strength (Gao et al., 2021; Hagedorn et al., 2016). Previous studies using young eucalypt trees (Epron et al., 2016) and a rainfall event in a naturally dry pine forest (Gao et al., 2021) reported that C transport velocity from crown to trunk base or soil was related to C source or sink strength, which typically decreases under drought and increases after drought release (Hagedorn et al., 2016; Joseph et al., 2020; Nikolova et al., 2009; Zang et al., 2014). Furthermore, there is increasing evidence that C source strength and C supply may be “sink controlled” (Fatichi et al., 2014; Gavito et al., 2019; Hagedorn et al., 2016; Körner, 2015). Conversely, drought-related reductions of phloem conduit diameter are expected to further restrict the phloem transport during the first weeks after stress release even if the phloem sap viscosity and C source/sink strength recover.

This present study was performed in the framework of the Kranzberg roof (KROOF) project, which was initiated to elucidate the drought responses of mature European beech (*Fagus sylvatica* L.) and Norway spruce (*Picea abies* [L.] KARST.; see details in Grams et al., 2021). Both tree species were exposed to recurrent summer droughts from 2014 to 2018 and leaf water potential reached values as low as −1.8 MPa, causing distinct drought effects such as reduced stem and fine root growth (Grams et al., 2021; Pretzsch et al., 2020; Zwetsloot & Bauerle, 2021) and acclimation in tree hydraulics (Tomasella et al., 2018). To predict the trajectories of forests under future climates, it is important to understand, to what extent tree functionality recovers after drought release and how fast. To answer this question, former drought plots were watered in early summer 2019 (Grams et al., 2021). In parallel with watering, we performed a whole-tree ¹³C labeling experiment on mature spruce trees to assess the resilience of their C transport processes, that is, the ability to recover to the level of control trees (Lloret et al., 2011).

We divided the C transport path from the crown to the soil CO₂ efflux into two parts (Figure 1), as drought release may affect them differently. (1) Aboveground transport from the crown (leaves) to the trunk base (aboveground transport hereafter), and (2) belowground transport from the trunk base to the soil CO₂ efflux (belowground transport hereafter). In addition, we also investigated a third process, (3) incorporation of current photoassimilates in living fine roots (Figure 1). The aboveground transport comprises sugar export from leaves and transport along the woody structures in the

FIGURE 1 Overview of the carbon transport paths assessed in this study. (1) Aboveground carbon transport rates (CTR_{above} , in $m\ h^{-1}$) from crown to trunk base (assessed as stem CO_2 efflux), (2) Belowground carbon transport rates (CTR_{below} , in $m\ h^{-1}$) from trunk base to soil CO_2 efflux, and (3) Incorporation time (in h) of current photoassimilates from trunk base to fine root tips



phloem. The aboveground C transport rates (CTR_{above} in $m\ h^{-1}$) indicate how fast newly assimilated C can be supplied to belowground sinks. The belowground transport includes the phloem transport along roots and the CO_2 diffusion in the soil. The belowground C transport rates (CTR_{below}) indicate the rates of C flux from belowground plant tissues to the atmosphere, which is an important flux in analyzing forest C cycling. Based on the “sink-control” mechanism, we hypothesize that both CTR_{above} [H1] and CTR_{below} [H2] recover within 2 weeks in parallel to C sink and/or C source strength. The timing of the incorporation of current photoassimilates in fine roots indicates how fast trees use the available C to grow and restore the belowground tissues. Since a high C demand is expected in fine root growth of recovering trees upon drought release, the incorporation time can be even shorter in recovering trees compared to control trees. Therefore, our third hypothesis is that upon drought release, incorporation of current photoassimilates is faster in fine roots of trees recovering from drought than in control trees [H3].

In a similar experiment by Gao et al. (2021) conducted in a naturally dry pine forest after a rainfall event is the only study to date investigating CTR of mature trees after drought release. We still lack

knowledge on the recovery of highly productive forests under ongoing climate change. Furthermore, there is no study considering the effect of water availability on the above- and belowground transport individually. We show for the first time the resilience of the whole-tree C transport after repeated summer droughts in a highly productive Norway spruce forest stand of great ecological and economic relevance in central Europe (Caudullo et al., 2016).

2 | MATERIALS AND METHODS

2.1 | Experimental site

This study was conducted in a mixed forest with c. 90-year-old European beech and c. 70-year-old Norway spruce trees in Kranzberg Forest, located in southern Germany/Bavaria ($11^{\circ}39'42''E$, $48^{\circ}25'12''N$; 490 m a.s.l.). The experimental site consists of 12 plots with three to seven beech and spruce trees each. At this site, a long-term throughfall exclusion (TE) and subsequent watering experiment was conducted as described in detail

in Grams et al. (2021). Briefly, six plots were assigned to TE plots equipped with roofs and the other six plots without roofs to control plots (CO). All plots were trenched to 1 m of soil depth 4 years before the experiments started (Pretzsch et al., 2014). The mature beech and spruce trees in TE plots were then exposed to summer drought for five consecutive growing seasons (2014–2018). To investigate trees' recovery processes, in early summer 2019, all TE plots were watered with c. 90 mm over 36 h and the soil water content increased to the level of the CO plots within 1 week (for further details see Grams et al., 2021). In parallel with the watering, we conducted a ^{13}C labeling experiment on four CO and three TE spruce trees on neighboring plots (Figure 2a, for details see Table S1). In addition to the two labeled plots, we assessed three spruce trees each on additional CO and TE plots as non-labeled controls (Table S2). A canopy crane located next to these plots enabled the measurements of leaf photosynthesis, leaf water potential, and leaf osmotic potential in sun-lit canopy.

2.2 | Weather data

The mean photosynthetic photon flux density during the labeling period accounted to 788 ± 534 (SD) $\mu\text{mol m}^{-2} \text{s}^{-1}$ (Figure 3a). During the daytime (from 5 am to 7 pm, CET) on the labeling days, mean temperature was 18.8 ± 4.3 (SD) $^{\circ}\text{C}$ (Figure 3b) and mean vapor pressure deficit was 0.6 ± 0.4 (SD) kPa. There were several rain periods during labeling on day 3, 7, and 9. Only on day 9, however, weak but continuous rainfall event with a high wind speed occurred throughout the daytime, accumulating to 7.8 mm (Figure 3b). Due to this weather conditions, a smaller $\delta^{13}\text{C}$ shift in canopy air was achieved on day 9 (see below).

2.3 | CO_2 exposure and assessment of canopy air

The whole crowns of all spruce trees on the CO and TE plot, that is, four and three trees, respectively, were fumigated with ^{13}C -depleted

tank CO_2 ($\delta^{13}\text{C}$ of $-44.3 \pm 0.2\text{‰}$) using the isoFACE system described earlier (Grams et al., 2011; Kuptz et al., 2011). Depending on its crown size, each tree crown was equipped with 9–17 micro-perforated PVC tubes hanging vertically from a carrier structure (Figure 2b). These fumigation tubes were then connected to the CO_2 tank and the ^{13}C -depleted CO_2 was released directly within the seven tree crowns.

The atmospheric CO_2 concentration and $\delta^{13}\text{C}$ in tree canopy ($\delta^{13}\text{C}_a$) were continuously monitored during the labeling using a cavity ring-down spectroscopy (CRDS, ESP-1000; PICARRO). Two air measurement points were installed per tree c. 2 m inside the sun-lit crowns at 1 m distance from the stem (east and west orientation, one CO tree had only one measurement point, Figure 2a and Table S2). We took care that these sampling points had enough distances from the fumigation tubes (c. 1 m). A sample point above the canopy was used as a reference. The sample air was continuously transported to the CRDS by membrane pumps via PVC tubes. A computer-automated multiplexer system switched every 5 min between measurement positions and averages of the last 3 min were recorded by the CRDS. According to the mean CO_2 concentration of all 13 measurement points in canopy, which was measured continuously by an infra-red gas analyzer (BINOS 100 4P; Rosemount-Emerson Electric Co.), a mass flow controller regulated the amount of the CO_2 exposure through fumigation tubes. To calibrate the CRDS, two commercially available calibration gases were used (Ref.1: $-9.7 \pm 0.3\text{‰}$ and Ref.2: $-27.8 \pm 0.3\text{‰}$; Thermo Fisher Scientific). All $\delta^{13}\text{C}$ values in this study were referenced to international standards (Vienna Pee Dee Belemnite).

The ^{13}C labeling started in parallel with the watering and continued for 14 days, that is, from July 4, 2019 (day 0) to July 17, 2019 (day 13), from 5 am to 7 pm (CET). We targeted the mean CO_2 concentration in canopy air at +130 ppm relative to the ambient air above the canopy to create a shift of -8.3‰ . Due to variable wind exposition, however, each tree received different amounts of added CO_2 . In CO trees, the mean canopy CO_2 concentration increased to 541 ± 16 ppm during labeling (Figure 3c, see values for individual trees in Table S1), shifting the $\delta^{13}\text{C}_a$ by

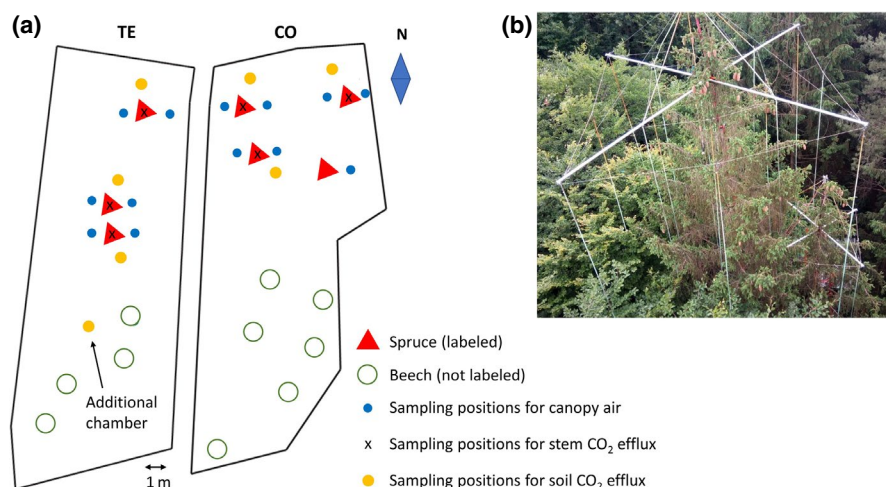


FIGURE 2 (a) Overview of the two ^{13}C -labeled plots (CO = control, TE = throughfall exclusion), giving positions of trees (red triangles = labeled spruce trees, green open circles = beech), sampling positions of canopy air (blue circles), stem CO_2 efflux (x), and soil CO_2 efflux (yellow circles). (b) Picture of the structure for the ^{13}C labeling with PVC tubes hanging vertically through the spruce crowns

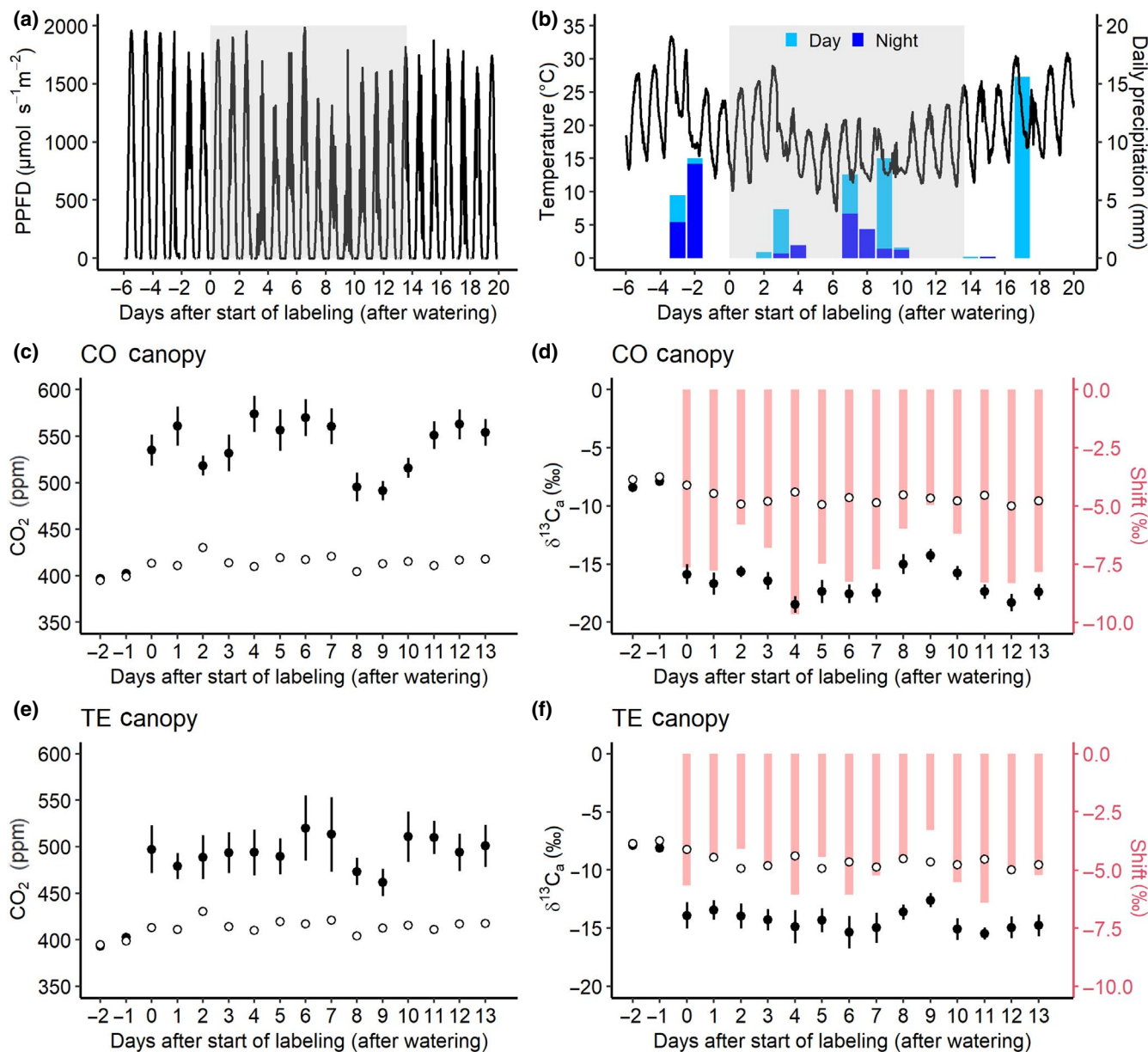


FIGURE 3 (a) Photosynthetic photon flux density (PPFD) before, during, and after labeling. (b) Temperature (lines) and precipitation (bars) before, during, and after labeling. Precipitation is given as daytime (5 am–7 pm CET, fumigation hours, light blue), and nighttime (7 pm–5 am, dark blue). The ticks on the x-axis indicate 0 am of each day. The labeling started in parallel with the watering on day 0 and continued during daytime until day 13 (marked with gray areas). (c, e) Daily mean CO_2 concentration and (d, f) $\delta^{13}\text{C}$ of canopy air ($\delta^{13}\text{C}_a$) of control (CO) and previously drought-stressed (throughfall exclusion, TE) trees during labeling hours (5 am–7 pm), respectively. The closed circles are the averages of the canopy air and the open circles are the non-labeled reference air measured above the canopy. The mean daily shift in $\delta^{13}\text{C}_a$ was expressed with red bars. Error bars give SE. Error bars of the reference air (open circles) are removed, as they are much shorter than the size of the circles due to the large amount of measurement points

$-7.3 \pm 0.5\%$ on average (Figure 3d). In contrast, TE trees received less ^{13}C -depleted CO_2 with an increase in the mean canopy CO_2 concentration to 495 ± 23 ppm (Figure 3e), causing smaller mean shift of $\delta^{13}\text{C}_a$ by $-5.1 \pm 1.3\%$ (Figure 3f) compared to CO trees. Furthermore, during the weak but longer rainfall event associated with a high wind speed on day 9, a smaller mean shift in $\delta^{13}\text{C}_a$ was achieved in both CO and TE trees. Mean CO_2 concentration and $\delta^{13}\text{C}$ of the ambient air above the canopy were 413 ppm and -9.2% during labeling hours.

To track the current photoassimilates through the tree/soil system, we used the two experimentally induced changes in $\delta^{13}\text{C}_a$: (1) Turn-on of CO_2 exposure with ^{13}C -depleted tank CO_2 on day 0 of watering. This part of the experiment was used to calculate the arrival time of the ^{13}C -depleted tracer in the observed C sinks in the first week after watering. (2) Turn-off of the CO_2 exposure system and subsequent increase in $\delta^{13}\text{C}$ in the canopy air back to the initial, ambient level on day 13 of watering. In this part of the experiment, the arrival of unlabeled tracer (C with ambient $\delta^{13}\text{C}$)

in the studied C sinks was used to calculate CTR 2 weeks after watering.

2.4 | Measurement of phloem sugar

On day -1, 7, 13, and 21 around midday, phloem tissue samples were collected at the breast height of four labeled CO and three labeled TE trees using a cork borer (two disks with diameter of 5 mm for each tree, Tables S2 and S3). The dead bark was removed and the remaining phloem samples were immediately frozen on dry ice and subsequently freeze-dried. The dried material was milled to fine powder using a steel ball-mill (Retsch) and about 70 mg per sample were transferred into a 2 ml reaction vial and mixed with 1.5 ml deionized water. The fractions of water-soluble compounds were then extracted in a water bath at 85°C for 30 min and further purified to neutral sugars using commercial available ion-exchange cartridges (OnGuard II H, A, & P; Dionex) as described in detail by Lehmann et al. (2020). An aliquot of 1 mg of the neutral sugar fraction was then transferred to 5 × 9 mm silver capsules (Saentis Analytical AG), frozen at -20°C, freeze-dried, and the capsules were closed before isotopic analysis. The C isotopic composition of phloem sugars ($\delta^{13}\text{C}_{\text{phloem}}$) was analyzed with a thermal conversion elemental analyzer (PYRO cube; Elementar) that was coupled via a ConFlo III reference system to an isotope-ratio mass spectrometer (Finnigan Delta Plus XP, all supplied by Thermo Fisher Scientific). The typical measurement precision for in-house sugar standards was 0.3‰ (SD).

2.5 | Measurement of stem CO₂ efflux

Rates of stem CO₂ efflux and its stable C isotope composition ($\delta^{13}\text{C}_{\text{stem}}$) before and after watering were recorded using an isotope ratio infrared spectrometer (IRIS, DeltaRay, Thermo Fisher Scientific; Braden-Behrens et al., 2017). A total of 12 spruce trees were measured, three ¹³C-labeled and three non-labeled trees in each treatment, that is, CO and TE ($n = 3$; Figure 2a; Tables S2 and S3). The non-labeled trees were used to correct for changes in ¹³C discrimination caused by the watering and weather fluctuations. Plexiglas (Röhm GmbH) chambers (61–204 cm²) were attached at ca. 1 m height on each stem after removing mosses, lichens, and algae. After a leak test using a slight overpressure (c. 2000 Pa), each chamber was supplied with reference air of a constant CO₂ concentration of c. 413 ppm. Excess air was exhausted before entering the chamber to avoid an overpressure. The mixture of reference air plus stem-derived CO₂ of each chamber was continuously pumped through PVC tubes to a computer-automated manifold with 16 channels, which changed the channel flowing to IRIS every 5 min. The CO₂ concentration and the stable C isotope composition of the reference air were determined between measurement cycles (c. every 80 min). The same reference gases as for the CRDS system were used for calibration of the IRIS system (see above).

The rate of stem-derived CO₂ efflux was calculated according to mass balance equation as described by Gamnitzer et al. (2009), using the mean values of the closest two measurements of the reference air.

$$\text{Stem CO}_2 \text{ efflux} (\mu\text{mol m}^{-2} \text{ s}^{-1}) = \frac{F_{\text{air}}}{V_{\text{mol}} A_{\text{chamber}}} ([\text{CO}_2]_{\text{sample}} - [\text{CO}_2]_{\text{reference}}),$$

where F_{air} gives the air flow through the chamber (L s⁻¹); V_{mol} , the molar volume of gases (22.4 L mol⁻¹); A_{chamber} , the chamber base area (m²); $[\text{CO}_2]_{\text{sample}}$ and $[\text{CO}_2]_{\text{reference}}$, the CO₂ concentration (ppm) of sample air from stem chambers and reference air, respectively.

$\delta^{13}\text{C}_{\text{stem}}$ was calculated by the following equation using a two end-member mixing model (Dawson et al., 2002),

$$\delta^{13}\text{C}_{\text{stem}} (\text{‰}) = \frac{([\text{CO}_2]_{\text{sample}} \times \delta^{13}\text{C}_{\text{sample}}) - ([\text{CO}_2]_{\text{reference}} \times \delta^{13}\text{C}_{\text{reference}})}{[\text{CO}_2]_{\text{sample}} - [\text{CO}_2]_{\text{reference}}},$$

where $\delta^{13}\text{C}_{\text{sample}}$ and $\delta^{13}\text{C}_{\text{reference}}$ give the $\delta^{13}\text{C}$ signature of sample air from stem chambers and that of reference air, respectively.

$\delta^{13}\text{C}_{\text{stem}}$ can be affected by CO₂ transported from belowground in xylem sap (Teskey et al., 2008). However, Kuptz et al. (2011) observed a positive correlation in $\delta^{13}\text{C}$ between stem phloem and stem CO₂ efflux in spruce trees at the same experimental site. In this study, we also found a positive linear correlation between $\delta^{13}\text{C}_{\text{stem}}$ and $\delta^{13}\text{C}_{\text{phloem}}$ (slope = 0.94, $R^2 = .30$, $p < .01$; Figure S1). Likewise, $\delta^{13}\text{C}_{\text{stem}}$ showed no significant difference between daytime and nighttime (data not shown). Therefore, as reported in previous studies (Kodama et al., 2008; Kuptz et al., 2011; Ubierna et al., 2009), we concluded that CO₂ in xylem sap had negligible effect on $\delta^{13}\text{C}_{\text{stem}}$. Thus, we assessed the $\delta^{13}\text{C}_{\text{stem}}$ as a surrogate of $\delta^{13}\text{C}_{\text{phloem}}$.

2.6 | Measurement of soil CO₂ efflux

Soil CO₂ efflux rates and its isotopic C composition ($\delta^{13}\text{C}_{\text{soil}}$) were measured using a Li-8100 automated soil CO₂ flux system with a Li-8150 multiplexer (Li-Cor Inc.), connected to an IRIS. The air stream leaving the Li-8100 was sampled by the IRIS at a flow rate of 80 ml min⁻¹ and added back to the chamber air stream. Three automatically operating soil chambers (8100-104) per treatment, that is, CO and TE, were installed with 1 m distance from the spruce trees (Figure 2a; Table S2). Additionally, one chamber was installed close to the non-labeled beech trees in the TE plot (Figure 2a), which was used to correct for effects of physical CO₂ diffusion due to watering (see the last paragraph of this section). Each chamber enclosed a permanently installed soil collar, which was inserted 2–3 cm into the soil 3 days before the measurements started. All chambers were measured at a frequency of c. 30 min (Table S3). Measurement time per chamber was adapted based on the CO₂ efflux rate: 5 min in the TE plot and 2:30 min in the CO plot. $\delta^{13}\text{C}_{\text{soil}}$ was calculated using the Keeling plot approach (Keeling, 1958, 1961). Each single measurement was quality controlled based on the fit of the linear regressions. For soil CO₂ efflux values were kept if $R^2 \geq .8$ and for

$\delta^{13}\text{C}_{\text{soil}}$ based on the Keeling plot approach if $R^2 \geq .9$. To calibrate the IRIS, two commercially available calibration gases were used (Ref.1: $-9.9 \pm 0.3\text{‰}$ and Ref.2: $-27.8 \pm 0.3\text{‰}$, Thermo Fisher Scientific).

During watering of the TE plots, the soil pores fill with water and the lighter ^{13}C -depleted CO_2 gets pushed-out (Andersen et al., 2010; Subke et al., 2009; Unger et al., 2010). This interfered with our labeling experiment. Hence, we corrected for the $\delta^{13}\text{C}_{\text{soil}}$ of the TE plot based on measurements of the additional chamber close to the non-labeled beech trees (see details in Figures S2 and S3). Due to a limitation in the number of soil chambers, a non-labeled chamber was not available for the CO plot. For purposes not related to this study, the CO plot was slightly watered (c. 12 mm over 12 h) in parallel to the TE plots. As we did not observe any significant effect of the watering on the $\delta^{13}\text{C}_{\text{soil}}$ of the wet CO plot (Figure 4c), there was no need to apply this correction here.

2.7 | Measurement of root tips

Fine roots were collected on day -7 and repeatedly after the watering with an interval of 1–2 days until day 25 (Table S3), from random sampling positions (17–18 samples per treatment and day, Table S2). The collected samples were carefully washed in petri dishes, and representative living root tips were cut off under a stereomicroscope. Individual root tips were placed in pre-weighed tin capsules and dried at 60°C . Their stable C isotope composition ($\delta^{13}\text{C}_{\text{root}}$) was determined with an isotope-ratio mass spectrometer (delta V Advantage; Thermo Fisher Scientific) coupled to an Elemental Analyzer (Euro EA; Eurovector). Due to the very small sample quantities (the smallest samples with c. $3 \mu\text{g C}$), the C-blank (c. $0.6 \mu\text{g C}$) of the tin capsules and their $\delta^{13}\text{C}$ were taken into account in the evaluation. As with $\delta^{13}\text{C}_{\text{stem}}$, $\delta^{13}\text{C}_{\text{root}}$ of non-labeled plots was assessed to correct for the effect of watering and weather fluctuations.

2.8 | Calculation of arrival time and CTR

To determine the arrival time of the two tracers (^{13}C -depleted tracer after the start of labeling, and unlabeled tracer after the end of labeling) in stem/soil CO_2 efflux and living root tips, the courses of $\delta^{13}\text{C}$ were fitted by piecewise function (Figure 4). Since ^{13}C -depleted CO_2 decreases $\delta^{13}\text{C}$, the arrival time of the ^{13}C -depleted tracer was defined as the point when $\delta^{13}\text{C}$ started to decrease. First, $\delta^{13}\text{C}$ data of each C sink were cut to contain only two linear segments before and after the arrival of the tracers. Then, we performed a linear regression for the $\delta^{13}\text{C}$ data ("lm" function, R package "stats," version: 3.6.1). Finally, the intersection of two linear fits was determined using "segmented" function (R package "segmented," version: 1.3-0, red lines fitted to the $\delta^{13}\text{C}$ data). This function calculated a new regression model and automatically estimated the break point (intersection) of two lines including standard errors, where the linear relationship changed. This intersection was then defined as the arrival time of the ^{13}C -depleted tracer (red vertical lines in Figure 4a–f). In the case of soil CO_2 efflux,

the first line before arrival was fitted as a horizontal line (Figure 4c,d). After the end of labeling, $\delta^{13}\text{C}$ of each C sink started to increase again, as the unlabeled tracer (with ambient $\delta^{13}\text{C}$ values) arrived. This point of increasing $\delta^{13}\text{C}$ was calculated with the same method described above (blue lines fitted to the $\delta^{13}\text{C}$ data) and was then defined as the arrival time of unlabeled C (blue vertical lines in Figure 4a–f). In the case of root tips, it was not possible to assign each root to the belonging tree. Therefore, all values were pooled for each treatment (Figure 4e,f), providing only one arrival time for each treatment.

Using the arrival time in stem and soil CO_2 efflux, the $\text{CTR}_{\text{above}}$ (aboveground C transport rates from crown to trunk base in m h^{-1} , Figure 1) and $\text{CTR}_{\text{below}}$ (belowground C transport rates from trunk base to soil CO_2 efflux in m h^{-1} , Figure 1) were calculated by:

$$\text{CTR}(\text{m h}^{-1}) = \frac{d}{tl}$$

For $\text{CTR}_{\text{above}}$, tl (in h) gives the time lag between the start respectively end of labeling and the arrival time of the tracers at trunk base (stem CO_2 efflux). d (in m) represents the distance between the mean crown height (the middle of the crown, Table S1) of the tree and the height of the stem chamber. For $\text{CTR}_{\text{below}}$, tl (in h) gives the time lag between the arrival time of the tracers at trunk base and the arrival time at soil CO_2 efflux, with d (in m) representing the height of the stem chamber plus 1 m, since each soil chamber was placed at 1 m distance from each trunk. The real transport distance from trunk base to soil chamber can vary depending on the structure of roots. We assumed that there is no time lag between arrival of current photoassimilates at trunk base/roots and the use of them in stem/root CO_2 efflux. We did not calculate CTR to living root tips, since the transport distance was unknown due to random sampling positions. Therefore, for the incorporation time of current photoassimilates in fine roots, the time lags between the arrival time of the tracers at trunk base and the arrival time at root tips were compared between CO and TE trees instead (Figure 1).

The additional soil chamber in the TE plot enabled to correct for the effects of watering on $\delta^{13}\text{C}_{\text{soil}}$ (see details in Figures S2 and S3). Due to stable weather conditions in the first week of the labeling with only few short and weak rain events, we were able to calculate the arrival time of ^{13}C -depleted tracer in soil CO_2 efflux. However, unstable weather conditions during the second part of the experiment (day 7–13) did not allow to calculate the arrival time of unlabeled tracer in soil CO_2 efflux (they caused negative time lags). Reduced C gain on day 9 increased the $\delta^{13}\text{C}_{\text{soil}}$ already before the unlabeled tracer arrived in soil CO_2 efflux, likely as more ^{13}C -enriched old C was used (Steinmann et al., 2004; Wingate et al., 2010). Thus, we excluded the $\text{CTR}_{\text{below}}$ calculated using unlabeled tracer 2 weeks after watering.

2.9 | Measurement of light-saturated CO_2 assimilation rates (A_{sat}), predawn leaf water potential (Ψ_{PD}), and leaf osmotic potential (π_{O})

The light-saturated CO_2 assimilation rates at CO_2 concentration of 400 ppm (A_{sat} , expressed on the basis of total needle surface area)

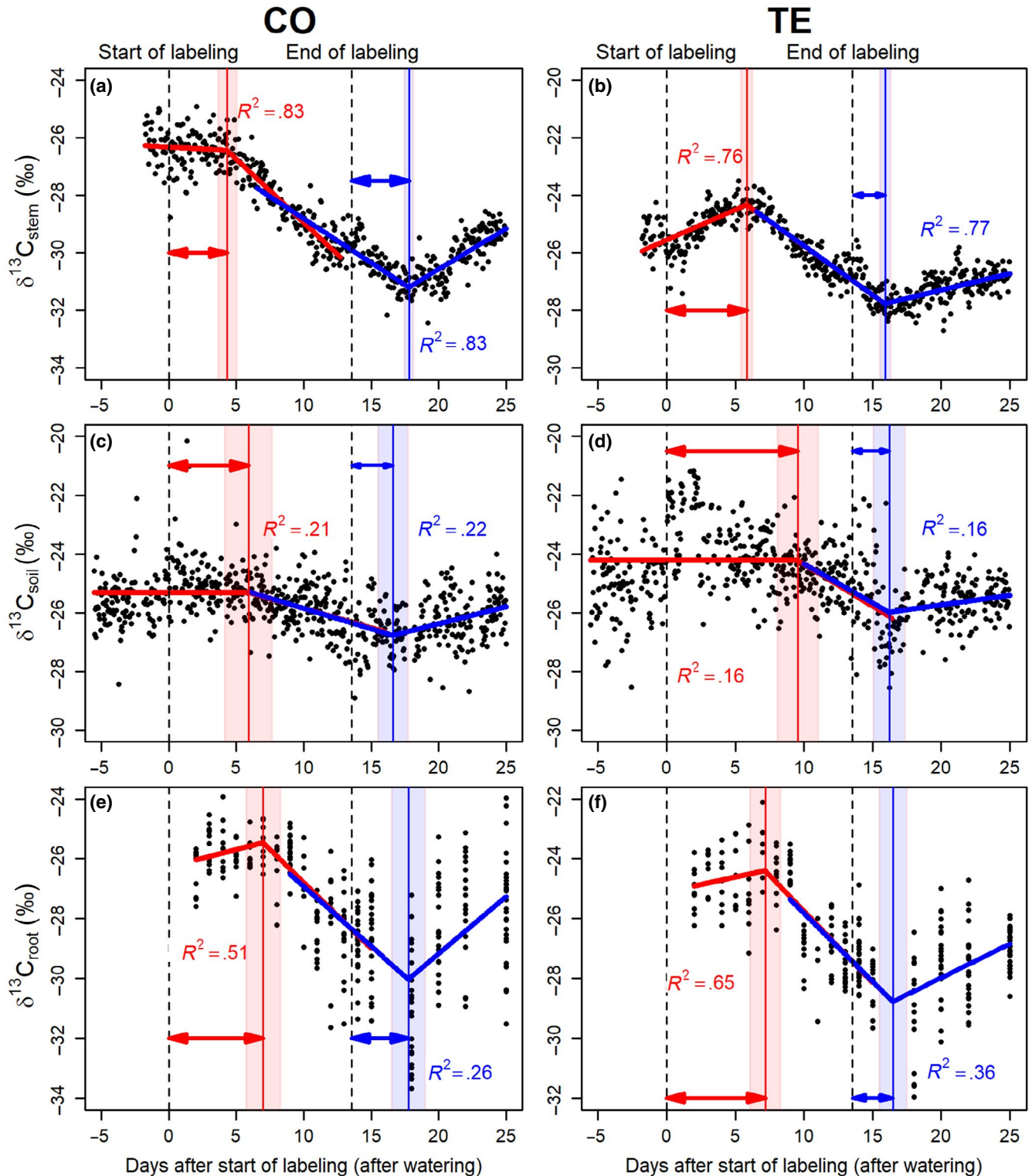


FIGURE 4 Examples for the calculation of the arrival time of the ^{13}C -tracers, using: (a, b) $\delta^{13}\text{C}$ of stem CO_2 efflux ($\delta^{13}\text{C}_{\text{stem}}$) of one control (CO) and one previously drought-stressed (throughfall exclusion, TE) tree, (c, d) $\delta^{13}\text{C}$ of soil CO_2 efflux ($\delta^{13}\text{C}_{\text{soil}}$) of one CO and one TE soil chamber, and (e, f) $\delta^{13}\text{C}$ of living root tips ($\delta^{13}\text{C}_{\text{root}}$) of CO and TE trees. Dashed vertical lines are the start and the end of labeling. The red and blue lines fitted to the data show the results of the piecewise functions to estimate the arrival time of ^{13}C -depleted and unlabeled tracer, respectively (see Section 2). The intersections of two lines, marked with solid red and blue vertical lines are the calculated arrival times in the first week and 2 weeks after the watering, respectively. These arrival times (displayed here with arrows) were then used to calculate the above- and belowground carbon transport rates ($\text{CTR}_{\text{above}}$, $\text{CTR}_{\text{below}}$) and the incorporation time in fine roots (see Section 2). The red and blue shaded area give the 95% confidence interval of the intersections. The data of the other trees are displayed in Figure S4 (stem CO_2 efflux) and in Figures S3 and S5 (soil CO_2 efflux). All the root samples were pooled for each plot (CO and TE)

were measured on fully sun-exposed 1-year-old needles using a LI-6800 gas exchange system (Li-Cor Inc.) between 8 am and 3 pm (CET), before (around day -14) and after watering on days 4 and 14 (Table S3). In TE trees, when annual branch growth was not sufficiently long to cover the measurement chamber, needles from the previous year(s) were also included. Because of the small number of replicates in the present labeling plots (access by the canopy crane was limited by the labeling infrastructure), we additionally measured four spruce trees of each treatment in other plots (in total $n = 6$; Table S2). During the measurements, we set the light intensity to $1500 \mu\text{mol m}^{-2} \text{s}^{-1}$ and kept the leaf temperature at 25°C . The relative humidity was set to 60–65%. After the measurements, the needles were harvested and scanned (Epson Perfection 4990 Photo; Epson Deutschland GmbH). The projected needle surface area was multiplied by the factor 3.2 to determine the total needle surface area (Goisser et al., 2016).

Pre-dawn leaf water potential (Ψ_{PD}) and leaf osmotic potential (π_{O}) on fully sun-exposed twigs were determined on day -6, 2, 7, and 22 ($n = 6$, same trees used for A_{sat} , Tables S2 and S3). Ψ_{PD} was measured using a Scholander pressure bomb (mod. 1505D; PMS Instrument Co.) before sunrise (3 am–5 am CET). π_{O} was determined with pressure volume curves (PV curves), following Tomasella et al. (2018). Collected twigs (two needle age classes) were rehydrated, and subsequently, their weight and water potential were repeatedly measured.

2.10 | Statistical analysis

We analyzed all data using R (version 4.0.3) in R studio (version 1.3.1093). The treatment effect on the CTR and the time lags were tested using a t test. Beforehand, we tested the homogeneity of variances (F -test) and the normality of the data (Shapiro test). Since the homogeneity of variances between $\text{CTR}_{\text{above}}$ and $\text{CTR}_{\text{below}}$ was violated, we tested their difference with `wilcox.test` (package: stats, version: 3.6.1). The differences in A_{sat} , rates of stem/soil CO_2 efflux, Ψ_{PD} , and π_{O} were tested using a linear-mixed model (package: nlme, version: 3.1-151). We defined the treatment and day as fixed, and tree/chamber as random effects. Since A_{sat} , Ψ_{PD} , and π_{O} were also measured in other plots, the plot was defined as a random effect. For every model, we tested the homogeneity of variances (Levene test) and the normality of the residuals (Shapiro test). If any fixed factor was significant, we performed a post-hoc test with Tukey correction (package: lsmeans, version: 2.30-0). The correlation between π_{O} and Ψ_{PD} was fitted with the following sigmoid curve.

$$\pi_{\text{O}} = d + \frac{a - d}{1 + e^{-\frac{\Psi_{\text{PD}} - c}{b}}}$$

where a represents the start value of π_{O} before watering, b the slope coefficient of the regression, c the instant of the regression inflection point, and d the end value of π_{O} .

3 | RESULTS

3.1 | Aboveground transport rates ($\text{CTR}_{\text{above}}$) from crown to trunk base

The ^{13}C -depleted CO_2 was successfully taken up by tree crowns and transported downwards along the stem after the start of labeling. For example, $\delta^{13}\text{C}_{\text{stem}}$ of one CO tree in Figure 4a was $-26.1 \pm 0.1\%$ before the start of labeling and remained almost constant for 4 days after the start of labeling. Then, $\delta^{13}\text{C}_{\text{stem}}$ suddenly decreased after the ^{13}C -depleted tracer arrived. Similar courses of $\delta^{13}\text{C}_{\text{stem}}$ were observed in all six labeled trees assessed in this study (Figure 4b; Figure S4). Despite similar transport distance of 28.4 ± 0.3 and 27.0 ± 0.9 m in CO and TE trees, respectively (Table S1), the arrival of the ^{13}C -depleted tracer in stem CO_2 efflux was significantly delayed in TE trees compared to CO trees ($p < .05$). The ^{13}C -depleted tracer was found in stem CO_2 efflux of CO trees 95 ± 10 h after the start of labeling and watering, whereas in TE trees the tracer arrived after 163 ± 12 h. $\text{CTR}_{\text{above}}$, calculated from these arrival times, was $0.16 \pm 0.01 \text{ m h}^{-1}$ and thus about half in TE spruce compared to CO spruce with $0.30 \pm 0.06 \text{ m h}^{-1}$ (Figure 5a; $p = .06$). Already 2 weeks after watering, $\text{CTR}_{\text{above}}$ determined with the arrival of unlabeled tracer did not differ between treatments anymore, because of a significant increase in $\text{CTR}_{\text{above}}$ of TE trees to $0.39 \pm 0.13 \text{ m h}^{-1}$ (Figure 5b). $\text{CTR}_{\text{above}}$ of CO trees remained almost constant during the study period ($0.32 \pm 0.05 \text{ m h}^{-1}$ 2 weeks after watering).

3.2 | Leaf osmotic potential (π_{O}) and predawn water potential (Ψ_{PD})

π_{O} increased with Ψ_{PD} following a sigmoidal fit (Figure 6; $p < .001$). Before watering, Ψ_{PD} of the TE trees was on average $-0.93 \pm 0.03 \text{ MPa}$, which was significantly lower than that of CO trees with $-0.59 \pm 0.02 \text{ MPa}$ ($p < .05$). On day 7, Ψ_{PD} was then similar between treatments with -0.61 ± 0.02 and $-0.69 \pm 0.05 \text{ MPa}$ in CO and TE trees, respectively ($p > .6$). The lowest π_{O} of $-2.44 \pm 0.05 \text{ MPa}$ was observed for TE trees before watering, which was significantly lower than in CO trees with $-1.67 \pm 0.04 \text{ MPa}$ ($p < .01$). Correlated with Ψ_{PD} , π_{O} of TE trees increased by 0.5 MPa until day 22 to $-2.00 \pm 0.04 \text{ MPa}$. Nevertheless, on day 22, π_{O} of TE trees was still somewhat lower than in CO trees ($p < .1$) that stayed around -1.6 MPa throughout the study.

3.3 | Belowground transport rates ($\text{CTR}_{\text{below}}$) from trunk base to soil CO_2 efflux

The labeling with ^{13}C -depleted CO_2 also caused a sudden decrease in $\delta^{13}\text{C}_{\text{soil}}$, but with a smaller shift compared to $\delta^{13}\text{C}_{\text{stem}}$ (Figure 4c,d). In the first week after watering, the ^{13}C -depleted tracer was detected in soil CO_2 efflux under CO trees 73 ± 22 h

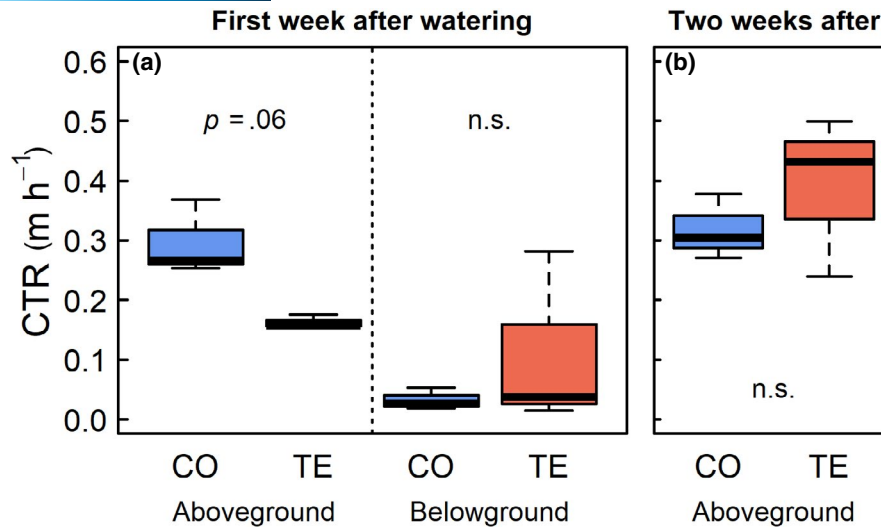


FIGURE 5 (a) Aboveground and belowground carbon transport rates (CTR) in the first week after watering determined by the arrival time of the ^{13}C -depleted tracer after the start of labeling; Aboveground CTR ($\text{CTR}_{\text{above}}$ in text), from crown to trunk base (detected as stem CO_2 efflux); belowground CTR ($\text{CTR}_{\text{below}}$ in text), from trunk base to soil CO_2 efflux. (b) $\text{CTR}_{\text{above}}$ 2 weeks after watering, determined by the arrival time of the unlabeled tracer in stem CO_2 efflux after the end of labeling. p -value and n.s. (no significance) give the results of t tests comparing CO (control) and TE (previously drought-stressed, throughfall exclusion) trees

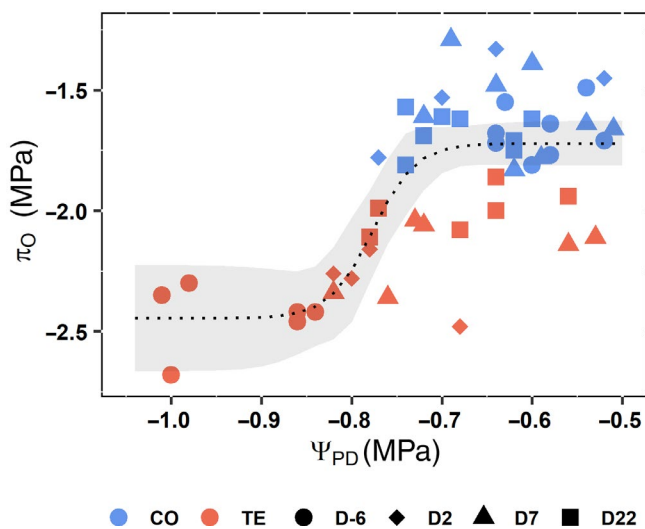


FIGURE 6 Correlation between leaf osmotic potential (π_0) and predawn leaf water potential (Ψ_{PD}) of control (CO, blue) and previously drought-stressed trees (throughfall exclusion, TE, red). Circles show the measurements 6 days before watering, diamonds on day 2 (2 days after watering), triangles on day 7, and rectangles on day 22. The dotted curve displays the prediction of the sigmoid curve (all points were fitted together). The gray area gives the 95% confidence interval

after the detection in the stem CO_2 efflux. The time lag was similar in TE trees with 62 ± 37 h ($p > .8$). $\text{CTR}_{\text{below}}$, calculated from these time lags, was not significantly different between CO and TE trees with 0.03 ± 0.01 and 0.11 ± 0.08 m h^{-1} , respectively (Figure 5a, $p > .7$). The large variance of TE trees was caused by one tree with a high $\text{CTR}_{\text{below}}$ (0.28 m h^{-1}). $\text{CTR}_{\text{below}}$ was significantly lower than $\text{CTR}_{\text{above}}$ ($p < .05$).

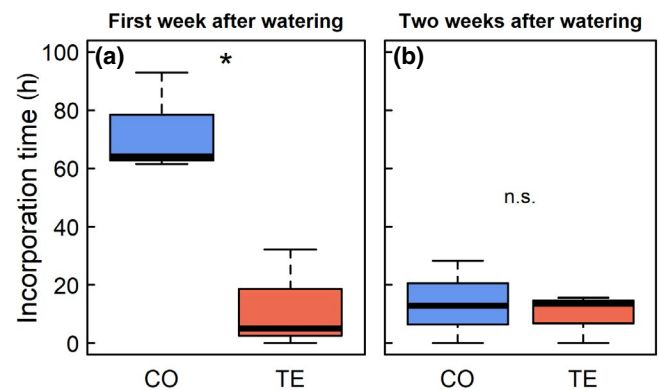


FIGURE 7 Incorporation time of current photoassimilates in living root tips (time lag between the arrival time at trunk base and arrival time in living root tips), (a) in the first week after watering, determined with the ^{13}C -depleted tracer after the start of labeling, and (b) 2 weeks after watering, determined with the unlabeled tracer after the end of labeling. Asterisk ($p < .05$) and n.s. (no significance) give the results of t tests comparing CO (control) and TE (previously drought-stressed, throughfall exclusion) trees

3.4 | Incorporation of current photoassimilates in living fine roots

In the first week after watering, the ^{13}C -depleted tracer was detected in the living root tips of TE trees within 12 ± 10 h after the detection in the stem CO_2 efflux, whereas CO trees incorporated the current photoassimilates much later, that is, within 73 ± 10 h ($p < .05$; Figure 7a). Two weeks after watering, the incorporation time of the unlabeled tracer significantly decreased in CO trees to 14 ± 8 h after the detection at the trunk base ($p < .05$), which was similar to that of TE trees (10 ± 5 h, $p > .7$; Figure 7b).

TABLE 1 Light-saturated CO₂ assimilation rates (A_{sat}) before (around day -14) and after (day 4 and 14) the watering (means \pm SE, $n = 6$, expressed on the basis of total needle area), and rates of stem and soil CO₂ efflux before (day -1) and after (day 4 and 14/15) watering (means \pm SE, $n = 3$) in CO (control) and TE (previously drought-stressed, throughfall exclusion) trees. The lowercase letters indicate the significant differences among treatments and days, determined by a post-hoc test after applying a linear-mixed model. A_{sat} , stem CO₂ efflux, and soil CO₂ efflux were tested separately

	Before	Day 4	Day 14/15
A_{sat} ($\mu\text{mol CO}_2 \text{ m}^{-2} \text{ s}^{-1}$)			
CO	2.7 \pm 0.2 ^a	2.6 \pm 0.3 ^a	2.3 \pm 0.3 ^a
TE	2.1 \pm 0.3 ^a	2.4 \pm 0.3 ^a	2.1 \pm 0.2 ^a
Stem CO ₂ efflux ($\mu\text{mol CO}_2 \text{ m}^{-2} \text{ s}^{-1}$)			
CO	2.8 \pm 0.8 ^a	2.9 \pm 0.7 ^a	3.3 \pm 0.8 ^a
TE	3.3 \pm 0.7 ^a	2.8 \pm 0.2 ^a	3.3 \pm 0.6 ^a
Soil CO ₂ efflux ($\mu\text{mol CO}_2 \text{ m}^{-2} \text{ s}^{-1}$)			
CO	6.7 \pm 0.4 ^a	5.4 \pm 0.3 ^b	6.6 \pm 0.4 ^a
TE	1.7 \pm 0.1 ^c	1.8 \pm 0.1 ^c	2.1 \pm 0.2 ^c

3.5 | Changes in C source/sink relations upon watering

Before watering, light-saturated CO₂ assimilation rates (A_{sat}) were $2.7 \pm 0.2 \mu\text{mol m}^{-2} \text{ s}^{-1}$ and thus hardly higher in CO compared to TE spruce with $2.1 \pm 0.3 \mu\text{mol m}^{-2} \text{ s}^{-1}$ (Table 1; $p > .6$). Watering did not significantly affect the A_{sat} of TE spruce, which remained almost constant under both treatments until day 14 (on day 4: CO, 2.6 ± 0.3 ; TE, 2.4 ± 0.3 ; on day 14: CO, 2.3 ± 0.3 ; TE, $2.1 \pm 0.2 \mu\text{mol m}^{-2} \text{ s}^{-1}$).

Similarly, the rates of stem CO₂ efflux did not significantly differ between treatments before watering (Table 1; $p > .9$), although the CO₂ efflux was slightly higher in TE with $3.3 \pm 0.7 \mu\text{mol m}^{-2} \text{ s}^{-1}$ compared to CO spruce with $2.8 \pm 0.8 \mu\text{mol m}^{-2} \text{ s}^{-1}$. Upon watering, the stem CO₂ efflux rates remained almost constant with 2.9 ± 0.7 and 3.3 ± 0.8 in CO, and 2.8 ± 0.2 and $3.3 \pm 0.6 \mu\text{mol m}^{-2} \text{ s}^{-1}$ in TE trees on days 4 and 14.

Before watering, rates of soil CO₂ efflux were $1.7 \pm 0.1 \mu\text{mol m}^{-2} \text{ s}^{-1}$ under TE trees, which were much lower than under CO trees with $6.7 \pm 0.4 \mu\text{mol m}^{-2} \text{ s}^{-1}$ ($p < .01$; Table 1). Soil CO₂ efflux rates under TE trees around $2.0 \mu\text{mol m}^{-2} \text{ s}^{-1}$ hardly increased after watering and remained significantly lower than those under CO trees with 5.4 ± 0.3 and $6.6 \pm 0.4 \mu\text{mol m}^{-2} \text{ s}^{-1}$ on days 4 and 15, respectively.

4 | DISCUSSION

This study aims to elucidate the whole-tree C transport in highly productive Norway spruce forests upon watering in a long-term climate-change experiment with repeated experimental summer droughts. In the last decades, Norway spruce forests have been

showing immense dieback through severe drought (Arend et al., 2021; Boczoń et al., 2018; Hentschel et al., 2014; Rosner et al., 2016; Solberg, 2004). Also in our experimental site, we lost a couple of TE spruce trees during the drought period (Grams et al., 2021). In the present study, we ask whether surviving trees recover both the aboveground C transport, that is, from the crown to the trunk base, and the belowground C transport, that is, from the trunk base to the soil CO₂ efflux after drought release. As the third transport process, we show how fast the current photoassimilates are incorporated in fine roots after drought release.

4.1 | Aboveground transport from crown to trunk base recovered within 2 weeks after drought release

The observed $\text{CTR}_{\text{above}}$ of CO spruce (c. 0.30 m h^{-1}) is somewhat higher than the average of gymnosperm trees calculated in a meta-analysis (0.22 m h^{-1} , Liesche et al., 2015), and corresponds to the values observed at the same site 10 years before (Kuptz et al., 2011). The repeated summer droughts restricted the $\text{CTR}_{\text{above}}$ of mature spruce. In the first week after drought release, the arrival of ¹³C-depleted tracer was still delayed by 2–3 days in TE trees, indicating a 46% reduction in $\text{CTR}_{\text{above}}$ compared to CO spruce (Figure 5a). In a counterpart experiment with pine trees growing on a naturally dry site (Gao et al., 2021), CTR from crown to rhizosphere doubled upon watering, similar to findings on mature spruce trees in the present study. This delay was likely to be caused by longer MRT of sugars in leaves (Dannoura et al., 2019; Epron et al., 2012; Hesse et al., 2019; Ruehr et al., 2009; Zang et al., 2014) and/or slower phloem transport (Hesse et al., 2019; Sevanto, 2014).

About 2 weeks after watering, $\text{CTR}_{\text{above}}$ of TE trees significantly increased to the level of CO trees, while $\text{CTR}_{\text{above}}$ of CO trees remained constant (Figure 5b). However, neither C source strength, that is, photosynthesis rates nor sink strength, assessed here as stem and soil CO₂ efflux, significantly increased within the first 2 weeks after watering (Table 1). Likewise, unaffected soil CO₂ efflux rates during 2 weeks after drought release were also observed in other Norway spruce forests, likely due to slow recovery of microbial activity (Muhr & Borken, 2009; Schindlbacher et al., 2012). Considering that ratio of autotrophic (root-derived) to heterotrophic (microbial) soil respiration under the present spruce trees is known to decrease during drought (Nikolova et al., 2009), autotrophic respiration also likely remained low after drought release. Thus, changes of C source/sink relations are unlikely to be a major cause for the impaired $\text{CTR}_{\text{above}}$. This led to the rejection of H1 that $\text{CTR}_{\text{above}}$ would recover with C source and/or sink strength, which is different from the study of Gao et al. (2021) on pine trees.

Although still not fully recovered to the rather constant level of CO trees, π_0 of TE trees increased until day 22 after watering in parallel with Ψ_{PD} (Figure 6). This indicates a declined C demand for osmotic adjustments, implying a decrease in leaf sugar concentration and MRT after drought release. Therefore, the delayed

sugar export from leaves under drought was likely a component of slower C translocation from the crown to the trunk base. A quick recovery of MRT of sugars in leaves was also observed in beech saplings after drought release (Zang et al., 2014). In addition, since Ψ_{PD} of TE trees was significantly lower than that of CO trees before watering and increased to the control level by day 7 (Figure 6), increased phloem viscosity due to water limitation in the xylem might be another cause for the slower phloem transport under drought (Epron et al., 2016; Woodruff, 2014). In principle, CTR may be reduced by intensified leakage–retrieval of transported sugars in the phloem (van Bel, 2003; De Schepper et al., 2013; Epron et al., 2016), however, there is no evidence to date that this mechanism is enhanced under drought (Salmon et al., 2019). Considering the rapid increase in CTR_{above} within 2 weeks, reduction in phloem conduit diameter is unlikely to have occurred, which is in line with unaffected branch phloem lumen area of the same TE spruce trees (Giai Petit, University of Padova, in preparation). Miller et al. (2020) also reported an unaffected sieve cell production of mature spruce under summer drought. Furthermore, phloem production of the present spruce likely peaked before watering under moderate water stress (c. -0.9 MPa), since it has been found to peak before mid-June in spruce trees (Gričar et al., 2014; Jyske et al., 2015; Miller et al., 2020). This explains the different results on other tree species including conifers, which decreased phloem growth and diameter under more severe water stress (Dannoura et al., 2019; Woodruff, 2014).

It is important to note that the xylem water potential and to some extent also π_o were continuously increasing after watering until the ^{13}C -depleted tracer arrived in stem CO_2 efflux around day 7 in TE trees. Therefore, the drought-induced reduction in CTR_{above} might have been even more pronounced before the watering. Most importantly, the aboveground CTR from crown to trunk base of mature spruce fully recovered within 2 weeks after watering, hence showing high resilience to long-term and recurrent summer droughts.

4.2 | Belowground transport from trunk base to soil CO_2 efflux was similar between treatments already in the first week after watering

The observed CTR_{below} of CO trees (c. 0.03 $m\ h^{-1}$) was about 10 times lower than CTR_{above} (Figure 5a), which is in line with the study of Mencuccini and Hölttä (2010) reporting on a slower belowground transport compared to transport along the stem phloem. The variance of CTR_{below} in TE trees was high, likely due to the soil heterogeneities and unknown root structures from the trunk base to the spot of soil CO_2 efflux assessments. Already in the first week after watering, CTR_{below} was similar between CO and TE trees. However, conversely to our expectation, rates of soil CO_2 efflux did not increase after watering (as discussed above), which led to the rejection of H2 that CTR_{below} would recover in parallel with increasing C sink or source strength. Upon watering, water potential in leaves fully recovered within 1 week (Figure 6) and can be expected to have

increased faster in roots in parallel with increasing soil water potential (Fiscus, 1972; Gleason et al., 2017; McCully, 1999). Therefore, we suggest a fast and full recovery of root phloem transport within few days, that is, even before the ^{13}C -depleted tracer arrived at the trunk base (i.e., around day 7). Moreover, speed of soil CO_2 diffusion was likely similar in soils of both treatments, as gas diffusion in soils is negatively correlated with soil water content (Kuz'yakov & Gavrichkova, 2010) that was very similar in TE and CO plots within few days after watering (Grams et al., 2021).

Since the distance of the aboveground transport is much longer than belowground in tall mature trees, particularly in shallow rooting spruce trees, the drought-reduced transport rates from crown to soil CO_2 efflux are mainly caused by the restricted aboveground C transport from crown to trunk base. However, short young trees or deep rooting mature trees have higher ratio of belowground to total transport distance. Thus, the belowground C transport from trunk base to soil CO_2 efflux might play a significant role for the whole-tree transport processes and forest C cycling (Gao et al., 2021), since CTR_{below} is much lower than CTR_{above} . Most importantly, not only aboveground but the whole-tree CTR from crown to soil CO_2 efflux showed a full recovery within 2 weeks after watering, hence indicating high resilience to long-term and recurrent summer droughts.

4.3 | Incorporation of current photoassimilates in fine roots was faster in trees recovering from drought than in control trees

The ^{13}C -depleted tracer was detected in living root tips of TE trees within 12 h after the arrival at the trunk base, but only 60 h later in CO trees (Figure 7a), confirming H3 that incorporation of current photoassimilates is faster in trees recovering from drought. The faster use of the tracers in living root tips of TE trees compared to controls coincided with the growth of new roots that started within few days after watering (personal observations on site), suggesting a higher C demand in fine roots of TE trees. However, the enhanced fine root growth upon watering in TE plots was not reflected in soil CO_2 efflux, likely due to a small contribution of respiration of fine roots grown after watering to total soil CO_2 efflux: that is, small biomass share of growing fine roots to total roots. Furthermore, Nikolova et al. (2020) found on the same spruce trees that respiration rates of fine roots and proportion of absorptive fine roots to the total root biomass were both small. A preferential investment of current photoassimilates following high C sink strength of growing fine roots has also been observed in young beech trees upon drought release (Hagedorn et al., 2016) and in naturally drought-stressed mature pine trees after a rainfall event (Gao et al., 2021; Joseph et al., 2020).

Not only previously drought-stressed spruce but also control trees responded with fast C incorporation in living fine roots after increase in soil water availability. During an intensive rain event on day 17 (following a short dry spell), fine root growth was likely induced in the shallow soil layers (Joseph et al., 2020; Meier & Leuschner, 2008). This may explain the fast arrival of unlabeled tracer in root

tips in both treatments 2 weeks after drought release (Figure 7b). Our results suggest, therefore, that the speed of incorporation of current photoassimilates in living root tips of mature spruce trees is strongly dependent on the C demand for root production, that is, “sink controlled” as suggested earlier (Faticchi et al., 2014; Gavito et al., 2019; Hagedorn et al., 2016; Körner, 2015). In contrast to previous studies (Gao et al., 2021; Hagedorn et al., 2016), the increased “sink demand” by stimulated fine root growth in mature spruce did not significantly affect the whole-tree CTR from crown to soil, since they were still reduced in the first week after drought release (Figure 5a). Above all, mature drought-stressed spruce trees respond to drought release by quickly supplying the growing root tips with current photoassimilates. In addition to the high resilience in whole-tree C transport, this response is essential to regenerate the water-absorbing root system.

5 | CONCLUSION

The present study reveals high resilience of the whole-tree C transport system in Norway spruce forests even after recurrent summer droughts. Once spruce trees manage to survive drought periods, their whole-tree C transport system may be expected to recover quickly after drought release. This ensures high resilience of C supply with current photoassimilates, in particular to belowground sinks such as growing fine roots. Once the water-absorbing root system is restored, long-term recovery of C uptake and supply to further sinks can be expected. However, recovery of the C transport is only one of the many important prerequisites for the recovery of tree productivity. Thus, long-term observations of C source and sink activities upon drought release are necessary to elucidate the recovery potential of productivity in central European forests dominated by Norway spruce stands.

ACKNOWLEDGMENTS

We thank Thomas Feuerbach (TUM) for technical support and maintenance of the measurement equipment. We also thank Timo Gebhardt, Karl-Heinz Häberle, Josef Heckmair, Peter Kuba, bachelor/master students (TUM), Laura Pohlenz, Ramona Werner, and ecology volunteers (Helmholtz Zentrum München) for support during the fieldwork, Phillip Papastefanou (TUM) for support with the calculation of CTR, Timo Knüver (KIT) for his support with the soil respiration unit, and Manuela Laski and Manuela Oettli for laboratory support (both WSL). This study was funded by the German Research Foundation (DFG) through grants GR 1881/5-1, MA1763/10-1, PR555/2-1, PR292/22-1 and by the Bavarian State Ministries of the Environment and Consumer Protection as well as Food, Agriculture and Forestry (W047/Kroof II). RR and NKR were supported by the German Research Foundation through its Emmy Noether Program (RU 1657/2-1). MML was supported by the Ambizione grant (179978) from the Swiss National Science Foundation (SNSF). BDH was funded by a doctoral scholarship from the German Federal Environmental Foundation (DBU, AZ 20018/535). Open Access funding enabled and organized by Projekt DEAL.

CONFLICT OF INTEREST

The authors declare that there is no conflict of interest.





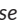





AUTHOR CONTRIBUTIONS

TEEG and KP designed the experiment. KH, VR, and TEEG prepared and conducted the ¹³C labeling experiment. All authors contributed to the data collection. KH analyzed and interpreted the data with supports from TEEG, JD, and VR. KH wrote the manuscript with contributions of all authors.

DATA AVAILABILITY STATEMENT

The data that support the findings of this study are openly available in mediaTUM at <https://doi.org/10.14459/2021mp1637391>.

ORCID

Kyohsuke Hikino  <https://orcid.org/0000-0002-6981-3988>
 Vincent P. Riedel  <https://orcid.org/0000-0003-1685-8135>
 Romy Rehschuh  <https://orcid.org/0000-0001-9140-0306>
 Nadine K. Ruehr  <https://orcid.org/0000-0001-5989-7463>
 Benjamin D. Hesse  <https://orcid.org/0000-0003-1113-9801>
 Marco M. Lehmann  <https://orcid.org/0000-0003-2962-3351>
 Franz Buegger  <https://orcid.org/0000-0003-3526-4711>
 Fabian Weigl  <https://orcid.org/0000-0003-3973-6341>
 Karin Pritsch  <https://orcid.org/0000-0001-6384-2473>
 Thorsten E. E. Grams  <https://orcid.org/0000-0002-4355-8827>

REFERENCES

- Allen, C. D., Breshears, D. D., & McDowell, N. G. (2015). On underestimation of global vulnerability to tree mortality and forest die-off from hotter drought in the Anthropocene. *Ecosphere*, 6(8), art129. <https://doi.org/10.1890/ES15-00203.1>
- Allen, C. D., Macalady, A. K., Chenchouni, H., Bachelet, D., McDowell, N., Vennetier, M., Kitzberger, T., Rigling, A., Breshears, D. D., Hogg, E. H., Gonzalez, P., Fensham, R., Zhang, Z., Castro, J., Demidova, N., Lim, J.-H., Allard, G., Running, S. W., Semerci, A., & Cobb, N. (2010). A global overview of drought and heat-induced tree mortality reveals emerging climate change risks for forests. *Forest Ecology and Management*, 259(4), 660–684. <https://doi.org/10.1016/j.foreco.2009.09.001>
- Andersen, C. P., Ritter, W., Gregg, J., Matyssek, R., & Grams, T. E. E. (2010). Below-ground carbon allocation in mature beech and spruce trees following long-term, experimentally enhanced O₃ exposure in Southern Germany. *Environmental Pollution*, 158(8), 2604–2609. <https://doi.org/10.1016/j.envpol.2010.05.008>
- Arend, M., Link, R. M., Patthey, R., Hoch, G., Schuldt, B., & Kahmen, A. (2021). Rapid hydraulic collapse as cause of drought-induced mortality in conifers. *Proceedings of the National Academy of Sciences of the United States of America*, 118(16), e2025251118. <https://doi.org/10.1073/pnas.2025251118>
- Barthel, M., Hammerle, A., Sturm, P., Baur, T., Gentsch, L., & Knohl, A. (2011). The diel imprint of leaf metabolism on the δ¹³C signal of soil respiration under control and drought conditions. *The New Phytologist*, 192(4), 925–938. <https://doi.org/10.1111/j.1469-8137.2011.03848.x>
- Boczoń, A., Kowalska, A., Ksepko, M., & Sokotowski, K. (2018). Climate warming and drought in the Białowieża Forest from 1950–2015 and their impact on the dieback of Norway spruce stands. *Water*, 10(11), 1950–2015. <https://doi.org/10.3390/w10111502>

- Braden-Behrens, J., Yan, Y., & Knohl, A. (2017). A new instrument for stable isotope measurements of ^{13}C and ^{18}O in CO_2 – Instrument performance and ecological application of the Delta Ray IRIS analyzer. *Atmospheric Measurement Techniques*, 10(11), 4537–4560. <https://doi.org/10.5194/amt-10-4537-2017>
- Caudullo, G., Tinner, W., & De Rigo, D. (2016). *Picea abies* in Europe: Distribution, habitat, usage and threats. In J. San-Miguel-Ayanz, D. de Rigo, G. Caudullo, T. Houston Durrant, & A. Mauri (Eds.), *European atlas of forest tree species* (pp. 114–116). Publications Office of the EU, e012300+ pp.
- Ciais, P. H., Reichstein, M., Viovy, N., Granier, A., Ogée, J., Allard, V., Aubinet, M., Buchmann, N., Bernhofer, C., Carrara, A., Chevallier, F., De Noblet, N., Friend, A. D., Friedlingstein, P., Grünwald, T., Heinesch, B., Keronen, P., Knohl, A., Krinner, G., ... Valentini, R. (2005). Europe-wide reduction in primary productivity caused by the heat and drought in 2003. *Nature*, 437(7058), 529–533. <https://doi.org/10.1038/nature03972>
- Collins, M., Knutti, R., Arblaster, J., Dufresne, J.-L., Fichetef, T., Friedlingstein, P., Gao, X., Gutowski, W. J., Johns, T., Krinner, G., Shongwe, M., Tebaldi, C., Weaver, A. J., & Wehner, M. (2013). Long-term climate change: Projections, commitments and irreversibility. In T. F. Stocker, D. Qin, G.-K. Plattner, M. Tignor, S. K. Allen, J. Boschung, A. Nauels, Y. Xia, V. Bex, & P. M. Midgley (Eds.), *Climate change 2013: The physical science basis. Contribution of working group I to the fifth assessment report of the Intergovernmental Panel on Climate Change* (pp. 1029–1136). Cambridge University Press.
- Dannoura, M., Epron, D., Desalme, D., Massonnet, C., Tsuji, S., Plain, C., Priault, P., & Gérant, D. (2019). The impact of prolonged drought on phloem anatomy and phloem transport in young beech trees. *Tree Physiology*, 39(2), 201–210. <https://doi.org/10.1093/treephys/tpy070>
- Dawson, T. E., Mambelli, S., Plamboeck, A. H., Templer, P. H., & Tu, K. P. (2002). Stable isotopes in plant ecology. *Annual Review of Ecology and Systematics*, 33(1), 507–559. <https://doi.org/10.1146/annurev.ecolsys.33.020602.095451>
- De Schepper, V., De Swaef, T., Bauweraerts, I., & Steppe, K. (2013). Phloem transport: A review of mechanisms and controls. *Journal of Experimental Botany*, 64(16), 4839–4850. <https://doi.org/10.1093/jxb/ert302>
- Epron, D., Bahn, M., Derrien, D., Lattanzi, F. A., Pumpanen, J., Gessler, A., Högberg, P., Maillard, P., Dannoura, M., Gérant, D., & Buchmann, N. (2012). Pulse-labelling trees to study carbon allocation dynamics: A review of methods, current knowledge and future prospects. *Tree Physiology*, 32(6), 776–798. <https://doi.org/10.1093/treephys/tps057>
- Epron, D., Cabral, O. M. R., Laclau, J.-P., Dannoura, M., Packer, A. P., Plain, C., Battie-Laclau, P., Moreira, M. Z., Trivelin, P. C. O., Bouillet, J.-P., Gérant, D., & Nouvellon, Y. (2016). In situ ^{13}C pulse labelling of field-grown eucalypt trees revealed the effects of potassium nutrition and throughfall exclusion on phloem transport of photosynthetic carbon. *Tree Physiology*, 36(1), 6–21. <https://doi.org/10.1093/treephys/tpv090>
- Epron, D., & Dreyer, E. (1996). Starch and soluble carbohydrates in leaves of water-stressed oak saplings. *Annales Des Sciences Forestières*, 53(2–3), 263–268. <https://doi.org/10.1051/forest:19960209>
- Fatichi, S., Leuzinger, S., & Körner, C. (2014). Moving beyond photosynthesis: From carbon source to sink-driven vegetation modeling. *The New Phytologist*, 201(4), 1086–1095. <https://doi.org/10.1111/nph.12614>
- Fiscus, E. L. (1972). In situ measurement of root-water potential. *Plant Physiology*, 50(1), 191–193. <https://doi.org/10.1104/pp.50.1.191>
- Gammitzer, U., Schäufele, R., & Schnyder, H. (2009). Observing ^{13}C labelling kinetics in CO_2 respired by a temperate grassland ecosystem. *The New Phytologist*, 184(2), 376–386. <https://doi.org/10.1111/j.1469-8137.2009.02963.x>
- Gao, D., Joseph, J., Werner, R. A., Brunner, I., Zürcher, A., Hug, C., Wang, A., Zhao, C., Bai, E., Meusburger, K., Gessler, A., & Hagedorn, F. (2021). Drought alters the carbon footprint of trees in soils-tracking the spatio-temporal fate of ^{13}C -labelled assimilates in the soil of an old-growth pine forest. *Global Change Biology*. <https://doi.org/10.1111/gcb.15557>
- Gavito, M. E., Jakobsen, I., Mikkelsen, T. N., & Mora, F. (2019). Direct evidence for modulation of photosynthesis by an arbuscular mycorrhiza-induced carbon sink strength. *The New Phytologist*, 223(2), 896–907. <https://doi.org/10.1111/nph.15806>
- Gleason, S. M., Wiggans, D. R., Bliss, C. A., Young, J. S., Cooper, M., Willi, K. R., & Comas, L. H. (2017). Embolized stems recover overnight in *Zea mays*: The role of soil water, root pressure, and nighttime transpiration. *Frontiers in Plant Science*, 8, 662. <https://doi.org/10.3389/fpls.2017.00662>
- Goisser, M., Geppert, U., Rötzer, T., Paya, A., Huber, A., Kerner, R., Bauerle, T., Pretzsch, H., Pritsch, K., Häberle, K. H., Matyssek, R., & Grams, T. (2016). Does belowground interaction with *Fagus sylvatica* increase drought susceptibility of photosynthesis and stem growth in *Picea abies*? *Forest Ecology and Management*, 375, 268–278. <https://doi.org/10.1016/j.foreco.2016.05.032>
- Grams, T. E. E., Hesse, B. D., Gebhardt, T., Weikl, F., Rötzer, T., Kovacs, B., Hikino, K., Hafner, B. D., Brunn, M., Bauerle, T. L., Häberle, K.-H., Pretzsch, H., & Pritsch, K. (2021). The Kroof experiment: Realization and efficacy of a recurrent drought experiment plus recovery in a beech/spruce forest. *Ecosphere*, 12(3). <https://doi.org/10.1002/ecs2.3399>
- Grams, T. E. E., Werner, H., Kuptz, D., Ritter, W., Fleischmann, F., Andersen, C. P., & Matyssek, R. (2011). A free-air system for long-term stable carbon isotope labeling of adult forest trees. *Trees*, 25(2), 187–198. <https://doi.org/10.1007/s00468-010-0497-7>
- Gričar, J., Prislán, P., Gryc, V., Vavrčík, H., de Luis, M., & Cufar, K. (2014). Plastic and locally adapted phenology in cambial seasonality and production of xylem and phloem cells in *Picea abies* from temperate environments. *Tree Physiology*, 34(8), 869–881. <https://doi.org/10.1093/treephys/tpu026>
- Hagedorn, F., Joseph, J., Peter, M., Luster, J., Pritsch, K., Geppert, U., Kerner, R., Molinier, V., Egli, S., Schaub, M., Liu, J.-F., Li, M., Sever, K., Weiler, M., Siegwolf, R. T. W., Gessler, A., & Arend, M. (2016). Recovery of trees from drought depends on belowground sink control. *Nature Plants*, 2, 16111. <https://doi.org/10.1038/NPLAN.TS.2016.111>
- Hartmann, H., Ziegler, W., Kolle, O., & Trumbore, S. (2013). Thirst beats hunger – Declining hydration during drought prevents carbon starvation in Norway spruce saplings. *The New Phytologist*, 200(2), 340–349. <https://doi.org/10.1111/nph.12331>
- Hartmann, H., Ziegler, W., & Trumbore, S. (2013). Lethal drought leads to reduction in nonstructural carbohydrates in Norway spruce tree roots but not in the canopy. *Functional Ecology*, 27(2), 413–427. <https://doi.org/10.1111/1365-2435.12046>
- Hentschel, R., Rosner, S., Kayler, Z. E., Andreassen, K., Børja, I., Solberg, S., Tveito, O. E., Priesack, E., & Gessler, A. (2014). Norway spruce physiological and anatomical predisposition to dieback. *Forest Ecology and Management*, 322, 27–36. <https://doi.org/10.1016/j.foreco.2014.03.007>
- Hesse, B. D., Goisser, M., Hartmann, H., & Grams, T. E. E. (2019). Repeated summer drought delays sugar export from the leaf and impairs phloem transport in mature beech. *Tree Physiology*, 39(2), 192–200. <https://doi.org/10.1093/treephys/tpy122>
- Hölttä, T., Mencuccini, M., & Nikinmaa, E. (2009). Linking phloem function to structure: Analysis with a coupled xylem-phloem transport model. *Journal of Theoretical Biology*, 259(2), 325–337. <https://doi.org/10.1016/j.jtbi.2009.03.039>
- Hölttä, T., Vesala, T., Sevanto, S., Perämäki, M., & Nikinmaa, E. (2006). Modeling xylem and phloem water flows in trees according to

- cohesion theory and Münch hypothesis. *Trees*, 20(1), 67–78. <https://doi.org/10.1007/s00468-005-0014-6>
- Hsiao, T. C. (1973). Plant responses to water stress. *Annual Review of Plant Physiology*, 24(1), 519–570. <https://doi.org/10.1146/annurev.pp.24.060173.002511>
- IPCC. (2007). Summary for policymakers. In M. L. Parry, O. F. Canziani, J. P. Palutikof, P. J. van der Linden, & C. E. Hanson (Eds.), *Climate change 2007: Impacts, adaptation and vulnerability. Contribution of working group II to the fourth assessment report of the intergovernmental panel on climate change* (pp. 7–22). Cambridge University Press.
- IPCC. (2014). *Climate change 2014: Synthesis report. Contribution of working groups I, II and III to the fifth assessment report of the intergovernmental panel on climate change* [Core Writing Team, R. K. Pachauri, & L. A. Meyer (Eds.)]. IPCC, 151 pp.
- Joseph, J., Gao, D., Backes, B., Bloch, C., Brunner, I., Gleixner, G., Haeni, M., Hartmann, H., Hoch, G., Hug, C., Kahmen, A., Lehmann, M. M., Li, M.-H., Luster, J., Peter, M., Poll, C., Rigling, A., Rissanen, K. A., Ruehr, N. K., ... Gessler, A. (2020). Rhizosphere activity in an old-growth forest reacts rapidly to changes in soil moisture and shapes whole-tree carbon allocation. *Proceedings of the National Academy of Sciences of the United States of America*, 117(40), 24885–24892. <https://doi.org/10.1073/pnas.2014084117>
- Jyske, T. M., Suuronen, J.-P., Pranovich, A. V., Laakso, T., Watanabe, U., Kuroda, K., & Abe, H. (2015). Seasonal variation in formation, structure, and chemical properties of phloem in *Picea abies* as studied by novel microtechniques. *Planta*, 242(3), 613–629. <https://doi.org/10.1007/s00425-015-2347-8>
- Keeling, C. D. (1958). The concentration and isotopic abundances of atmospheric carbon dioxide in rural areas. *Geochimica Et Cosmochimica Acta*, 13(4), 322–334. [https://doi.org/10.1016/0016-7037\(58\)90033-4](https://doi.org/10.1016/0016-7037(58)90033-4)
- Keeling, C. D. (1961). The concentration and isotopic abundances of carbon dioxide in rural and marine air. *Geochimica Et Cosmochimica Acta*, 24(3–4), 277–298. [https://doi.org/10.1016/0016-7037\(61\)90023-0](https://doi.org/10.1016/0016-7037(61)90023-0)
- Kodama, N., Barnard, R. L., Salmon, Y., Weston, C., Ferrio, J. P., Holst, J., Werner, R. A., Saurer, M., Rennenberg, H., Buchmann, N., & Gessler, A. (2008). Temporal dynamics of the carbon isotope composition in a *Pinus sylvestris* stand: From newly assimilated organic carbon to respired carbon dioxide. *Oecologia*, 156(4), 737–750. <https://doi.org/10.1007/s00442-008-1030-1>
- Körner, C. (2015). Paradigm shift in plant growth control. *Current Opinion in Plant Biology*, 25, 107–114. <https://doi.org/10.1016/j.pbi.2015.05.003>
- Kuptz, D., Fleischmann, F., Matyssek, R., & Grams, T. E. E. (2011). Seasonal patterns of carbon allocation to respiratory pools in 60-yr-old deciduous (*Fagus sylvatica*) and evergreen (*Picea abies*) trees assessed via whole-tree stable carbon isotope labeling. *The New Phytologist*, 191(1), 160–172. <https://doi.org/10.1111/j.1469-8137.2011.03676.x>
- Kuzyakov, Y., & Gavrichkova, O. (2010). REVIEW: Time lag between photosynthesis and carbon dioxide efflux from soil: A review of mechanisms and controls. *Global Change Biology*, 16(12), 3386–3406. <https://doi.org/10.1111/j.1365-2486.2010.02179.x>
- Lehmann, M. M., Egli, M., Brinkmann, N., Werner, R. A., Saurer, M., & Kahmen, A. (2020). Improving the extraction and purification of leaf and phloem sugars for oxygen isotope analyses. *Rapid Communications in Mass Spectrometry*, 34(19), e8854. <https://doi.org/10.1002/rcm.8854>
- Lemoine, R., La Camera, S., Atanassova, R., Dédaldéchamp, F., Allario, T., Pourtau, N., Bonnemain, J.-L., Laloi, M., Coutos-Thévenot, P., Maurousset, L., Faucher, M., Girousse, C., Lemonnier, P., Parrilla, J., & Durand, M. (2013). Source-to-sink transport of sugar and regulation by environmental factors. *Frontiers in Plant Science*, 4, 272. <https://doi.org/10.3389/fpls.2013.00272>
- Liesche, J., Windt, C., Bohr, T., Schulz, A., & Jensen, K. H. (2015). Slower phloem transport in gymnosperm trees can be attributed to higher sieve element resistance. *Tree Physiology*, 35(4), 376–386. <https://doi.org/10.1093/treephys/tpv020>
- Lloret, F., Keeling, E. G., & Sala, A. (2011). Components of tree resilience: Effects of successive low-growth episodes in old ponderosa pine forests. *Oikos*, 120(12), 1909–1920. <https://doi.org/10.1111/j.1600-0706.2011.19372.x>
- McCully. (1999). Root xylem embolisms and refilling. Relation To water potentials of soil, roots, and leaves, and osmotic potentials of root xylem Sap. *Plant Physiology*, 119(3), 1001–1008. <https://doi.org/10.1104/pp.119.3.1001>
- McDowell, N., Pockman, W. T., Allen, C. D., Breshears, D. D., Cobb, N., Kolb, T., Plaut, J., Sperry, J., West, A., Williams, D. G., & Yezzer, E. A. (2008). Mechanisms of plant survival and mortality during drought: Why do some plants survive while others succumb to drought? *The New Phytologist*, 178(4), 719–739. <https://doi.org/10.1111/j.1469-8137.2008.02436.x>
- Meier, I. C., & Leuschner, C. (2008). Belowground drought response of European beech: Fine root biomass and carbon partitioning in 14 mature stands across a precipitation gradient. *Global Change Biology*, 14(9), 2081–2095. <https://doi.org/10.1111/j.1365-2486.2008.01634.x>
- Mencuccini, M., & Hölttä, T. (2010). The significance of phloem transport for the speed with which canopy photosynthesis and below-ground respiration are linked. *The New Phytologist*, 185(1), 189–203. <https://doi.org/10.1111/j.1469-8137.2009.03050.x>
- Miller, T. W., Stangler, D. F., Larysch, E., Seifert, T., Spiecker, H., & Kahle, H.-P. (2020). Plasticity of seasonal xylem and phloem production of Norway spruce along an elevational gradient. *Trees*, 34(5), 1281–1297. <https://doi.org/10.1007/s00468-020-01997-6>
- Muhr, J., & Borken, W. (2009). Delayed recovery of soil respiration after wetting of dry soil further reduces C losses from a Norway spruce forest soil. *Journal of Geophysical Research*, 114(G4). <https://doi.org/10.1029/2009JG000998>
- Nikolova, P. S., Bauerle, T. L., Häberle, K.-H., Blaschke, H., Brunner, I., & Matyssek, R. (2020). Fine-root traits reveal contrasting ecological strategies in European beech and Norway spruce during extreme drought. *Frontiers in Plant Science*, 11, 1211. <https://doi.org/10.3389/fpls.2020.01211>
- Nikolova, P. S., Raspe, S., Andersen, C. P., Mainiero, R., Blaschke, H., Matyssek, R., & Häberle, K.-H. (2009). Effects of the extreme drought in 2003 on soil respiration in a mixed forest. *European Journal of Forest Research*, 128(2), 87–98. <https://doi.org/10.1007/s10342-008-0218-6>
- Pretzsch, H., Grams, T. E. E., Häberle, K.-H., Pritsch, K., Bauerle, T. L., & Rötzer, T. (2020). Growth and mortality of Norway spruce and European beech in monospecific and mixed-species stands under natural episodic and experimentally extended drought. Results of the KROOF throughfall exclusion experiment. *Trees*, 34(4), 957–970. <https://doi.org/10.1007/s00468-020-01973-0>
- Pretzsch, H., Rötzer, T., Matyssek, R., Grams, T. E. E., Häberle, K.-H., Pritsch, K., Kerner, R., & Munch, J.-C. (2014). Mixed Norway spruce (*Picea abies* [L.] Karst) and European beech (*Fagus sylvatica* [L.] stands under drought: From reaction pattern to mechanism. *Trees*, 28(5), 1305–1321. <https://doi.org/10.1007/s00468-014-1035-9>
- Rosner, S., Světlík, J., Andreassen, K., Børja, I., Dalsgaard, L., Evans, R., Luss, S., Tveito, O. E., & Solberg, S. (2016). Novel hydraulic vulnerability proxies for a boreal conifer species reveal that opportunists may have lower survival prospects under extreme climatic events. *Frontiers in Plant Science*, 7, 831. <https://doi.org/10.3389/fpls.2016.00831>
- Ruehr, N. K., Grote, R., Mayr, S., & Arneth, A. (2019). Beyond the extreme: Recovery of carbon and water relations in woody plants following heat and drought stress. *Tree Physiology*, 39(8), 1285–1299. <https://doi.org/10.1093/treephys/tpz032>

- Ruehr, N. K., Offermann, C. A., Gessler, A., Winkler, J. B., Ferrio, J. P., Buchmann, N., & Barnard, R. L. (2009). Drought effects on allocation of recent carbon: From beech leaves to soil CO₂ efflux. *The New Phytologist*, 184(4), 950–961. <https://doi.org/10.1111/j.1469-8137.2009.03044.x>
- Ryan, M. G., & Asao, S. (2014). Phloem transport in trees. *Tree Physiology*, 34(1), 1–4. <https://doi.org/10.1093/treephys/tpt123>
- Salmon, Y., Dietrich, L., Sevanto, S., Hölttä, T., Dannoura, M., & Epron, D. (2019). Drought impacts on tree phloem: From cell-level responses to ecological significance. *Tree Physiology*, 39(2), 173–191. <https://doi.org/10.1093/treephys/tpy153>
- Schindlbacher, A., Wunderlich, S., Borken, W., Kitzler, B., Zechmeister-Boltenstern, S., & Jandl, R. (2012). Soil respiration under climate change: Prolonged summer drought offsets soil warming effects. *Global Change Biology*, 18(7), 2270–2279. <https://doi.org/10.1111/j.1365-2486.2012.02696.x>
- Sevanto, S. (2014). Phloem transport and drought. *Journal of Experimental Botany*, 65(7), 1751–1759. <https://doi.org/10.1093/jxb/ert467>
- Sevanto, S. (2018). Drought impacts on phloem transport. *Current Opinion in Plant Biology*, 43, 76–81. <https://doi.org/10.1016/j.cpb.2018.01.002>
- Solberg, S. (2004). Summer drought: A driver for crown condition and mortality of Norway spruce in Norway. *Forest Pathology*, 34(2), 93–104. <https://doi.org/10.1111/j.1439-0329.2004.00351.x>
- Steinmann, K., Siegwolf, R. T. W., Saurer, M., & Körner, C. (2004). Carbon fluxes to the soil in a mature temperate forest assessed by ¹³C isotope tracing. *Oecologia*, 141(3), 489–501. <https://doi.org/10.1007/s00442-004-1674-4>
- Subke, J.-A., Vallack, H. W., Magnusson, T., Keel, S. G., Metcalfe, D. B., Högberg, P., & Ineson, P. (2009). Short-term dynamics of abiotic and biotic soil ¹³CO₂ effluxes after in situ ¹³CO₂ pulse labelling of a boreal pine forest. *The New Phytologist*, 183(2), 349–357. <https://doi.org/10.1111/j.1469-8137.2009.02883.x>
- Teskey, R. O., Saveyn, A. N., Steppe, K., & McGuire, M. A. (2008). Origin, fate and significance of CO₂ in tree stems. *The New Phytologist*, 177(1), 17–32. <https://doi.org/10.1111/j.1469-8137.2007.02286.x>
- Tomasella, M., Beikircher, B., Häberle, K.-H., Hesse, B., Kallenbach, C., Matyssek, R., & Mayr, S. (2018). Acclimation of branch and leaf hydraulics in adult *Fagus sylvatica* and *Picea abies* in a forest through-fall exclusion experiment. *Tree Physiology*, 38(2), 198–211. <https://doi.org/10.1093/treephys/tpx140>
- Ubierna, N., Marshall, J. D., & Cernusak, L. A. (2009). A new method to measure carbon isotope composition of CO₂ respired by trees: Stem CO₂ equilibration. *Functional Ecology*, 23(6), 1050–1058. <https://doi.org/10.1111/j.1365-2435.2009.01593.x>
- Unger, S., Máguas, C., Pereira, J. S., David, T. S., & Werner, C. (2010). The influence of precipitation pulses on soil respiration – Assessing the “Birch effect” by stable carbon isotopes. *Soil Biology and Biochemistry*, 42(10), 1800–1810. <https://doi.org/10.1016/j.soilbio.2010.06.019>
- van Bel, A. J. E. (2003). The phloem, a miracle of ingenuity. *Plant, Cell & Environment*, 26(1), 125–149. <https://doi.org/10.1046/j.1365-3040.2003.00963.x>
- van Mantgem, P. J., Stephenson, N. L., Byrne, J. C., Daniels, L. D., Franklin, J. F., Fulé, P. Z., Harmon, M. E., Larson, A. J., Smith, J. M., Taylor, A. H., & Veblen, T. T. (2009). Widespread increase of tree mortality rates in the western United States. *Science*, 323(5913), 521–524. <https://doi.org/10.1126/science.1165000>
- Wang, A., Siegwolf, R. T. W., Joseph, J., Thomas, F. M., Werner, W., Gessler, A., Rigling, A., Schaub, M., Saurer, M., Li, M.-H., & Lehmann, M. M. (2021). Effects of soil moisture, needle age and leaf morphology on carbon and oxygen uptake, incorporation and allocation: A dual labeling approach with ¹³CO₂ and H₂¹⁸O in foliage of a coniferous forest. *Tree Physiology*, 41(1), 50–62. <https://doi.org/10.1093/treephys/tpaa114>
- Wingate, L., Ogée, J., Burrett, R., Bosc, A., Devaux, M., Grace, J., Loustau, D., & Gessler, A. (2010). Photosynthetic carbon isotope discrimination and its relationship to the carbon isotope signals of stem, soil and ecosystem respiration. *The New Phytologist*, 188(2), 576–589. <https://doi.org/10.1111/j.1469-8137.2010.03384.x>
- Winkler, A., & Oberhuber, W. (2017). Cambial response of Norway spruce to modified carbon availability by phloem girdling. *Tree Physiology*, 37(11), 1527–1535. <https://doi.org/10.1093/treephys/tpx077>
- Woodruff, D. R. (2014). The impacts of water stress on phloem transport in Douglas-fir trees. *Tree Physiology*, 34(1), 5–14. <https://doi.org/10.1093/treephys/tpt106>
- Zang, U., Goisser, M., Grams, T. E. E., Häberle, K.-H., Matyssek, R., Matzner, E., & Borken, W. (2014). Fate of recently fixed carbon in European beech (*Fagus sylvatica*) saplings during drought and subsequent recovery. *Tree Physiology*, 34(1), 29–38. <https://doi.org/10.1093/treephys/tpy110>
- Zwetsloot, M. J., & Bauerle, T. L. (2021). Repetitive seasonal drought causes substantial species-specific shifts in fine-root longevity and spatio-temporal production patterns in mature temperate forest trees. *The New Phytologist*, 231(3), 974–986. <https://doi.org/10.1111/nph.17432>

SUPPORTING INFORMATION

Additional supporting information may be found in the online version of the article at the publisher's website.

How to cite this article: Hikino, K., Danzberger, J., Riedel, V. P., Rehschuh, R., Ruehr, N. K., Hesse, B. D., Lehmann, M. M., Buegger, F., Weigl, F., Pritsch, K., & Grams, T. E. E. (2022). High resilience of carbon transport in long-term drought-stressed mature Norway spruce trees within 2 weeks after drought release. *Global Change Biology*, 28, 2095–2110. <https://doi.org/10.1111/gcb.16051>

Supplementary figures and tables

High resilience of carbon transport in long-term drought stressed mature Norway spruce trees within two weeks after drought release

Kyohsuke Hikino, Jasmin Danzberger, Vincent P. Riedel, Romy Rehschuh, Nadine K. Ruehr, Benjamin D. Hesse, Marco M. Lehmann, Franz Buegger, Fabian Weikl, Karin Pritsch, Thorsten E. E. Grams

Supplementary figures

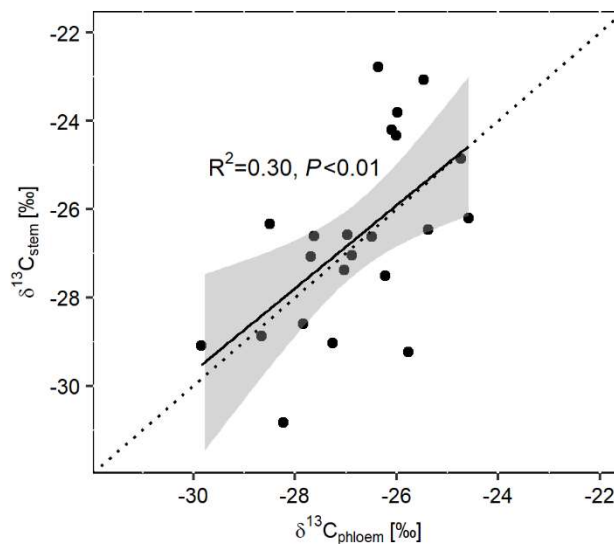


Figure S 1: Correlation between $\delta^{13}\text{C}$ of stem CO_2 efflux ($\delta^{13}\text{C}_{\text{stem}}$) and $\delta^{13}\text{C}$ of stem phloem sugar ($\delta^{13}\text{C}_{\text{phloem}}$). The dashed line is 1:1 line and the solid line is the calculated regression line (slope = 0.94). The gray area displays the 95% confidence interval.

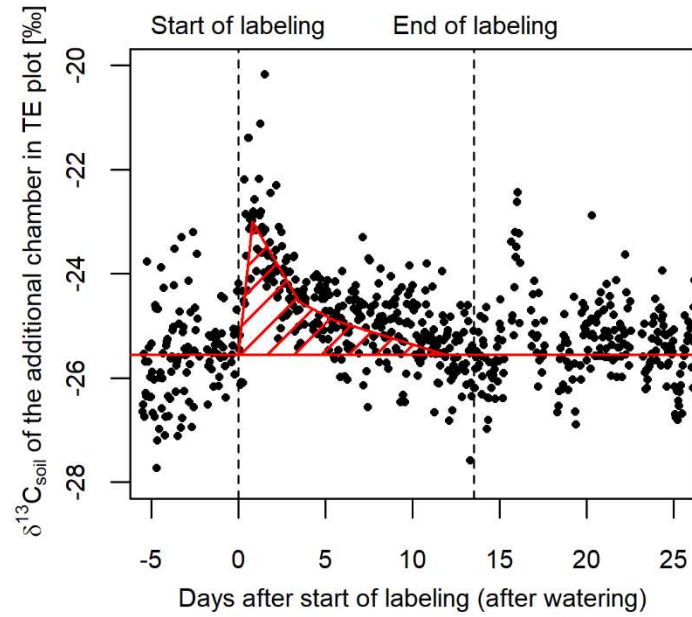


Figure S 2: $\delta^{13}\text{C}$ of the additional soil chamber ($\delta^{13}\text{C}_{\text{soil}}$) close to the non-labeled beech trees in the TE (previously drought-stressed, throughfall exclusion) plot (see Figure 2a). Dashed lines indicate start and end of labeling. The red horizontal line displays the mean $\delta^{13}\text{C}_{\text{soil}}$ before the start of labeling. The shift of $\delta^{13}\text{C}_{\text{soil}}$ after watering/start of labeling (roughly marked with red striped area for the first 12 days) was subtracted from the $\delta^{13}\text{C}_{\text{soil}}$ of the soil chambers under labeled trees in the TE plot (for details see Figure S3).

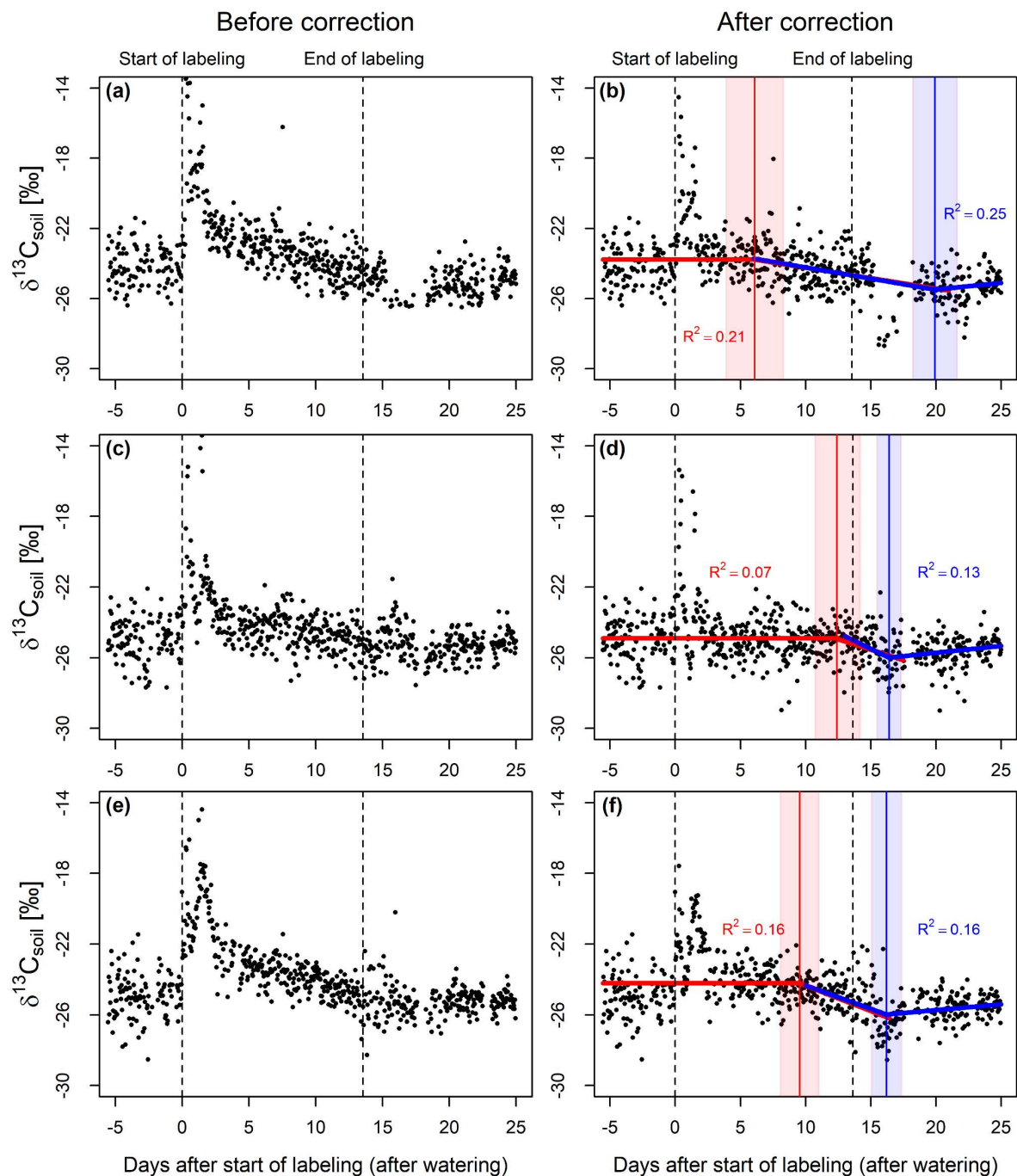


Figure S 3: The correction of $\delta^{13}\text{C}$ of soil CO_2 efflux ($\delta^{13}\text{C}_{\text{soil}}$) under labeled, previously drought-stressed trees (TE, throughfall exclusion, $n = 3$) using the additional soil chamber (see Figure S2): $\delta^{13}\text{C}_{\text{soil}}$ of three TE soil chamber before (a, c, e) and after the correction (b, d, f), respectively. The gap between the values before and after the watering (start of labeling) was properly corrected, enabling to calculate the arrival time of the tracers with piecewise functions. Dashed lines indicate the start and the end of the labeling period. The red and blue lines fitted to the data show the results of the piecewise functions (see Materials and Methods in the main document). The red and blue vertical lines give the calculated arrival time of ^{13}C -depleted (after turn-on of the CO_2 exposure) and unlabeled tracer (after turn-off of the CO_2 exposure), respectively. The red and blue shaded area show the 95% confidence interval of the intersections.

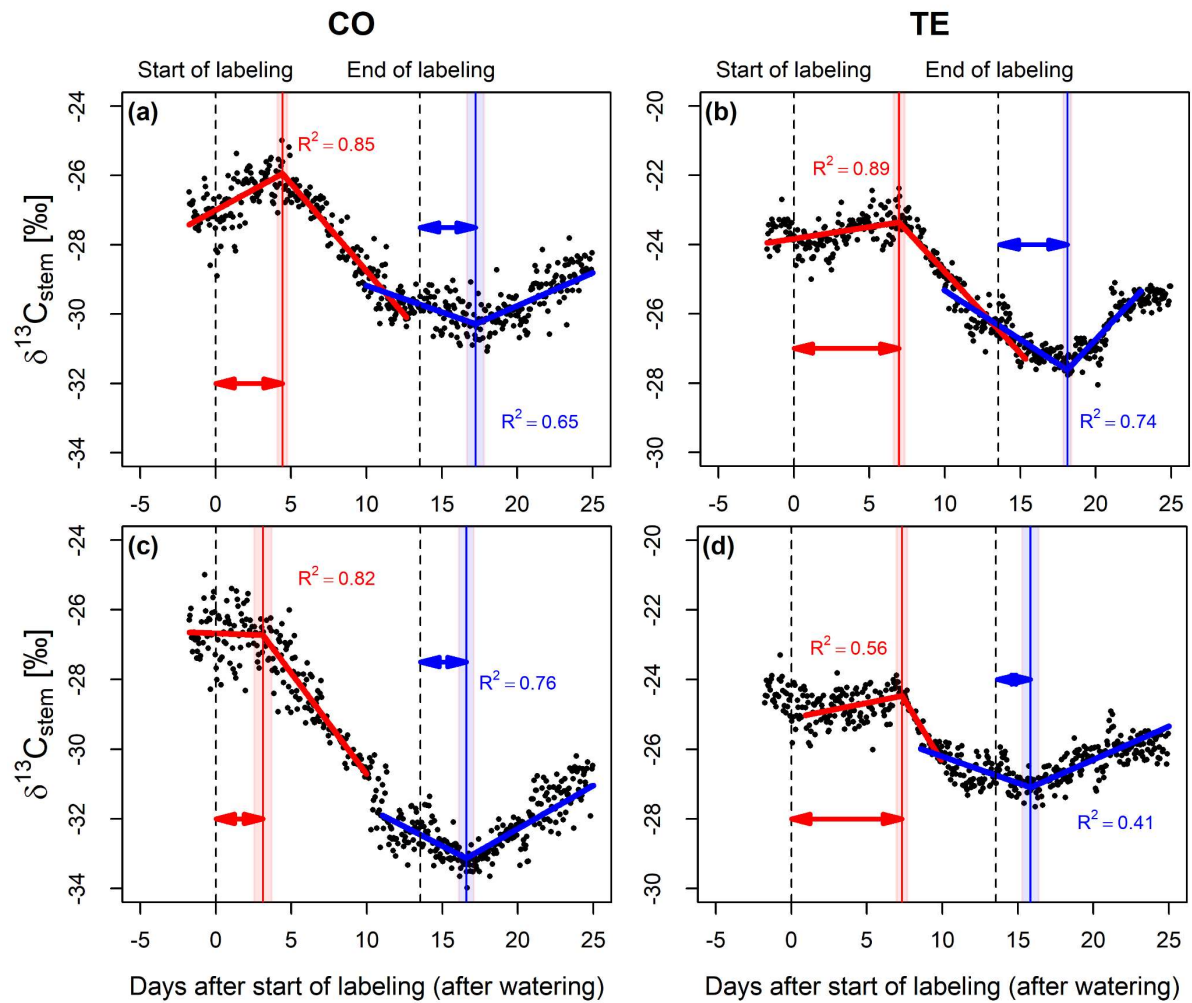


Figure S 4: The other data of $\delta^{13}\text{C}$ of stem CO_2 efflux ($\delta^{13}\text{C}_{\text{stem}}$) in CO (control, a, c) and TE (previously drought-stressed, throughfall exclusion, b,d) plots, used for the calculation of the arrival time of the ^{13}C -tracers (see Materials and Methods in the main document, Figure 4). Dashed vertical lines are the start and the end of labeling. The red and blue lines fitted to the data show the results of the piecewise functions to estimate the arrival time of ^{13}C -depleted and unlabeled tracer, respectively. The intersections of two lines, marked with solid red and blue vertical lines are the calculated arrival times in the first week and two weeks after the watering, respectively. These arrival times (displayed here with arrows) were then used to calculate the aboveground carbon transport rates ($\text{CTR}_{\text{above}}$). The red and blue shaded area give the 95% confidence interval of the intersections.

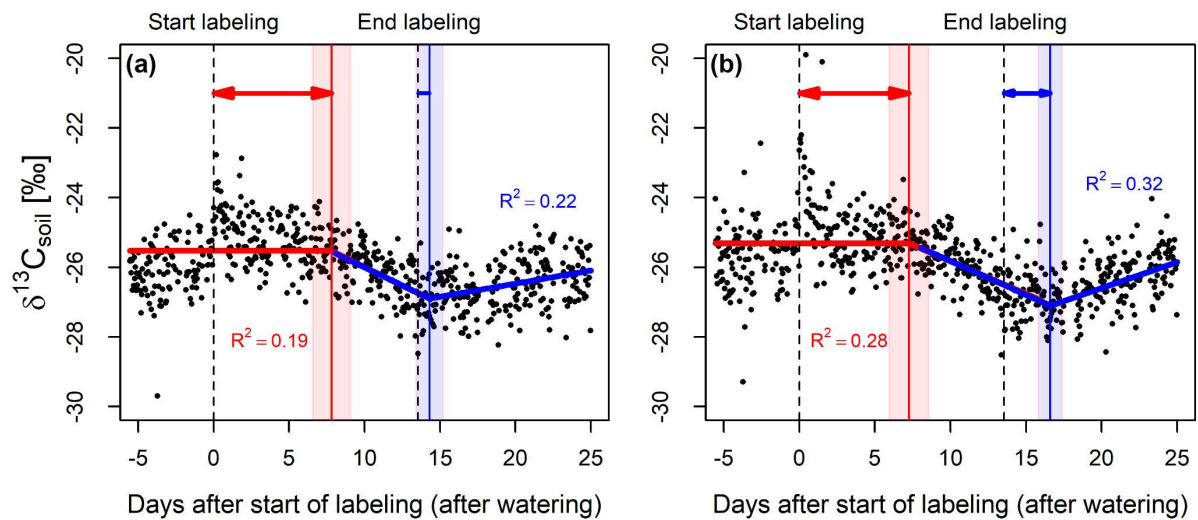


Figure S 5: The other data of $\delta^{13}\text{C}$ of soil CO_2 efflux ($\delta^{13}\text{C}_{\text{soil}}$) in CO (control) plot, used for the calculation of the arrival time of the ^{13}C -tracers (see Materials and Methods in the main document, Figure 4). Dashed vertical lines are the start and the end of labeling. The red and blue lines fitted to the data show the results of the piecewise functions to estimate the arrival time of ^{13}C -depleted and unlabeled tracer, respectively. The intersections of two lines, marked with solid red and blue vertical lines are the calculated arrival times in the first week and two weeks after the watering, respectively. These arrival times (displayed here with arrows) were then used to calculate the belowground carbon transport rates ($\text{CTR}_{\text{below}}$). The red and blue shaded area give the 95% confidence interval of the intersections.

Supplementary tables

Table S 1: Diameter at breast height (DBH), mean crown height (middle of the crown), and daily mean shift of CO₂ concentration and stable carbon isotope composition ($\delta^{13}\text{C}_a$) of canopy air during labeling hours (5 am – 7 pm CET) of four labeled control (CO) and three labeled throughfall exclusion (TE, previously drought stressed) trees. Shifts are given in means \pm SE. The fourth tree on the CO plot was not the object of the calculation of arrival time and C transport rates (CTR), therefore, its mean crown height was not measured.

	DBH [cm]	Mean crown height [m]	Shift of CO ₂ concentration [ppm]	Shift of $\delta^{13}\text{C}_a$ [‰]
CO_1	30.5	28.6	111 \pm 8	-6.7 \pm 0.4
CO_2	34.9	27.9	112 \pm 8	-6.7 \pm 0.4
CO_3	46.3	28.7	119 \pm 8	-7.2 \pm 0.4
CO_4	37.7	-	162 \pm 10	-8.8 \pm 0.4
TE_1	45.1	27.3	72 \pm 5	-5.0 \pm 0.3
TE_2	27.3	25.4	132 \pm 8	-7.3 \pm 0.4
TE_3	38.3	28.4	35 \pm 5	-2.9 \pm 0.3

Table S 2: Number of trees and sampling positions assessed for this study in labeled and non-labeled plots in each treatment: i.e. control (CO) and throughfall exclusion (TE, previously drought stressed). n.a.= not assessed. A_{sat} (light-saturated CO₂ assimilation rates), Ψ_{PD} (Pre-dawn leaf water potential), π_{O} (leaf osmotic potential).

Number of trees/ sampling positions	Labeled		Non-labeled	
	CO	TE	CO	TE
Spruce tree	4	3	3	3
Canopy air	7	6	1	1
Stem CO ₂ efflux	3	3	3	3
Soil CO ₂ efflux	3	3	n.a.	1
Root tips	18	17	11	5
Stem phloem	4	3	n.a.	n.a.
A_{sat} , Ψ_{PD} , π_{O}	2	2	4	4

RESEARCH ARTICLE

Dynamics of initial carbon allocation after drought release in mature Norway spruce—Increased belowground allocation of current photoassimilates covers only half of the carbon used for fine-root growth

Kyohsuke Hikino¹  | Jasmin Danzberger²  | Vincent P. Riedel¹  | Benjamin D. Hesse¹  | Benjamin D. Hafner³  | Timo Gebhardt¹ | Romy Rehschuh⁴  | Nadine K. Ruehr⁴  | Melanie Brunn⁵  | Taryn L. Bauerle³  | Simon M. Landhäuser⁶  | Marco M. Lehmann⁷  | Thomas Rötzer⁸  | Hans Pretzsch⁸  | Franz Buegger²  | Fabian Weikl^{1,2}  | Karin Pritsch²  | Thorsten E. E. Grams¹ 

¹Professorship for Land Surface-Atmosphere Interactions, Ecophysiology of Plants, TUM School of Life Sciences, Technical University of Munich, Freising, Germany

²Institute of Biochemical Plant Pathology, Helmholtz Zentrum München – German Research Center for Environmental Health (GmbH), Neuherberg, Germany

³School of Integrative Plant Science, Cornell University, Ithaca, New York, USA

⁴Karlsruhe Institute of Technology, Institute of Meteorology and Climate Research—Atmospheric Environmental Research (KIT/IMK-IFU), Garmisch-Partenkirchen, Germany

⁵Institute for Environmental Sciences, University Koblenz-Landau, Landau, Germany

⁶Department of Renewable Resources, University of Alberta, Edmonton, Alberta, Canada

⁷Swiss Federal Institute for Forest, Snow and Landscape Research (WSL), Forest Dynamics, Birmensdorf, Switzerland

⁸Forest Growth and Yield Science, TUM School of Life Sciences, Technical University of Munich, Freising, Germany

Correspondence

Kyohsuke Hikino, Professorship for Land Surface-Atmosphere Interactions, Ecophysiology of Plants, TUM School of Life Sciences, Technical University of Munich, Hans-Carl-von-Carlowitz Platz 2, 85354 Freising, Germany.
Email: kyohsuke.hikino@tum.de

Jasmin Danzberger, Institute of Biochemical Plant Pathology, Helmholtz Zentrum München – German Research Center for Environmental Health (GmbH), Ingolstaedter Landstr. 1, 85764 Neuherberg, Germany.
Email: jasmin.danzberger@helmholtz-muenchen.de

Abstract

After drought events, tree recovery depends on sufficient carbon (C) allocation to the sink organs. The present study aimed to elucidate dynamics of tree-level C sink activity and allocation of recent photoassimilates (C_{new}) and stored C in c. 70-year-old Norway spruce (*Picea abies*) trees during a 4-week period after drought release. We conducted a continuous, whole-tree ^{13}C labeling in parallel with controlled watering after 5 years of experimental summer drought. The fate of C_{new} to growth and CO_2 efflux was tracked along branches, stems, coarse- and fine roots, ectomycorrhizae and root exudates to soil CO_2 efflux after drought release. Compared with control trees, drought recovering trees showed an overall 6% lower C sink activity and 19% less allocation of C_{new} to aboveground sinks, indicating a low priority for aboveground sinks during recovery. In contrast, fine-root growth in recovering trees was seven times greater than that of controls. However, only half of the C used for new fine-root

Kyohsuke Hikino and Jasmin Danzberger contributed equally to this work and share the first authorship.

This is an open access article under the terms of the [Creative Commons Attribution](https://creativecommons.org/licenses/by/4.0/) License, which permits use, distribution and reproduction in any medium, provided the original work is properly cited.

© 2022 The Authors. *Global Change Biology* published by John Wiley & Sons Ltd.

Present address

Vincent P. Riedel, Julius-von-Sachs-Institute of Biological Sciences, Ecophysiology and Vegetation Ecology, University of Würzburg, Julius-von-Sachs-Platz 3, Würzburg, 97082, Germany

Romy Rehschuh, Institute of General Ecology and Environmental Protection, Technische Universität Dresden, Piennner Str. 7, Tharandt, 01737, Germany

Funding information

Deutsche Bundesstiftung Umwelt, Grant/Award Number: AZ 20018/535; Deutsche Forschungsgemeinschaft, Grant/Award Number: GR 1881/5-1, MA1763/10-1, PR292/22-1, PR555/2-1 and RU1657/2-1; Schweizerischer Nationalfonds zur Förderung der Wissenschaftlichen Forschung, Grant/Award Number: 179978; Technische Universität München

growth was comprised of C_{new} while the other half was supplied by stored C. For drought recovery of mature spruce trees, in addition to C_{new} , stored C appears to be critical for the regeneration of the fine-root system and the associated water uptake capacity.

KEYWORDS

^{13}C labeling, belowground carbon allocation, carbon partitioning, climate change, drought recovery, forest ecosystems, *Picea abies*, watering

1 | INTRODUCTION

Forests store ~45% of terrestrial carbon (C), which is in form of carbon dioxide (CO_2) a rapidly increasing greenhouse gas (IPCC, 2021). Thus, conditions and C sequestration capacity of forests have a large impact on the global C cycle (Bonan, 2008; Lal et al., 2018). As a consequence of climate change, forests are globally facing repeated droughts leading to immense tree dieback (Allen et al., 2010; Hartmann et al., 2018; Schuldt et al., 2020). Under these circumstances, tree survival depends not only on water availability, but also on C supply to each above- and belowground tree organs (Hartmann et al., 2020; Ruehr et al., 2019; Sala et al., 2010). Previous studies revealed that allocation of both, structural (i.e., growth) and non-structural (i.e., maintenance and storage) C, was altered to increase tree survival: for example, enhanced C allocation to root growth (Gaul et al., 2008; Hommel et al., 2016; Meier & Leuschner, 2008; Poorter et al., 2012) and C storage (Blessing et al., 2015; Chuste et al., 2020; Hart et al., 2021).

Because the frequency of drought events is predicted to increase in the future (IPCC, 2021), recovery from these events is an important aspect of tree survival, which has attracted less attention compared with direct drought effects (Ruehr et al., 2019). On the one hand, drought release can increase aboveground C sink activity for repair processes such as growth of new xylem and embolism refilling (Brodersen & McElrone, 2013; Ruehr et al., 2019; Zang et al., 2014) or C storage to prepare for future droughts (Galiano et al., 2017; Rehschuh et al., 2021). On the other hand, drought release can stimulate belowground C sinks such as root production, mycorrhizal and microbial activity, and associated soil respiration (Brunner et al., 2019; Gao et al., 2021; Hagedorn et al., 2016; Joseph et al., 2020; Werner et al., 2021). Fine-root growth dynamics are especially challenging to assess

(Ruehr et al., 2019), are typically tree species-specific, and therefore difficult to generalize (Nikolova et al., 2020; Zwetsloot & Bauerle, 2021).

To improve our understanding of the tree recovery processes from drought, it is crucial to analyze the whole-tree C allocation including belowground sinks, which has been often restricted to young trees (Brüggemann et al., 2011; Hartmann et al., 2018). Recovery of tree function can be expected only if the increased C sink activity after drought release can be met by available C that is newly assimilated C (C_{new} , see Table 1 for terms and abbreviations) and stored C. A previous study using young European beech trees directly related allocation of C_{new} belowground to the capacity of trees to recover from drought (Hagedorn et al., 2016). However, for mature trees, recovery from repeated drought events is critically understudied and experimental evidence on the allocation of both C_{new} and stored C for tree recovery processes is still scarce (Gao et al., 2021; Joseph et al., 2020; Werner et al., 2021).

The present study was conducted as part of the Kranzberg forest roof (KROOF) project, which was established to investigate mature Norway spruce (*Picea abies* [L.] Karst.) trees exposed to 5 years of experimental summer droughts (Grams et al., 2021). This long-term repetitive drought treatment significantly reduced leaf and twig growth (Tomasella et al., 2018), stem growth (Pretzsch et al., 2020), fine-root growth (Nickel et al., 2018; Zwetsloot & Bauerle, 2021), total C uptake (Brunn et al., 2022), and C storage pools (Hesse et al., 2021) in Norway spruce. To gain insight into the recovery processes, the drought-stressed trees were watered in early summer of the sixth year (Grams et al., 2021). In parallel with the watering, we performed a continuous ^{13}C labeling and assessed the use of both C_{new} and stored C at the whole-tree level for tree recovery from drought.

In this study, leaves were considered C sources, and we focused on the allocation of newly assimilated C (C_{new}) exported

TABLE 1 Terms and abbreviations used in this study

Terms	Unit	Abbreviations	Explanation
Newly assimilated C	gC	C_{new}	Labeled, newly assimilated C
Stored C	gC	-	C originating from C reserves within a tree
C sink activity	$\text{gC tree}^{-1} 28 \text{ days}^{-1}$	-	Total C that was used for growth and respiratory sinks (cumulative sum during 28 days after drought release)
Amount of C_{new}	$\text{gC tree}^{-1} 28 \text{ days}^{-1}$	-	Total amount of C_{new} allocated to each C sink (cumulative sum during 28 days after drought release)
Proportional allocation of C_{new}	%	-	Proportion of C_{new} in each C sink to the total C_{new} detected in the whole tree
Fraction of labeled C	%	f_{Label}	Proportion of C_{new} to the C sink activity at each measurement point
Contribution of C_{new} to each C sink activity	%	$\text{cont}C_{\text{new}}$	Proportion of C_{new} to the C sink activity at the new isotopic equilibrium (asymptote of Equation 11)

from leaves to the different above- and belowground sinks. We examined the following three aspects: (i) whole-tree C sink activity (in g C used for growth and respiration, see Table 1), (ii) allocation of C_{new} , and (iii) contribution of C_{new} to each C sink activity ($\text{cont}C_{\text{new}}$). We expected the regeneration of the water-absorbing fine roots to be a high priority for drought-recovering spruce trees and thus we hypothesized a higher C sink activity belowground and correspondingly a lower C sink activity aboveground compared with control trees [H1] and that the high belowground C sink activity of recovering trees would be supported by preferential allocation of C_{new} into belowground sinks at the expense of aboveground sinks [H2]. Due to reduced leaf and twig growth under drought, the total C uptake per tree can be expected to be much lower in recovering trees even after drought release compared with controls. Thus, we further hypothesized that for recovering trees, the relative contribution of C_{new} to the different sinks (i.e., $\text{cont}C_{\text{new}}$) would be lower compared with control trees, particularly when sink activity is increased [H3].

2 | MATERIALS AND METHODS

2.1 | Experimental site and ^{13}C labeling

The present study was conducted at the Kranzberg Forest experimental site, a mixed forest in southern Germany (11°39'42" E, 48°25'12" N; 490 m a.s.l.). A long-term drought experiment was established in 2014, which is described in detail by Grams et al. (2021). In brief, this experimental site consists of 12 plots with c. 70-year-old Norway spruce (*P. abies* [L.] Karst.) trees. The plots were trenched 4 years before the start of the drought treatment and separated by buried plastic tarps from the surrounding soil (Pretzsch et al., 2014). Half of the plots were equipped with under-canopy roofs, thereby excluding precipitation throughfall throughout the entire growing season (from April to November) between 2014 and 2018 and leading to recurrent summer droughts; remaining control plots were exposed to natural rainfall events. Accordingly, 459 ± 21 mm ($69 \pm 7\%$ of the

annual precipitation) was excluded during the growing seasons and predawn leaf water potential of drought-stressed trees significantly decreased to as low as -1.8 MPa (Grams et al., 2021). In early summer of 2019, all drought plots were watered to initiate the recovery processes (Grams et al., 2021) by supplying c. 90 mm water over 40 h to increase the soil water content to the control level (around 20%–30%, Grams et al., 2021). Accordingly, the predawn leaf water potential of previously drought-stressed trees fully recovered from -0.93 ± 0.03 MPa to -0.69 ± 0.05 MPa within 7 days after watering, while that of control trees remained constant at -0.61 ± 0.02 MPa (Grams et al., 2021; Hikino et al., 2022). In parallel with the watering, we conducted a continuous ^{13}C labeling experiment in four control and three recovering spruce trees on two neighboring plots (Figure 1a, for details see Hikino et al., 2022). In brief, each tree (average height of 32.3 ± 0.7 m, Table S1) was equipped with perforated PVC tubes, which continuously released ^{13}C -depleted CO_2 ($\delta^{13}\text{C}$ of $-44.3 \pm 0.2\%$) into the entire crowns from 5 a.m. to 7 p.m. (CET). The CO_2 exposure started at the same time as watering on July, 4th 2019 (day 0), lasted until July, 17th 2019 (day 13) and CO_2 concentration and its stable C isotopic signature ($\delta^{13}\text{C}$) were monitored by means of a cavity ring-down spectroscopy (CRDS, ESP-1000; PICARRO). The change of the CO_2 concentration and $\delta^{13}\text{C}$ of individual crown air during labeling were on average $+126$ ppm and -7.3% for control trees, $+80$ ppm and -5.1% for recovering trees, due to different wind exposure of each tree. The individual shift in crown air (Table S1) was considered in the tree-specific analyses. To assess the whole-tree C allocation, we investigated the following C sinks (Figure 2): Growth and/or CO_2 efflux of branch, upper and lower stem, coarse-root, fine-root, ectomycorrhizae (ECM), fine-root exudates, and soil. Because the ^{13}C label in soil CO_2 efflux showed a peak 14–20 days after the start of labeling/watering and a rapid decrease until day 28 (Hikino et al., 2022), C allocation during the first 4 weeks (28 days) of drought release was considered. In addition to the seven labeled trees, three control and three recovering spruce trees on non-labeled plots were assessed to correct for the effect of watering and weather influences on $\delta^{13}\text{C}$ of studied parameters.

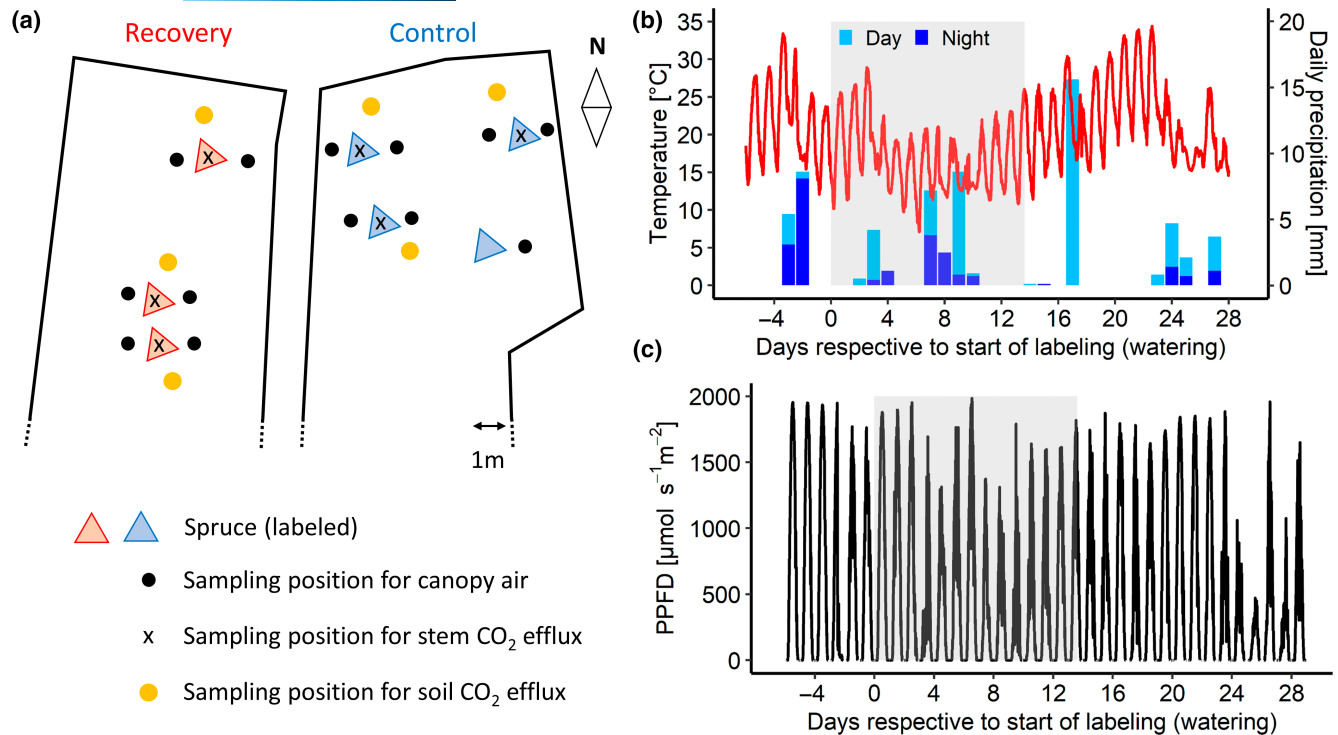


FIGURE 1 (a) Overview of the two ^{13}C -labeled plots: Control and recovery (previously drought-stressed), giving positions of trees (red and blue triangles = labeled spruce trees), sampling points of canopy air (black circles), stem CO_2 efflux (x), and soil CO_2 efflux (yellow circles). Modified from Hikino et al. (2022). (b) Temperature (red lines), daily precipitation (blue bars), and (c) photosynthetic photon flux density (PPFD) before and after the watering until day 28. Precipitation amount is split into day (5 a.m.–7 p.m. CET, fumigation hours, light blue), and night (7 p.m.–5 a.m., dark blue). Day 0 is the day of the watering. The gray areas show the labeling days (day 0–13). ^{13}C labeling started in parallel with the watering on day 0.

2.2 | Weather data

Daytime (from 5 a.m. to 7 p.m., CET), mean temperature during the experiment (i.e., 0–28 days after watering) was 21.4 ± 5.4 (1SD) °C (Figure 1b) with a mean vapor pressure deficit of 0.6 ± 0.4 (1SD) kPa. There were prolonged periods with minor daytime precipitation on days 9 (7.8 mm) and 17 (15.6 mm). The mean daytime photosynthetically active photon flux density was 772 ± 545 (1SD) $\mu\text{mol m}^{-2} \text{s}^{-1}$ (38 ± 14 [1SD] $\text{mol m}^{-2} \text{day}^{-1}$, Figure 1c).

2.3 | Sample collection

After the 2019 growing season, increment cores (diameter 0.5 cm) were collected at three different stem heights (breast height, crown base, mid-crown), and from coarse-roots (Figure 2) and immediately dried at 64°C for 72 h. Tree rings from 2019 were separated with a razor blade and subsequently thin-sectioned (c. 5 μm) in radial direction, using a microtome (Sledge Microtome G.S.L.1; Schenkung Dapples).

To record the isotopic signature of fine-root tips and mycorrhizae and trace fine-root growth, vital fine-roots (diameter ≤ 2 mm) were selected based on their turgid appearance and active meristems, and placed in mesh bags as follows. In April 2019, eight fine-roots for each sampling day and treatment were excavated

within the first 10 cm of the soil, photographed, placed in 1/3 soil filled nylon mesh bags (12.5 \times 6.5 cm, mesh width 80 μm , open area of 29%), sprayed with water to enhance root soil contact, and covered with soil. Seven days before and weekly after the watering, roots were harvested from the mesh bags and photographed. Additional fine roots from 0 to 10 cm depth were also randomly sampled within the plots daily to gain a more detailed time resolution of the change in C isotope signature (Table S2). Thus, a total of 1166 root tips were sampled. After sampling, vital ECM and non-mycorrhizal root tips were distinguished by the presence/absence of a hyphal mantle using a stereomicroscope (M125; Leica), and dried for 1 h at 60°C.

Root exudates were collected according to the method described by Phillips et al. (2008) and Brunn et al. (2022). Excavated root branches were rinsed with a nutrient solution (0.5 mM NH_4NO_3 , 0.1 mM KH_2PO_4 , 0.2 mM K_2SO_4 , 0.15 mM MgSO_4 , 0.3 mM CaCl_2) after attached soil was gently removed with tweezers. Roots were then left to recover in a 1:1 mixture of native soil from the site and sand for 48 h, cleaned, and placed into 30 ml glass syringes with sterile glass beads. Syringes were flushed three times with the nutrient solution, equilibrated for 48 h, flushed again, and left shielded with aluminum foil and leaf litter. Between days –5 and 7, and 20 and 24 (Table S2), exudates trapped in the syringes were collected from the same root branches every 48 h by adding 30 ml of nutrient solution, extracted using a membrane pump, filtered through sterile

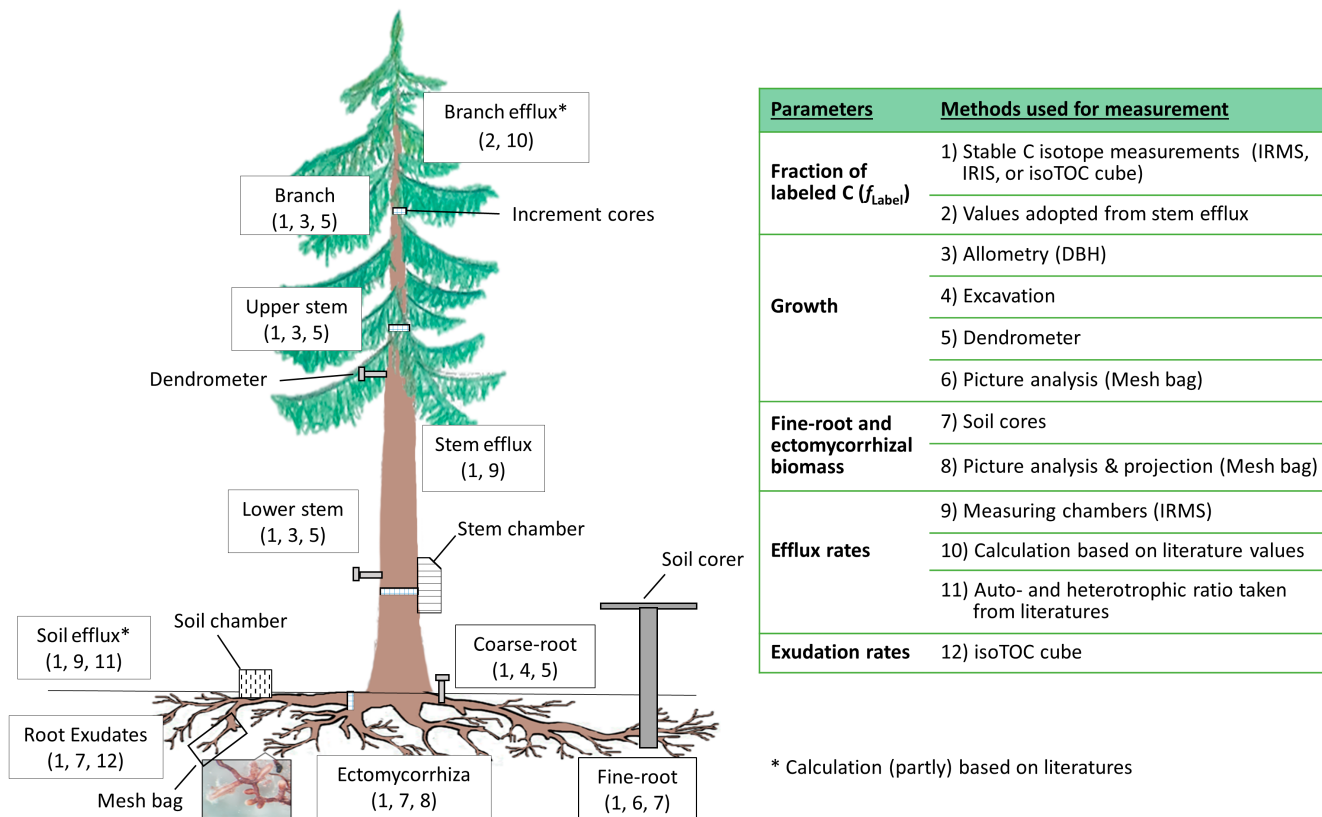


FIGURE 2 Overview of C sinks and sampling/calculation methods used for this study. In few cases, data from literature were adopted for calculations (i.e., branch CO_2 efflux and autotrophic soil CO_2 efflux).

syringe filters (0.22 μm , ROTILABO® MCE; Carl Roth GmbH + Co. KG), and stored at -20°C . A blank syringe without roots served as a reference. Root branches were harvested after exudate collection, dried, and total dry biomass recorded to normalize exudation rates to root mass.

2.4 | Analysis of stable C isotopic composition ($\delta^{13}\text{C}$), rates of CO_2 efflux, and root exudates

$\delta^{13}\text{C}$ of tree ring slices (stem and coarse-roots) and vital root tips (ECM and non-mycorrhizal) were determined with an isotope ratio mass spectrometer (IRMS, delta V Advantage; Thermo Fisher Scientific) coupled to an Elemental Analyzer (Euro EA; Eurovector).

Rates and $\delta^{13}\text{C}$ of stem CO_2 efflux were assessed approx. every 80 min at c. 1 m height on stems of six labeled ($n = 3$ per treatment, Figures 1a and 2) and six non-labeled trees as controls with custom-built stem chambers connected to an isotope ratio infrared spectrometer (IRIS, DeltaRay; Thermo Fisher Scientific), as described in detail by Hikino et al. (2022). Soil CO_2 efflux chambers (Li-8100; Li-Cor, Inc.) were installed at a 1 m distance from each measured tree ($n = 3$, Figures 1a and 2), connected to a Li-8150 (Li-Cor, Inc.) multiplexer and a second IRIS. Rates and $\delta^{13}\text{C}$ of soil CO_2 efflux were then recorded every 30 min (Table S2). $\delta^{13}\text{C}$ of the three soil chambers in the recovering plot was corrected for the physical back-diffusion of

soil air during watering (Andersen et al., 2010; Subke et al., 2009; Unger et al., 2010), using an additional chamber installed next to non-labeled trees in the same plot.

$\delta^{13}\text{C}$ and total organic C concentration of root exudate samples were analyzed with an isoTOC cube (Elementar).

2.5 | Calculation of total C sink activity

Below, cumulative sum of C sink activity during 28 days (in $\text{gC}_{\text{tree}}^{-1} 28\text{days}^{-1}$) after drought release was calculated for each C sink (Figure 2).

2.5.1 | Stem and branch growth

The total growth during the 2019 growing season (Y in kg tree^{-1}) was determined with an allometric function provided for Norway spruce by Forrester et al. (2017), using the diameter at breast height (DBH, d in cm, Table S1) as input parameter:

$$\text{For stem } \ln(Y) = -2.5027 + 2.3404 \cdot \ln(d) \quad (1)$$

$$\text{For branch } \ln(Y) = -3.3163 + 2.1983 \cdot \ln(d) \quad (2)$$

Because crown length was c. 1/3 of the total tree height (Table S1), 1/9 of the total stem growth was assigned to the upper

stem (from top to crown base) and the remaining 8/9 to the lower stem (from crown base to trunk base), assuming a conical shape of the stems.

The total annual growth in 2019 was then multiplied by the proportional growth (in %) during the 28 days after watering (ratio of the radial growth during 28 days to the total annual growth), determined by automatic point dendrometers (DR-type; Ecomatik) installed at 50% tree height (used for branch and upper stem) and breast height (used for lower stem, Figure 2; see Methods S1). The % C of samples was ascertained by IRMS measurement (same for coarse-root growth, fine-root growth, and ECM).

2.5.2 | Branch CO₂ efflux

Total branch and twig surface area was estimated for each tree (Table S3) using field data including length, number, and mean diameter of branches and twigs, separated into each needle class and sun/shade crowns. Based on earlier studies on spruce trees at the same site using a infrared gas analyser (Binos 4b; Emerson Process Management; Kuptz et al., 2011; Reiter, 2004), maintenance respiration rates (R_M), growth respiration rates (R_G), and total CO₂ efflux of branch CO₂ efflux (R_{branch}) were calculated as follows:

$$R_{\text{branch}} = R_M + R_G \quad (3)$$

$$R_M = R_{M10} \cdot Q_{10}^{\frac{T-10}{10}} \quad (4)$$

$$R_G = \frac{330 - \text{DOY}}{330 - 130} \cdot R_{G10\text{max}} \cdot Q_{10}^{\frac{T-10}{10}} \quad (5)$$

where R_{M10} represents the maintenance respiration rates at 10°C (0.13 μmol m⁻² s⁻¹ for sun branch, and 0.048 μmol m⁻² s⁻¹ for shade branch), $R_{G10\text{max}}$ the maximum growth respiration at 10°C (0.23 μmol m⁻² s⁻¹ for sun branch, and 0.12 μmol m⁻² s⁻¹ for shade branch), Q_{10} the temperature sensitivity (2.45 for both sun and shade branches), and T the temperature. Since rates of stem CO₂ efflux did not significantly differ between control and recovering trees, rates of branch CO₂ efflux were also assumed to be similar.

2.5.3 | Stem CO₂ efflux

Stem efflux rates of each tree (Figure S1a,b) were multiplied by the stem surface area (Table S3), which was calculated using DBH and tree height, assuming a conical shape of the stems. For stems above 6.5 m, efflux rates at the breast height were multiplied by 1.4 as previously assessed on spruce trees from the same site (Kuptz et al., 2011). The mean rates of stem CO₂ efflux of three measured control trees were used for the fourth control tree, which was not assessed in this study (Figure 1a).

2.5.4 | Coarse-root growth

Coarse roots were counted, and the length of one coarse root (root diameter ≥2 mm) per tree was measured on site after excavating. Using root wood density of 0.416 g cm⁻³ (Pretzsch et al., 2018), mean diameter, length, and ring width from 2019 based on coring, the total coarse-root growth in 2019 was determined, and subsequently multiplied by the proportional growth during the 28 days after watering, according to automatic dendrometers installed at one coarse root (diameter of 9.4 ± 1.1 cm) on each tree (Ecomatik, Figure 2) as described above for stem and branch growth.

2.5.5 | Fine-root growth and ECM

To avoid massive soil disturbance in the long-term plots, not more than one coarse-root per tree was excavated. Thus it was not possible to assign the ECM samples, non-mycorrhizal root tips, or root exudates unequivocally to a specific tree. Special care was taken to gain representative samples by avoiding clustered sampling spots and covering the whole area underneath the labeled spruce each sampling day. For this reason, the total C sink activity of fine-root growth, ECM, and root exudates was first extrapolated to the area occupied by spruce trees (Figure 1a). From coring within the plot, we knew that fine-roots of spruce were evenly spread in the spruce area. The total spruce tree C sink activity belowground was then assigned to individual trees according to the area occupied by each tree using a positive exponential relationship between DBH and root biomass (Table S1, spatial contribution belowground and area; Häberle et al., 2012).

The initial fine-root biomass (mg cm⁻³) was determined with fine roots taken from 10 soil cores (diameter of 1.4 cm) within the first 10 cm of the uppermost soil layers on day -7. Because the biomass values of the two labeled plots differed from all other sampled plots and the previous years, the average initial biomass of all control and recovery plots of the experimental site, which agrees to fine-root area values of Brunn et al. (2022) on the same site and year, was accounted for further calculations. To calculate the fine-root biomass at 10–30 cm depth and thus the total initial fine-root biomass from 0 to 30 cm soil depth (M_{FR30}), a root biomass ratio between upper (0–10 cm) and lower (10–30 cm) soil layer was used, measured in summer 2018 on the same plots (Table 2). The total fine-root gain in the spruce area (Table 2) was calculated:

$$\text{Fine root length growth rate} = \frac{\text{Root length growth}}{\text{Initial root length in mesh bag}} \quad (6)$$

where the initial root length on day -7 and root length growth was determined by image analysis of respective pre- and post-harvest mesh bag root pictures via ImageJ (version 1.53a; National Institute of Health). The biomass gain per soil volume (mg cm⁻³) was then calculated (Equation 7), assuming a constant fine-root diameter, corrected

TABLE 2 Fine-root (FR) biomass (BM) and its ratio between upper (0–10 cm depth, U) and lower (10–30 cm depth, L) soil layer in summer 2018 to calculate the initial BM and root growth in the lower layer in 2019: In control and recovery (previously drought-stressed) plots

	FR BM summer 2018 (mg cm ⁻³)	FR BM ratio U/L	M _{FR} (mg cm ⁻³)	M _{ECM} (mg cm ⁻³)	FR BM gain (g)	FR length growth rate
Control	1.1 (U)	2.0	1.0 (U)	0.3 (U)	1113	0.1±0.0
	0.6 (L)		0.5 (L)	0.1 (L)		
Recovery	0.6 (U)	1.3	0.9 (U)	0.1 (U)	5905	0.3±0.2
	0.5 (L)		0.7 (L)	0.1 (L)		

Note: Initial FR BM (M_{FR}) and ECM BM (M_{ECM}) display the BM before the watering. FR BM gain reflects the cumulative sum of growth within the plot of each treatment during 28 days after watering (total g biomass per treatment, i.e., sum of four trees for control and three trees for recovery plot). FR length growth rate represents the mean ratio of fine-root growth to initial length during 28 days after watering (calculated by Equation 6, given with SE).

by the average biomass gain on day -7 to exclude root growth between mesh bag placement and first harvest, and extrapolated to the soil volume of the plot at 0–30 cm depth.

$$\text{fine root biomass gain} = \text{fine root length growth rate} \times \text{dry mass per soil volume} \quad (7)$$

Helmisaari et al. (2009) found the most spruce fine roots in the upper soil layer and Zwetsloot and Bauerle (2021) reported no changes in vertical root distribution of the present spruce during drought compared with controls which support a sufficient coverage of our calculated fine-root biomass. For determination of fine-root biomass, we manually selected vital fine-roots based on the same morphologic criteria as for the fine-roots included in mesh bags, which was used to calculate root growth. Within the mesh bag roots, we found that 96% of the sampled fine-roots in control and 57% in recovering trees were colonized by ectomycorrhizal fungi. Assuming no significant change in ECM biomass on root tips during our 28 day study period, since full formation of ECM takes longer (Ineichen & Wiemken, 1992), the biomass of mycorrhized fine-roots (M_{FR-ECM}) at 0–30 cm depth was calculated based on the initial fine-root biomass at 0–30 cm (M_{FR30} , Table 2):

$$M_{FR-ECM} = \frac{M_{FR30}}{100} \times 96 \text{ (or 57)} \quad (8)$$

ECM biomass (M_{ECM}) was calculated based on the finding by Helmisaari et al. (2007, 2009), that ECM make up 28% of one spruce fine-root's biomass, determined under the same terms as in our study (mature spruce trees, root diameter <2 mm, most fine-roots found within 0–10 cm depth):

$$M_{ECM} = \frac{M_{FR-ECM}}{100} \times 28 \quad (9)$$

2.5.6 | Root exudates

The total root exudates C contribution was calculated for the soil at 0–30 cm depth using the organic C concentration in root exudates and the total fine-root biomass determined by soil cores.

2.5.7 | Soil CO₂ efflux

Soil efflux rates of each tree (Figure S1c,d) were multiplied by the area belowground occupied by each tree (Table S1). The mean rates of soil CO₂ efflux close to the three measured control trees were used for the fourth control tree, which was not assessed (Figure 1a). For the contribution of autotrophic respiration (root-derived including rhizosphere) to total soil respiration (autotrophic + heterotrophic), we used as value 51% in control and 38% in recovering trees based on previous measurements on spruce trees at the same site in July during 1 year with drought and 1 year without drought (Nikolova et al., 2009). We assumed that the contribution of autotrophic respiration did not significantly change after drought release, as soil CO₂ efflux rates under recovering trees remained unaffected by the drought release (Hikino et al., 2022).

2.6 | Calculation of fraction of labeled C (f_{Label}) and contribution of C_{new} to each C sink activity (contC_{new})

Fraction of labeled C (f_{Label}) was calculated at each measurement point using the following equation (Kuptz et al., 2011):

$$f_{Label} = \frac{\delta^{13}C_{old} - \delta^{13}C_{sample}}{\delta^{13}C_{old} - \delta^{13}C_{new}} \quad (10)$$

where $\delta^{13}C_{old}$ gives the mean $\delta^{13}C$ before the start of labeling, $\delta^{13}C_{sample}$ is the $\delta^{13}C$ of each measurement, and $\delta^{13}C_{new}$ represents $\delta^{13}C$ at the new isotopic equilibrium (Figure S2, for the calculation of $\delta^{13}C_{new}$ see Methods S2). Rarely occurring negative f_{Label} values were set to zero. f_{Label} of stem CO₂ efflux was used for branch CO₂ efflux, which was not assessed in this study.

contC_{new}, representing f_{Label} at the new isotopic equilibrium, was determined by fitting the course of f_{Label} with the following sigmoid curve (Figures S3 and S4).

$$f_{Label} = \frac{\text{cont C}_{new}}{1 + e^{-\frac{t-t_0}{b}}} \quad (11)$$

where t is the time of measurement, t_0 the inflection point of the curve, and b the slope coefficient of the regression. $\text{contC}_{\text{new}}$ would be one (100%) if C sink was supplied solely with C_{new} and zero (0%) if supplied exclusively by stored C. Since f_{Label} decreased again after the end of labeling, only f_{Label} before reaching the maximum were used for the fitting.

Similar to C sink activity, we pooled all samples of ECM, non-mycorrhizal root tips, and root exudates for the calculation of $\text{contC}_{\text{new}}$ for control and recovering trees. Thus, only one value was available for each treatment, so that a statistical test between treatments was not possible for these three C sinks. $\text{contC}_{\text{new}}$ to soil CO_2 efflux was divided by the contribution of autotrophic part to calculate the $\text{contC}_{\text{new}}$ to autotrophic soil CO_2 efflux.

2.6.1 | Methods used for branch, stem, and coarse-root growth

For branch, stem, and coarse-root growth, $\delta^{13}\text{C}_{\text{old}}$ and $\delta^{13}\text{C}_{\text{sample}}$ (for Equation 10) were determined by fitting the $\delta^{13}\text{C}$ of tree ring slices with a piecewise function (R package "segmented", version: 1.3-0) as described by Hikino et al. (2022; for details see Methods S3; Figure S5). The applied labeling with ^{13}C -depleted CO_2 caused a sudden and steep decrease of $\delta^{13}\text{C}$, after the ^{13}C -depleted tracer was incorporated into the tree ring. The $\delta^{13}\text{C}$ value at this point was determined with a piecewise function (marked by the green horizontal dashed lines in Figure S5a,b) and then defined as $\delta^{13}\text{C}_{\text{old}}$. After the steep decrease, $\delta^{13}\text{C}$ increased again as unlabeled C arrived after the end of labeling. The minimum $\delta^{13}\text{C}$ value at this point was determined with the same method (purple horizontal dashed lines) and defined as $\delta^{13}\text{C}_{\text{sample}}$. In addition to the labeled trees, we also determined the natural shifts of $\delta^{13}\text{C}$ of non-labeled control trees for each treatment ($n = 3$) to correct $\delta^{13}\text{C}_{\text{sample}}$ for the effect of watering, weather fluctuation, and seasonal changes (Helle & Schleser, 2004). Finally, using $\delta^{13}\text{C}_{\text{old}}$, corrected $\delta^{13}\text{C}_{\text{sample}}$, and Equation (10), f_{Label} was calculated.

For the course of f_{Label} (Figure S6), C transport rates determined by Hikino et al. (2022) were used to define the day on which the first ^{13}C -depleted tracer arrived at each tree height (i.e., when f_{Label} started to increase). A linear increase of f_{Label} was assumed until the new isotopic equilibrium was reached, that is $\text{contC}_{\text{new}}$. $\text{contC}_{\text{new}}$ calculated with the samples from the middle of the crown was used for branch and upper stem growth. For the lower stem growth, we used the mean $\text{contC}_{\text{new}}$ calculated for the crown base and breast height.

2.7 | Calculation of allocation of newly assimilated C (C_{new}) to each C sink

Total amount of C_{new} allocated to each C sink during 28 days after drought release was calculated as the cumulative sum of C_{new} after multiplying C sink activity and their respective f_{Label} .

As soon as f_{Label} started to decrease due to the end of labeling, sigmoid curves (Equation 11) or in the case of branch, stem, and coarse-root growth (Figure S6) a constant f_{Label} was used. For soil CO_2 efflux, total C sink activity (autotrophic + heterotrophic) was multiplied with respective f_{Label} , since C isotopic signatures and f_{Label} comprise the mixed signal of both autotrophic and heterotrophic efflux. Using the amount of C_{new} (in gC), proportional allocation of C_{new} (in %) to each sink was calculated for each tree.

2.8 | Statistical analysis

All data were analyzed using R (version 4.0.3) in R studio (version 1.3.1093). For the non-linear regression (Equation 11), nls function (package: stats, version: 4.0.3) was applied. The differences in C sink activity, $\text{contC}_{\text{new}}$, and allocation of C_{new} between control and recovering trees were tested with a t -test for each C sink. Beforehand, we tested the homogeneity of variances (F -test) and the normality of the data (Shapiro test). If these prerequisites were violated, data were either transformed (logarithms, square root, multiplicative inverse), or wilcox.test (package: stats, version: 4.0.3) was used. Proportional allocation of C_{new} was tested using a linear-mixed model (package: nlme, version: 3.1-151). We defined the treatment and above- and belowground sinks as fixed, and tree as a random effect. Beforehand, we tested the homogeneity of variances (Levene test) and the normality of the residuals (Shapiro test). If the fixed factor was significant, a post-hoc test with Tukey correction (package: lsmeans, version: 2.30-0) was performed. All results are given in $\text{mean} \pm \text{SE}$, unless otherwise noted.

3 | RESULTS

3.1 | Total C sink activity

We assessed the cumulative sum of C sink activity for each sink (in $\text{gCtree}^{-1} 28 \text{ days}^{-1}$, Figure 3) during the first 4 weeks after drought release. In aboveground sinks, the recovering trees had a significantly lower sink activity for branch CO_2 efflux with $558 \pm 86 \text{ gC}$ ($p < .01$, Figure 3) than control trees with $1205 \pm 131 \text{ gC}$. The activity of the other aboveground sinks was slightly but insignificantly lower in recovering trees compared with controls.

In belowground sinks of recovering trees, fine-root growth was the major C sink with $965 \pm 136 \text{ gC}$, which was seven times higher than that of control trees ($136 \pm 12 \text{ gC}$, $p < .001$). Sink activity of coarse roots and ECM was $126 \pm 48 \text{ gC}$, and $302 \pm 43 \text{ gC}$ in recovering trees, respectively, which was similar to controls with $98 \pm 43 \text{ gC}$ and $306 \pm 27 \text{ gC}$. Autotrophic soil CO_2 efflux under recovering trees was significantly lower with $649 \pm 123 \text{ gC}$ than under control trees with $1643 \pm 220 \text{ gC}$ ($p = .01$). Sink activity of root exudates tended to be higher under recovering trees than

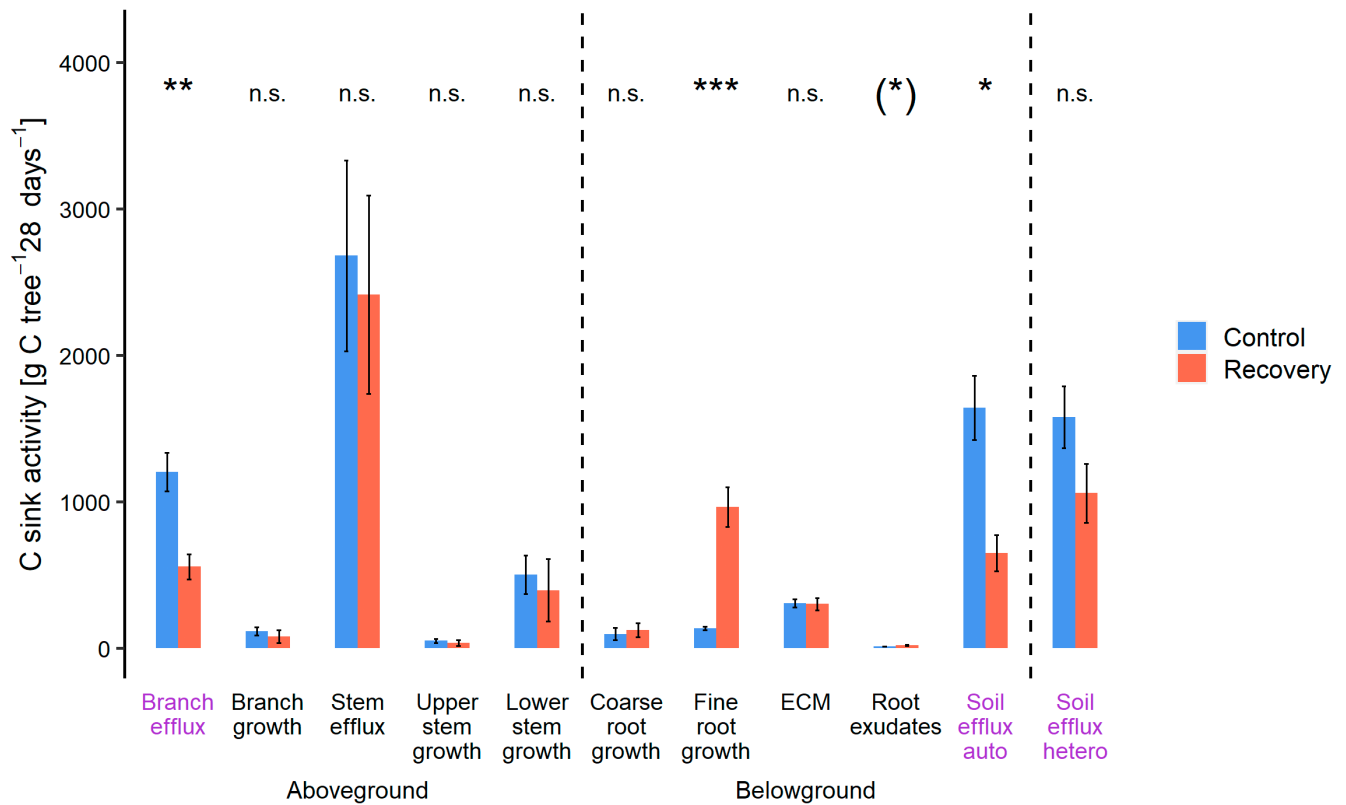


FIGURE 3 Total C sink activity (cumulative sum during 28 days after watering in $\text{g C tree}^{-1} 28 \text{ days}^{-1}$) in each above- and belowground sink in four control and three recovering (previously drought-stressed) trees (mean \pm SE): In branch CO_2 efflux, branch growth, stem CO_2 efflux, upper and lower stem growth, coarse-root growth, fine-root growth, ectomycorrhizae (ECM), root exudates, and soil CO_2 efflux (autotrophic and heterotrophic). C sinks which were (partly) not directly measured are marked with purple color. Asterisks indicate significant results based on t-tests comparing control and recovering trees, *** $p < .001$; ** $p < .01$; * $p < .05$; (*), $p < .1$; n.s., not significant.

controls ($p < .1$) although it was very small with $<20 \text{ g C}$ in both treatments.

3.2 | Allocation of newly assimilated C (C_{new})

We calculated the cumulative sum of C_{new} allocated to each sink (in $\text{g C tree}^{-1} 28 \text{ days}^{-1}$, Figure 4b) during the first 4 weeks after drought release, and the proportional allocation of C_{new} to the total C_{new} detected in the whole tree (in %, Figure 4a). At the whole-tree level, recovering trees tended to shift allocation towards belowground sinks (although not significant, $p = .14$, Figure 4a), that is, $60 \pm 7\%$ to aboveground and $40 \pm 7\%$ to belowground sinks, compared with control trees ($79 \pm 3\%$ aboveground and $21 \pm 3\%$ belowground).

Recovering trees tended to allocate less C_{new} to branch CO_2 efflux with $317 \pm 83 \text{ g}$ ($p = .07$), to branch growth with $19 \pm 13 \text{ g}$ ($p = .15$), and to upper stem growth with $8 \pm 6 \text{ g}$ ($p = .17$), compared with control trees with $766 \pm 145 \text{ g C}$, $52 \pm 15 \text{ g C}$, and $23 \pm 7 \text{ g C}$, respectively. Lower stem growth of recovering trees received $76 \pm 44 \text{ g}$ of C_{new} , which was similar to that of control trees with $66 \pm 6 \text{ g C}$. Allocation to stem CO_2 efflux in recovering trees ($1209 \pm 439 \text{ g C}$)

was slightly but insignificantly lower than that of control trees with $1557 \pm 474 \text{ g C}$. Looking at the proportional allocation (Figure 4a), branch efflux, branch growth, and upper stem growth of recovering trees received $13 \pm 0\%$, $<1 \pm 0\%$, and $<1 \pm 0\%$ of total C_{new} detected, which all tended to be lower than that of control trees with $26 \pm 2\%$, $2 \pm 0\%$, and $1 \pm 0\%$, respectively ($p < .1$). Proportional allocation to stem CO_2 efflux was also slightly but insignificantly lower in recovering ($44 \pm 6\%$) than in control trees ($48 \pm 5\%$).

Belowground, the most prominent difference between control and recovering trees was the allocation of C_{new} to growing fine-roots with $406 \pm 57 \text{ g C}$ in recovering and only $38 \pm 3 \text{ g C}$ in control trees ($p < .001$). This makes fine-root growth the major belowground sink for the allocation of C_{new} after drought release, representing $18 \pm 4\%$ of the total C_{new} detected in recovering trees ($1 \pm 0\%$ in control trees, $p < .001$). In coarse-root growth, a strong tendency of a higher allocation ($p < .1$) was detected in recovering trees ($20 \pm 8 \text{ g C}$ and proportional allocation of $1 \pm 0\%$) compared with controls ($4 \pm 3 \text{ g C}$ representing $<1 \pm 0\%$). Allocation to root exudates was also significantly higher ($p < .05$) in recovering trees with $17 \pm 2 \text{ g C}$ than in control controls with $7 \pm 1 \text{ g C}$ (but both $<1\%$). In contrast, there was no significant difference in ECM ($171 \pm 24 \text{ g C}$ and $8 \pm 2\%$ in recovering, $174 \pm 16 \text{ g C}$ and $6 \pm 1\%$ in control trees).

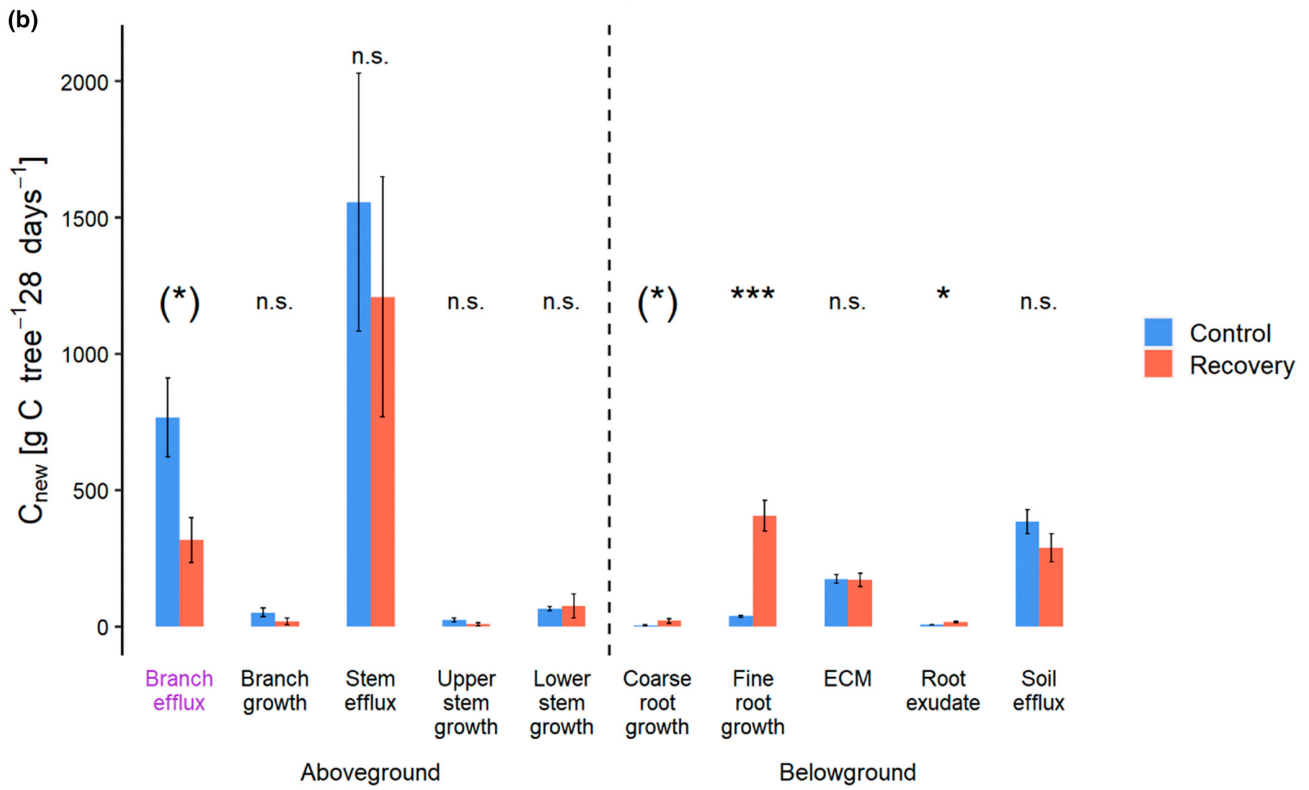
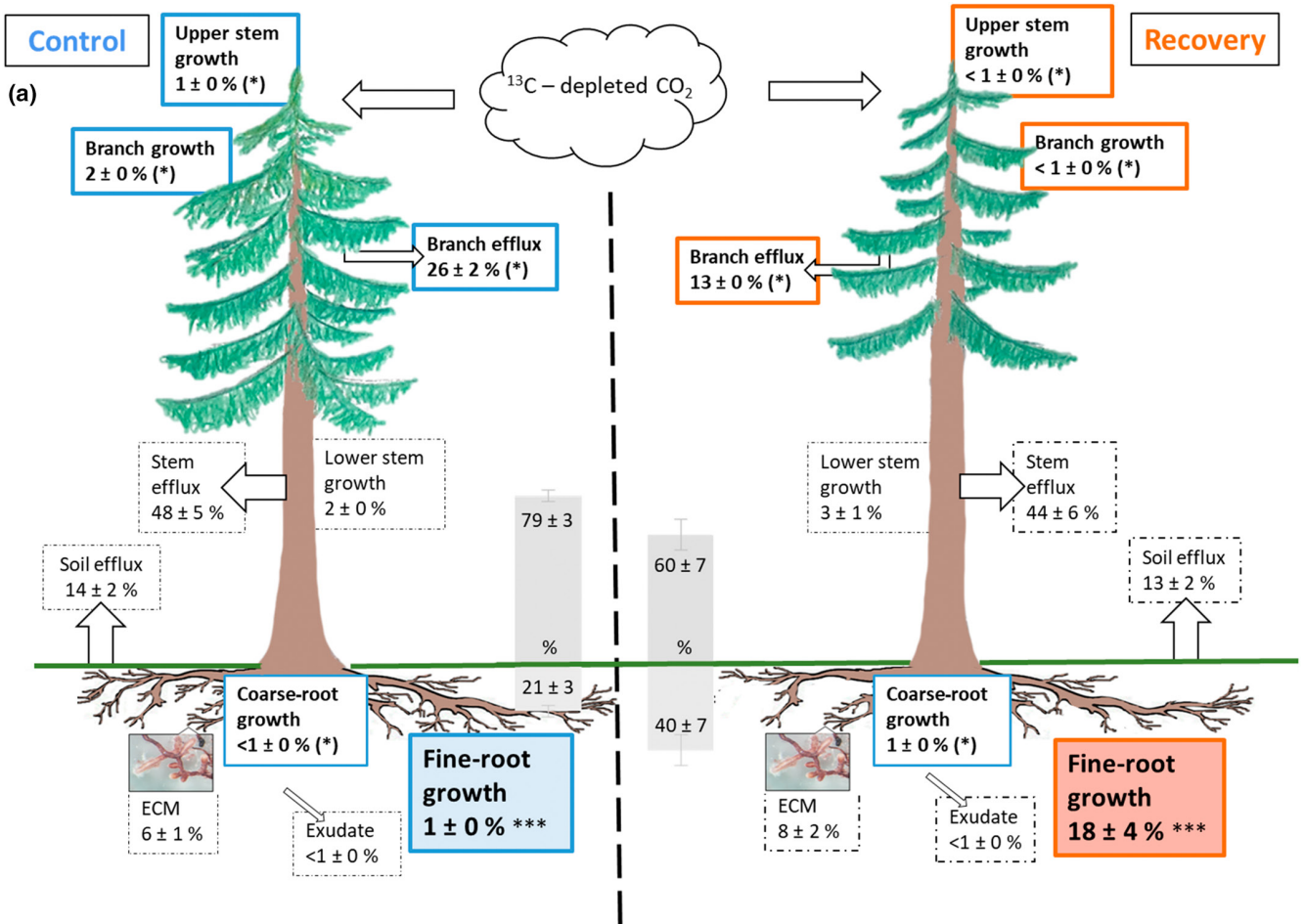
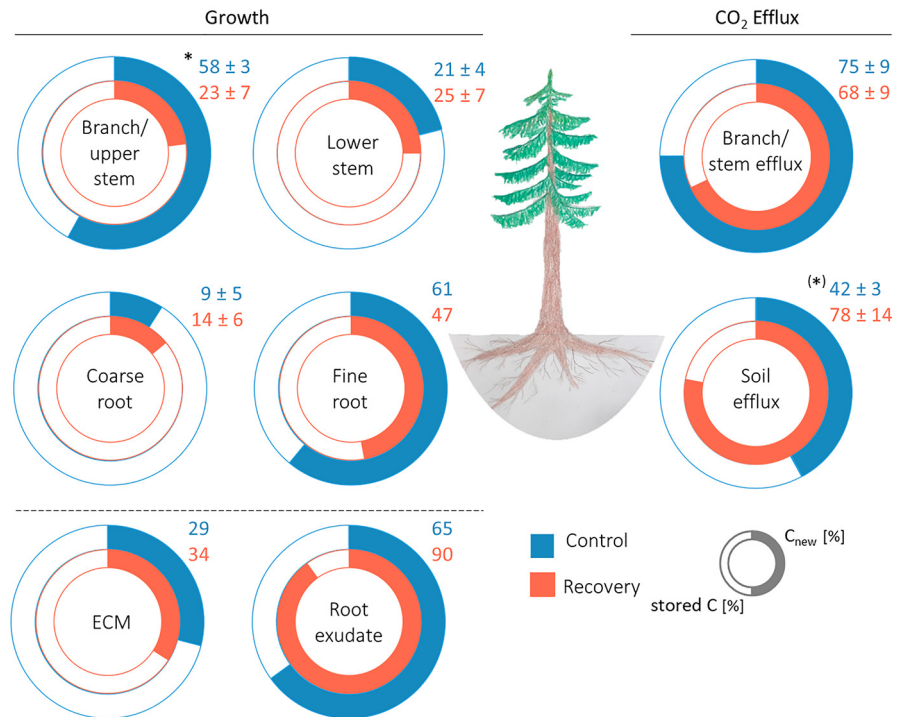


FIGURE 4 (a) Proportional allocation of newly assimilated C (C_{new}) to total C_{new} detected and (b) amount of C_{new} (cumulative sum during 28 days after watering in $\text{gC tree}^{-1} 28 \text{ days}^{-1}$) allocated to each above- and belowground sink in four control and three recovering (previously drought-stressed) trees, that is, branch CO_2 efflux, branch growth, stem CO_2 efflux, upper and lower stem growth, coarse-root growth, fine-root growth, ectomycorrhizae (ECM), root exudates, and autotrophic soil CO_2 efflux (mean \pm SE). C sinks which were not directly measured in this study are marked with purple color. Asterisks give the results of *t*-tests or linear-mixed model comparing control and recovering trees, *** $p < .001$; * $p < .05$; (*), $p < .1$; n.s., not significant.

FIGURE 5 Contribution of newly assimilated C (C_{new}) to each C sink activity at the new isotopic equilibrium ($\text{cont}C_{\text{new}}$ in %) in each above- and belowground C sink, that is, stem and branch CO_2 efflux, branch and upper stem growth, lower stem growth, coarse-root growth, fine-root growth, ectomycorrhizae (ECM), root exudates, and autotrophic soil CO_2 efflux, in control and recovering (previously drought-stressed) trees. Numbers next to the charts give means \pm SE of each treatment. Asterisk indicates a significant difference between control and recovering trees, * $p < .05$; (*), $p < .1$. For fine-root, ECM, and root exudate, there are no SE, since we pooled all samples for the calculation of $\text{cont}C_{\text{new}}$. Statistical tests for these three sinks were thus not possible.



Allocation to soil CO_2 efflux was slightly but insignificantly lower in recovering trees ($289 \pm 51 \text{ gC}$, $13 \pm 2\%$) compared with controls ($384 \pm 44 \text{ g}$, $14 \pm 2\%$).

3.3 | Contribution of C_{new} to each C sink activity ($\text{cont}C_{\text{new}}$)

$\text{cont}C_{\text{new}}$ represents the contribution (in %) of C_{new} to meet the C sink activity (Figure 5). Belowground sinks with high C sink activity tended to show low contribution of C_{new} .

In aboveground sinks, C_{new} contributed to $23 \pm 7\%$ of the C sink activity of upper stem and branch growth in recovering trees, which was significantly lower ($p = .02$) compared with controls with $58 \pm 3\%$. In other aboveground sinks of recovering trees, $\text{cont}C_{\text{new}}$ was similar between control and recovering trees.

In belowground sinks of recovering trees, C_{new} contributed to 47% of the fine-root growth, which was lower compared with control trees with 61%. In root exudates and autotrophic soil CO_2 efflux, $\text{cont}C_{\text{new}}$ tended to be higher in recovering trees with 90% and $78 \pm 14\%$ ($p = .08$), compared with controls with 65% and $42 \pm 3\%$. Remaining belowground sinks showed similar $\text{cont}C_{\text{new}}$ between control and recovering trees.

4 | DISCUSSION

The present study elucidates the C sink activity and the allocation of C_{new} and stored C in mature Norway spruce upon drought release after 5 years of experimental summer drought. The recovering trees increased C sink activity of fine-root growth upon drought release, while that of aboveground growth and CO_2 efflux tended to be less (Figure 3), confirming H1 that belowground sink activity would increase with a parallel decrease aboveground. The high belowground C sink activity was supported by a preferential C_{new} allocation to the root system (Figure 4a,b), with a parallel decrease of C_{new} allocation aboveground, which is in line with H2: preferential allocation C_{new} belowground at the expense of aboveground sinks. $\text{cont}C_{\text{new}}$ to fine-root growth was lower in recovering trees compared with controls (Figure 5), which was driven by the high belowground C sink activity in recovering trees, confirming H3 that contribution of C_{new} would be lower under high sink activity. As a result, the preferential allocation of C_{new} to fine-roots was not sufficient to meet the increased C sink activity of these growing roots.

The broad measurement data set used here allowed for scaling from the organ to whole-tree level. Although a broad overview is gained, some uncertainties remain, in particular estimates of branch CO_2 efflux and partitioning of soil CO_2 efflux into autotrophic and

heterotrophic processes due to the lack of direct measurements. However, these uncertainties do not change the main conclusions of this study that enhanced fine-root growth was supported by both, C_{new} and stored C. For example for soil CO_2 efflux, the contribution of autotrophic respiration in control trees may be significantly lower than assumed (e.g. as low as 5%, Muhr & Borken, 2009), which would even reinforce our conclusions that recovering trees increased belowground sink activity compared with controls. Moreover, the contribution of autotrophic respiration might have decreased after drought release (Schindlbacher et al., 2012), but overall it cannot be lower than $\text{cont}C_{\text{new}}$ to total soil CO_2 efflux, that is, around 20%–36%. Within these boundaries, significance of the results do not change.

4.1 | Preferential allocation of C_{new} to enhanced fine-root growth after drought release

In control trees, majority of the aboveground C demand was found in the respiratory sinks. Small C demand and allocation of C_{new} to the aboveground growth in the control trees might be explained by seasonal variations (Arneith et al., 1998; DeLucia et al., 2007), as only 15%–20% of the annual radial growth occurred during the study period (data not shown). Compared with control trees, Norway spruce recovering from drought tended to show lower aboveground C sink activity (Figure 3). Similarly, these recovering trees tended to allocate less C_{new} to aboveground growth and CO_2 efflux (Figure 4b), and had a lower proportional allocation of C_{new} to aboveground (Figure 4a). A comparable decreased allocation of C_{new} to aboveground organs during drought recovery has also been observed in saplings of other tree species (Galiano et al., 2017; Hagedorn et al., 2016). The lower allocation of C_{new} to aboveground sinks likely resulted from reduced C sink activity aboveground as branch and stem growth had significantly decreased during drought (Pretzsch et al., 2020; Tomasella et al., 2018) and remained lower compared with controls 4 weeks after drought release (Figure 3). Before watering in early July, predawn leaf water potential of the recovering trees was c. -0.9 MPa (Grams et al., 2021), which is much higher than the water potential of -4 MPa that could cause a 50% loss of branch xylem conductivity determined for the same trees (Tomasella et al., 2018). Therefore, aboveground repair processes, which would increase the amount of C used for CO_2 efflux (Bucci et al., 2003; Secchi & Zwieniecki, 2011; Trugman et al., 2018; Zang et al., 2014), were unlikely to have played a significant role in the recovery of these trees. This is further supported by rates of stem CO_2 efflux of recovering trees after drought release (Hikino et al., 2022) which were unaffected. Accordingly, smaller growth and the lack of repair processes, both explain the lower C sink activity of aboveground respiratory sinks in recovering trees compared with controls (Figure 3).

Belowground, we observed a seven times greater C sink activity of fine-root growth in recovering trees after drought release compared with controls (Figure 3), which was supported by the preferential allocation of C_{new} to roots (Figure 4a,b). A strong reduction

of fine-root growth was observed throughout the drought period (Nickel et al., 2018; Zwetsloot & Bauerle, 2021), corroborating the need to restore the essential functions of fine-roots for resource uptake (Bardgett et al., 2014; Germon et al., 2020; Solly et al., 2018). Thus, the faster transport of C_{new} to fine-root tips (Hikino et al., 2022) and the increased allocation of C_{new} both facilitated the fine-root growth upon drought release. C sink activity and the allocation of C_{new} to coarse-root growth also increased in recovering trees compared with controls (Figure 4a,b), likely supporting the increased fine-root growth and water transport (Zhang & Wang, 2015). Our findings are in agreement with Joseph et al. (2020) who reported that naturally drought-stressed mature pine trees invested more C_{new} into root biomass after rainfall compared with long-term irrigated trees, while the allocation of C_{new} to aboveground sinks was slightly lower. These findings support the optimal partitioning theory by Bloom et al. (1985) stating that plants allocate C to the organ which is responsible for the uptake of the limiting resource—in our case water, most likely along with dissolved nutrients (Gessler et al., 2017).

Ectomycorrhizae of recovering spruce trees showed a similar C sink activity (Figure 3) and similar allocation of C_{new} as control trees (Figure 4a,b). This is in contrast to young beech trees, which preferentially allocated newly assimilated C to ECM during recovery from drought (Hagedorn et al., 2016). Species-specific root traits particularly under and following drought most likely explain these contrasting C allocation patterns. Beech forms fine-roots with a short lifespan and sustains fine-root formation under drought (Nikolova et al., 2020; Zwetsloot & Bauerle, 2021). Beech ECMs, thus, need to be continuously formed resulting in fast C turnover and a high C sink activity of ECMs immediately after drought release (Hagedorn et al., 2016). In contrast, spruce trees with long-lived fine-roots and slow C turnover, show a temporal dormancy during drought by suberization and reduced growth to prevent resource loss (Nikolova et al., 2020). Our findings on unaffected C allocation to vital ECM on trees that experienced long-term drought are in accordance with previous results on sustained functionality of the ectomycorrhizal symbiosis under drought (Fuchslueger et al., 2014; Nickel et al., 2018). In addition, the lack of an increased C allocation to ECM may reflect an asynchrony between fast fine-root growth after watering with the supply of C_{new} from day 7 on (Hikino et al., 2022) and slower ECM formation (duration around 4 weeks, Ineichen & Wiemken, 1992) on newly grown roots. Therefore, we suggest that C allocation in newly formed ECM peaked later in spruce and was not captured during this 4-week study period.

Root exudation was a negligible C sink with less than 1% of total C sink activity (Figure 3) and of C_{new} (Figure 4a), thus similar to Mediterranean conifer saplings (Rog et al., 2021), but somewhat lower than in other natural forest stands with 2%–6% of total C_{new} (Abramoff & Finzi, 2016; Gougherty et al., 2018) and saplings with up to 30% of total C_{new} (Liese et al., 2018). Allocation of C_{new} to root exudates, which was already small during the drought period (approx. 1%–2%, Brunn et al., 2022), remained small after drought release. Furthermore, allocation in the recovering trees tended to be

higher than in the controls, which is consistent with findings during the drought phase (Brunn et al., 2022).

The increased C sink activity and allocation of C_{new} to root growth in the recovering trees was not reflected in soil CO_2 efflux, that is, lower soil CO_2 efflux rates (Figure 3) and lower allocation of C_{new} to autotrophic soil CO_2 efflux compared with control trees even after drought release (Figure 4a,b), despite the similar soil water content between treatments after drought release (Grams et al., 2021). Sun et al. (2020) state that maintenance respiration of spruce fine-roots accounts for 70% of the total respiration (maintenance and growth). Due to increased suberization during drought (Nikolova et al., 2020; Zwetsloot & Bauerle, 2021), root maintenance respiration was likely decreased (Barnard & Jorgensen, 1977). This reduction cannot be compensated by increased root-growth, which only accounts for 30% of the initial fine-root biomass (Table 2, fine-root length growth rate). This result also suggests that soil microbial activity, which was potentially reduced during drought (Nikolova et al., 2009), did not increase immediately after drought release as observed in other Norway spruce forests (Muhr & Borken, 2009; Schindlbacher et al., 2012). During repeated drought, the microbial communities might have adapted to drought conditions leading to a higher C use efficiency and thus reduces respiration with the number of repetitive droughts (Canarini et al., 2021; de Nijs et al., 2019; Evans & Wallenstein, 2012). Therefore, in contrast to previous studies on young beech and slow-growing, mature pine trees (Gao et al., 2021; Hagedorn et al., 2016; Joseph et al., 2020), we assume that microbial biomass did not receive an enhanced amount of C_{new} after drought release, which is supported by the low allocation of C_{new} to root exudates.

4.2 | Use of the stored C is essential for fine-root growth during recovery

Despite the preferential allocation of C_{new} to fine-root recovery, less than half of the increased fine-root growth in recovering trees was supported by C_{new} (Figure 5), which was lower than in control trees (61%) and what had been reported for other species (c. 75%; Lynch et al., 2013; Matamala et al., 2003). This suggests that the relative contribution of C_{new} decreases with high C sink activity belowground, which was also observed in autotrophic soil CO_2 efflux of controls (Figures 3 and 5). Likewise for coarse-root growth, around 86% of the present C was comprised of stored C (Figure 5), indicating the importance of stored C for root growth during drought recovery. Increased suberization and reduced respiration of fine-roots in recovery plots during drought (Nikolova et al., 2020; Zwetsloot & Bauerle, 2021) was accompanied by twice the starch concentration stored in these fine-roots before watering compared with the controls (data not shown). Reduction of these starch concentrations to the level of control trees within the first 7 days after watering indicates that they were most likely used for initial fine-root growth after drought release, which is similar to observations by Yang et al. (2016) in Chinese fir saplings.

Lack of complete depletion might indicate an existence of regulation mechanism through enzymes degrading starch (Tsamir-Rimon et al., 2021). Furthermore, in addition to the starch conversion, reversal of osmotic potential in leaves (Hikino et al., 2022) and also in other organs likely released large amounts of osmolytes during first 4 weeks after watering, which became available for other C sinks (Tsamir-Rimon et al., 2021). Indeed, a reduced $\text{cont}C_{\text{new}}$ allocated to branches and upper stem growth in the recovering trees compared with controls might indicate a direct incorporation of C derived from the released osmolytes to sinks in the crowns, allowing C_{new} to bypass towards belowground sinks. C storage pools of the spruce trees (in leaves, branches, stem, and roots) had significantly decreased during the drought period (Hesse et al., 2021), and thus remobilized C from osmolytes also likely played a significant role as a C source.

5 | CONCLUSION

Restoring water uptake is crucial for long-term drought recovery of whole-tree functionality and preparation for upcoming drought periods. Following drought release, we found recovering spruce trees prioritized root growth by preferential allocation of new photoassimilates (i.e., C_{new}). The high belowground C sink activity was not entirely met by C_{new} and was largely subsidized by stored C. This highlights the role of both, the availability of C stores and the allocation of new photoassimilates to support repair and regrowth of functional tissues. It remains an open question whether (and how) the belowground C sink activity can be met over longer periods, even years, following drought release. Our findings also highlight the importance of belowground C sinks for analyses of post-drought growth increment and C stores of trees. If the altered C allocation towards belowground sinks persists in the following growing seasons, the drought effect on stem growth may remain for years. Thus, long-term observation of above- and belowground biomass partitioning is necessary to elucidate the longstanding consequences of altered C allocation upon drought release for forest productivity and C storage dynamics.

AUTHOR CONTRIBUTIONS

Thorsten E. E. Grams and Karin Pritsch originally designed the experiment. Kyohsuke Hikino, Vincent P. Riedel, and Thorsten E. E. Grams prepared and performed the ^{13}C labeling. Kyohsuke Hikino, Jasmin Danzberger, Vincent P. Riedel, Benjamin D. Hesse, Benjamin D. Hafner, Timo Gebhardt, Romy Rehschuh, Nadine K. Ruehr, Melanie Brunn, Simon M. Landhäusser, Marco M. Lehmann, Thomas Rötzer, Franz Buegger, Fabian Weikl, Karin Pritsch, and Thorsten E. E. Grams collected and processed the samples/data. Kyohsuke Hikino and Jasmin Danzberger finalized the experimental design, analyzed and interpreted the data with supports from Thorsten E. E. Grams, Karin Pritsch, Benjamin D. Hesse, Benjamin D. Hafner, Franz Buegger, Fabian Weikl, Romy Rehschuh, Nadine K. Ruehr, Simon M. Landhäusser, Marco M. Lehmann, Timo Gebhardt, Thomas Rötzer,

Hans Pretzsch, and Taryn L. Bauerle. Kyohsuke Hikino and Jasmin Danzberger wrote the manuscript and all authors revised and edited the manuscript. Kyohsuke Hikino and Jasmin Danzberger contributed equally.

ACKNOWLEDGMENTS

We would like to thank Thomas Feuerbach who set up and maintained the labeling and measurement equipment. We also appreciate supports during the fieldworks by Karl-Heinz Häberle, Josef Heckmair, Peter Kuba, bachelor/master students (TUM), Laura Pohlenz, Ramona Werner, and ecology volunteers (Helmholtz-Zentrum München). We also thank Pak S. Chow (UAlberta) for sample processing, Florian Motte (TUM) for providing data of diameter at breast height and for support during sampling of coarse-roots, Patrick Wordell-Dietrich (TU Dresden) for support in $\delta^{13}\text{C}$ -analysis of root exudates, and Timo Knüver (KIT) for his support with the soil CO_2 efflux unit. This study was funded by the German Research Foundation (DFG) through grants GR 1881/5-1, MA1763/10-1, PR555/2-1, PR292/22-1 and by the Bavarian State Ministries of the Environment and Consumer Protection as well as Food, Agriculture and Forestry (W047/Kroof II). RR and NKR were supported by the German Research Foundation through its Emmy Noether Program (RU1657/2-1). MML was supported by the Ambizione grant (No. 179978) from the Swiss National Science Foundation (SNSF). BDHe was funded by a doctoral scholarship from the German Federal Environmental Foundation (DBU, AZ 20018/535). Open Access funding enabled and organized by Projekt DEAL.

CONFLICT OF INTEREST

The authors declare that there is no conflict of interest.

DATA AVAILABILITY STATEMENT

The data that support the findings of this study are openly available in mediaTUM (doi: [10.14459/2022mp1663853](https://doi.org/10.14459/2022mp1663853)).

ORCID

Kyohsuke Hikino  <https://orcid.org/0000-0002-6981-3988>
 Jasmin Danzberger  <https://orcid.org/0000-0002-1683-7345>
 Vincent P. Riedel  <https://orcid.org/0000-0003-1685-8135>
 Benjamin D. Hesse  <https://orcid.org/0000-0003-1113-9801>
 Benjamin D. Hafner  <https://orcid.org/0000-0003-2348-9200>
 Romy Rehschuh  <https://orcid.org/0000-0001-9140-0306>
 Nadine K. Ruehr  <https://orcid.org/0000-0001-5989-7463>
 Melanie Brunn  <https://orcid.org/0000-0002-5692-8575>
 Taryn L. Bauerle  <https://orcid.org/0000-0003-2741-2593>
 Simon M. Landhäusser  <https://orcid.org/0000-0002-4466-1607>
 Marco M. Lehmann  <https://orcid.org/0000-0003-2962-3351>
 Thomas Rötzer  <https://orcid.org/0000-0003-3780-7206>
 Hans Pretzsch  <https://orcid.org/0000-0002-4958-1868>
 Franz Buegger  <https://orcid.org/0000-0003-3526-4711>
 Fabian Weikl  <https://orcid.org/0000-0003-3973-6341>
 Karin Pritsch  <https://orcid.org/0000-0001-6384-2473>
 Thorsten E. E. Grams  <https://orcid.org/0000-0002-4355-8827>

REFERENCES

- Abramoff, R. Z., & Finzi, A. C. (2016). Seasonality and partitioning of root allocation to rhizosphere soils in a midlatitude forest. *Ecosphere*, 7(11), e01546. <https://doi.org/10.1002/ecs2.1547>
- Allen, C. D., Macalady, A. K., Chenchouni, H., Bachelet, D., McDowell, N. G., Vennetier, M., Kitzberger, T., Rigling, A., Breshears, D. D., Hogg, E. H., Gonzalez, P., Fensham, R., Zhang, Z., Castro, J., Demidova, N., Lim, J.-H., Allard, G., Running, S. W., Semerci, A., & Cobb, N. (2010). A global overview of drought and heat-induced tree mortality reveals emerging climate change risks for forests. *Forest Ecology and Management*, 259(4), 660–684. <https://doi.org/10.1016/j.foreco.2009.09.001>
- Andersen, C. P., Ritter, W., Gregg, J., Matyssek, R., & Grams, T. E. E. (2010). Below-ground carbon allocation in mature beech and spruce trees following long-term, experimentally enhanced O_3 exposure in southern Germany. *Environmental Pollution*, 158(8), 2604–2609. <https://doi.org/10.1016/j.envpol.2010.05.008>
- Arneth, A., Kelliher, F. M., McSeveny, T. M., & Byers, J. N. (1998). Net ecosystem productivity, net primary productivity and ecosystem carbon sequestration in a *Pinus radiata* plantation subject to soil water deficit. *Tree Physiology*, 18(12), 785–793. <https://doi.org/10.1093/treephys/18.12.785>
- Bardgett, R. D., Mommer, L., & de Vries, F. T. (2014). Going underground: Root traits as drivers of ecosystem processes. *Trends in Ecology & Evolution*, 29(12), 692–699. <https://doi.org/10.1016/j.tree.2014.10.006>
- Barnard, E. L., & Jorgensen, J. R. (1977). Respiration of field-grown loblolly pine roots as influenced by temperature and root type. *Canadian Journal of Botany*, 55(6), 740–743. <https://doi.org/10.1139/b77-088>
- Blessing, C. H., Werner, R. A., Siegwolf, R., & Buchmann, N. (2015). Allocation dynamics of recently fixed carbon in beech saplings in response to increased temperatures and drought. *Tree Physiology*, 35(6), 585–598. <https://doi.org/10.1093/treephys/tpv024>
- Bloom, A. J., Chapin, F. S., & Mooney, H. A. (1985). Resource limitation in plants—an economic analogy. *Annual Review of Ecology and Systematics*, 16(1), 363–392. <https://doi.org/10.1146/annurev.es.16.110185.002051>
- Bonan, G. B. (2008). Forests and climate change: Forcings, feedbacks, and the climate benefits of forests. *Science (New York, N.Y.)*, 320(5882), 1444–1449. <https://doi.org/10.1126/science.1155121>
- Brodersen, C. R., & McElrone, A. J. (2013). Maintenance of xylem network transport capacity: A review of embolism repair in vascular plants. *Frontiers in Plant Science*, 4, 108. <https://doi.org/10.3389/fpls.2013.00108>
- Brüggemann, N., Gessler, A., Kayler, Z., Keel, S. G., Badeck, F., Barthel, M., Boeckx, P., Buchmann, N., Brugnoli, E., Esperschütz, J., Gavrichkova, O., Ghashghaie, J., Gomez-Casanovas, N., Keitel, C., Knohl, A., Kuptz, D., Palacio, S., Salmon, Y., Uchida, Y., & Bahn, M. (2011). Carbon allocation and carbon isotope fluxes in the plant-soil-atmosphere continuum: A review. *Biogeosciences*, 8(11), 3457–3489. <https://doi.org/10.5194/bg-8-3457-2011>
- Brunn, M., Hafner, B. D., Zwetsloot, M. J., Weikl, F., Pritsch, K., Hikino, K., Ruehr, N. K., Sayer, E. J., & Bauerle, T. L. (2022). Carbon allocation to root exudates is maintained in mature temperate tree species under drought. *New Phytologist*, 235, 965–977. <https://doi.org/10.1111/nph.18157>
- Brunner, I., Herzog, C., Galiano, L., & Gessler, A. (2019). Plasticity of fine-root traits under long-term irrigation of a water-limited scots pine forest. *Frontiers in Plant Science*, 10, 701. <https://doi.org/10.3389/fpls.2019.00701>
- Bucci, S. J., Scholz, F. G., Goldstein, G., Meinzer, F. C., & Sternberg, L. D. S. L. (2003). Dynamic changes in hydraulic conductivity in petioles of two savanna tree species: Factors and mechanisms contributing to the refilling of embolized vessels. *Plant, Cell & Environment*, 26(10), 1633–1645. <https://doi.org/10.1046/j.0140-7791.2003.01082.x>

- Canarini, A., Schmidt, H., Fuchslueger, L., Martin, V., Herbold, C. W., Zezula, D., Gündler, P., Hasibeder, R., Jecmenica, M., Bahn, M., & Richter, A. (2021). Ecological memory of recurrent drought modifies soil processes via changes in soil microbial community. *Nature Communications*, 12(1), 5308. <https://doi.org/10.1038/s41467-021-25675-4>
- Chuste, P.-A., Maillard, P., Bréda, N., Levillain, J., Thirion, E., Wortemann, R., & Massonnet, C. (2020). Sacrificing growth and maintaining a dynamic carbohydrate storage are key processes for promoting beech survival under prolonged drought conditions. *Trees*, 34(2), 381–394. <https://doi.org/10.1007/s00468-019-01923-5>
- de Nijs, E. A., Hicks, L. C., Leizeaga, A., Tietema, A., & Rousk, J. (2019). Soil microbial moisture dependences and responses to drying–rewetting: The legacy of 18 years drought. *Global Change Biology*, 25(3), 1005–1015. <https://doi.org/10.1111/gcb.14508>
- DeLucia, E. H., Drake, J. E., Thomas, R. B., & Gonzalez-Meler, M. (2007). Forest carbon use efficiency: Is respiration a constant fraction of gross primary production? *Global Change Biology*, 13(6), 1157–1167. <https://doi.org/10.1111/j.1365-2486.2007.01365.x>
- Evans, S. E., & Wallenstein, M. D. (2012). Soil microbial community response to drying and rewetting stress: Does historical precipitation regime matter? *Biogeochemistry*, 109(1–3), 101–116. <https://doi.org/10.1007/s10533-011-9638-3>
- Forrester, D. I., Tachauer, I., Annighoefer, P., Barbeito, I., Pretzsch, H., Ruiz-Peinado, R., Stark, H., Vacchiano, G., Zlatanov, T., Chakraborty, T., Saha, S., & Sileshi, G. W. (2017). Generalized biomass and leaf area allometric equations for European tree species incorporating stand structure, tree age and climate. *Forest Ecology and Management*, 396, 160–175. <https://doi.org/10.1016/j.foreco.2017.04.011>
- Fuchslueger, L., Bahn, M., Fritz, K., Hasibeder, R., & Richter, A. (2014). Experimental drought reduces the transfer of recently fixed plant carbon to soil microbes and alters the bacterial community composition in a mountain meadow. *The New Phytologist*, 201(3), 916–927. <https://doi.org/10.1111/nph.12569>
- Galiano, L., Timofeeva, G., Saurer, M., Siegwolf, R., Martínez-Vilalta, J., Hommel, R., & Gessler, A. (2017). The fate of recently fixed carbon after drought release: Towards unravelling C storage regulation in *Tilia platyphyllos* and *Pinus sylvestris*. *Plant, Cell & Environment*, 40(9), 1711–1724. <https://doi.org/10.1111/pce.12972>
- Gao, D., Joseph, J., Werner, R. A., Brunner, I., Zürcher, A., Hug, C., Wang, A., Zhao, C., Bai, E., Meusburger, K., Gessler, A., & Hagedorn, F. (2021). Drought alters the carbon footprint of trees in soils—tracking the spatio-temporal fate of ¹³C-labelled assimilates in the soil of an old-growth pine forest. *Global Change Biology*, 27, 2491–2506. <https://doi.org/10.1111/gcb.15557>
- Gaul, D., Hertel, D., Borken, W., Matzner, E., & Leuschner, C. (2008). Effects of experimental drought on the fine root system of mature Norway spruce. *Forest Ecology and Management*, 256(5), 1151–1159. <https://doi.org/10.1016/j.foreco.2008.06.016>
- Germon, A., Laclau, J.-P., Robin, A., & Jourdan, C. (2020). Tamm review: Deep fine roots in forest ecosystems: Why dig deeper? *Forest Ecology and Management*, 466, 118135. <https://doi.org/10.1016/j.foreco.2020.118135>
- Gessler, A., Schaub, M., & McDowell, N. G. (2017). The role of nutrients in drought-induced tree mortality and recovery. *New Phytologist*, 214(2), 513–520. <https://doi.org/10.1111/nph.14340>
- Gougherty, S. W., Bauer, J. E., & Pohlman, J. W. (2018). Exudation rates and $\delta^{13}\text{C}$ signatures of tree root soluble organic carbon in a riparian forest. *Biogeochemistry*, 137(1–2), 235–252. <https://doi.org/10.1007/s10533-017-0415-9>
- Grams, T. E. E., Hesse, B. D., Gebhardt, T., Weikl, F., Rötzer, T., Kovacs, B., Hikino, K., Hafner, B. D., Brunn, M., Bauerle, T. L., Häberle, K.-H., Pretzsch, H., & Pritsch, K. (2021). The Kroof experiment: Realization and efficacy of a recurrent drought experiment plus recovery in a beech/spruce forest. *Ecosphere*, 12(3), e03399. <https://doi.org/10.1002/ecs2.3399>
- Häberle, K.-H., Weigt, R., Nikolova, P. S., Reiter, I. M., Cermak, J., Wieser, G., Blaschke, H., Rötzer, T., Pretzsch, H., & Matyssek, R. (2012). Case study “Kranzberger Forst”: Growth and defence in European beech (*Fagus sylvatica* L.) and Norway spruce (*Picea abies* [L.] Karst.). In R. Matyssek, H. Schnyder, W. Oßwald, D. Ernst, J. C. Munch, & H. Pretzsch (Eds.), *Ecological studies. Growth and defence in plants* (Vol. 220, pp. 243–271). Springer. https://doi.org/10.1007/978-3-642-30645-7_11
- Hagedorn, F., Joseph, J., Peter, M., Luster, J., Pritsch, K., Geppert, U., Kerner, R., Molinier, V., Egli, S., Schaub, M., Liu, J.-F., Li, M., Sever, K., Weiler, M., Siegwolf, R. T. W., Gessler, A., & Arend, M. (2016). Recovery of trees from drought depends on belowground sink control. *Nature Plants*, 2, 16111. <https://doi.org/10.1038/NPLANTS.2016.111>
- Hart, A. T., Merlin, M., Wiley, E., & Landhäuser, S. M. (2021). Splitting the difference: Heterogeneous soil moisture availability affects aboveground and belowground reserve and mass allocation in trembling Aspen. *Frontiers in Plant Science*, 12, 654159. <https://doi.org/10.3389/fpls.2021.654159>
- Hartmann, H., Bahn, M., Carbone, M., & Richardson, A. D. (2020). Plant carbon allocation in a changing world – Challenges and progress: Introduction to a virtual issue on carbon allocation: Introduction to a virtual issue on carbon allocation. *The New Phytologist*, 227(4), 981–988. <https://doi.org/10.1111/nph.16757>
- Hartmann, H., Moura, C. F., Anderegg, W. R. L., Ruehr, N. K., Salmon, Y., Allen, C. D., Arndt, S. K., Breshears, D. D., Davi, H., Galbraith, D., Ruthrof, K. X., Wunder, J., Adams, H. D., Bloemen, J., Cailleret, M., Cobb, R., Gessler, A., Grams, T. E. E., Jansen, S., ... O'Brien, M. (2018). Research frontiers for improving our understanding of drought-induced tree and forest mortality. *The New Phytologist*, 218(1), 15–28. <https://doi.org/10.1111/nph.15048>
- Helle, G., & Schleser, G. H. (2004). Beyond CO₂-fixation by rubisco - An interpretation of ¹³C/¹²C variations in tree rings from novel intra-seasonal studies on broad-leaf trees. *Plant, Cell & Environment*, 27(3), 367–380. <https://doi.org/10.1111/j.0016-8025.2003.01159.x>
- Helmisaari, H.-S., Derome, J., Nöjd, P., & Kukkola, M. (2007). Fine root biomass in relation to site and stand characteristics in Norway spruce and scots pine stands. *Tree Physiology*, 27(10), 1493–1504. <https://doi.org/10.1093/treephys/27.10.1493>
- Helmisaari, H.-S., Ostonen, I., Löhmus, K., Derome, J., Lindroos, A.-J., Merilä, P., & Nöjd, P. (2009). Ectomycorrhizal root tips in relation to site and stand characteristics in Norway spruce and scots pine stands in boreal forests. *Tree Physiology*, 29(3), 445–456. <https://doi.org/10.1093/treephys/tpn042>
- Hesse, B. D., Hartmann, H., Rötzer, T., Landhäuser, S. M., Goisser, M., Weikl, F., Pritsch, K., & Grams, T. E. (2021). Mature beech and spruce trees under drought – Higher C investment in reproduction at the expense of whole-tree NCS stores. *Environmental and Experimental Botany*, 191, 104615. <https://doi.org/10.1016/j.envexpbot.2021.104615>
- Hikino, K., Danzberger, J., Riedel, V. P., Rehschuh, R., Ruehr, N. K., Hesse, B. D., Lehmann, M. M., Buegger, F., Weikl, F., Pritsch, K., & Grams, T. E. E. (2022). High resilience of carbon transport in long-term drought stressed mature Norway spruce trees within two weeks after drought release. *Global Change Biology*, 28, 2095–2110. <https://doi.org/10.1111/gcb.16051>
- Hommel, R., Siegwolf, R., Zavadlav, S., Arend, M., Schaub, M., Galiano, L., Haeni, M., Kayler, Z. E., & Gessler, A. (2016). Impact of interspecific competition and drought on the allocation of new assimilates in trees. *Plant Biology (Stuttgart, Germany)*, 18(5), 785–796. <https://doi.org/10.1111/plb.12461>
- Ineichen, K., & Wiemken, V. (1992). Changes in the fungus-specific, soluble-carbohydrate pool during rapid and synchronous ectomycorrhiza formation of *Picea abies* with *Pisolithus tinctorius*. *Mycorrhiza*, 2(1), 1–7. <https://doi.org/10.1007/BF00206277>
- IPCC. (2021). Summary for policymakers. In V. Masson-Delmotte, P. Zhai, A. Pirani, S. L. Connors, C. Péan, S. Berger, N. Caud, Y. Chen,

- L. Goldfarb, M. I. Gomis, M. Huang, K. Leitzell, E. Lonnoy, J. B. R. Matthews, T. K. Maycock, T. Waterfield, O. Yelekçi, R. Yu, & B. Zhou (Eds.), *Climate change 2021: The physical science basis. Contribution of working group I to the sixth assessment report of the intergovernmental panel on climate change* (pp. 3–32). Cambridge University Press. <https://doi.org/10.1017/9781009157896.001>
- Joseph, J., Gao, D., Backes, B., Bloch, C., Brunner, I., Gleixner, G., Haeni, M., Hartmann, H., Hoch, G., Hug, C., Kahmen, A., Lehmann, M. M., Li, M.-H., Luster, J., Peter, M., Poll, C., Rigling, A., Rissanen, K. A., Ruehr, N. K., ... Gessler, A. (2020). Rhizosphere activity in an old-growth forest reacts rapidly to changes in soil moisture and shapes whole-tree carbon allocation. *Proceedings of the National Academy of Sciences of the United States of America*, 117(40), 24885–24892. <https://doi.org/10.1073/pnas.2014084117>
- Kuptz, D., Fleischmann, F., Matyssek, R., & Grams, T. E. E. (2011). Seasonal patterns of carbon allocation to respiratory pools in 60-yr-old deciduous (*Fagus sylvatica*) and evergreen (*Picea abies*) trees assessed via whole-tree stable carbon isotope labeling. *The New Phytologist*, 191(1), 160–172. <https://doi.org/10.1111/j.1469-8137.2011.03676.x>
- Lal, R., Smith, P., Jungkunst, H. F., Mitsch, W. J., Lehmann, J., Nair, P. R., McBratney, A. B., de Moraes Sá, J. C., Schneider, J., Zinn, Y. L., Skorupa, A. L., Zhang, H.-L., Minasny, B., Srinivasrao, C., & Ravindranath, N. H. (2018). The carbon sequestration potential of terrestrial ecosystems. *Journal of Soil and Water Conservation*, 73(6), 145A–152A. <https://doi.org/10.2489/jswc.73.6.145A>
- Liese, R., Lübke, T., Albers, N. W., & Meier, I. C. (2018). The mycorrhizal type governs root exudation and nitrogen uptake of temperate tree species. *Tree Physiology*, 38(1), 83–95. <https://doi.org/10.1093/treephys/tpx131>
- Lynch, D. J., Matamala, R., Iversen, C. M., Norby, R. J., & González-Meler, M. A. (2013). Stored carbon partly fuels fine-root respiration but is not used for production of new fine roots. *The New Phytologist*, 199(2), 420–430. <https://doi.org/10.1111/nph.12290>
- Matamala, R., González-Meler, M. A., Jastrow, J. D., Norby, R. J., & Schlesinger, W. H. (2003). Impacts of fine root turnover on forest NPP and soil C sequestration potential. *Science (New York, N.Y.)*, 302(5649), 1385–1387. <https://doi.org/10.1126/science.1089543>
- Meier, I. C., & Leuschner, C. (2008). Belowground drought response of European beech: Fine root biomass and carbon partitioning in 14 mature stands across a precipitation gradient. *Global Change Biology*, 14(9), 2081–2095. <https://doi.org/10.1111/j.1365-2486.2008.01634.x>
- Muhr, J., & Borken, W. (2009). Delayed recovery of soil respiration after wetting of dry soil further reduces C losses from a Norway spruce forest soil. *Journal of Geophysical Research*, 114, G04023. <https://doi.org/10.1029/2009JG000998>
- Nickel, U. T., Weikl, F., Kerner, R., Schäfer, C., Kallenbach, C., Munch, J. C., & Pritsch, K. (2018). Quantitative losses vs. qualitative stability of ectomycorrhizal community responses to 3 years of experimental summer drought in a beech-spruce forest. *Global Change Biology*, 24(2), e560–e576. <https://doi.org/10.1111/gcb.13957>
- Nikolova, P. S., Bauerle, T. L., Häberle, K.-H., Blaschke, H., Brunner, I., & Matyssek, R. (2020). Fine-root traits reveal contrasting ecological strategies in European beech and Norway spruce during extreme drought. *Frontiers in Plant Science*, 11, 1211. <https://doi.org/10.3389/fpls.2020.01211>
- Nikolova, P. S., Raspe, S., Andersen, C. P., Mainiero, R., Blaschke, H., Matyssek, R., & Häberle, K.-H. (2009). Effects of the extreme drought in 2003 on soil respiration in a mixed forest. *European Journal of Forest Research*, 128(2), 87–98. <https://doi.org/10.1007/s10342-008-0218-6>
- Phillips, R. P., Erlitz, Y., Bier, R., & Bernhardt, E. S. (2008). New approach for capturing soluble root exudates in forest soils. *Functional Ecology*, 22(6), 990–999. <https://doi.org/10.1111/j.1365-2435.2008.01495.x>
- Poorter, H., Niklas, K. J., Reich, P. B., Oleksyn, J., Poot, P., & Mommer, L. (2012). Biomass allocation to leaves, stems and roots: Meta-analyses of interspecific variation and environmental control. *The New Phytologist*, 193(1), 30–50. <https://doi.org/10.1111/j.1469-8137.2011.03952.x>
- Pretzsch, H., Biber, P., Schütze, G., Kemmerer, J., & Uhl, E. (2018). Wood density reduced while wood volume growth accelerated in central European forests since 1870. *Forest Ecology and Management*, 429, 589–616. <https://doi.org/10.1016/j.foreco.2018.07.045>
- Pretzsch, H., Grams, T., Häberle, K.-H., Pritsch, K., Bauerle, T. L., & Rötzer, T. (2020). Growth and mortality of Norway spruce and European beech in monospecific and mixed-species stands under natural episodic and experimentally extended drought. Results of the KROOF throughfall exclusion experiment. *Trees*, 34(4), 957–970. <https://doi.org/10.1007/s00468-020-01973-0>
- Pretzsch, H., Rötzer, T., Matyssek, R., Grams, T. E. E., Häberle, K.-H., Pritsch, K., Kerner, R., & Munch, J.-C. (2014). Mixed Norway spruce (*Picea abies* [L.] Karst) and European beech (*Fagus sylvatica* [L.]) stands under drought: From reaction pattern to mechanism. *Trees*, 28(5), 1305–1321. <https://doi.org/10.1007/s00468-014-1035-9>
- Rehseh, R., Rehseh, S., Gast, A., Jakab, A.-L., Lehmann, M. M., Saurer, M., Gessler, A., & Ruehr, N. K. (2021). Tree allocation dynamics beyond heat and hot drought stress reveal changes in carbon storage, belowground translocation and growth. *New Phytologist*, 233, 687–704. <https://doi.org/10.1111/nph.17815>
- Reiter, I. M. (2004). *Space-related resource investments and gains of adult beech (Fagus sylvatica) and spruce (Picea abies) as a quantification of aboveground competitiveness*. (Doctoral thesis). Technical University of Munich, Munich. <http://mediatum.ub.tum.de/?id=603496>
- Rog, I., Jakoby, G., & Klein, T. (2021). Carbon allocation dynamics in conifers and broadleaved tree species revealed by pulse labeling and mass balance. *Forest Ecology and Management*, 493, 119258. <https://doi.org/10.1016/j.foreco.2021.119258>
- Ruehr, N. K., Grote, R., Mayr, S., & Arneith, A. (2019). Beyond the extreme: Recovery of carbon and water relations in woody plants following heat and drought stress. *Tree Physiology*, 39(8), 1285–1299. <https://doi.org/10.1093/treephys/tpz032>
- Sala, A., Piper, F., & Hoch, G. (2010). Physiological mechanisms of drought-induced tree mortality are far from being resolved. *The New Phytologist*, 186(2), 274–281. <https://doi.org/10.1111/j.1469-8137.2009.03167.x>
- Schindlbacher, A., Wunderlich, S., Borken, W., Kitzler, B., Zechmeister-Boltenstern, S., & Jandl, R. (2012). Soil respiration under climate change: Prolonged summer drought offsets soil warming effects. *Global Change Biology*, 18(7), 2270–2279. <https://doi.org/10.1111/j.1365-2486.2012.02696.x>
- Schuldt, B., Buras, A., Arend, M., Vitasse, Y., Beierkuhnlein, C., Damm, A., Gharun, M., Grams, T. E., Hauck, M., Hajek, P., Hartmann, H., Hiltbrunner, E., Hoch, G., Holloway-Phillips, M., Körner, C., Larysch, E., Lübke, T., Nelson, D. B., Rammig, A., ... Kahmen, A. (2020). A first assessment of the impact of the extreme 2018 summer drought on central European forests. *Basic and Applied Ecology*, 45, 86–103. <https://doi.org/10.1016/j.baae.2020.04.003>
- Secchi, F., & Zwieniecki, M. A. (2011). Sensing embolism in xylem vessels: The role of sucrose as a trigger for refilling. *Plant, Cell & Environment*, 34(3), 514–524. <https://doi.org/10.1111/j.1365-3040.2010.02259.x>
- Solly, E. F., Brunner, I., Helmsaari, H.-S., Herzog, C., Leppälammikujansuu, J., Schöning, I., Schrupf, M., Schweingruber, F. H., Trumbore, S. E., & Hagedorn, F. (2018). Unravelling the age of fine roots of temperate and boreal forests. *Nature Communications*, 9(1), 3006. <https://doi.org/10.1038/s41467-018-05460-6>
- Subke, J.-A., Vallack, H. W., Magnusson, T., Keel, S. G., Metcalfe, D. B., Höglberg, P., & Ineson, P. (2009). Short-term dynamics of abiotic and biotic soil ¹³CO₂ effluxes after in situ ¹³CO₂ pulse labelling of a boreal pine forest. *New Phytologist*, 183(2), 349–357. <https://doi.org/10.1111/j.1469-8137.2009.02883.x>
- Sun, L., Hirano, T., Yazaki, T., Teramoto, M., & Liang, N. (2020). Fine root dynamics and partitioning of root respiration into growth and maintenance components in cool temperate deciduous and evergreen

- forests. *Plant and Soil*, 446(1–2), 471–486. <https://doi.org/10.1007/s11104-019-04343-z>
- Tomasella, M., Beikircher, B., Häberle, K.-H., Hesse, B. D., Kallenbach, C., Matyssek, R., & Mayr, S. (2018). Acclimation of branch and leaf hydraulics in adult *Fagus sylvatica* and *Picea abies* in a forest through-fall exclusion experiment. *Tree Physiology*, 38(2), 198–211. <https://doi.org/10.1093/treephys/tpx140>
- Trugman, A. T., Detto, M., Bartlett, M. K., Medvigy, D., Anderegg, W. R. L., Schwalm, C., Schaffer, B., & Pacala, S. W. (2018). Tree carbon allocation explains forest drought-kill and recovery patterns. *Ecology Letters*, 21(10), 1552–1560. <https://doi.org/10.1111/ele.13136>
- Tsamir-Rimon, M., Ben-Dor, S., Feldmesser, E., Oppenheimer-Shaanan, Y., David-Schwartz, R., Samach, A., & Klein, T. (2021). Rapid starch degradation in the wood of olive trees under heat and drought is permitted by three stress-specific beta amylases. *New Phytologist*, 229(3), 1398–1414. <https://doi.org/10.1111/nph.16907>
- Unger, S., Máguas, C., Pereira, J. S., David, T. S., & Werner, C. (2010). The influence of precipitation pulses on soil respiration – Assessing the “Birch effect” by stable carbon isotopes. *Soil Biology and Biochemistry*, 42(10), 1800–1810. <https://doi.org/10.1016/j.soilbio.2010.06.019>
- Werner, C., Meredith, L. K., Ladd, S. N., Ingrisch, J., Kübert, A., van Haren, J., Bahn, M., Bailey, K., Bamberger, I., Beyer, M., Blomdahl, D., Byron, J., Daber, E., Deleeuw, J., Dippold, M. A., Fudyma, J., Gil-Loaiza, J., Honeker, L. K., Hu, J., ... Williams, J. (2021). Ecosystem fluxes during drought and recovery in an experimental forest. *Science (New York, N.Y.)*, 374(6574), 1514–1518. <https://doi.org/10.1126/science.abj6789>
- Yang, Q., Zhang, W., Li, R., Xu, M., & Wang, S. (2016). Different responses of non-structural carbohydrates in above-ground tissues/organs and root to extreme drought and re-watering in Chinese fir (*Cunninghamia lanceolata*) saplings. *Trees*, 30(5), 1863–1871. <https://doi.org/10.1007/s00468-016-1419-0>
- Zang, U., Goisser, M., Grams, T. E. E., Häberle, K.-H., Matyssek, R., Matzner, E., & Borken, W. (2014). Fate of recently fixed carbon in European beech (*Fagus sylvatica*) saplings during drought and subsequent recovery. *Tree Physiology*, 34(1), 29–38. <https://doi.org/10.1093/treephys/tpt110>
- Zhang, X., & Wang, W. (2015). The decomposition of fine and coarse roots: Their global patterns and controlling factors. *Scientific Reports*, 5, 9940. <https://doi.org/10.1038/srep09940>
- Zwetsloot, M. J., & Bauerle, T. L. (2021). Repetitive seasonal drought causes substantial species-specific shifts in fine-root longevity and spatio-temporal production patterns in mature temperate forest trees. *New Phytologist*, 231, 974–986. <https://doi.org/10.1111/nph.17432>

SUPPORTING INFORMATION

Additional supporting information can be found online in the Supporting Information section at the end of this article.

How to cite this article: Hikino, K., Danzberger, J., Riedel, V. P., Hesse, B. D., Hafner, B. D., Gebhardt, T., Rehschuh, R., Ruehr, N. K., Brunn, M., Bauerle, T. L., Landhäuser, S. M., Lehmann, M. M., Rötzer, T., Pretzsch, H., Buegger, F., Weikl, F., Pritsch, K., & Grams, T. E. E. (2022). Dynamics of initial carbon allocation after drought release in mature Norway spruce—Increased belowground allocation of current photoassimilates covers only half of the carbon used for fine-root growth. *Global Change Biology*, 00, 1–17. <https://doi.org/10.1111/gcb.16388>

1 **Supporting information**

2 **Article title:** Dynamics of initial C allocation after drought release in mature Norway spruce -
 3 Increased belowground allocation of current photoassimilates covers only half of the C used for
 4 fine-root growth

5 **Authors:** Kyohsuke Hikino, Jasmin Danzberger, Vincent P. Riedel, Benjamin D. Hesse,
 6 Benjamin D. Hafner, Timo Gebhardt, Romy Rehschuh, Nadine K. Ruehr, Melanie Brunn,
 7 Taryn L. Bauerle, Simon M. Landhäusser, Marco M. Lehmann, Thomas Rötzer, Hans Pretzsch,
 8 Franz Buegger, Fabian Weikl, Karin Pritsch, Thorsten E. E. Grams

9

10

11

12

13

14

15

16 *Table S1: Detailed data of the labeled four control and three recovering (previously drought-stressed)*
 17 *trees: Diameter at breast height (DBH), tree height, height of the crown base, the daily mean change of*
 18 *stable carbon isotope composition ($\delta^{13}\text{C}$) and CO_2 concentration in crown air during labeling, spatial*
 19 *contribution and area of each tree for the calculation of belowground C sink activity and allocation of*
 20 *newly assimilated C (C_{new}): in fine-root growth, ectomycorrhizae (ECM), root exudates, and soil CO_2*
 21 *efflux (see Material and Methods). The changes are given in means \pm SE.*

Tree	DBH [cm]	Tree height [m]	Height of the crown base [m]	Change in crown air $\delta^{13}\text{C}$ [‰]	Change in CO_2 concentration [ppm]	Spatial contribution belowground [%]	Area [m²]
Conrol_1	30.5	33.7	23.6	-6.7 \pm 0.4	111 \pm 8	21	11
Conrol_2	34.9	32.6	23.1	-6.7 \pm 0.4	112 \pm 8	23	13
Control_3	46.3	34.3	23.1	-7.2 \pm 0.4	119 \pm 8	31	17
Control_4	37.7	32.5	21.0	-8.8 \pm 0.4	162 \pm 10	25	14
Recovery_1	45.1	32.0	22.7	-5.0 \pm 0.3	72 \pm 5	41	26
Recovery_2	27.3	28.3	22.5	-7.3 \pm 0.4	132 \pm 8	25	16
Recovery_3	38.3	33.6	23.3	-2.9 \pm 0.3	35 \pm 5	36	22

22

27 *Table S3: Total length and surface area of branch/twig and stem estimated for each tree based on field*
 28 *data. Data of branches and twigs are separated into sun and shade crowns.*

	Sun branch/twig length [m]	Sun branch/twig area [m²]	Shade branch/twig length [m]	Shade branch/twig area [m²]	Stem area (< 6.5 m) [m²]	Stem area (> 6.5 m) [m²]
Conrol_1	3359	40	1287	14	6	11
Conrol_2	3847	45	1474	18	7	12
Control_3	5103	60	1956	25	9	17
Control_4	4140	38	1590	21	7	12
Recovery_1	1883	21	1411	22	9	15
Recovery_2	1138	13	853	12	5	8
Recovery_3	1597	20	1198	14	7	14

29

30

31 **Methods S1: Determination of proportional growth using dendrometer**

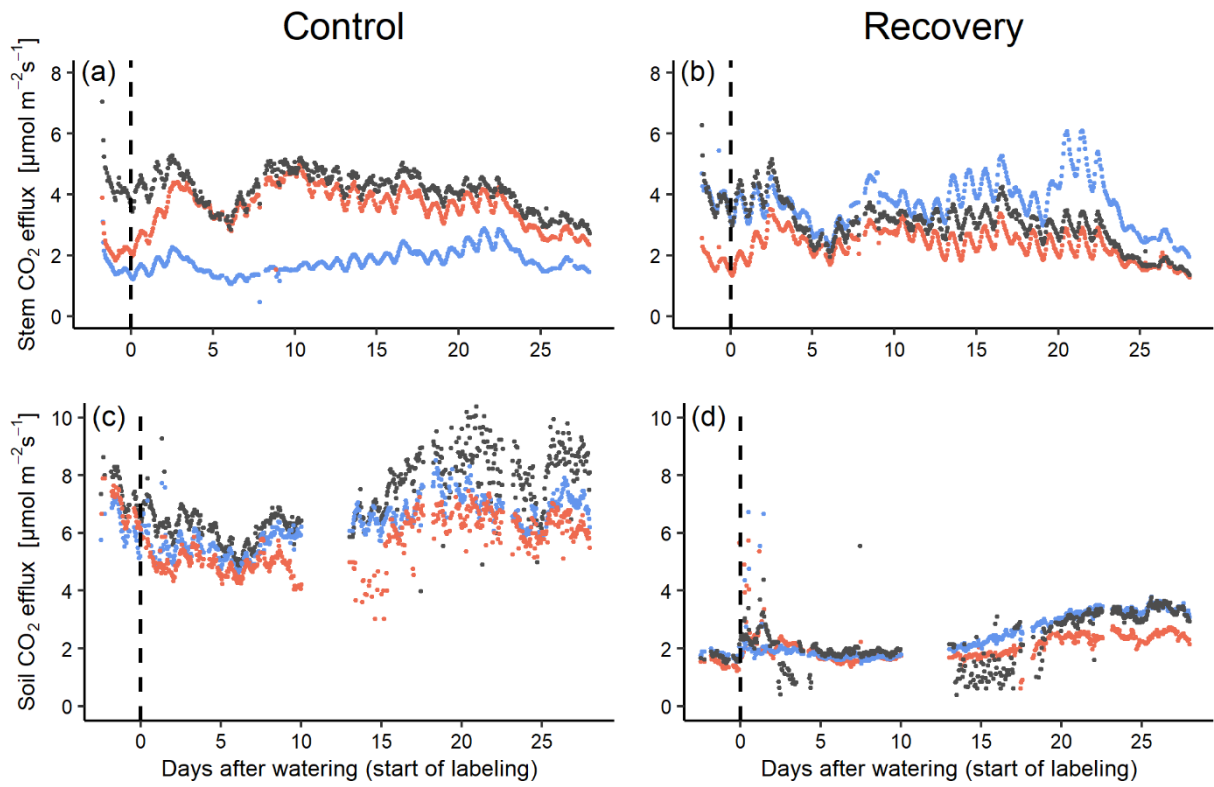
32 To determine the proportional growth (in %) during the 28 days after watering (ratio of the
 33 radial growth during 28 days to the total annual growth), dendrometer data at 6 am was used
 34 and fitted with the following sigmoid curve:

35
$$X = d + \frac{a - d}{1 + e^{\frac{DOY - c}{b}}} \text{ (Eqn. S1),}$$

36 where X is the output voltage (in mV) corresponding to the radial growth, DOY is the day of
 37 year, a is the starting value of X before the growing season, b the slope coefficient of the
 38 regression, c the inflection point of the curve, and d the end value of X after the growing season.

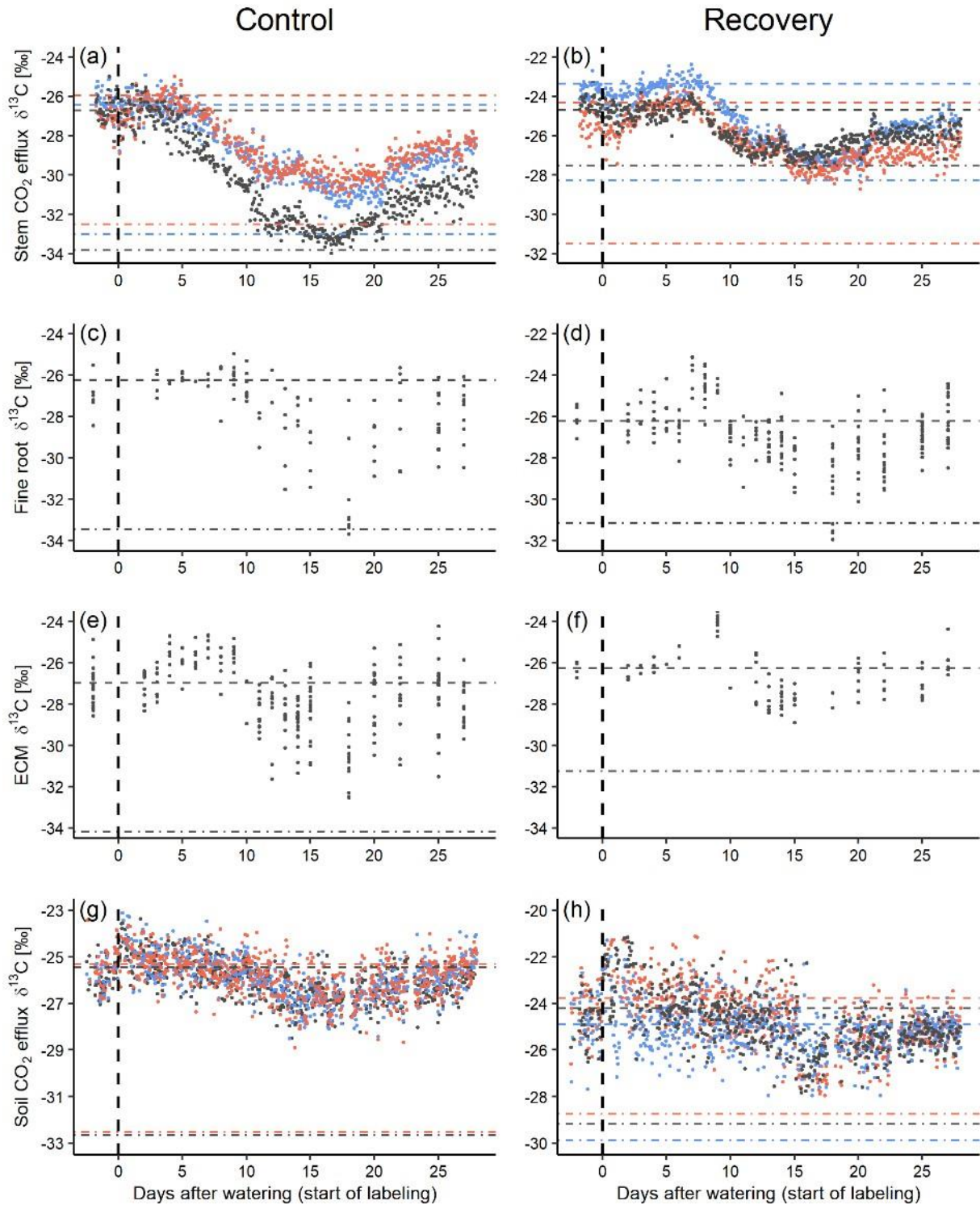
39 Using these curves, proportional growth was calculated by relating the growth during the 28
 40 days to the total annual growth. Since only two labeled trees per treatment were assessed with
 41 the dendrometers, additional spruce trees in neighboring plots were included in the evaluation
 42 of the proportional growth (n = 9 for control and n = 6 for recovering trees).

43



44

45 *Fig. S1: Rates of stem (a, b) and soil CO₂ efflux (c, d) in control (left) and recovery (right) trees during*
 46 *the study period. Each color represents each measurement tree (n = 3).*



47

48 *Fig. S2: Raw $\delta^{13}\text{C}$ data ($\delta^{13}\text{C}_{sample}$) used for Eqn. 10. (a,b) stem CO_2 efflux, (c,d) non-mycorrhized fine-*
 49 *root tips, (e, f) ectomycorrhizae (ECM), and (g,h) soil CO_2 efflux, separated in control trees (left) and*
 50 *recovering (previously drought-stressed, right) trees. Different colors represent each measurement tree*
 51 *($n = 3$) for stem CO_2 efflux and soil CO_2 efflux. All measurements were pooled for non-mycorrhizal root*
 52 *tips and ECM. Horizontal dashed and dot-dash lines display $\delta^{13}\text{C}_{old}$ and $\delta^{13}\text{C}_{new}$ in Eqn. 10, respectively.*
 53 *$\delta^{13}\text{C}_{new}$ was calculated with Eqn. S2,S3 using $\delta^{13}\text{C}_{old}$ and the individual change in crown air $\delta^{13}\text{C}$ (Table*
 54 *S1).*

55

56

57 **Methods S2: Calculation of $\delta^{13}\text{C}_{\text{new}}$ for Eqn. 10**

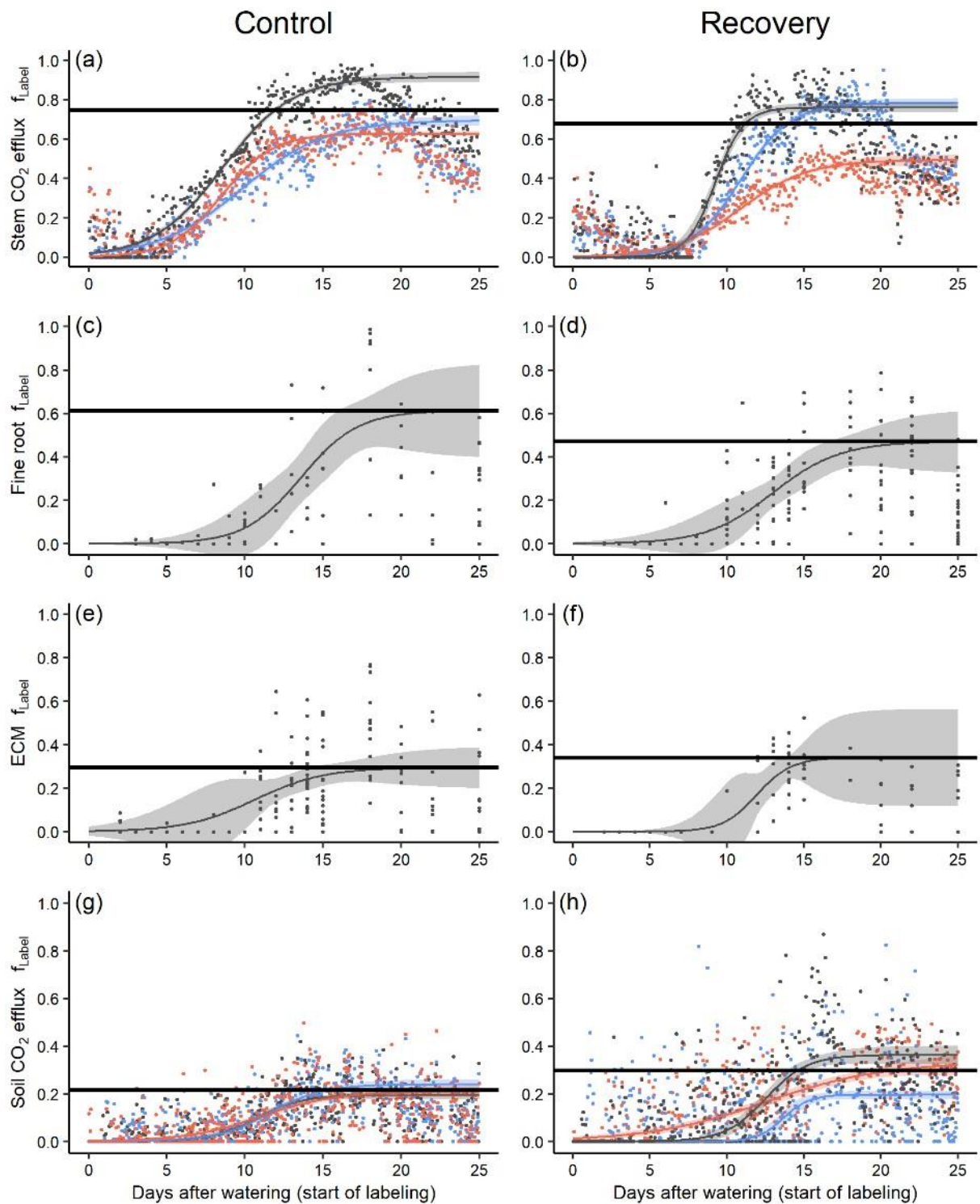
58 $\delta^{13}\text{C}_{\text{new}}$ for Eqn. 10 was calculated as described by Kuptz *et al.* (2011), following (Schnyder *et*
59 *al.*, 2003):

60
$$\delta^{13}\text{C}_{\text{A-O}} (\text{‰}) = \left(\frac{1000 + \delta^{13}\text{C}_{\text{Air-Unlabeled}}}{1000 + \delta^{13}\text{C}_{\text{Old}}} - 1 \right) \times 1000 \text{ (Eqn. S2),}$$

61 which gives the mean apparent ^{13}C discrimination ($\delta^{13}\text{C}_{\text{A-O}}$) between unlabeled crown air
62 (reference air above canopy, $\delta^{13}\text{C}_{\text{Air-Unlabeled}}$) and $\delta^{13}\text{C}_{\text{Old}}$.

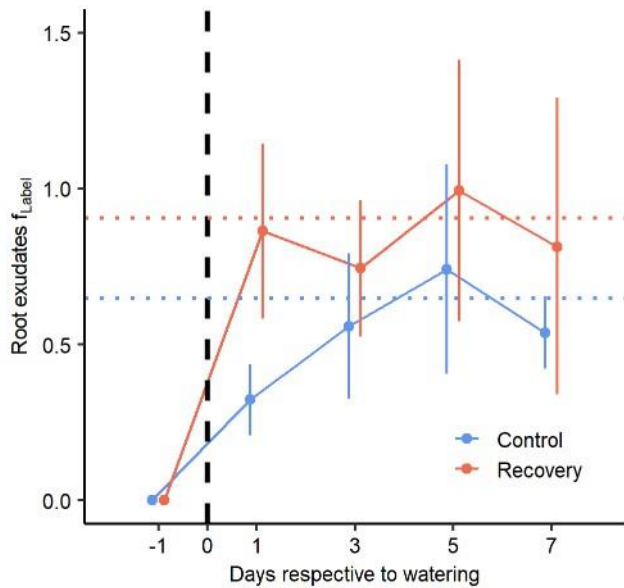
63
$$\delta^{13}\text{C}_{\text{new}} (\text{‰}) = 1000 \times \frac{1000 + \delta^{13}\text{C}_{\text{Air-Labeled}}}{1000 + \delta^{13}\text{C}_{\text{A-O}}} - 1000 \text{ (Eqn. S3),}$$

64 where $\delta^{13}\text{C}_{\text{Air-Labeled}}$ is the mean $\delta^{13}\text{C}$ of crown air of each tree. For belowground sinks that were
65 not assigned to specific trees, mean $\delta^{13}\text{C}_{\text{Air-Labeled}}$ of four (control) or three (recovering) trees
66 was used.



67

68 *Fig. S3: f_{Label} (fraction of labeled C) and sigmoid curves with 95% confidence intervals to calculate the*
 69 *$contC_{new}$ (contribution of C_{new} to C sink activity) to stem CO_2 efflux (a,b), non-mycorrhizal fine-root tips*
 70 *(c,d), ectomycorrhizae (ECM, e,f), and soil CO_2 efflux (g,h), separated in control trees (left) and*
 71 *recovering (previously drought-stressed, right) trees. Different colors represent each measurement tree*
 72 *($n = 3$) for stem CO_2 efflux and soil CO_2 efflux. All measurements were pooled for non-mycorrhizal root*
 73 *tips and ECM. Only f_{Label} before reaching the maximum were used for the fitting, since f_{Label} decreased*
 74 *again after the end of labeling. Black horizontal lines display the mean $contC_{new}$.*



75

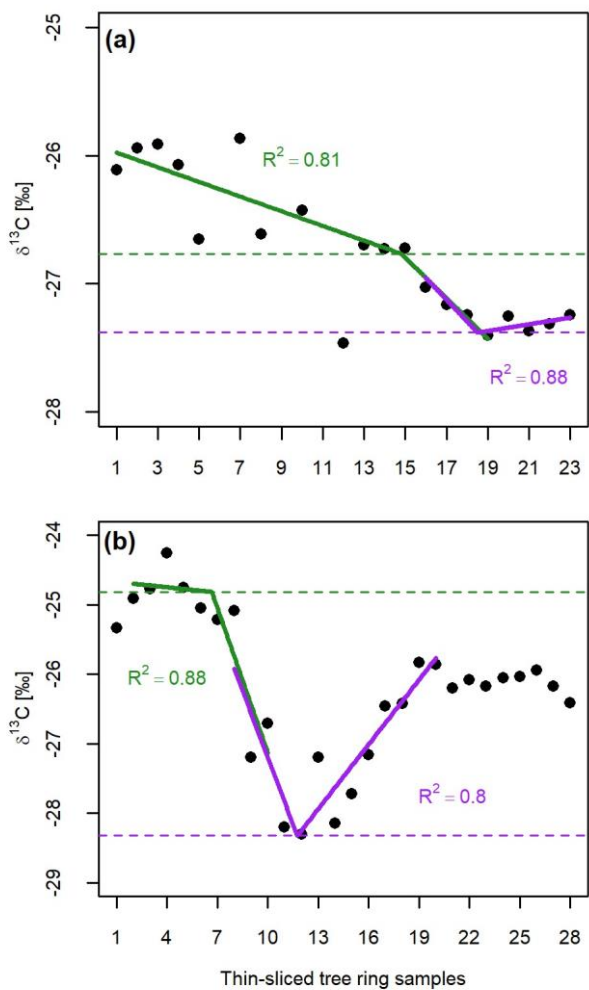
76 Fig. S4: f_{Label} (fraction of labeled C) and $contC_{new}$ (contribution of C_{new} to C sink activity) to root exudates
 77 in control (blue) and recovering trees (previously drought-stressed, red). The calculated $contC_{new}$ is
 78 shown in horizontal dotted lines for control (blue) and recovering trees (red), respectively. The data are
 79 displayed in mean \pm SE.

80 **Methods S3: Detailed descriptions for the calculation of fraction of labeled C (f_{Label}) and**
 81 **contribution of C_{new} to each C sink activity ($contC_{new}$) for branch, stem, and coarse-root**
 82 **growth**

83 For branch, stem, and coarse-root growth, $\delta^{13}C_{old}$ and $\delta^{13}C_{sample}$ (for Eqn. 10) were determined
 84 by fitting the $\delta^{13}C$ of tree ring slices with a piecewise function (Hikino *et al.*, 2022). The applied
 85 labeling with ^{13}C -depleted CO_2 caused a sudden and steep decrease of $\delta^{13}C$, after the ^{13}C -
 86 depleted tracer was incorporated in the tree ring and was thus defined as tracer arrival. To
 87 determine this point, linear segments before and after the start of the steep decrease (e.g. slices
 88 1 - 19 for the sample in Fig. S5a) were extracted from the course of the $\delta^{13}C$ data. Then, these
 89 linear segments were fitted by linear regression (“lm” function, R package “stats”, version:
 90 3.6.1). Subsequently, the “segmented” function (R package “segmented”, version: 1.3-0) was
 91 used to determine the point where the linear relationship (slope and intercept) changes, giving
 92 the intersection between the two green lines as exemplified in Fig. S5. The $\delta^{13}C$ value at this
 93 point (marked by the green horizontal dashed lines in Fig. S5a,b) was then defined as $\delta^{13}C_{old}$.

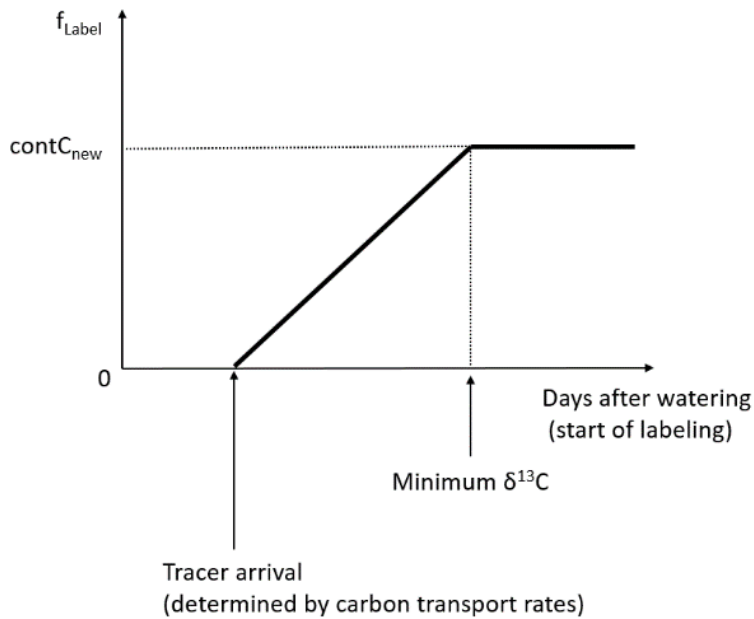
94 After the steep decrease, $\delta^{13}C$ started to increase again as unlabeled C arrived after the end of
 95 labeling. We determined this minimum value of $\delta^{13}C$ by fitting with the piecewise function
 96 using the same method (intersection between the purple linear segments fitted to the data in Fig.
 97 S5). The $\delta^{13}C$ value at this point (purple horizontal dashed lines) was then defined as $\delta^{13}C_{sample}$.
 98 In addition to the labeled trees, we also determined the natural shifts of $\delta^{13}C$ of non-labeled

99 control trees for each treatment (n = 3). These shifts without the effect of the labeling were
 100 subtracted from the $\delta^{13}\text{C}_{\text{sample}}$ determined above to correct for the effect of watering, weather
 101 fluctuation, and seasonal changes (Helle & Schleser, 2004). Finally, using $\delta^{13}\text{C}_{\text{old}}$, corrected
 102 $\delta^{13}\text{C}_{\text{sample}}$, and Eqn. 10, f_{Label} was calculated. Since we could not apply the sigmoid curve (Eqn.
 103 11) to determine $\text{contC}_{\text{new}}$, the calculated f_{Label} was defined as $\text{contC}_{\text{new}}$. Thus, we could not
 104 consider that the new isotopic equilibrium was not completely reached by the labeling. However,
 105 since c. 98% of the calculated $\text{contC}_{\text{new}}$ to stem CO_2 efflux was reached with the recorded f_{Label}
 106 data (Fig. S3a,b), the underestimation of $\text{contC}_{\text{new}}$ to the branch, stem, and the coarse-root
 107 growth is likely negligible.



108

109 *Fig. S5: Two examples for the calculation of $\text{contC}_{\text{new}}$ (contribution of C_{new} to C sink activity) to stem*
 110 *and coarse-root growth, using piecewise functions. X-axis is each tree ring sample thin-sectioned in*
 111 *radial direction (c. 5 μm thick). The green and purple line segments fitted to the data show the results*
 112 *of the piecewise functions for the arrival of ^{13}C -depleted tracer (green) and minimum $\delta^{13}\text{C}$ (purple),*
 113 *respectively. $\delta^{13}\text{C}$ at the intersections of two line segments of the respective color, marked with*
 114 *horizontal dashed lines, are the calculated $\delta^{13}\text{C}_{\text{old}}$ and $\delta^{13}\text{C}_{\text{sample}}$, respectively. These values were then*
 115 *used for the calculation of $\text{contC}_{\text{new}}$ (see main text and Methods S3).*



116

117 *Fig. S6: Estimation of the course of f_{Label} (fraction of labeled C) in branch, stem, and coarse-root growth,*
 118 *using $contC_{new}$ (contribution of C_{new} to C sink activity) and the arrival time of the ^{13}C -depleted tracer.*
 119 *f_{Label} between tracer arrival and the minimum $\delta^{13}C$ was assumed to increase linearly.*

120

121

122 References

123 **Helle G, Schleser GH. 2004.** Beyond CO₂-fixation by Rubisco - an interpretation of ¹³C/¹²C
 124 variations in tree rings from novel intra-seasonal studies on broad-leaf trees. *Plant, cell &*
 125 *environment* **27**: 367–380.

126 **Hikino K, Danzberger J, Riedel VP, Rehschuh R, Ruehr NK, Hesse BD, Lehmann MM,**
 127 **Buegger F, Weigl F, Pritsch K et al. 2022.** High resilience of carbon transport in long-term
 128 drought stressed mature Norway spruce trees within two weeks after drought release. *Global*
 129 *Change Biology*. doi: 10.1111/gcb.16051.

130 **Kuptz D, Fleischmann F, Matyssek R, Grams TEE. 2011.** Seasonal patterns of carbon
 131 allocation to respiratory pools in 60-yr-old deciduous (*Fagus sylvatica*) and evergreen (*Picea*
 132 *abies*) trees assessed via whole-tree stable carbon isotope labeling. *The New phytologist* **191**:
 133 160–172.

134 **Schnyder H, Schäufele R, Lötscher M, Gebbing T. 2003.** Disentangling CO₂ fluxes: direct
 135 measurements of mesocosm-scale natural abundance ¹³CO₂ / ¹²CO₂ gas exchange, ¹³C
 136 discrimination, and labelling of CO₂ exchange flux components in controlled environments.
 137 *Plant, cell & environment* **26**: 1863–1874.

138